Universitat de Lleida

Towards the characterisation of adaptive syndromes of Mediterranean pines: insights through innovative tree phenotyping techniques

Filippo Santini

http://hdl.handle.net/10803/668898

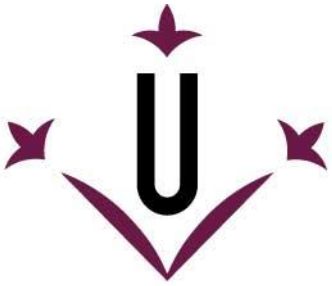

Universitat de Lleida

PhD THESIS

Towards the characterisation of adaptive syndromes of Mediterranean pines: insights through innovative tree phenotyping techniques

Filippo Santini

PhD program: Forest and Natural Environment Management

Supervisor
Jordi Voltas

2020

This thesis has been carried out at the Laboratory of Silviculture, Department of Crop and Forest Sciences, University of Lleida, Spain. The author was supported by a University of Lleida pre-doctoral scholarship. The research was funded by the Spanish Government [MINECO/FEDER grant number AGL2015-68274-C3-3-R]. The work reported in Chapter 5 was partially supported by the Russian Science Foundation (project number 14-14-00219-P, mathematical approach).

Ai miei nonni, che mi hanno insegnato
che aver studiato non è una condizione
imprescindibile, ne tantomeno sufficiente,
per essere una buona persona

TABLE OF CONTENTS

LIST OF PUBLICATIONS

This thesis is based on the work contained in the following publications:

- Santini F., Ferrio J.P., Hereş A.M., Notivol E., Piqué M., Serrano L., Shestakova T.A., Sin E., Vericat P., Voltas, J. (2018) Scarce population genetic differentiation but substantial spatiotemporal phenotypic variation of water-use efficiency in *Pinus sylvestris* at its western distribution range. *European Journal of Forest Research*, 137, 863-878.

- Santini F., Kefauver S.C., Resco de Dios V., Araus J.L., Voltas J. (2019) Using unmanned aerial vehicle-based multispectral, RGB and thermal imagery for phenotyping of forest genetic trials: A case study in *Pinus halepensis*. *Annals of Applied Biology*, 174, 262-276.

- Santini F., Climent J.M., Voltas J. (2019) Phenotypic integration and life history strategies among populations of *Pinus halepensis*: an insight through structural equation modelling. *Annals of Botany*. doi: 10.1093/aob/mcz088

- Santini F., Serrano L., Kefauver S.C., Abdullah-Al M., Aguilera M., Sin E., Voltas J. (2019) Morpho-physiological variability of *Pinus nigra* populations reveals climate-driven local adaptation but weak water use differentiation. *Environmental and Experimental Botany*, 166, 103828

SUMMARY

The *in-situ* adaptation of tree species in the context of the ongoing climate change is determined by intra-specific genetic variation and phenotypic plasticity, which can be evaluated by testing multiple populations in common gardens. For this purpose, new technologies allowing the ecophysiological characterisation of adult trees can improve our capacity to disentangle patterns of adaptive variation in forest species, providing fundamental information to forecast their ability to cope with environmental changes.

In this thesis, I studied the nature and extent of intra-specific genetic variation in important functional traits of *Pinus halepensis* Mill., *Pinus nigra* Arnold and *Pinus sylvestris* L., three widespread and socio-economically important conifers typical of the Mediterranean basin and characterised by contrasting ecological niches. Variability in growing conditions among the distribution range of each species has driven intra-specific differentiation in functional traits and life-history strategies among populations, a variation that remains nevertheless largely unexplored. To analyse the extent of intra-specific differentiation in these pines, I characterised adult trees growing in three common gardens, each one testing populations of a single species. To this end, I combined well-established phenotyping techniques with remote sensing data obtained with RGB, multispectral and thermal cameras mounted on an Unmanned Aerial Vehicle (UAV). In the case of *P. sylvestris*, the potential genetic variation in growth and intrinsic water use efficiency (WUE_i) was also compared to the magnitude of plastic differentiation detected in natural populations.

UAV-imagery revealed a strong genetic differentiation in leaf area and summer transpiration among populations of *P. halepensis*, which was in turn associated with variation in growth rate. Combining this information with already available data, a clear divergence in adaptive strategies was detected in this species, seemingly driven by variation in water availability and fire occurrence across the species distribution range. Fast growing populations showing high leaf area, low rooting depth and high summer transpiration emerged in contrast to drought-adapted populations characterised by slow growth rate, reduced transpiration, deep rooting and high investment in reproduction and reserve accumulation. By developing a straightforward methodology to retrieve tree-level data from aerial images, I associated phenotypic variation among individuals of Aleppo pine with genomic variation at Single Nucleotide Polymorphism loci (SNPs), providing an insight into the molecular basis of phenotypic differentiation in this species.

In *P. nigra*, an appreciable genetic differentiation was detected among populations in growth traits, reserve accumulation, photosynthetic efficiency and leaf area. The main drivers of this variation were minimum annual temperatures and continentality, with populations experiencing harsher winter conditions being characterised by a more efficient photosynthetic apparatus, a slow growth and a high accumulation of non-structural carbohydrates. On the other hand, water availability had a weak role as driver of genetic adaptive variation in this species. Additionally, populations did not differ in traits related to water use, such as WUE_i, stem water potential and rooting patterns.

Similarly, a weak genetic differentiation in WUE_i emerged among populations of *P. sylvestris*. However, variation in WUE_i in natural stands, mainly related to spatio-temporal plastic adjustment to soil water holding capacity, was sizeable and much higher than genetic variation. This indicates a prominent role of plasticity over genetic adaptation as determinant of phenotypic variation in *P. sylvestris* for WUE_i. Moreover, plastic variation in WUE_i among natural stands directly affected water-use efficiency at the ecosystem level, as revealed by satellite-derived remote sensing data.

Altogether, this thesis provided a deep insight into intra-specific adaptive variation in key phenotypic traits of three important Mediterranean conifers characterised by contrasting ecological niches. In the context of the ongoing climate change, this information is crucial to understand the future dynamics (e.g. range expansion or contraction) of these species. Under a future scenario of reduced water availability in Mediterranean regions, the *in-situ* selection of drought-adapted individuals or their migration from drought-adapted populations will likely play a fundamental role in the adaptation of *P. halepensis*. Conversely, lack of evidence of genetic differentiation in traits related to drought resistance suggests that the persistence and future distribution of *P. nigra* and *P. sylvestris* around the Mediterranean basin will likely rely on the extent of phenotypic plasticity and on the colonization of higher altitude and more humid areas.

In addition, this thesis provided a strong support for the use of UAV-derived imagery as phenotyping tool in forest species, highlighting the valuable information that can be obtained with this methodology. The different approaches developed in this work are described in detail in the thesis, emphasising the strengths and pitfalls of remote sensing data obtained with UAVs as high-throughput phenotyping technique for forest species.

RESUMEN

La adaptación *in-situ* de las especies arbóreas está determinada, en el contexto del cambio climático, por la variación genética intraespecífica y la plasticidad fenotípica, fenómenos que pueden evaluarse analizando múltiples poblaciones mediante ensayos de procedencia. Las nuevas tecnologías permiten la caracterización ecofisiológica de árboles adultos y pueden mejorar nuestra capacidad de descifrar patrones de variación adaptativa en especies forestales, proporcionando información fundamental para predecir su capacidad de respuesta a los cambios ambientales.

En esta tesis, se estudiaron patrones de variación genética intraespecífica de rasgos funcionales de *Pinus halepensis* Mill., *Pinus nigra* Arnold y *Pinus sylvestris* L., tres coníferas características de la cuenca mediterránea que destacan por ocupar nichos ecológicos diferenciados. La variabilidad de las condiciones de crecimiento propias de la distribución geográfica de cada especie ha propiciado la diferenciación intraespecífica de rasgos funcionales y estrategias vitales. Sin embargo, esta variación permanece en gran parte inexplorada. Para analizar el alcance de la diferenciación intraespecífica en estos pinos, se caracterizaron árboles adultos en tres ensayos de procedencia. Se combinaron técnicas de fenotipado bien establecidas con datos de teledetección obtenidos con cámaras RGB, multiespectrales y térmicas acopladas a un vehículo aéreo no tripulado (*unmanned aerial vehicle*, UAV). En el caso de *P. sylvestris*, la variación genética en el crecimiento y la eficiencia intrínseca del uso del agua (EUA_i) se comparó además con la magnitud de la diferenciación plástica detectada en poblaciones naturales.

Las imágenes de UAV revelaron la existencia de diferenciación genética significativa en el área foliar y en la transpiración en verano de distintas poblaciones de *P. halepensis*, que resultó estar asociada con la variación en crecimiento aéreo. Combinando esta información con datos ya disponibles se detectó una clara divergencia intraespecífica en las estrategias adaptativas de esta conífera, determinada por la variación en la disponibilidad de agua y la ocurrencia de incendios a lo largo de la distribución geográfica de la especie. Las poblaciones de rápido crecimiento, caracterizadas por una extensa área foliar, baja profundidad de enraizamiento y alta transpiración en verano, se diferenciaron de las poblaciones adaptadas a la sequía, que presentaban una tasa de crecimiento lenta, transpiración reducida, enraizamiento profundo y una alta inversión en reproducción y acumulación de reservas.

Mediante el desarrollo de una metodología para la recolección semiautomática de datos a nivel de árbol a partir de imágenes aéreas, la variación fenotípica entre individuos de *P. halepensis* se asoció a la variación genómica en loci SNP (*Single Nucleotide Polymorphism*).

Esta asociación proporcionó información acerca de la base molecular de la diferenciación fenotípica en esta especie.

En *P. nigra*, se detectó diferenciación genética entre poblaciones apreciable en caracteres de crecimiento, así como en acumulación de reservas, eficiencia fotosintética y área foliar. Los principales promotores de esta variación fueron las temperaturas mínimas anuales y la continentalidad, de manera que las poblaciones que experimentan condiciones invernales más severas en origen presentaron un aparato fotosintético más eficiente, un crecimiento lento y una alta acumulación de reservas. Por otro lado, la disponibilidad de agua tuvo una importancia marginal como determinante de la variación genética adaptativa en esta especie. Además, las poblaciones no difirieron en rasgos relacionados con el uso del agua tales como EUA_i, el potencial hídrico de mediodía y la extracción de agua del suelo a diferentes profundidades.

Asimismo se detectó una escasa diferenciación genética en EUA_i entre poblaciones de *P. sylvestris*. Sin embargo, la variación de EUA_i, en rodales naturales, determinada principalmente por el ajuste plástico a nivel espacial y temporal, fue considerable y mucho mayor que la variación genética en esta especie. Esto sugiere una mayor importancia de la plasticidad frente la adaptación genética como factor responsable de la variación fenotípica en *P. sylvestris* para EUA_i. Además, datos obtenidos mediante satélites mostraron que la variación plástica individual en EUA_i afectó a la eficiencia del uso del agua a nivel del ecosistema en rodales monoespecíficos regulares de la especie.

En su conjunto, esta tesis proporciona una visión de la variación adaptativa intraespecífica de rasgos fenotípicos clave en tres importantes coníferas mediterráneas con nichos ecológicos diferentes. En el contexto del cambio climático actual, esta información es crucial para comprender la dinámica futura de estas especies. En un escenario próximo de reducida disponibilidad de agua en la región mediterránea, el establecimiento de individuos adaptados a la sequía mediante la selección *in-situ* o el flujo genético desde otras poblaciones tendrá un rol fundamental en la persistencia de *P. halepensis*. Por otro lado, la falta de evidencias de diferenciación genética en rasgos relacionados con el uso de agua sugiere que, probablemente, la distribución futura de *P. nigra* y *P. sylvestris* en la cuenca del Mediterráneo dependerán del grado de plasticidad fenotípica en estas especies y de la colonización de áreas más húmedas.

Además, los resultados de esta tesis subrayan el uso de imágenes derivadas de UAVs como potenciales herramientas de fenotipado masivo en especies forestales, destacando la información que se puede obtener con esta metodología. Las diferentes metodologías desarrolladas en este trabajo se describen en detalle en la tesis, destacando los pros y contras del uso de UAVs para el fenotipado de especies forestales.

RESUM

L'adaptació in-situ de les espècies arbòries està determinada, en el context del canvi climàtic, per la variació genètica intraespecífica i per la plasticitat fenotípica, fenòmens que es poden estudiar avaluant múltiples poblacions en assaigs genètics. Per a aquest propòsit, les noves tecnologies permeten la caracterització ecofisiològica d'arbres adults i poden millorar la nostra capacitat de desxifrar patrons de variació adaptativa en espècies forestals, proporcionant informacions fonamentals per pronosticar la seva capacitat de fer front als canvis ambientals.

En aquesta tesi, es van estudiar patrons de variació genètica intraespecífica en caracters funcionals de *Pinus halepensis* Mill., *Pinus nigra* Arnold i *Pinus sylvestris* L., tres coníferes d'importància socioeconòmica típiques de la conca mediterrània i caracteritzades per ocupar nínxols ecològics diferents. La variabilitat en les condicions de desenvolupament dins la distribució geogràfica de cada espècie ha determinat la diferenciació intraespecífica en trets funcionals i en estratègies vitals, una variació que, però, segueix sent en gran part inexplorada. Per analitzar l'abast de la diferenciació intraespecífica en aquests pins, es van caracteritzar arbres adults en tres assaigs genètics. Un conjunt de tècniques de fenotipat ben establertes van ser combinades amb dades de teledetecció obtingudes amb càmeres RGB, multiespectrals i tèrmiques muntades en un vehicle aeri no tripulat (*unmanned aerial vehicle*, UAV). En el cas de *P. sylvestris*, la variació genètica en el creixement i en l'eficiència intrínseca de l'ús de l'aigua (EUA_i) es va comparar amb el grau de diferenciació plàstica detectada en poblacions naturals.

Les imatges d'UAV van indicar una diferenciació genètica significativa en paràmetres relacionats amb l'àrea foliar i transpiració estival entre poblacions de *P. halepensis*, que es va associar amb la variació en la taxa de creixement. Combinant aquesta informació amb dades ja disponibles, es va detectar una clara divergència intraespecífica en les estratègies adaptatives d'aquest pi, determinada per la variació en la disponibilitat d'aigua i l'ocurrència d'incendis dins la distribució geogràfica de l'espècie. Poblacions amb un ràpid creixement caracteritzades per una extensa àrea foliar, escassa profunditat d'arrelament i alta transpiració estival es van diferenciar de poblacions adaptades a la sequera, caracteritzades per una taxa de creixement lenta, transpiració reduïda, arrelament profund i alta inversió en reproducció i acumulació de reserves.

Mitjançant el desenvolupament d'una metodologia per a la recol·lecció semiautomàtica de dades individualitzades a partir d'imatges aèries, la variació fenotípica entre individus de *P. halepensis* es va associar a la variació genòmica en loci SNP (*Single Nucleotide Polymorphism*).

Aquesta associació va proporcionar informació en relació a la base molecular de la diferenciació fenotípica en aquesta espècie.

En *P. nigra*, es va detectar variació genètica apreciable entre les poblacions en caracters de creixement, acumulació de reserves, eficiència fotosintètica i àrea foliar. Les principals causes d'aquesta variació van ser les temperatures mínimes anuals i la continentalitat, de manera que les poblacions que experimenten condicions hivernals més severes van presentar un aparell fotosintètic més eficient, un creixement lent i una alta acumulació de reserves. D'altra banda, la disponibilitat d'aigua va tenir una importància marginal com a impulsor de la variació genètica adaptativa en aquesta espècie. A més, les poblacions no van diferir en trets relacionats amb l'ús de l'aigua, com EUA_i, potencial hídric en fust i patrons d'arrelament.

De la mateixa manera, es va detectar una petita diferenciació genètica en EUA_i entre poblacions de *P. sylvestris*. No obstant això, la variació en EUA_i en rodals naturals d'aquesta espècie, principalment determinada per l'ajust plàstic a nivell espacial i temporal relacionat amb la capacitat de retenció d'aigua del sòl, va ser considerable i molt més gran que la variació genètica, indicant una major importància de la plasticitat sobre la variació genètica com a determinant de canvis fenotípics en *P. sylvestris* per EUA_i. A més, la variació plàstica individual en EUA_i va afectar l'eficiència de l'ús de l'aigua a nivell de l'ecosistema en rodals monoespecífics regulars de l'espècie, com indiquen les dades extretes de satèl·lits.

En conjunt, aquesta tesi ha proporcionat una visió de la variació adaptativa intraespecífica en trets fenotípics de tres importants coníferes mediterrànies caracteritzades per ocupar nínxols ecològics diferenciats. En el context del canvi climàtic en curs, aquesta informació és crucial per comprendre la dinàmica futura (expansió o contracció) de la distribució d'aquestes espècies. En un escenari futur d'una reduïda disponibilitat d'aigua a les regions mediterrànies, la selecció natural in situ d'individus adaptats a la sequera o la migració de poblacions probablement jugaran un paper fonamental en l'adaptació de *P. halepensis*. D'altra banda, la manca d'evidències de diferenciació genètica en caracters relacionats amb la resistència a la sequera suggereix que la persistència i distribució futura de *P. nigra* i *P. sylvestris* a la conca del Mediterrani dependran probablement del grau de plasticitat fenotípica d'aquestes espècies i de la colonització de zones de major altitud o més humides.

A més, els resultats d'aquesta tesi donen suport a l'ús d'imatges derivades d'UAVs com a eina de fenotipat en espècies forestals, destacant-ne la variada informació que es pot obtenir amb aquesta eina. Les diferents metodologies desenvolupades en aquest treball es descriuen en detall a la tesi, emfatitzant els avantatges i inconvenients de l'ús d'UAV com a tècnica de fenotipat d'espècies forestals.

GENERAL INTRODUCTION

BACKGROUND

Forest ecosystems cover a large part of our planet, greatly influencing a wide range of processes from local to global scales (Melillo *et al.,* 2013). Forests are fundamental actors in water and carbon cycles and are tightly linked to soil and nutrient dynamics. They also retain a large part of Earth's biodiversity and, ultimately, they provide countless ecosystem services with enormous economic and social implications (Gibbson *et al.,* 2000). However, forest ecosystems are currently threatened by environmental changes directly and indirectly induced by human activities. Among those, the ongoing climate change is one of the main factors altering forest dynamics worldwide (Bonan, 2008). Global warming impacts on the distribution of forest species, resulting in range shifts and local extinctions that are difficult to forecast (Aitken *et al.,* 2008; Chen *et al.,* 2011). The results of these changes may dramatically alter forest dynamics and processes, producing unpredictable impacts on ecosystems and, also, on human societies.

Across the Mediterranean basin, water availability is the main limiting factor for forest development. Under the current scenario of a global temperature increase of 1.5-2 °C by the end of this century (Hoegh-Guldberg *et al.,* 2018), models predict a reduction in precipitation up to 40% in some areas of the Mediterranean basin, although with large variability at local scale (Giorgi and Lionello, 2008). In this context, the main challenge that Mediterranean forests will likely have to face is an increment in extreme and prolonged drought events, which may result in increasing episodes of drought-induced forest diebacks, as already reported (Allen *et al.,* 2010; Sánchez-Salguero *et al.,* 2010; Camarero *et al.,* 2017). Indeed, prolonged droughts can directly exacerbate tree mortality through carbon starvation and hydraulic failure (Wang *et al.,* 2012) and, at the same time, they can indirectly affect forest survival through the intensification of pests occurrence and severity (Allen *et al.,* 2010; Jactel *et al.,* 2012). Moreover, a further disturbance affecting forest dynamics in Mediterranean ecosystems is the variation in forest fire regimes associated with climate change (Pausas, 2004). Fire is a main ecological factor in Mediterranean forests, shaping species distribution and dynamics (Pausas, 2015). However, the current increasing trend towards more recurrent and larger fires may alter the composition of Mediterranean forests impacting on long-term survival of many species.

Altogether, Mediterranean ecosystems are facing large and multifaceted environmental transformations which will likely affect species distribution and may threaten, in some cases, forest survival. With the accumulating evidence of global warming effects on forest ecosystems,

disentangling the ability of forest species to handle such environmental changes has turned into a priority in forest ecology (Guittar *et al.,* 2016).

PHENOTYPIC PLASTICITY AND GENETIC ADAPTATION

Apart from migration to more suitable areas, tree populations can respond to environmental changes through phenotypic plasticity and genetic adaptation (Nicotra *et al.,* 2010; Benito Garzón *et al.,* 2011). Phenotypic plasticity is defined as the amount of phenotypic variation expressed by an individual genotype in response to different growing conditions (Bradshaw, 1965, 2006). In other words, plasticity is the ability of individuals to quickly adjust their phenotype when experiencing changes in environmental conditions. Considering tree populations instead of single individuals, phenotypic plasticity refers to the arrays of phenotypes that individuals with a common genetic background (i.e. belonging to genetically homogenous populations) can show in response to different environmental conditions. Morpho-physiological plasticity has a marked adaptive value especially in the case of sessile organisms such as trees, allowing individuals and populations to cope with environmental changes up to a threshold in which variation in environmental factors exceeds the ability of trees to adjust their phenotypes (Valladares *et al.,* 2014). Indeed, phenotypic plasticity in phenology, leaf traits and growth (among others) have been described in tree populations as adaptive mechanism to cope with environmental changes (e.g.; Kramer, 1995; dosAnjos *et al.,* 2015; Gárate-Escamilla *et al.,* 2019).

Phenotypic plasticity allows individuals to adjust their phenotype in an order of time spanning from seconds to years, depending on the considered trait. On the other hand, environmental cues act across much longer time periods as forces selecting genotypes that perform better under particular conditions. The primary result of this process is inter-specific differentiation, which leads to species-specific adaptation to particular ecological niches. However, selective pressures varying within the distribution range of single species also generate variation in functional traits at the intra-specific level (Alberto *et al.,* 2013). This is particularly true in the case of tree species whose distribution ranges frequently embrace a wide variety of habitats. Indeed, intra-specific genetic variation has been widely reported in many forest species for phenotypic traits including growth and survival (Kleinschmit, 1993; Kobe, 1996), reproductive effort (Climent *et al.,* 2008), water use (Voltas *et al.,* 2015), leaf traits (Forey *et al.,* 2016) or wood anatomy (Hajek *et al.,* 2016), among others. This variation shapes the functional adaptations of populations and their capacity to thrive in particular environments (Bussotti *et al.,* 2015). In this regard, intra-specific genetic variation is also crucial for adaptation to new

environmental conditions. Following the standard postulates of evolutionary theory, standing variation within the genetic pool of a species retains the potential for species adaptation in a changing world (Bolnick *et al.*, 2011). Intra-specific genetic variation in morpho-physiological functional traits is therefore a key player in forest functioning and responses in the context of ongoing global warming (Benito Garzón *et al.*, 2011; Guittar *et al.*, 2016).

A further aspect that must be taken into account in the analysis of adaptation of forest trees is that intra-specific genetic variation among populations is usually not limited to one or few traits. Indeed, adaptive variation is often driven by environmental cues impacting on different functional traits, resulting in phenotypic co-variation between life-history traits (mainly growth, reproduction, defence and survival). Moreover, the allocation of resources to a particular plant compartment or physiological process impacts on the overall economy of a tree, generating an ulterior constrain on the variation of single traits (Milla and Reich, 2011). This co-variation is known as phenotypic integration or, at the intra-specific level, as evolutionary integration, and defines the disposition of several traits to evolve jointly during the divergence of populations (Armbruster *et al.*, 2014). As a result of this process, contrasting life strategies often characterise different populations of the same species. If high quality data on intra-specific variation in several traits are available, disentangling patterns of phenotypic integration can therefore help to understand the adaptive strategies that different populations embrace – or could embrace under environmental changes – to face specific constraints (Murren, 2002).

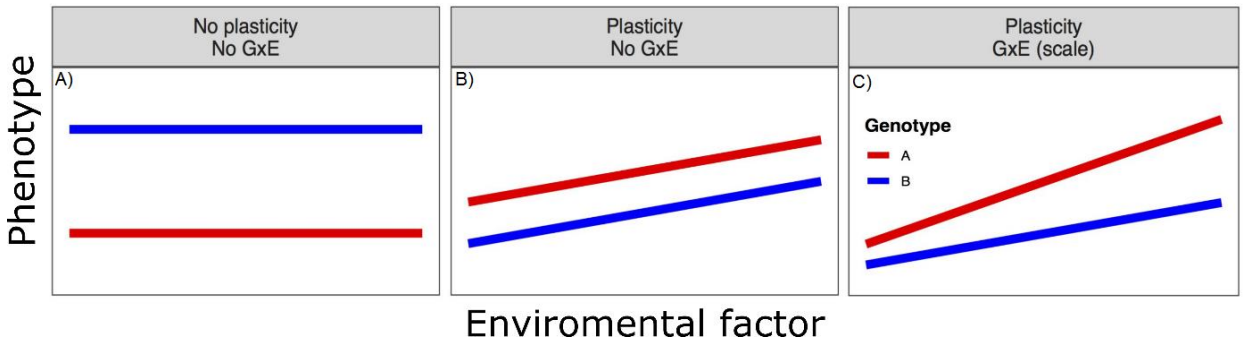

Figure 1. Modified from Kusmec *et al.* (2018). Intra-specific genetic variation results in phenotypic differences among genotypes, which is constant across environments in absence of phenotypic plasticity (A). In the presence of plastic responses, genotypes express different phenotypes across different environments. The extent of phenotypic plastic variation can be constant (B) or, in case of genetic variation in plasticity, variable across genotypes (C).

COMMON GARDEN EXPERIMENTS

As already stressed, phenotypic plasticity and genetic variation concur as partially independent processes determining phenotypic variation at the intra-specific level (Bradshaw, 1965). However, differentiating plastic and genetic components simultaneously influencing phenotypic variation is not an easy task. Moreover, the extent of phenotypic plasticity is also under genetic control, resulting in intra-specific variation of phenotypic adjustment among populations of the same species (Bradshaw, 2006).

Generally, common garden experiments are used to test the nature and magnitude of genetic and plastic components shaping phenotypic differences among populations (Kusmec *et al.*, 2018). Trees originating from populations growing in contrasting environments can be planted in semi-natural conditions in common garden experiments (Mátyás, 1996; de Villemereuil *et al.*, 2016). Under the same growing conditions, phenotypic variation among trees or populations is mainly due to genetic differentiation, with variation related to plastic adjustments of phenotypes to possible intra-trial variation in growing conditions being accounted in the experimental design. Relevant phenotypic differences among populations in a single common garden are therefore usually interpreted as indicative of the genetic basis of phenotypic variation, i.e. intra-specific genetic variation (Mátyás, 1996). On the other hand, the performance of the same set of populations can be assessed in replicated common gardens across different environments (i.e. multi-environment trials). In this case, phenotypic differences recorded for a specific population in different environments are indicative of plastic variation. Finally, the interaction between population and site effects in a multi-environment trial provides an estimation of genetic variation in phenotypic plasticity among populations (Li *et al.*, 2017).

Although common gardens have been established for many forest species, there is a poor availability of multi-environmental trials allowing the partitioning of genetic and plastic effects in phenotypic traits of Mediterranean tree species. Even though relevant exceptions exist (e.g. Klein *et al.*, 2013; di Matteo and Voltas, 2016; Voltas *et al.*, 2018; Sbay and Zas, 2018), multi-environmental trials are often extremely unbalanced with regard to the populations involved, thus preventing a straightforward measurement of phenotypic plasticity. On the other hand, common garden experiments have been largely employed to evaluate intra-specific genetic variation in tree performance. This information has been used for long time to choose the best genetic material for reforestations or timber production (Mátyás, 1996). In the last two decades, however, the interest in common garden experiments have shifted from mere silvicultural purposes to the study of evolutionary adaptation of tree populations to environmental conditions, primarily to climate (Mátyás, 1994; Carter, 1996). This approach has revealed a wide range of

intra-specific genetic differentiation in numerous forest species, providing insights to the distribution of adaptive variation among populations and being nowadays the standard methodology for studying intra-specific genetic variation (Bussotti *et al.*, 2015).

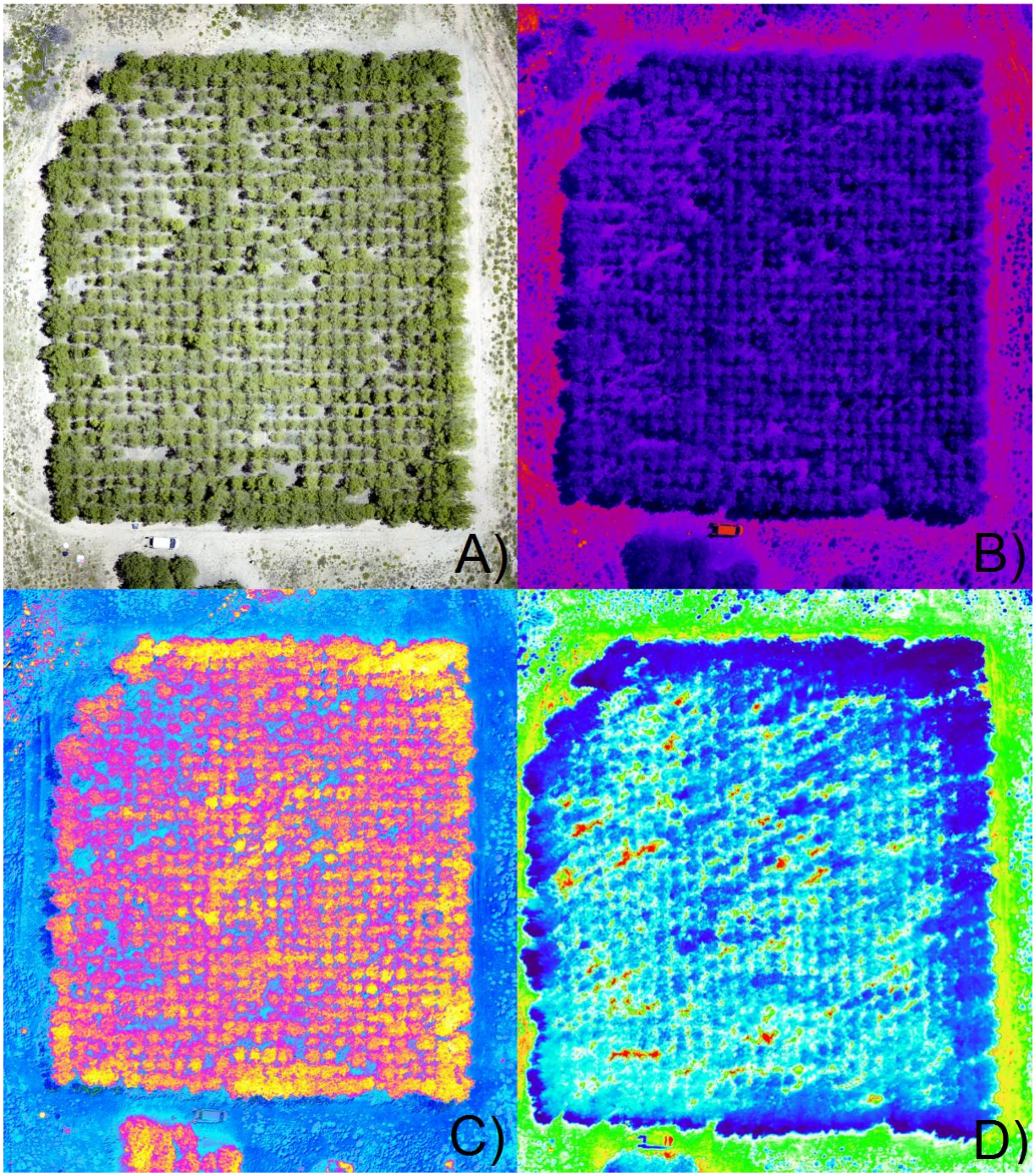

Figure 2. Aerial images of a common garden test of *Pinus halepensis* in Altura, central Spain. A) RGB image, B) infrared image, C) NDVI image and D) thermal image.

UAV IMAGERY FOR TREE-LEVEL PHENOTYPING

A major limitation when studying adaptation in forest trees in terms of their functional variability is related to the difficulties for obtaining meaningful phenotypic data for a representative number of individuals, an issue that is particularly evident in the case of adult trees (Ludovisi *et al.*, 2017). For this reason, many studies investigating patterns of adaptive variation in common garden experiments are carried out at the seedling or juvenile stage, when data collection is easier (Mátyás, 1996). However, this approach results in a limited characterisation of phenotypic variation in organisms with a lifespan of decades or centuries.

In this regard, the rapid development of new technologies can assist to overcome the issue of effective phenotyping for a relevant number of trees (Colaço *et al.*, 2018; Ampatzidis *et al.*, 2019). Developed in the context of the genetic improvement of crop and fruit species, the so-called high-throughput phenotyping techniques are rapidly spreading as effective tools for studying phenotypic variation in economically relevant plants (Araus and Cairns, 2014; Araus *et al.*, 2018). Among the vast array of new technologies for vegetation characterisation, the use of remote sensing data derived with Unmanned Aerial Vehicles (UAVs) has had a particular success in the field of forest sciences (Dash *et al.*, 2016). UAVs are cost-effective tools which can be equipped with different cameras and sensors to record images in a wide range of wavelengths (Fahlgren *et al.*, 2015; Sankaran *et al.*, 2015). RGB (red, green, blue) images can be used for implementing structure-from-motion 3D reconstructions of trees and to retrieve morphological data such as stem diameter, tree height or crown surface (Ota *et al.*, 2015; Iglhaut *et al.*, 2019). Differences in the reflectance at specific wavelengths are recorded with multispectral cameras and provide information on a range of processes, including phenology, forest decay, spreading of pathogens, and tree variation in leaf area and photosynthetic pigments (Roberts *et al.*, 2016; Torresan *et al.*, 2017). Thermal cameras are also used to retrieve canopy temperature, which provides information of tree water status (Gonzalez-Dugo *et al.*, 2013; Ludovisi *et al.*, 2017). The advantages of UAVs imagery in monitoring forest ecosystems are related to the high spatial and temporal resolution at which data can be obtained, which allows the retrieval of records on an individual basis (Gambella *et al.*, 2016). Images taken with cameras mounted on UAVs can have a spatial resolution varying from dozens of centimetres to less than 1 cm, depending on the sensor that is used and on flight height. Moreover, UAVs can be used to collect data with a daily or even hourly temporal resolution, which are of particular importance when studying phenomena such as disease spread, phenology or forest fires, among others (Torresan *et al.*, 2017).

Altogether, the flexibility in terms of spatial and temporal resolution and the wide variability of sensors that can be employed have made UAV imagery a powerful and cost-effective tool that can be easily adapted to a vast range of studies in forest sciences (Torresan *et al.,* 2017). However, a field that has remained unexplored is the suitability of UAV-derived imagery in analysing phenotypic variation in common gardens of forest species. On the other hand, UAV images have been successfully employed to evaluate phenotypic variation among varieties of crops or in fruit orchards (Candiago *et al.*, 2015; Sankaran *et al.*, 2015). Based on these results, UAV imagery is a promising tool to evaluate variation among trees populations tested in common garden experiments, thus representing a possible cost-effective technique to study adaptive variation in forest species.

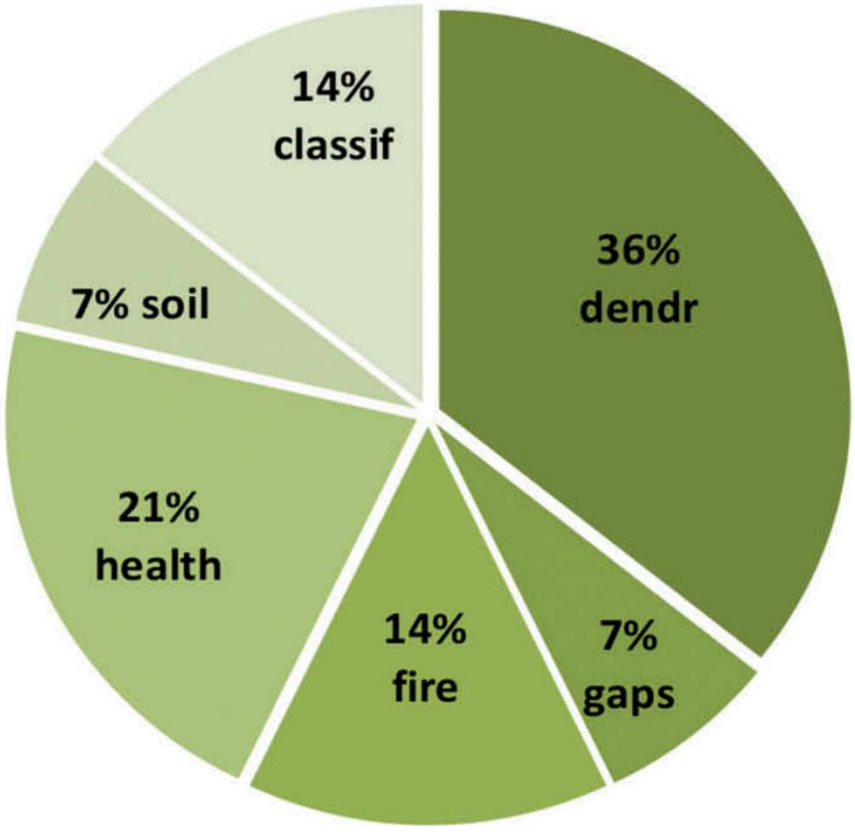

Figure 3. Modified from Torresan *et al.* (2017). Percentages of studies involving UAVs to different applications in European forests. UAVs imagery has been used to perform dendrometric measurements, forest classification and gap quantification, and also to assess forest health status, monitor forest fires and to study soil proprieties.

GENOTYPE-PHENOTYPE ASSOCIATION

Passing from populations to the individual tree perspective, a further possible application of UAV-based phenotyping in provenance trials is the study of genotype-phenotype associations to provide insights into the genetic basis of adaptation (Houle *et al.,* 2010; Großkinsky *et al.,* 2015). Indeed, the last few years have witnessed an increasing availability of cost-effective genotyping tools rising probably faster than the development of high-throughput phenotyping technologies. Nowadays, the genetic characterisation of several individuals at numerous genetic markers is possible even for non-model species such as forest trees. The result of this process is the increasing number of genome-wide association studies (GWAS) in forest species. These studies correlate phenotypic traits with genotypic variation across hundreds of individuals and genomic loci, aiming at understanding the genetic basis of phenotypic differentiation (Araus *et al.,* 2018).

The most commonly used markers in these studies are Single Nucleotide Polymorphisms (SNPs), that is, loci in which the genetic code varies among individuals only at a single nucleotide in a specific genomic position. Each variation in a SNP locus is present at a certain frequency in the species, allowing the study of the possible association between SNP variation and phenotype of individuals. SNPs whose variation is found to be associated with phenotypic differentiation can be located in proximity to genetic polymorphism causing the phenotypic variation or can be quantitative trait nucleotides themselves (i.e. single polymorphism influencing phenotype). This approach has been used to disentangle the genetic basis of phenotypic variation in forest trees (Khan and Korban, 2012; Jaramillo-Correa *et al.,* 2016). However, a prerequisite for the application of GWAS is the availability, together with genotypic data, of accurate phenotyping information. In this regard, UAV imagery as phenotyping tool of common gardens can assist to narrow the knowledge gap in genotype-phenotype association studies in forest trees.

SATELLITES

Dating back to the 1970s and far before the advent of UAV imagery, remote sensing data derived from Earth monitoring satellites have been employed for studying forest dynamics (Boyd and Danson, 2005). Nowadays, the continuous increase in freely available satellite data with high spatial and temporal resolution has made possible the assessment of cover and composition of forests along with a wide range of their biophysical properties, including health, productivity and fires occurrence (Wang *et al.,* 2010).

Differences between satellite and UAV-based remote sensing monitoring are related to the geographical areas that can be covered and the spatial resolution that can be obtained (Pádua

et al., 2017). UAV flights can generate high resolution images suitable for tree-level assessments, but limited to the restricted geographical area than can be covered in a single flight. On the other hand, satellite images are available for much larger land extensions, virtually covering all Earth surface. Although the spatial resolution of these data is yet not enough to allow tree-level analysis, satellite remote sensing data are suitable for monitoring a wide array of processes at the ecosystem level.

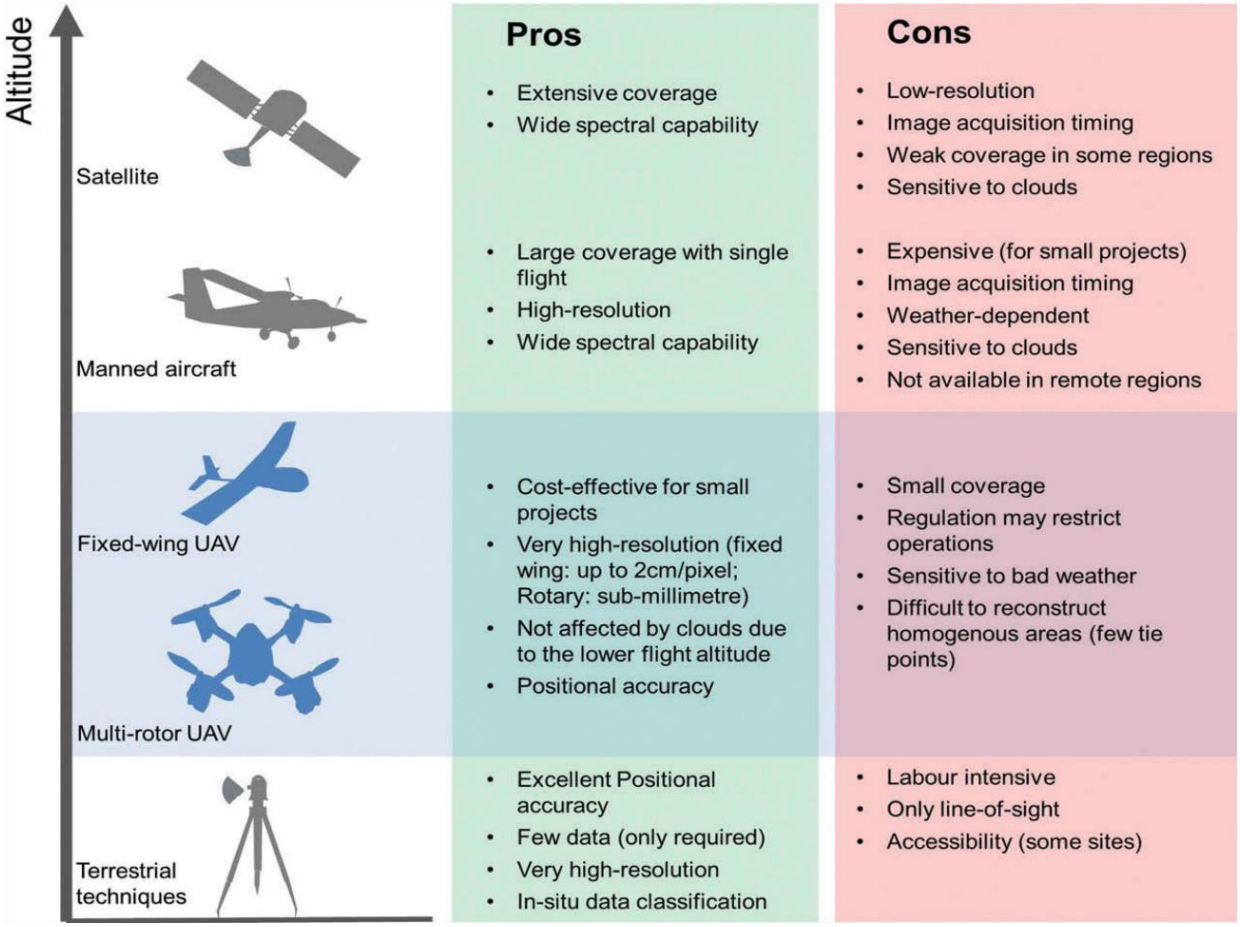

Figure 4. From Pádua *et al.* (2017). Pros and cons of different existing remote-sensing technologies compared to terrestrial phenotyping tools. UAV imagery provides very high-resolution but small area coverage, while satellite data are suitable for monitoring large surfaces.

MEDITERRANEAN PINES

The worldwide-distributed *Pinus* genus comprises about 120 species that colonize a variety of environments, ranging from semi-arid areas to rainforests and from sea level to high mountain ecosystems (Richardson, 2000). Ten pines species are naturally occurring around the Mediterranean basin where they provide fundamental ecosystem services reflected in their important socio-economic value (Klaus, 1989; Barbéro *et al.*, 1998). Among these species, *Pinus halepensis* (Mill.), *Pinus nigra* (Arnold) and *Pinus sylvestris* (L.) constitute a significant part of the Iberian Peninsula forests and, also, of other regions of the central-western part of the Mediterranean basin. These pines occupy different ecological niches and are adapted to extremely variable environments. *P. halepensis* characterises coastal and low altitude forests in the Iberian, Italian and Balkan peninsulas and in North Africa. Broadly speaking, this species shows considerable morpho-physiological adaptations to drought and forest fires typically found in Mediterranean environments (Barbéro *et al.*, 1998). Such adaptations include, among others, a strong regulation of water loss through stomatal regulation, an efficient hydraulic system, and, in relation to forest fire, a thick bark, cone serotiny and short-life cycles (Schiller, 2000; Tapias *et al.*, 2004). Although pines can be generally considered drought-avoidant species (Irvine *et al.*, 1998), coastal pines (e.g. *Pinus halepensis*, *P. pinea*) are substituted at medium elevation by species less resistant to drought. Among those, *P. nigra* plays a primary role in many medium-altitude Mediterranean mountain forests, being distributed from the Iberian Peninsula to Anatolia. This species is more susceptible to summer drought than coastal pines, showing, on the other hand, adaptation to cold stress (Climent *et al.*, 2009; Matías *et al.*, 2017). High mountain forests of the central-western Mediterranean basin are characterised by the presence of the Eurosiberian species *P. sylvestris*, which is a species typical of boreal forests of Europe and Asia but that is also present in Mediterranean mountains with its southernmost populations (Durrant *et al.*, 2016).

Although inter-specific differentiation shapes adaptation to a particular range of environmental conditions for a given species, it is worth noting that the populations of a species can also be found in very contrasting environments. As an example, populations of *P. halepensis* grow from semi-arid (i.e. less than 400 mm of annual precipitation) to humid (up to 1000 mm of precipitation) environments across the Mediterranean basin (Mauri *et al.*, 2016). As a result, an appreciable intra-specific variation in many adaptive traits is present among populations of Mediterranean pines. Indeed, data from common garden experiments show that low-altitude species such as *P. halepensis* are characterised by intra-specific differentiation in traits related to water use and fire resistance, including water uptake patterns (Voltas *et al.*, 2015), hydraulic

conductivity (Tognetti *et al.,* 1997), stomatal regulation (Klein *et al.,* 2013) and cone serotiny (Hernández-Serrano *et al.,* 2014) among others. In mountain species (i.e. *P. nigra* and *P. sylvestris*) intra-specific variation in water use is less evident, while populations of these species are characterised by variation in other traits such as cold resistance (Kreyling *et al.,* 2012), nutrient acquisition (Oleksyn *et al.,* 2003) or phenology (Notivol *et al.,* 2007).

Disentangling the extent and nature of intra-specific adaptive variation in Mediterranean pines is a current issue for understanding their potential to adapt to ongoing environmental changes. Climate change is indeed impacting on the natural dynamics of Mediterranean pine forests, with effects that are difficult to forecast (Benito Garzón *et al.,* 2008). In this regard, key information on the distribution of intra-specific adaptive variation is lacking for many pine species typical of forests around the Mediterranean basin. Although common garden experiments have been established for many of these species to study intra-specific genetic variation, information is widely available only for few phenotypic traits (e.g. growth or survival) and many studies have been performed at juvenile stages. This lack of information is a serious limitation for understanding the ability of Mediterranean pines to cope with environmental changes, and studies investigating adaptive variation in meaningful traits at adult stage are urgently needed (Alberto *et al.,* 2013; Bussotti *et al.,* 2015).

OBJECTIVES OF THIS THESIS

The main objective of this thesis is to characterise patterns of adaptive variation among populations of *P. halepensis* (Aleppo pine), *P. nigra* (European Black pine) and *P. sylvestris* (Scots pine), three widely distributed pine species which occupy contrasting ecological niches respectively at low, medium and high altitudes in the central-western part of the Mediterranean basin. For this purpose, three common gardens were investigated, each testing populations of one species. In this regard, a second general goal of the thesis is to evaluate the suitability of UAV-derived remote sensing data as phenotyping tool in common gardens of forest species and to develop a straightforward methodology for retrieving phenotyping data from UAV imagery. Specifically, the general objectives of the thesis are:

Objective 1. To characterise intra-specific genetic variation (Chapters 1-5) and phenotypic plasticity (Chapter 5) in relevant functional traits as determinants of phenotypic variation among populations of three Mediterranean pines occupying divergent ecological niches.

Objective 2. To identify environmental drivers of phenotypic variation in relevant functional traits in relation to the different constrains that each species faces across its distribution range (Chapters 2, 4 and 5).

Objective 3. To assess the use of high resolution images obtained with UAVs for characterising morpho-physiological features of populations of Mediterranean pines growing in common garden experiments (Chapters 1 to 4).

Besides these general goals which are transversal to many chapters of the thesis, specific objectives developed in single chapters are:

Objective 4. To investigate the presence of divergent ecological strategies among populations of Aleppo pine, as the results of intra-specific variation (Chapter 1) and phenotypic integration (i.e. co-variation) in functional traits (Chapter 2).

Objective 5. To study the genetic basis of phenotypic differentiation in *P. halepensis* by coupling high-throughput genotypic information and phenotypic data (Chapter 3).

Objective 6. To investigate intra-specific variation in functional traits and contrasting adaptive strategies among populations of *P. nigra* by combining standard phenotypic approaches and UAV imagery (Chapter 4).

Objective 7. To investigate intra-specific variation in growth and water use-efficiency in *P. sylvestris* and to compare the extent of this variation to differences detected among natural populations and related to plastic responses (Chapter 5).

Objective 8. To assess the possible influence of tree-level variation in functional traits on ecosystem processes by scaling-up the extent of phenotypic variation in *P. sylvestris* populations from individual to ecosystem level through remote sensing satellite data (Chapter 5).

THESIS OVERVIEW AND ORGANIZATION

This thesis is organised in five chapters. Chapters 1 to 4 focus exclusively on intra-specific genetic variation of adaptive traits in *P. halepensis* (Chapters 1 to 3) and *P. nigra* (Chapter 4), respectively. In the case of Aleppo pine, the availability of high-quality phenotypic and

genotypic data obtained in the common garden of this species allowed not only to investigate intra-specific genetic variation in adaptive traits, but also to test for phenotypic integration between different traits and to study the association between genotypic and phenotypic differentiation. In the case of *P. sylvestris* (Chapter 5), the study was focused not only on intra-specific genetic variation, but it also analysed the extent of phenotypic plasticity for the considered traits. Specifically:

In Chapter 1, I used UAV imagery to analyse intra-specific genetic variation in leaf area, photosynthetic pigments and transpiration among 56 populations of *P. halepensis* growing in a common garden experiment. To this end, I developed a methodology to obtain phenotypic data at plot level from RGB, multispectral and thermal images, which were used to retrieve vegetation indices and canopy temperature as surrogates of meaningful phenotypic traits.

In Chapter 2, I combined the information obtained in Chapter 1 with already available phenotypic data (i.e. records of growth, reproductive effort, rooting patterns and accumulation of non-structural carbohydrates) collected in the same common garden. This information was used to develop a Structural Equation Model which tested for phenotypic integration of 11 traits among 56 populations of Aleppo pine.

In Chapter 3, I performed a genetic wide association study (GWAS) to analyse the genetic basis of phenotypic variation in *P. halepensis*. To this purpose, I developed a methodology for the automatic identification of tree crowns in UAV images of the common garden in order to automatically obtain individual tree phenotypic records. These data were combined with the genotypes of the individuals at 235 SNPs loci, in order to analyse the association of particular phenotypes with genetic variation in specific areas of the pine genome.

In Chapter 4, I studied the intra-specific genetic variation in growth, reserves accumulation, intrinsic water use efficiency (WUE_i), rooting patterns, leaf area and photosynthetic pigments among 18 populations and four subspecies of *P. nigra* growing in a common garden. To this purpose, I combined well-established phenotyping techniques (i.e. analysis of non-structural carbohydrates in wood, carbon stable isotopes in cellulose, and oxygen and hydrogen isotopes of xylem water) with UAV images to phenotype adult individuals growing in the trial.

Finally, in Chapter 5 I used a third common garden to analyse intra-specific genetic variation in growth and WUE_i among 22 populations of *P. sylvestris.* In this latter case, the poor maintenance and the non-homogenous growing conditions of the trial prevented the use of UAV imagery and limited the phenotypic traits that could be analysed. Moreover, the genetic differentiation in growth and WUE was found to be very low among populations tested in the

trial (see Chapter 5 for details). For this reason, I compared the levels of differentiation observed in the trial (i.e. intra-specific genetic variation) with the spatial and temporal variation in growth and WUE found in (approximately) genetically homogenous natural populations of *P. sylvestris*, as indicative of phenotypic plasticity in these traits. Finally, the phenotypic variation in WUE detected in natural stands of *P. sylvestris* was up-scaled to ecosystem level water use efficiency using high-resolution satellite images.

REFERENCES

Aitken S.N., Yeaman S., Holliday J.A., Wang T., Curtis-McLane S. (2008) Adaptation, migration or extirpation: climate change outcomes for tree populations: climate change outcomes for tree populations. *Evolutionary Applications*, 1, 95–111.

Alberto F.J., Aitken S.N., Alía R., González-Martínez S.C., Hänninen H., Kremer A., Lefèvre F., Lenormand T., Yeaman S., Whetten R., Savolainen O. (2013) Potential for evolutionary responses to climate change - evidence from tree populations. *Global Change Biology*, 19, 1645–1661.

Allen C.D., Macalady A.K., Chenchouni H. *et al.* (2010) A global overview of drought and heat-induced tree mortality reveals emerging climate change risks for forests. *Forest Ecology and Management*, 259, 660–684.

Ampatzidis Y., Partel V., Meyering B., Albrecht U. (2019) Citrus rootstock evaluation utilizing UAV-based remote sensing and artificial intelligence. *Computers and Electronics in Agriculture*, 164, 104900.

Araus J.L., Cairns J.E. (2014) Field high-throughput phenotyping: the new crop breeding frontier. *Trends in Plant Science*, 19, 52–61.

Araus J.L., Kefauver S.C., Zaman-Allah M., Olsen M.S., Cairns J.E. (2018) Translating high-throughput phenotyping into genetic gain. *Trends in Plant Science*, 23, 451–466.

Armbruster W.S., Pelabon C., Bolstad G.H., Hansen T.F. (2014) Integrated phenotypes: understanding trait covariation in plants and animals. *Philosophical Transactions of the Royal Society B: Biological Sciences*, 369, 20130245–20130245.

Barbéro M., Loisel R., Quézel P., Richardson D.M., Romane F. (1998). Pines of the Mediterranean basin. In Richardson D.M. (eds) *Ecology and Biogeography of Pinus*, pp. 153-170.

Benito Garzón M., Sánchez de Dios R., Sainz Ollero H. (2008) Effects of climate change on the distribution of Iberian tree species. *Applied Vegetation Science*, 11, 169–178.

Benito Garzón M., Alía R., Robson T.M., Zavala M.A. (2011) Intra-specific variability and plasticity influence potential tree species distributions under climate change: Intra-specific variability and plasticity. *Global Ecology and Biogeography*, 20, 766–778.

Bolnick D.I., Amarasekare P., Araújo M.S., Bürger R., Levine J.M., Novak M., Rudolf V.H.W., Schreiber S.J., Urban M.C., Vasseur D.A. (2011) Why intraspecific trait variation matters in community ecology. *Trends in Ecology and Evolution*, 26, 183–192.

Bonan G.B. (2008) Forests and climate change: forcings, feedbacks, and the climate benefits of forests. *Science*, 320, 1444–1449.

Boyd D.S., Danson F.M. (2005) Satellite remote sensing of forest resources: three decades of research development. *Progress in Physical Geography: Earth and Environment*, 29, 1–26.

Bradshaw A.D. (1965) Evolutionary significance of phenotypic plasticity in plants, *Advances in Genetics*, 13, 115–155.

Bradshaw A.D. (2006) Unravelling phenotypic plasticity ? Why should we bother? *New Phytologist*, 170, 644–648.

Bussotti F., Pollastrini M., Holland V., Brüggemann W. (2015) Functional traits and adaptive capacity of European forests to climate change. *Environmental and Experimental Botany*, 111, 91–113.

Camarero J.J., Linares J.C., Sangüesa-Barreda G., Sánchez-Salguero R., Gazol A., Navarro-Cerrillo R.M., Carreira J.A. (2017) The multiple causes of forest decline in Spain: drought, historical logging, competition and biotic stressors. In M.M. Amoroso, L.D. Daniels, P.J. Baker, and J.J. Camarero (eds.) *Dendroecology*, pp. 307–323. Cham: Springer International Publishing.

Candiago S., Remondino F., De Giglio M., Dubbini M., Gattelli M. (2015) evaluating multispectral images and vegetation indices for precision farming applications from uav images. *Remote Sensing*, 7, 4026–4047.

Carter K.K. (1996). Provenance tests as indicators of growth response to climate change in 10 north temperate tree species. *Canadian Journal of Forest Research*, 26, 1089-1095.

Chen I.-C., Hill J.K., Ohlemuller R., Roy D.B., Thomas C.D. (2011) Rapid range shifts of species associated with high levels of climate warming. *Science*, 333, 1024–1026.

Climent J., Prada M.A., Calama R., Chambel M.R., de Ron D.S., Alía R. (2008) To grow or to seed: ecotypic variation in reproductive allocation and cone production by young female Aleppo pine (*Pinus halepensis*, Pinaceae). *American Journal of Botany*, 95, 833–842.

Climent J., Costa e Silva F., Chambel M.R., Pardos M., Almeida M.H. (2009) Freezing injury in primary and secondary needles of Mediterranean pine species of contrasting ecological niches. *Annals of Forest Science*, 66, 407–407.

Colaço A.F., Molin J.P., Rosell-Polo J.R., Escolà A. (2018) Application of light detection and ranging and ultrasonic sensors to high-throughput phenotyping and precision horticulture: current status and challenges. *Horticulture Research*, 5, 35.

Dash J., Pont D., Brownlie R., Dunningham A., Watt M., Pearse, G. (2016) Remote sensing for precision forestry. *NZ Journal of Forestry*, 60, 15.

de Villemereuil P., Gaggiotti O.E., Mouterde M., Till-Bottraud I. (2016). Common garden experiments in the genomic era: new perspectives and opportunities. *Heredity*, 116, 249.

di Matteo G., Voltas J. (2016) Multienvironment evaluation of *Pinus pinaster* provenances: evidence of genetic trade-offs between adaptation to optimal conditions and resistance to the Maritime Pine Bast Scale (*Matsucoccus feytaudi*). *Forest Science*, 62, 553-563.

dosAnjos L., Oliva M.A., Kuki K.N., Mielke M.S., Ventrella M.C., Galvão M.F., Pinto L.R.M. (2015) Key leaf traits indicative of photosynthetic plasticity in tropical tree species. *Trees*, 29, 247–258.

Durrant T.H., De Rigo D., Caudullo G. (2016) *Pinus sylvestris* in Europe: distribution, habitat, usage and threats. *European atlas of forest tree species*, 132-133.

Fahlgren N., Gehan M.A., Baxter I. (2015) Lights, camera, action: high-throughput plant phenotyping is ready for a close-up. *Current Opinion in Plant Biology*, 24, 93–99.

Forey E., Langlois E., Lapa G., Korboulewsky N., Robson T.M., Aubert M. (2016) Tree species richness induces strong intraspecific variability of beech (*Fagus sylvatica*) leaf traits and alleviates edaphic stress. *European Journal of Forest Research*, 135, 707–717.

Gambella F., Sistu L., Piccirilli D., Corposanto S., Caria M., Arcangeletti E., Proto A.R., Chessa G., Pazzona A. (2016) Forest and UAV: a bibliometric review. *Contemporary Engineering Sciences*, 9, 1359–1370.

Gárate-Escamilla H., Hampe A., Vizcaíno-Palomar N., Robson T.M., Benito Garzón M. (2019) Range-wide variation in local adaptation and phenotypic plasticity of fitness-related traits in *Fagus sylvatica* and their implications under climate change. *Global Ecology and Biogeography*, 28, 1336–1350.

Gibson C.C., McKean M.A., Ostrom E. (eds.) (2000). *People and forests: Communities, Institutions, and Governance*. Mit Press.

Giorgi F., Lionello P. (2008) Climate change projections for the Mediterranean region. *Global and Planetary Change*, 63, 90–104.

Gonzalez-Dugo V., Zarco-Tejada P., Nicolás E., Nortes P.A., Alarcón J.J., Intrigliolo D.S., Fereres E. (2013) Using high resolution UAV thermal imagery to assess the variability in the water status of five fruit tree species within a commercial orchard. *Precision Agriculture*, 14, 660–678.

Großkinsky D.K., Svensgaard J., Christensen S., Roitsch T. (2015) Plant phenomics and the need for physiological phenotyping across scales to narrow the genotype-to-phenotype knowledge gap. *Journal of Experimental Botany*, 66, 5429–5440.

Guittar J., Goldberg D., Klanderud K., Telford R.J., Vandvik V. (2016) Can trait patterns along gradients predict plant community responses to climate change? *Ecology*, 97, 2791–2801.

Klaus W, Ehrendorfer F. (1989). Mediterranean pines and their history. In Ehrendorfer F. (eds) *Woody plants—evolution and distribution since the Tertiary*, pp. 133-163. Springer, Vienna.

Hajek P., Kurjak D., von Wühlisch G., Delzon S., Schuldt B. (2016) Intraspecific variation in wood anatomical, hydraulic, and foliar traits in ten European beech provenances differing in growth yield. *Frontiers in Plant Science*, 7.

Hernández-Serrano A., Verdú M., Santos-del-Blanco L., Climent J., González-Martínez S.C., Pausas J.G. (2014) Heritability and quantitative genetic divergence of serotiny, a fire-persistence plant trait. *Annals of Botany*, 114, 571–577.

Houle D., Govindaraju D.R., Omholt S. (2010) Phenomics: the next challenge. *Nature Reviews Genetics*, 11, 855–866.

Hoegh-Guldberg, O.D., Jacob D., Taylor M. et *al.* (2018) Impacts of 1.5ºC Global Warming on Natural and Human Systems. In First P.J. (eds.) *Global Warming of 1.5°C. An IPCC Special Report on the impacts of global warming of 1.5°C above pre-industrial levels and related global greenhouse gas emission pathways, in the context of strengthening the global response to the threat of climate change, sustainable development, and efforts to eradicate poverty* In Press.

Iglhaut J., Cabo C., Puliti S., Piermattei L., O'Connor J., Rosette J. (2019) Structure from Motion photogrammetry in forestry: a review. *Current Forestry Reports*, 5, 155–168.

Jactel H., Petit J., Desprez-Loustau M.L., Delzon S., Piou D., Battisti A., Koricheva J. (2012). Drought effects on damage by forest insects and pathogens: a meta-analysis. *Global Change Biology*, 18, 267-276.

Jaramillo-Correa J.P., Prunier J., Vázquez-Lobo A., Keller S.R., Moreno-Letelier A. (2015). Molecular signatures of adaptation and selection in forest trees. *Advances in Botanical Research*, 74, 265-306.

Khan M.A., Korban, S.S. (2012) Association mapping in forest trees and fruit crops. *Journal of Experimental Botany*, 63, 4045-4060.

Klein T., Di Matteo G., Rotenberg E., Cohen S., Yakir D. (2013) Differential ecophysiological response of a major Mediterranean pine species across a climatic gradient. *Tree Physiology*, 33, 26–36.

Kleinschmit J. (1993) Intraspecific variation of growth and adaptive traits in European oak species. *Annales des sciences forestières*, 50, 166–185.

Kobe R.K. (1996) Intraspecific variation in sapling mortality and growth predicts geographic variation in forest composition. *Ecological Monographs*, 66, 181–201.

Kramer K. (1995) Phenotypic plasticity of the phenology of seven European tree species in relation to climatic warming. *Plant, Cell and Environment*, 18, 93–104.

Kreyling J., Wiesenberg G.L.B., Thiel D., Wohlfart C., Huber G., Walter J., Jentsch A., Konnert M., Beierkuhnlein C. (2012) Cold hardiness of *Pinus nigra* Arnold as influenced by geographic origin, warming, and extreme summer drought. *Environmental and Experimental Botany*, 78, 99–108.

Kusmec A., de Leon N., Schnable P.S. (2018) Harnessing phenotypic plasticity to improve maize yields. *Frontiers in Plant Science*, 9.

Li Y., Suontama M., Burdon R.D., Dungey H.S. (2017) Genotype by environment interactions in forest tree breeding: review of methodology and perspectives on research and application. *Tree Genetics and Genomes*, 13, 60.

Ludovisi R., Tauro F., Salvati R., Khoury S., Mugnozza Scarascia G., Harfouche A. (2017) UAV-Based thermal imaging for high-throughput field phenotyping of black poplar response to drought. *Frontiers in Plant Science*, 8.

Matías L., Castro J., Villar-Salvador P., Quero J.L., Jump A.S. (2017) Differential impact of hotter drought on seedling performance of five ecologically distinct pine species. *Plant Ecology*, 218, 201–212.

Mátyás C. (1994) Modeling climate change effects with provenance test data. *Tree physiology*, 14, 797-804.

Mátyás C. (1996) Climatic adaptation of trees: rediscovering provenance tests. *Euphytica*, 92, 45–54

Mauri A., Di Leo M., de Rigo D., Caudullo G. (2016) *Pinus halepensis* and *Pinus brutia* in Europe: distribution, habitat, usage and threats. In: San-Miguel-Ayanz J., de Rigo D., Caudullo G., Houston Durrant T., Mauri A. (eds) *European Atlas of Forest Tree Species*, pp. 122-123. Publ Off EU, Luxembourg.

Melillo J. M, McGuire A.D., Kicklighter D.W., Moore B., Vorosmarty C.J., Schloss A. L. (1993) Global climate change and terrestrial net primary production. *Nature*, 363, 234.

Milla R., Reich P. B. (2011) Multi-trait interactions, not phylogeny, fine-tune leaf size reduction with increasing altitude. *Annals of Botany*, 107, 455–465.

Murren C. J. (2002) Phenotypic integration in plants. *Plant Species Biology*, 17, 89–99.

Nicotra A.B., Atkin O.K., Bonser S.P., Davidson A.M., Finnegan E.J., Mathesius U., Poot P., Purugganan M.D., Richards C.L., Valladares F., van Kleunen M. (2010) Plant phenotypic plasticity in a changing climate. *Trends in Plant Science*, 15, 684–692.

Notivol E., García-Gil M.R., Alía R., Savolainen O. (2007) Genetic variation of growth rhythm traits in the limits of a latitudinal cline in Scots pine. *Canadian Journal of Forest Research*, 37, 540–551.

Oleksyn J., Reich P.B., Zytkowiak R., Karolewski P., Tjoelker M.G. (2003) Nutrient conservation increases with latitude of origin in European *Pinus sylvestris* populations. *Oecologia*, 136, 220–235.

Ota T., Ogawa, M., Shimizu, K. *et al.* (2015) Aboveground biomass estimation using structure from motion approach with aerial photographs in a seasonal tropical forest. *Forests*, 6, 3882–3898.

Pádua L., Vanko J., Hruška J., Adão T., Sousa J.J., Peres E., Morais R. (2017) UAS, sensors, and data processing in agroforestry: a review towards practical applications. *International Journal of Remote Sensing*, 38, 2349–2391.

Pausas J.G. (2004) Changes in fire and climate in the eastern iberian peninsula (Mediterranean basin). *Climatic Change*, 63, 337–350.

Pausas J.G. (2015) Evolutionary fire ecology: lessons learned from pines. *Trends in Plant Science*, 20, 318–324.

Richardson D.M. (eds.) (2000) Ecology and biogeography of *Pinus*. Cambridge University Press.

Roberts D.A., Roth K.L., Perroy R.L. (2016) Hyperspectral vegetation indices. In: Huete A., Lyon J.G., Thenkabail P.S. (eds.) *Hyperspectral Remote Sensing of Vegetation*. pp. 309–328, Boca Raton, FL: CRC Press.

Sánchez-Salguero R., Navarro R.M., Camarero J.J., Fernández-Cancio Á. (2010) Drought-induced growth decline of Aleppo and maritime pine forests in south-eastern Spain. *Forest Systems*, 19, 458.

Sankaran S., Khot L.R., Espinoza C.Z., *et al.* (2015) Low-altitude, high-resolution aerial imaging systems for row and field crop phenotyping: A review. *European Journal of Agronomy*, 70, 112–123.

Sbay H., Zas R. (2018) Geographic variation in growth, survival, and susceptibility to the processionary moth (*Thaumetopoea pityocampa* Dennis and Schiff.) of *Pinus halepensis* Mill. and *P. brutia* Ten.: results from common gardens in Morocco. *Annals of Forest Science*, 75, 69.

Schiller G. (2000). Ecophysiology of *Pinus halepensis* Mill. and *P. brutia* Ten. In Ne'eman G., Trabaud L. (eds.) *Ecology, Biogeography and Management of Pinus halepensis and P. brutia Forest Ecosystems in the Mediterranean Basin*, pp 51-65.

Tapias R., Climent J., Pardos J.A., Gil L. (2004) Life histories of Mediterranean pines. *Plant Ecology*, 171, 53–68.

Tognetti R., Michelozzi M., Giovannelli A. (1997) Geographical variation in water relations, hydraulic architecture and terpene composition of Aleppo pine seedlings from Italian provinces. *Tree Physiology*, 17, 241–250.

Torresan C., Berton A., Carotenuto F., Di Gennaro S.F., Gioli B., Matese A., Miglietta F., Vagnoli C., Zaldei A., Wallace L. (2017) Forestry applications of UAVs in Europe: a review. *International Journal of Remote Sensing*, 38, 2427–2447.

Valladares F., Matesanz S., Guilhaumon F. *et al.* (2014) The effects of phenotypic plasticity and local adaptation on forecasts of species range shifts under climate change Ed W. Thuiller. *Ecology Letters*, 17, 1351–1364.

Voltas J., Lucabaugh D., Chambel M.R., Ferrio J.P. (2015) Intraspecific variation in the use of water sources by the circum-Mediterranean conifer *Pinus halepensis*. *New Phytologist*, 208, 1031–1041.

Voltas J., Shestakova T.A., Patsiou T., di Matteo G., Klein T. (2018) Ecotypic variation and stability in growth performance of the thermophilic conifer *Pinus halepensis* across the Mediterranean basin. *Forest Ecology and Management*, 424, 205–215.

Wang J., Sammis T.W., Gutschick V.P., Gebremichael M., Dennis S.O., Harrison R.E. (2010) Review of satellite remote sensing use in forest health studies. *The Open Geography Journal*, 3, 28-42.

Wang W, Peng C, Kneeshaw D.D., Larocque G.R., Luo Z. (2012). Drought-induced tree mortality: ecological consequences, causes, and modeling. *Environmental Reviews*, 20, 109-121.

MATERIALS AND METHODS - OVERVIEW

PROVENANCE TRIALS

A large part of the data was collected in three common gardens (also referred as provenance trials or genetic trials) located in Spain. One common garden was located in Altura (39°49′29″N, 00°34′22″W, Castellón province) and consisted of around 800 individuals of *P. halepensis* originating from 56 natural populations covering most of the range of the species. A second common garden, located in Valsaín (40°54′42″N, 04°00′50″W Segovia province), was composed of 200 individuals of *P. nigra* belonging to 18 range-wide populations of this species. Finally, around 1200 adult individuals of *P. sylvestris* originating from 16 Spanish and six German populations were tested in a third common garden located in Aragüés del Puerto (42°44'N, 00°37'W, Huesca province).

The trials were established in the 1990s by the Spanish government within the frame of a network of experimental common gardens aiming at testing the performance of Spanish populations of pines and to compare them to other Mediterranean populations. Specifically, the common garden of *P. sylvestris* was established in 1992, while the trials of *P. halepensis* and *P. nigra* were established in 1995. The individuals had therefore an age of around 25 years at the moment of sampling for this thesis, being considered as adult individuals.

All the common gardens were established following standard practises. Seeds were collected in natural populations of each species, being harvested for each population from 20-30 trees spaced at least 100 m apart. This was done to cover, as much as possible, intra-population variability. After being collected, the seeds were planted in forest nurseries in Spain, and 1-2 year-old seedlings were thereafter transferred to the trial sites, following different experimental designs. In the case of *P. nigra* and *P. sylvestris*, a completely randomised block design was used, while a Latinised row-column design (John and Williams, 1998) was employed in the common garden of *P. halepensis*. These experimental designs are used to randomise the allocation of the populations planted in the trials, aiming at reducing as much as possible the noise related to non-homogenous growing conditions at the trial sites.

STANDARD PHENOTYPING APPROACHES

A number of phenotypic traits were recorded in the common gardens using standard phenotyping techniques. Here I report the traits that were considered in more than one trial, while specific measurements performed in single common gardens are described in detail in the corresponding chapters of the thesis.

Growth and survival records

In the trials, growth measurements were performed by recording height and diameter at breast height (DBH) of each tree by using telescopic measuring sticks and tapes, respectively. Assuming the stem to be conical, DBH and height were used to calculate the stem volume over bark (Vob) following the equation:

$$Vob = (\pi/12) \times D^2 \times H \quad (1)$$

where D is the diameter at breast height and H is the tree height. Vob was used in some cases as surrogate of total above-ground biomass (Reinhardt *et al.*, 2006). The survival of each population in the trials was recorded at sampling time following visual inspection.

Carbon isotope composition of wood α-cellulose

The carbon isotope composition ($\delta^{13}C$) of wood α-cellulose was analysed as a well-established surrogate of intrinsic water use efficiency (WUE_i), defined as the ratio between carbon assimilation rate and stomatal conductance (Farquhar *et al.*, 1989). This approach was used in the case of the *P. sylvestris* and *P. nigra* trials, while for *P. halepensis* data collected with the same procedure were already available. Carbon isotope composition of wood was also used to study WUE_i variation in natural populations of *P. sylvestris*, although implementing a slightly different approach (see Chapter 5 for details). In the case of the common garden tests, increment borers were used to extract wood cores from the trees. Tree rings were visually cross-dated, and those corresponding to a representative period of years (5-10) were pooled together for carbon isotope analysis. This was done to obtain an estimation of mean WUE_i for each tree across years. The pooled rings were milled to a fine powder and α-cellulose was purified following the protocol described by Ferrio and Voltas (2005). Samples of α-cellulose underwent combustion using a Flash EA-1112 elemental analyser interfaced with a Finnigan MAT Delta C isotope ratio mass spectrometer (Thermo Fisher Scientific Inc., MA, USA). Carbon isotope composition ($\delta^{13}C$) was calculated as:

$$\delta^{13}C\ (‰) = (R_{sample} / R_{standard} - 1) \times 1000 \quad (2)$$

where R_{sample} and $R_{standard}$ are the isotope ratios ($^{13}C/^{12}C$) of the sample and of the Vienna Pee Dee Belemnite standard, respectively.

Non-structural carbohydrates

The concentration of non-structural carbohydrates (soluble sugars and starch) in sapwood was analysed to study the accumulation of carbon reserves in the case of *P. halepensis* and *P. nigra*. To this purpose, one healthy and sun-exposed branch with an approximate diameter of 1 cm was collected from the top part of the crown per each tree. The branches were bark-peeled and frozen in the field in dry ice. In the laboratory, branches were dried in an oven and then finely milled with a MM301 mixer mill (Retsch, Haan, Germany). Soluble sugars were extracted from 50 mg samples with 80% ethanol in a shaking water bath at 60 °C. The concentration of soluble sugars in the supernatant obtained after centrifugation was determined colourimetrically at 490 nm, using the phenol-sulphuric method described by Buysse and Merckx (1993). After ethanol extraction, the remaining undissolved precipitate was digested with amyloglucosidase to reduce starch to glucose, as described by Palacio *et al.* (2007). The resulting glucose was measured by the method of Buysse and Merckx (1993), from which the original starch concentration was determined.

AEREAL IMAGE COLLECTION

A multi-rotor UAV (Mikrokopter OktoXL, Moormerland, Germany) was used to obtain aerial images in the case of the *P. halepensis* and *P. nigra*. The flights took place at noon and with a completely clear sky to minimize shadow effects and changes in light intensity which could affect the optical properties of the images. The drone was flight under remote control at a fixed altitude, which was decided in each trial to combine the requirement to take overlapping pictures with the attainment of the highest possible resolution. The drone was equipped with three different cameras:

- A multispectral camera (MCA12; Tetracam Inc., Chatsworth, CA, US), which simultaneously captured 15.6-megapixel images in 10 wavelengths (450 ± 40, 550 ± 10, 570 ± 10, 670 ± 10, 700 ± 10, 720 ± 10, 840 ± 10, 860 ± 10, 900 ± 20, 950 ± 40 nm) in the visible and near infrared (NIR) regions of the spectrum. An extra sensor, incorporated in the multispectral camera, registered incident light (IL), hence resulting in real-time calibration of reflectance for each of the 10 wavelength images recorded during a flight.

- A Mirrorless Interchangeable Lens Camera (MILC) with an image sensor size of 17.3 × 13.0 mm, which was used for the acquisition of RGB images (Lumix GX7; Panasonic, Osaka, Japan). Images were taken at 16-megapixel resolution using a 20-mm focal length.

- A FLIR (Tau2 640; FLIR Systems, Nashua, NH, USA) camera carrying a vanadium oxide uncooled microbolometer equipped with a TEAX ThermalCapture module (TEAX Technology, Wilnsdorf, Germany), which was employed for the acquisition of thermal images.

The spatial resolution of the photographs changed according to flight altitude, but spanned between 1 cm (in the case to RBG images) and 6 cm per pixel (in the case of thermal camera). Images were taken at the rate of one every 5 s for the RGB and multispectral cameras, while, in the case of the thermal camera, images were extrapolated from a video with an image rate of 20 images per second. The multispectral images obtained during the flights were analysed in both the common gardens (i.e. *P. halepensis* and *P. nigra*), while images retrieved with RGB and thermal cameras were used only in the case of *P. halepensis*. A technical problem occurred during the flight which prevented the acquisition of good quality RGB and thermal images in the case of *P. nigra*.

The accuracy of the sensors' measurements was evaluated for the multispectral and thermal camera. In the case of the multispectral camera, accuracy of the reflectance measurements had been previously evaluated by comparing the camera records with the spectral reflectance of a durum wheat trial measured with an ASD field spectrometer (ASD, Boulder, CO, USA) (Kefauver *et al.*, unpublished data). The temperature measurements obtained with the UAV-mounted thermal camera for a vegetated, a completely white and a completely black surface were compared with ground-based measurements of the temperature recorded with an infrared thermometer. In both cases (i.e. multispectral and thermal), measurements were in agreement with ground-based records.

IMAGE PROCESSING

The approach used for image processing was slightly different in each case and is described in detailed in each single chapter. In general, for each flight the raw multispectral, RGB and thermal images were combined to produce orthomosaic images of the trials. Orthomosaics are aerial photographs that have been geometrically corrected – or orthorectified- to remove the effects of UAV flight (e.g. camera tilt) or topographic reliefs. To this purpose, images with a least 80% overlapping were used as input to the Agisoft PhotoScan Professional software (Agisoft LLC, St. Petersburg, Russia). This software identifies common features in overlapping pictures and generates an estimation of the camera position (i.e. coordinates and altitude) for each photo.

Using this information, an elevation model of the trial surface is produced and each image is subsequently orthorectified. The result of this process were multispectral and (only in the case of *P. halepensis*) RGB and thermal high-resolution orthomosaic images of the trials. In chapter 3, I also used RGB images to derive a canopy elevation model of *P. halepensis* trial. This model was then used for the automatic identification of single tree crowns (see Chapter 3 for details).

Generally, images corresponding to single experimental units (Chapters 1-2) or single trees (Chapters 3-4) were cropped from the orthomosaics. These images were used to calculate a wide range of vegetation indices based on the reflectance in specific wavelengths and, in the case of thermal images, to derive canopy temperatures. The indices were used as surrogates of traits such as leaf area, chlorophyll, anthocyanin, carotenoid, water concentration in the leaves and, also, transpiration. The indices that I used are described in details in Chapter I. In Chapter I, I tested a variety of indices, many of which were indicative of the same vegetation properties, thus resulting redundant. For this reason, in the following Chapters only a subset of indices was used.

REFERENCES

Buysse J.A.N., Merckx R. (1993) An improved colorimetric method to quantify sugar content of plant tissue. *Journal of Experimental Botany*, 44, 1627–1629.

Farquhar G.D., Ehleringer J.R., Hubick K.T. (1989) Carbon Isotope discrimination and photosynthesis. *Annual Review of Plant Physiology and Plant Molecular Biology*, 40, 503–537.

Ferrio J.P., Voltas J. (2005) Carbon and oxygen isotope ratios in wood constituents of *Pinus halepensis* as indicators of precipitation, temperature and vapour pressure deficit. *Tellus B*, 57, 164–173.

John J.A., Williams E.R. (1998) t-latinized designs. *Australian and New Zealand Journal of Statistics*, 40, 111-118.

Palacio S., Maestro M., Montserratmarti G. (2007) Seasonal dynamics of non-structural carbohydrates in two species of Mediterranean sub-shrubs with different leaf phenology. *Environmental and Experimental Botany*, 59, 34–42.

Reinhardt E., Scott J., Gray K., Keane R. (2006) Estimating canopy fuel characteristics in five conifer stands in the western United States using tree and stand measurements. *Canadian Journal of Forest Research*, 36, 2803–281.

CHAPTER I

Using UAV-based multispectral, RGB and thermal imagery for phenotyping of forest genetic trials: a case study in *Pinus halepensis*

F. Santini[a], S. C. Kefauver[b], V. Resco de Dios[a], J.L. Araus[b], J. Voltas[a*]

[a] Department of Crop and Forest Sciences – AGROTECNIO Center, University of Lleida, Av. Alcalde Rovira Roure 191, E-25198 Lleida, Spain.

[b] Integrative Crop Ecophysiology Group, Plant Physiology Section, Faculty of Biology, University of Barcelona, Av. Diagonal 643, E-08028 Barcelona, Spain

SUMMARY

The assessment of genetic differentiation in functional traits is fundamental towards understanding the adaptive characteristics of forest species. While traditional phenotyping techniques are costly and time-consuming, remote sensing data derived from cameras mounted on UAVs (unmanned aerial vehicles) provide potentially valid high-throughput information for assessing morphophysiological differences among tree populations. In this work, we test for genetic variation in vegetation indices and canopy temperature among populations of *Pinus halepensis* as proxies for canopy architecture, leaf area, photosynthetic pigments, photosynthetic efficiency and water use. The inter-population associations between vegetation properties and above-ground growth (stem volume) were also assessed. Three flights (July-2016, November-2016 and May-2017) were performed in a genetic trial consisting of 56 populations covering a large part of the species range. Multispectral (visible and near infrared wavelengths), RGB (red, green, blue) and thermal images were used to estimate canopy temperature and vegetation cover (VC) and derive several vegetation indices. Differences among populations emerged consistently across flights for vegetation cover and vegetation indices related to leaf area, indicating genetic divergence in crown architecture. Population differences in indices related to photosynthetic pigments emerged only in May-2017 and were probably related to a contrasting phenology of needle development. Conversely, the low population differentiation for the same indices in July-2016 and November-2016 suggested weak inter-population variation in the photosynthetic machinery of mature needles of *P. halepensis*. Population differences in canopy temperature found in July-2016 were indicative of variation in stomatal regulation under drought stress. Stem volume correlated with indices related to leaf area (positively) and with canopy temperature (negatively), indicating a strong influence of canopy properties and stomatal conductance on above-ground growth at the population level. Specifically, a combination of vegetation indices and canopy temperature accounted for about 60% of population variability in stem volume of adult trees. This is the first study to propose UAV remote sensing as an effective tool for screening genetic variation in morphophysiological traits of adult forest trees.

Key-words: Aleppo pine, common garden experiment, functional traits, leaf area, population differentiation, spectral imaging, stem volume, stomatal regulation

INTRODUCTION

The analysis of genetic variation in functional traits is fundamental towards understanding the adaptive properties of forest trees and to forecast responses to ongoing environmental changes (Bussotti *et al.,* 2015). Genetic trials are well suited for assessing adaptive variation among tree populations (Mátyás, 1996). Traits such as growth or phenology are typically evaluated in field trials (i.e. common garden experiments), occasionally in conjunction with functional characteristics such as reproductive effort (Santos-del-Blanco *et al.,* 2013), stem hydraulic properties or leaf gas exchange (Klein, 2014). However, large-scale phenotyping of forest genetic trials is methodologically challenging. The need to implement costly and time-consuming techniques is often a limitation for extensive phenotyping of adult trees (Ludovisi *et al.,* 2017). This constraint impacts negatively on the number of populations and traits that can be evaluated simultaneously, and may lead to the inadequate coverage of the suite of adaptive and plastic responses that are typical of forest species (Savolainen *et al.,* 2007).

Conversely, high-throughput phenotyping tools have been developed in plant sciences that enable a straightforward evaluation of hundreds of individuals with reduced economic and time costs (Großkinsky *et al.,* 2015; Lobos *et al.,* 2017). In this regard, remote sensing imagery acquired with unmanned aerial vehicles (UAVs) allows for an efficient morphophysiological characterisation of a large number of experimental units (Tattaris *et al.,* 2016). UAV-mounted multispectral and RGB (red, green, blue) cameras can detect light reflectance variation, while thermal cameras estimate canopy temperature (Sankaran *et al.,* 2015). Several vegetation indices can be derived through RGB and multispectral sensors, providing information about canopy properties, leaf area, leaf chemical composition and photosynthetic efficiency (Casadesús *et al.,* 2007; Fahlgren *et al.,* 2015; Xue and Su, 2017). Specific associations between functional traits and vegetation indices have been long established and are well described in the scientific literature (e.g., Roberts *et al.,* 2016; Xue and Su, 2017). These indices have been shown to be good predictors of physiological performance and productivity in field crops (Yu *et al.,* 2016; Gracia-Romero *et al.,* 2017) and forest species (Hernández-Clemente *et al.,* 2012). Moreover, thermal imagery provides information on canopy temperature that is linked to transpiration and plant water status (Costa *et al.,* 2013; Gonzalez-Dugo *et al.,* 2013). UAV-based remote sensing allows for high spatial resolution imagery and, therefore, is a promising tool for forest tree phenotyping. Indeed, UAVs are already being used for different purposes in forestry, including inventories, species classification, spatial gaps quantification, fire monitoring, and pest and pathogen mapping (Tang and Shao, 2015; Torresan *et al.,* 2017). To date, however, the potential

of UAVs as a tool for remote sensing assessments of intra-specific differentiation in phenotypic traits remains untested in adult forest trees (Ludovisi *et al.,* 2017).

In this work, we characterise the extent of inter-population differences in functional traits related to canopy architecture and tree physiology through high-resolution remote sensing data obtained in a common garden experiment. We focus on Aleppo pine (*Pinus halepensis* Mill.), the most widespread conifer of the Mediterranean basin. Aleppo pine is a drought-avoidant species that is prevalently distributed in the central-western part of the Mediterranean basin, where it provides important ecosystem services and it is widely used for reforestation (Pausas *et al.,* 2004; Choury *et al.,* 2017). Due to its circum-Mediterranean distribution range, *P. halepensis* can be found under contrasting growing conditions which, coupled with a complex history of demographic contractions and expansions, have shaped current intra-specific patterns of genetic variation (Serra-Varela *et al.,* 2017). In particular, population differentiation has been reported in this species for many key traits, including aerial growth (Schiller and Atzmon, 2009; Voltas *et al.,* 2018), phenology (Klein *et al.,* 2013), water uptake patterns (Voltas *et al.,* 2015), hydraulic conductivity (Tognetti *et al.,* 1997) and reproductive effort (Climent *et al.,* 2008).

We hypothesised that (i) morphophysiological properties related to drought resistance and inferred through remote sensing data should vary among populations of *P. halepensis* (Otieno *et al.,* 2005; Voltas *et al.,* 2008), and (ii) population differentiation in such properties can explain variation in above-ground growth. To test these hypotheses, we used UAV imagery as high-throughput phenotyping tool in a genetic trial of this conifer composed of adult individuals. More specifically, we sought to (i) assess genetic variation in canopy architecture, leaf area, photosynthetic pigments and stomatal regulation in three consecutive seasons of the year (summer, autumn, spring) as indicated by differentiation in vegetation cover, vegetation indices and canopy temperature, and (ii) explore the associations between ecophysiological properties and above-ground growth (stem volume) at the intra-specific level.

MATERIAL AND METHODS

Study site and plant material

The study was performed in a common garden experiment of *P. halepensis* located in Altura (39°49′29″N, 00°34′22″W, 640 m a.s.l.; Castellón province, eastern Spain, Figure 1A; Figure S1). The site has a mean annual temperature of 13.8°C and mean annual precipitation of 652 mm, of which 19% falls in summer (June to August). These climatic conditions are representative of the average values of the species' distribution range (Figure 1B). Seeds were collected in 1995 in 56 natural populations of *P. halepensis* covering most of the range of the

species (Appendix, Table S1, Figure S1). Seeds were harvested from 20-30 trees that were spaced at least 100 m apart and planted in a forest nursery in Spain. In 1997, one year old seedlings were planted systematically (2.5 m spacing on rows and columns) at the study site. Four seedlings from each provenance were planted in experimental units consisting of linear plots (Figure 1C). Four replicates were established following a Latinised row-column design (John and Williams, 1998) for a total of 896 seedlings (16 per population) tested in the trial. Each row had approximately 70 m long corresponding to seven plots and four trees per plot. In 2010 (at age 13), height and diameter at breast height were registered per tree, and data were used to calculate the stem volume over bark (Vob) following the equation:

$$Vob = (\pi/12) \times D^2 \times H \quad (1)$$

where D is the diameter at breast height and H is the tree height, assuming the stem to be conical. Vob was used as surrogate of total above-ground biomass (Reinhardt *et al.*, 2006). In 2016, survival was recorded at the plot level with a ground-based visual inspection.

Aerial data collection

Aerial images of the trial (Figure 1A) were obtained through a UAV (Mikrokopter OktoXL, Moormerland, Germany) flying under remote control at around 100 m of altitude. Three different cameras were mounted down-looking on the UAV in consecutive flights done during the same day. First, a multispectral camera (MCA12; Tetracam Inc., Chatsworth, CA, US) was operated which simultaneously captured 15.6-megapixel images in 10 wavelengths (450 ± 40, 550 ± 10, 570 ± 10, 670 ± 10, 700 ± 10, 720 ± 10, 840 ± 10, 860 ± 10, 900 ± 20, 950 ± 40 nm) in the visible and near infrared (NIR) regions of the spectrum. An extra sensor, incorporated in the multispectral camera, registered incident light (IL), hence resulting in real-time calibration of reflectance for each of the 10 wavelength images recorded during a flight. These images were pre-processed with the Tetracam PixelWrench software (Tetracam Inc., Chatsworth, CA, US) in order to correctly align the images. To ensure high quality image registration in the pre-processing stage, care was taken to keep forward motion limited to less than 5 m s^{-1} in the UAV flight. The accuracy of the reflectance measurements of the multispectral camera was evaluated in a previous study using the same sensor and UAV platform (Kefauver *et al.*, unpublished data). Particularly, the camera records were compared with the spectral reflectance of the same plots of a durum wheat trial measured with an ASD field spectrometer (ASD, Boulder, CO, USA), resulting in simple correlations varying between 0.95 and 0.97 for the 10 wavelengths. Second,

a Mirrorless Interchangeable Lens Camera (MILC) with an image sensor size of 17.3 × 13.0 mm was used for the acquisition of RGB images (Lumix GX7; Panasonic, Osaka, Japan). Images were taken at 16-megapixel resolution using a 20-mm focal length. Third, a FLIR (Tau2 640; FLIR Systems, Nashua, NH, USA) camera carrying a vanadium oxide uncooled microbolometer equipped with a TEAX ThermalCapture module (TEAX Technology, Wilnsdorf, Germany) was employed for the acquisition of thermal images. The temperature measurements obtained with the UAV-mounted thermal camera for a vegetated, a completely white and a completely black surface were compared with ground-based measurements of the temperature recorded with an infrared thermometer, resulting in a correlation of 0.96.

The spatial resolution of the photographs was *ca.* 1, 2.7 and 5.4 cm per pixel in the case of RGB, multispectral and thermal cameras, respectively. Images were taken at the rate of one every 5 s for the RGB and multispectral cameras, resulting in *ca.* 120 pictures obtained per flight (*ca.* 10 minutes long). In the case of the thermal camera, images were extrapolated from a video with a frame (image) rate of 20 images per second. Flights were done in summer (26 July 2016), autumn (17 November 2016) and spring conditions (25 May 2017) in two consecutive growing seasons, following a trajectory designed to spatially cover the entire study site (Figure 1A). The flights took place at noon and with a completely clear sky to minimize shadow effects and changes in light intensity. Environmental and sun conditions at the moment of the flights are reported in Table 1.

Image processing

For each flight the raw multispectral, RGB and thermal images were combined to produce orthomosaic images. The Agisoft PhotoScan Professional software (Agisoft LLC, St. Petersburg, Russia) was employed for this purpose using a variable number of images with at least 80% overlap. Nine orthomosaics resulted from this process (i.e. three orthomosaics per flight – one multispectral, one RGB and one thermal – and three flights) which were used for subsequent analyses. The open-source image analysis platform Fiji (Schindelin *et al.*, 2012) was used to identify and crop single linear plots (corresponding to four trees) in each orthomosaic (Figure 1C, 1D). In total, 224 single images (corresponding to the experimental units of the trial) were obtained for each flight and imagery (multispectral, RGB and thermal).

Multispectral indices

A number of vegetation indices (VIs) were derived from multispectral data based on the reflectance at 10 wavelengths (Table 2). The VIs were calculated for each pixel using a macro

code in the Fiji platform, and a mean value per plot was obtained afterwards. The indices are linked to different functional traits in relation to the wavelengths used for calculations. Several indices (based on red and NIR reflectance) are mainly linked to leaf area, being relatively insensitive to leaf chlorophyll content (Roberts *et al.*, 2016; Xue and Su, 2017). Specifically, these are:

- the Normalized Difference Vegetation Index (NDVI), which is broadly used and based on the reflectance in red and NIR wavelengths (Rouse *et al.*, 1974);
- the Enhanced Vegetation Index (EVI, Huete *et al.*, 2002), which is an optimized NDVI-based index developed to minimize the noise due to atmospheric reflectance;
- the Renormalized Difference Vegetation Index (RDVI, Roujean and Breon, 1995);
- the Optimized-Soil Adjusted Vegetation Index (OSAVI, Rondeaux *et al.*, 1996). RDVI and OSAVI were both proposed to minimize the effect of the background (i.e. soil) reflectance.

Alternatively, other indices include the reflectance in the green wavelengths and are negatively related to leaf chlorophyll content. These indices are:

- the Modified Chlorophyll Absorption Ratio Index (MCARI, Daughtry *et al.*, 2000);
- the Transformed Chlorophyll Absorption Ratio Index (TCARI, Haboudane *et al.*, 2002).

However, these indices are also sensitive to background reflectance and can be influenced by differences in leaf area (Daughtry *et al.*, 2000). A better estimation of leaf chlorophyll content can be obtained by correcting TCARI by an index that accounts for leaf area. In this regard, an index related to chlorophyll content and free of the effect of leaf area is:

- the ratio between TCARI and OSAVI (TCARI/OSAVI, Haboudane *et al.*, 2002; Zarco-Tejada *et al.*, 2004).

Alternative indices related to other leaf pigments and water content are:

- the Anthocyanin Reflectance Index 2 (ARI2, Gitelson *et al.*, 2001);
- the Carotenoid Reflectance Index 2 (CARI2, Gitelson *et al.*, 2002);
- the Water Band Index (WBI, Peñuelas *et al.*, 1993), which is related to the water content of leaves.

It must be taken into account that the values of vegetation indices, when calculated at the whole-plot level, arise as the combination of vegetation characteristics and vegetation cover (VC, or percentage of pixels containing vegetation). Phenotypic variation in vegetation properties within the canopy that influence such indices could be partly masked by phenotypic variation in crown size (i.e. VC). To overcome this issue, we applied a filter to distinguish between pixels containing vegetation and pixels containing soil. The filter was based on the NDVI index, which

was first developed to discriminate between vegetation and other surfaces (Richardson and Wiegand, 1977). The reflectance in NIR wavelengths of pure soil surface is slightly higher than the reflectance in red wavelengths, resulting in NDVI values of 0-0.2. Conversely, the NDVI is higher in vegetation surfaces, due to the high absorption in red wavelengths and the high reflectance in NIR wavelengths. Based on this, we applied an NDVI threshold of 0.5, considering as vegetated pixels those showing NDVI > 0.5 (Figure 1E). The multispectral VIs were recalculated using vegetated pixels as to be representative of differences in the properties of the vegetation, excluding differences in VC.

RGB vegetation indices

While multispectral indices have been used for long time as proxies of specific vegetation characteristics, RGB imagery has been only recently proposed as a low-cost alternative for plant phenotyping (Kefauver *et al.*, 2017; Gracia-Romero *et al.*, 2018). Indeed, a clear association with specific phenotypic traits is still lacking in the scientific literature for many RGB-derived VIs. As potential alternative to multispectral indices, several VIs based on colour properties and related to the degree of greenness of the image were retrieved from RGB images (Casadesús *et al.*, 2007), as described below.

RGB images corresponding to single experimental units (Figure 1C) were analysed using a version of the Breedpix 2.0 software implemented as a plug-in within Fiji (Casadesús and Villegas, 2014). This software calculates VIs on single pixels in each image and then provides a mean value per plot. In order to evaluate a wide range of RGB indices, three different models representing the colour space in different ways were considered to derive such indices. In the HSI (Hue, Saturation, Intensity) model (Judd, 1940), *Saturation* and *Intensity* describe the grade of purity of the colour and the light intensity, respectively, while *Hue* describes the colour itself in the form of an angle between 0° and 360°, where 0° means red, 60° means yellow, 120° means green and 180° means cyan. Derived from *Hue*, the Green Area (GA) index is defined as the percentage of green pixels in the image (*Hue* range from 60° to 180°). Two alternative models to HSI (CIELab and CIELuv) are defined according to the International Commission of Illumination (http://www.cie.co.a). In the CIELab model, the a^* component represents the green to red range, with a more positive value representing a purer red, and a more negative value indicating a greener colour. The b^* component defines the blue to yellow range, where more positive values are closer to a pure yellow and more negative ones are closer to pure blue. In the CIELuv model, the colour space is represented as a Cartesian system with two coordinates, u^* and v^*. The visible spectrum starts with blue at the bottom of the space, moving through green

in the upper left and to red in the upper right. It must be noted that the RGB-derived VIs described above are not calculated based on reflectance in specific wavelengths; instead, they are descriptors of the colour space. Alternatively, the RGB images can be used to calculate additional indices based on the reflectance in different wavelengths of the visible spectrum: the normalized green red difference index (NGRDI), which is based on the reflectance in the red and green bands, and the triangular greenness index (TGI), which includes also the reflectance in blue bands (Table 2).

The NDVI-based filter that was applied to the multispectral images to remove non-vegetated pixels could not be applied to RGB images due to the different type of imagery. For this reason, only whole plot RGB-indices (which includes vegetated and non-vegetated pixels) could be calculated.

Thermal images

Thermal images were used to retrieve information on canopy temperature. Since average plot temperature is related to vegetation cover, a filter based on an automatic Otsu's classification (Otsu, 1979) was applied to the thermal images in order to discriminate between vegetated and non-vegetated pixels. The algorithm assumes that images contain two classes of pixels (ground and vegetation) and automatically finds an optimum threshold (temperature) to separate between classes. Based on the pixels classified as "vegetation", a second estimation of vegetation cover was obtained (VC_T); these pixels were later used to derive the mean canopy temperature of each plot.

Statistical analyses

First, we evaluated the presence of significant inter-population variation in vegetation indices, vegetation cover and canopy temperature (as proxies of differentiation in canopy architecture, leaf area, photosynthetic pigments and water use) for each flight independently. Afterwards, the association between UAV-based vegetation characteristics and stem volume was tested. Prior to the analyses, plots having three dead trees were discarded, since dead trials could strongly bias the performance of neighbouring trees due to reduced competition. These plots represented only 2% of the total number of plots and showed strongly deviating values of VIs. Also, plots at the edges of the trial might have shown values influenced by reduced competition (i.e. border effects). Nevertheless, these plots (7%) were kept in the analyses because they did not show up as outliers. In total, 219 plots (corresponding to 818 trees) were used for statistical analyses.

Analysis of variance of individual traits

Stem volume, vegetation indices, vegetation cover and canopy temperature at the plot level were subjected to analysis of variance (ANOVA) for linear mixed-effects models in order to test for population differences in UAV-based phenotypic traits. ANOVAs were fitted independently for each flight date. Stem volume records were log-transformed prior to ANOVA to achieve homoscedasticity of residuals. ANOVAs consisted of fixed population, replicate and column terms and random column by replicate interaction and row nested to replicate terms.

For those indices showing significant population differences, Spearman's rank correlations involving population means were calculated across flights to check for consistency in population ranking.

Relationships between vegetation indices

The use of RGB-derived vegetation indices is relatively recent compared to multispectral imagery. While multispectral VIs based on specific reflectance bands have been linked to particular phenotypic traits (Roberts *et al.*, 2016; Xue and Su, 2017), few literature is available for many RGB indices considered in this work. In order to compare the information retrieved by RGB and multispectral VIs, simple correlations were calculated across populations. Moreover, the populations' least square means of the different vegetation indices and of canopy temperature were subjected to Principal Component Analysis (PCA) for each flight date and index type independently (multispectral, multispectral corrected by vegetation cover and RGB-derived), and PCA loadings were plotted to summarise the information contained in the different variables.

Population-level associations between stem volume and UAV-based imagery information

When significant population effects were detected, simple correlations involving log-transformed stem volume and VIs, vegetation cover or canopy temperature were calculated for each flight date using population means. This analysis aimed at indirectly test for the effects of a number of functional traits related to UAV imagery (canopy architecture, leaf area, photosynthetic pigments and water use) on population differentiation in above-ground growth. We assumed that the ranking of populations for stem volume remained stable at adult stage (age > 10 in *P. halepensis*), as reported elsewhere for pines (Li and Wu, 2005). Hence, growth data obtained in 2010 (at age 13) was compared with UAV imagery records.

The variability in stem volume across populations explained by vegetation properties (vegetation cover, vegetation indices and canopy temperature) was assessed through stepwise linear regression in July-2016 and May-2017. This analysis was not performed in November-

2016 due to the lack of reliable VIs estimation (see "Methodological limitations" in the Discussion section). The analyses were carried out using a bidirectional (forward and backward) elimination procedure based on input and output *F* probabilities of 0.15. The goodness of fit was evaluated considering the coefficient of determination (R^2) and the root-mean-square error (RMSE) of the regression. Different models were tested, either considering one particular family of VIs (RGB-derived indices, multispectral indices measured in either whole plots or vegetated pixels) or, alternatively, combining RGB-derived and multispectral indices. Vegetation cover was also included in the regressions involving multispectral indices. In the case of July-2016, the analyses were also performed including canopy temperature in the models (canopy temperature was not included in May-2017 because of lack of population differentiation for this trait).

RESULTS

Population variation in UAV-based imagery information and stem growth

The population term in the ANOVAs was significant ($P < 0.05$) for many VIs related to different functional traits and, also, for log-transformed stem volume (log-Vob, Table 3). Average population values of VIs are reported in Appendix for each flight (Table S2).

Most multispectral indices obtained at the plot level showed significant differences among populations, with the exceptions of TCARI/OSAVI, which was non-significant regardless of flight date. However, significant population differences in vegetation cover (VC), which may influence the variation in multispectral VIs, were found regardless of flight date (Table 3). Population means for VC varied between 52% and 69% in July-2016, between 51% and 67% in November-2016, and between 53% and 66% in May-2017. VC estimates were consistent across flights, as indicated by significant rank correlations and low absolute differences (<10%) at the plot level. Once the multispectral VIs were recalculated considering vegetated pixels only, significant population differences emerged for indices related to leaf area (i.e. NDVI, OSAVI, RDVI, EVI, MCARI and TCARI) across flight dates (Table 3). For those indices related to needle pigment composition (i.e. TCARI/OSAVI, ARI2 and CRI2) and water content (i.e. WBI), significant population differences were found only in May-2017. In the case of RGB-derived VIs, population differences were found in July-2016 (with the exception of TGI and *Intensity*) and May-2017. Population differentiation was also observed in November-2016, but only for three indices (a^*, u^* and GA).

For thermal data, we could not distinguish between soil and vegetation pixels in November-2016 owing to small differences in temperature between soil and canopy. For this

particular flight date, the mean temperature of the whole plot was used as response variable in the ANOVA. In July-2016 and May-2017, VC_T was significantly correlated with VC at the plot level, even if VC_T estimates were usually higher. Based exclusively on vegetated pixels, the ANOVA revealed population differences in canopy temperature only in July-2016, while population differentiation in temperature was not significant based on whole-plot (in November-2016) or vegetated pixels (in May-2017, Table 3).

For those indices showing population variation in different flights, significant Spearman correlations across flight dates indicated consistent population rankings (Table S3). Population ranking for vegetation cover was also consistent across flights.

Relationships between vegetation indices

The relationships between RGB-derived indices and multispectral indices at the population level provided information regarding the functional traits that could be potentially inferred by RGB imagery. Specifically, most RGB VIs were significantly correlated with the suite of multispectral indices related to leaf area obtained either for whole plots or for vegetated pixels only (Appendix, Table S4, S5, S6). Exceptions were TGI and *Intensity* (in July-2016) and *Hue* (in May-2017). Correlations between RGB-derived indices and multispectral indices related to pigment content (e.g. TCARI/OSAVI as indicator of needle chlorophyll content) were poorer and less consistent across flight dates (Appendix, Table S4, S5, S6). As an exception, TGI and *Intensity* were significantly correlated ($r \geq 0.55$) with TCARI/OSAVI in May-2017. Most RGB-derived and multispectral indices were also significantly correlated with VC across flight dates at the population level (Table 4).

The PCA loadings provided insights into the existing relationships among vegetation indices (see Figure 2 for the case of July-2016). For multispectral data, the relationships between indices were quite consistent across flights (with the exception of November-2016; results not shown), regardless of whether they were calculated on whole plots (Figure 2A) or on vegetated pixels only (Figure 2B). The indices related to leaf area (i.e., NDVI, RDVI, OSAVI, EVI, MCARI and TCARI) grouped together in the plot of loadings, opposite to canopy temperature (Figure 2A; Figure 2B). In turn, TCARI/OSAVI (informative of chlorophyll content) and WBI (of leaf water content) were negatively associated and unrelated to most other indices. Finally, ARI2 and CRI2 (informative of anthocyanins and carotenoid leaf content respectively) were poorly explained by the first two PCA dimensions. For RGB-derived indices, two patterns of associations could be distinguished regardless of flight date (see Figure 2C for the case of July-

2016). TGI and *Intensity* clustered together, being independent of the rest of indices, which in turn were tightly associated among them.

Population-level associations between stem volume and UAV-based imagery information

VIs often correlated significantly with log-Vob across populations (Table 4). The highest correlations were found in July-2016 and involved multispectral indices related to leaf area estimated on vegetated pixels ($r \geq 0.50$, Table 4). Significant correlations were often observed also in November-2016, regardless of index type. In May-2017, correlations with log-Vob were similar across different classes of indices (multispectral or RGB), with the exception of multispectral indices related to leaf pigments and water content, which resulted poorly correlated with log-Vob (Table 4). Vegetation cover was significantly correlated with log-Vob in July-2016, November-2016 and May-2017 ($r \geq 0.27$).

Canopy temperature was negatively correlated with log-Vob across populations in July-2016 (Figure 3). Also, canopy temperature was negatively and significantly correlated with multispectral indices related to leaf area as measured on vegetated pixels (i.e. NDVI, OSAVI, RDVI, EVI; $r = \leq - 0.52$). To account for the effect of leaf area on the relationship between canopy temperature and log-Vob, partial correlations controlling for such indices (NDVI, OSAVI, RDVI or EVI) were calculated across populations. These correlations were also significant ($r \leq - 0.49$).

Over 60% of the variability in growth was explained by a combination of vegetation properties. The best stepwise regression model of population differences in log-Vob was obtained in May-2017, and included a combination of multispectral and RGB indices measured on vegetated pixels ($R^2 = 0.63$, RMSE = 0.198, Table 5). Alternative regressions based on combinations of multispectral VIs showed lower R^2 and higher RMSE. In July-2016, the best predictive model was obtained combining canopy temperature and a multispectral index related to leaf area such as EVI ($R^2 = 0.60$, RMSE = 0.278). In general, regressions including canopy temperature were better predictors of log-Vob in July-2016, regardless of VI. Indeed, canopy temperature alone explained 57% variability among populations.

DISCUSSION

The potential of UAV-derived remote sensing data as phenotyping tool is widely acknowledged in plant sciences (Sankaran *et al.*, 2015). In this work, we have proposed a straightforward strategy for UAV-based characterisation of population differentiation in key functional traits of a forest tree species. Although several UAV-based applications have been described in forest

sciences (e.g., Hernández-Clemente *et al.,* 2012; Tang and Shao, 2015; Torresan *et al.,* 2017), this is to the best of our knowledge the first attempt to apply high-throughput phenotyping techniques based on aerial imagery in forest genetic trials comprising adult trees.

The extent of population differentiation in vegetation indices and canopy temperature as proxies of functional traits

Many multispectral indices measured on the whole plot varied among populations, suggesting genetic differentiation in several functional traits. However, these indices were also sensitive to variations in vegetation cover, which could have determined population differences for these indices (Purevdorj *et al.*, 1999). In particular, the confounding effect of vegetation cover on plot-level multispectral indices may explain the lack of population differentiation for some indices (e.g. NDVI, TCARI/OSAVI or CRI2), otherwise relevant when considering only vegetated pixels. Indeed, multispectral indices measured on vegetated pixels are free of changes in vegetation cover (i.e. canopy width), being representative of variations in other canopy properties (Xue and Su, 2017). In general, however, multispectral indices showed similar relationships when measured on the whole plot or on vegetated pixels, as revealed by PCAs.

NDVI-related multispectral indices (i.e. OSAVI, RDVI, EVI, MCARI and TCARI) measured on vegetated pixels showed significant population variation and similar population ranking across seasons, suggesting the existence of constitutive population differences in within-canopy characteristics in *P. halepensis*. As already stressed, these indices have been long used as indicators of variation in leaf area (e.g., Roberts *et al.,* 2016; Xue and Su, 2017) also at the individual tree level (Berni *et al.,* 2009). These evidences point to the existence of population differentiation in the number or area of needles per pixel, thereby indicating differences in canopy density as previously reported for other pine species (McRady and Jokela, 1996). Population differentiation was also found for vegetation cover across flights. Canopy structural properties such as branches' surface and distribution can impact on crown shape and concur with leaf area to determine differentiation in vegetation cover (Baldwin *et al.*, 1997; Weiskittel and Maguire, 2006). These findings suggest complex patterns of canopy architecture among populations of *P. halepensis*. Canopy structural properties have significant implications in many physiological traits, including foliage surface exposure and total radiation absorption (Niinemets, 2010). Reduced leaf area in some populations may also be associated to drought resistance as the result of a lower transpiring surface (Eamus *et al.*, 2000; Otieno *et al.*, 2005).

MCARI and TCARI take into account the reflectance in the green spectral region at 550 nm, revealing also potential differences in chlorophyll content of leaves (Daughtry *et al.,* 2000).

However, MCARI and TCARI were probably indicative of differences in leaf area, rather than in chlorophyll content, according to population differentiation observed across flight dates. This is because significant population differences emerged only in spring for TCARI/OSAVI, which is an index specifically informative of leaf chlorophyll content (Zarco-Tejada *et al.,* 2004; Wu *et al.,* 2008). In this regard, MCARI and TCARI (but also EVI, which includes reflectance in the blue band) showed lower, although significant, Spearman's correlations across flights compared to indices that consider only the reflectance in red and NIR (i.e. NDVI, OSAVI and RDVI). Other indices related to carotenoid, anthocyanin or water content in leaves also showed significant population variation in spring if calculated on vegetated pixels, which reinforces the existence of population differences in needle biochemical composition early in the growing season. Contrasting photosynthetic spring recovery or different phenology of needle emergence could explain variation in pigments and water content among pine populations in spring (Wong and Gamon, 2015). The scarce information available on needle phenology in *P. halepensis* indicates that new needles draw apart from the shoot in mid-spring, reaching the final size only in full summer (Weinstein, 1989). This evidence is consistent with our findings and points to differential needle development among populations of *P. halepensis*. On the other hand, our results indicate a lack of genetic differentiation in the photosynthetic apparatus (i.e. photosynthetic pigments) of mature needles of *P. halepensis,* which is consistent with a previous work carried out in the same trial suggesting weak differentiation in photosynthetic capacity among populations of *P. halepensis* (Voltas *et al.,* 2008).

In recent years, RGB imagery has been proposed as cost-effective alternative to multispectral records for plant phenotypic characterisation (Kefauver *et al.,* 2017; Gracia-Romero *et al.,* 2018). RGB imagery has limited possibilities for studying physiological processes such as gas exchange or leaf biochemistry (Großkinsky *et al.,* 2015). However, RGB-derived vegetation indices can be easily obtained from standard cameras and are suitable for studying the morphological characteristics of the vegetation. In this work, two distinct groups of RGB indices provided contrasting information on functional traits of *P. halepensis* populations. The first group included the *Intensity* parameter, which is indicative of the brightness of the picture, and the TGI index, which has been related to leaf chlorophyll content (Hunt *et al.,* 2011). The population differentiation in TGI in spring indicates variability in chlorophyll content in needles among populations of *P. halepensis* during spring, as suggested also by some multispectral indices. However, the tight association of TGI with *Intensity* cannot exclude a preponderant effect of pictures' brightness on TGI variation, making the interpretation of this index difficult. Conversely, a second group of indices showed significant population variation and consistent

genetic ranking across flights. Most of these indices are related to the overall "greenness" of the image and have been linked to leaf area in field crops (Hunt *et al.,* 2005; Casadesús and Villegas, 2014). In this regard, the strong and consistent correlations found at the population level between RGB and multispectral indices related to leaf area suggest that RGB indices are indicative of population differences in number of needles, in their total surface, or in both factors simultaneously. Our results suggest that RGB imagery can be a (partial) alternative to multispectral indices for tree phenotyping with UAV, as already proposed for herbaceous crops (Casadesús *et al.,* 2007; Kefauver *et al.,* 2017; Gracia-Romero *et al.,* 2018).

The population differentiation in canopy temperature observed in summer is indicative of divergence in transpiration rate (Gonzalez-Dugo *et al.,* 2013). Disentangling the effects of total leaf area and stomatal conductance on canopy temperature is complex, and canopy temperature was found to be correlated with vegetation indices related to leaf area. Notably, canopy temperature measured in July-2016 was also positively correlated with the carbon isotope composition ($\delta^{13}C$) of wood holocellulose for a subset of 25 populations evaluated in the same trial by Voltas *et al.* (2008, Figure S2). $\delta^{13}C$ is a commonly used integrative indicator of photosynthetic performance, with higher values implying reduced stomatal conductance in the absence of differences in photosynthetic rate (Farquhar *et al.,* 1989). This finding suggests that *thermal imagery is indicative of variation in both leaf area and stomatal regulation of gas exchange at the needle level* (Gonzalez-Dugo *et al.,* 2013), *and is* supportive of population differentiation in stomatal conductance in *P. halepensis* during the peak of summer (Voltas *et al.,* 2008).

Relationships between vegetation indices and stem volume

Volume over bark (Vob) is a good indicator of above-ground growth in *P. halepensis* as height versus diameter allometry is relatively constant among populations of the species (Vizcaíno-Palomar *et al.,* 2016). However, genetic differences have been described for P. halepensis in the allocation of resources to other functions such as reproduction, or to other compartments such as roots (Climent *et al.,* 2008; Cuesta *et al.,* 2010; Voltas *et al.,* 2015). Therefore, population differentiation in Vob could be indicative of either contrasting strategies in resource allocation or superior performance of specific populations showing enhanced growth. We can assume a strong influence of total needle area on Vob as indicated by consistent associations between Vob and NDVI-related indices across populations. This finding indicates that investment in needles is coupled with enhanced above-ground growth in P. halepensis, as already reported for other pines (Vose and Allen, 1988; McDowell *et al.,* 2007). Vegetation cover was also correlated with

Vob, suggesting complex associations between canopy architecture, canopy density and above-ground growth at the population level.

A negative relation between canopy temperature and Vob among populations was also detected. High canopy temperatures are indicative of decreased transpiration as combination of reduced leaf area and stomatal conductance (González-Dugo *et al.,* 2013). Since partial correlations between canopy temperature and stem volume were significant after accounting for indices related to leaf area, stomatal regulation is possibly concurring with decreasing transpiring area to limit carbon uptake, leading to reduced growth (Fardusi *et al.,* 2016). Thus, our results suggest that stomatal regulation is a crucial factor accounting for population differentiation in photosynthetic performance of *P. halepensis* under drought conditions. Conversely, low correlations between Vob and pigment-related indices (i.e. TCARI/OSAVI, CRI2 and ARI2) indicate a limited influence of needle phenology and development on population differentiation in above-ground growth.

RGB vegetation indices also showed significant correlations with stem volume, comparable to those obtained from multispectral indices, at least in May-2017. RGB-derived indices have been shown to be good predictors of aerial biomass and yield in crops (Casadesús and Villegas, 2014), in some cases outperforming multispectral indices (Kefauver *et al.,* 2017; Gracia-Romero *et al.,* 2018). Our results show that they can represent a cost-effective alternative to multispectral imagery as a surrogate of above-ground biomass in adult trees. Finally, the outcome of the stepwise regression analyses indicated that a combination of vegetation indices and thermal images can predict up to 60% of population differences in stem volume of adult trees. The best predictive models, involving either RGB and multispectral indices in May-2017, or a combination of a multispectral index and canopy temperature in July-2016, confirmed the concurring role of total leaf area and stomatal regulation in determining stem volume of *P. halepensis*.

Methodological limitations

UAVs are increasingly used to characterise genotypic variation in crop trials, which usually consist of isolated plots that are easily recognizable through aerial imagery (Sankaran *et al.*, 2015). In the case of genetic trials of forest species, a high tree density along with heterogeneous trial conditions can hamper the identification of experimental units, especially at adult stages. Moreover, forest trees are characterised by an extreme plasticity in the development of the crown, which can unpredictably grow to exploit the available light (Purves *et al.,* 2007). In aerial imagery, these issues can lead to important disturbances owing to the effects of overlapping

crowns of neighboring plots. We tried to overcome these issues by visually delimiting as carefully as possible crown expansions for each individual plot.

Another potential caveat is related to the existence of unwanted shading effects, which may affect vegetation reflectance and impact on the estimation of indices (Yamazaki *et al.*, 2009). Indeed, phenotypic variation in tree height could lead to systematic shading of some populations. We attempted to minimise this issue by performing flights at noon, but a shading influence on these indices cannot be ruled out, especially in November-2016, when the sun elevation over the horizon was low. In this regard, intricate relationships among indices, weak population differentiation and poor correlations with Vob were observed for this flight date, which suggests that autumn results should be taken cautiously. Finally, another possible limitation towards a precise phenotyping is that UAV-based imagery retrieves information mainly from the top crown of the tree, being less adequate to capture within-crown differences in functional characteristics. These differences are indeed relevant in forest species (Aranda *et al.*, 2004; Yamazaki *et al.*, 2009).

Concluding remarks

Plant phenotyping based on UAV remote sensing is coming to an increasing popularity in breeding programs for evaluating and selecting crop varieties for improved yield (Sankaran *et al.*, 2015; Lobos *et al.*, 2017). Here we assessed patterns of genotypic variability in functional traits of adult trees, which is a fundamental step towards the assessment of the adaptive potential of forest species to environmental changes (Bussotti *et al.*, 2015). By using well- established vegetation indices and aerial imagery, our results point to range-wide population differentiation in morphophysiological features related to stem volume in *P. halepensis*, indicating divergent ecophysiological responses and, possibly, changes in resource allocation to growth. This study therefore highlights UAV imagery as a valid high-throughput phenotypic tool with promise to bridge the gap between the molecular and field characterisation of forest tree species, potentially improving the prediction of adaptive responses in the context of global change.

ACKNOWLEDGMENTS

We thank the technical assistance of J. del Castillo.

AUTHOR CONTRIBUTIONS

J.V. and F.S. conceived and designed the research. F.S., S.C.K., and J.V. collected the data; F.S., V.R.D. and J.L.A. analysed the data; F.S. and J.V. wrote the manuscript, with contributions from the other authors.

REFERENCES

Aranda I., Pardo F., Gil L., Pardos J. (2004) Anatomical basis of the change in leaf mass per area and nitrogen investment with relative irradiance within the canopy of eight temperate tree species. *Acta Oecologica*, 25, 187–195.

Baldwin V.C., Peterson K.D., Burkhart H.E., Amateis R.L., Dougherty P.M. (1997) Equations for estimating loblolly pine branch and foliage weight and surface area distributions. *Canadian Journal of Forest Research*, 27, 918–927.

Berni J., Zarco-Tejada P.J., Suarez L., Fereres E. (2009) Thermal and narrowband multispectral remote sensing for vegetation monitoring from an unmanned aerial vehicle. *IEEE Transactions on Geoscience and Remote Sensing*, 47, 722–738.

Bussotti F., Pollastrini M., Holland V., Brüggemann W. (2015) Functional traits and adaptive capacity of European forests to climate change. *Environmental and Experimental Botany*, 111, 91–113.

Casadesús J., Kaya Y., Bort J. *et al.* (2007) Using vegetation indices derived from conventional digital cameras as selection criteria for wheat breeding in water-limited environments. *Annals of Applied Biology*, 150, 227–236.

Casadesús J., Villegas D. (2014) Conventional digital cameras as a tool for assessing leaf area index and biomass for cereal breeding: Conventional digital cameras for cereal breeding. *Journal of Integrative Plant Biology*, 56, 7–14.

Choury Z., Shestakova T.A., Himrane H., Touchan R., Kherchouche D., Camarero J.J., Voltas J. (2017) Quarantining the Sahara desert: growth and water-use efficiency of Aleppo pine in the Algerian Green Barrier. *European Journal of Forest Research*, 136, 139–152.

Climent J., Prada M.A., Calama R., Chambel M.R., de Ron D.S., Alia R. (2008) To grow or to seed: ecotypic variation in reproductive allocation and cone production by young female Aleppo pine (*Pinus halepensis*, Pinaceae). *American Journal of Botany*, 95, 833–842.

Costa J.M., Grant O.M., Chaves M.M. (2013) Thermography to explore plant–environment interactions. *Journal of Experimental Botany*, 64, 3937–3949.

Cuesta B., Vega J., Villar-Salvador P., Rey-Benayas J.M. (2010) Root growth dynamics of Aleppo pine (*Pinus halepensis* Mill.) seedlings in relation to shoot elongation, plant size and tissue nitrogen concentration. *Trees*, 24, 899–908.

Daughtry C.S.T., Walthall C.L., Kim M.S., De Colstoun E.B., McMurtrey J.E. (2000) Estimating corn leaf chlorophyll concentration from leaf and canopy reflectance. *Remote sensing of Environment*, 74, 229–239.

Eamus D., O'Grady A.P., Hutley L. (2000) Dry season conditions determine wet season water use in the wet–tropical savannas of northern Australia. *Tree Physiology*, 20, 1219–1226.

Fahlgren N., Gehan M.A., Baxter I. (2015) Lights, camera, action: high-throughput plant phenotyping is ready for a close-up. *Current Opinion in Plant Biology*, 24, 93–99.

Fardusi M.J., Ferrio J.P., Comas C., Voltas J., Resco de Dios V., Serrano L. (2016) Intra-specific association between carbon isotope composition and productivity in woody plants: A meta-analysis. *Plant Science*, 251, 110–118.

Farquhar G.D., Ehleringer J.R., Hubick K.T. (1989) Carbon isotope discrimination and photosynthesis. *Annual Review of Plant Physiology and Plant Molecular Biology*, 40, 503–537.

Gitelson A.A., Merzlyak M.N., Chivkunova O.B. (2001) Optical properties and nondestructive estimation of anthocyanin content in plant leaves. *Photochemistry and Photobiology*, 74, 38–45.

Gitelson A.A., Zur Y., Chivkunova O.B., Merzlyak M.N. (2002) Assessing carotenoid content in plant leaves with reflectance spectroscopy. *Photochemistry and Photobiology*, 75, 272–281.

Gonzalez-Dugo V., Zarco-Tejada P., Nicolás E., Nortes P.A., Alarcón J.J., Intrigliolo D.S., Fereres E. (2013) Using high resolution UAV thermal imagery to assess the variability in the water status of five fruit tree species within a commercial orchard. *Precision Agriculture*, 14, 660–678.

Gracia-Romero A., Kefauver S.C., Vergara-Díaz O., Zaman-Allah M.A., Prasanna B.M., Cairns J.E., Araus J.L. (2017) Comparative performance of ground vs. aerially assessed rgb and multispectral indices for early-growth evaluation of maize performance under phosphorus fertilization. *Frontiers in Plant Science*, 8, 2004.

Gracia-Romero A., Vergara-Díaz O., Thierfelder C., Cairns J., Kefauver S., Araus J. (2018) Phenotyping conservation agriculture management effects on ground and aerial remote sensing assessments of maize hybrids performance in Zimbabwe. *Remote Sensing*, 10, 349.

Großkinsky D.K., Svensgaard J., Christensen S., Roitsch T. (2015) Plant phenomics and the need for physiological phenotyping across scales to narrow the genotype-to-phenotype knowledge gap. *Journal of Experimental Botany*, 66, 5429–5440.

Haboudane D., Miller J.R., Tremblay N., Zarco-Tejada P.J., Dextraze L. (2002) Integrated narrow-band vegetation indices for prediction of crop chlorophyll content for application to precision agriculture. *Remote sensing of environment*, 81, 416–426.

Hernández-Clemente R., Navarro-Cerrillo R.M., Zarco-Tejada P.J. (2012) Carotenoid content estimation in a heterogeneous conifer forest using narrow-band indices and PROSPECT+ DART simulations. *Remote Sensing of Environment*, 127, 298–315.

Huete A., Didan K., Miura T., Rodriguez E.P., Gao X., Ferreira L.G. (2002) Overview of the radiometric and biophysical performance of the MODIS vegetation indices. *Remote sensing of environment*, 83, 195–213.

Hunt E.R., Cavigelli M., Daughtry C.S., Mcmurtrey J.E., Walthall C.L. (2005) Evaluation of digital photography from model aircraft for remote sensing of crop biomass and nitrogen status. *Precision Agriculture*, 6, 359–378.

Hunt E.R., Daughtry C.S.T., Eitel J.U.H., Long D.S. (2011) Remote Sensing leaf chlorophyll content using a visible band index. *Agronomy Journal*, 103, 1090–1099.

John J.A., Williams E.R. (1998) t-Latinized Designs. *Australian and New Zealand Journal of Statistics*, 40, 111–118.

Judd D.B. (1940) Hue saturation and lightness of surface colors with chromatic illumination. *Journal of the Optical Society of America*, 30, 2–32.

Kefauver S.C., Vicente R., Vergara-Díaz O., Fernandez-Gallego J.A., Kerfal S., López A., Melichar J.P.E., Serret M.D., Araus J.L. (2017) Comparative UAV and field phenotyping to assess yield and nitrogen use efficiency in hybrid and conventional barley. *Frontiers in Plant Science*, 8, 1733.

Klein T., Di Matteo G., Rotenberg E., Cohen S., Yakir D. (2013) Differential ecophysiological response of a major Mediterranean pine species across a climatic gradient. *Tree Physiology*, 33, 26–36.

Klein T. (2014) The variability of stomatal sensitivity to leaf water potential across tree species indicates a continuum between isohydric and anisohydric behaviours. *Functional Ecology*, 28, 1313–1320.

Li L., Wu H.X. (2005) Efficiency of early selection for rotation-aged growth and wood density traits in *Pinus radiata*. *Canadian Journal of Forest Research*, 35, 2019–2029.

Lobos G.A., Camargo A.V., del Pozo A., Araus J.L., Ortiz R., Doonan J.H. (2017) Editorial: plant phenotyping and phenomics for plant breeding. *Frontiers in Plant Science*, 8, 2181.

Ludovisi R., Tauro F., Salvati R., Khoury S., Mugnozza Scarascia G., Harfouche A. (2017) UAV-Based thermal imaging for high-throughput field phenotyping of black poplar response to drought. *Frontiers in Plant Science*, 8, 1681.

Mátyás C. (1996) Climatic adaptation of trees: rediscovering provenance tests. *Euphytica*, 92, 45–54.

McCrady R.L., Jokela E.J. (1996) Growth phenology and crown structure of selected loblolly pine families planted at two spacings. *Forest Science*, 42, 46–57.

McDowell N.G., Adams H.D., Bailey J.D., Kolb T.E. (2007) The role of stand density on growth efficiency, leaf area index, and resin flow in southwestern ponderosa pine forests. *Canadian Journal of Forest Research*, 37, 343–355.

Niinemets Ü. (2010) A review of light interception in plant stands from leaf to canopy in different plant functional types and in species with varying shade tolerance. *Ecological Research*, 25, 693–714.

Otieno D.O., Schmidt M.W.T., Adiku S., Tenhunen J. (2005) Physiological and morphological responses to water stress in two Acacia species from contrasting habitats. *Tree physiology*, 25, 361–371.

Otsu N. (1979) A threshold selection method from gray-level histograms. *IEEE transactions on systems, man, and cybernetics*, 9, 62–66.

Pausas J.G., Bladé C., Valdecantos A., Seva J.P., Fuentes D., Alloza J.A., Vilagrosa A., Bautista S., Cortina J., Vallejo R. (2004) Pines and oaks in the restoration of Mediterranean landscapes of Spain: new perspectives for an old practice—a review. *Plant ecology*, 171, 209–220.

Peñuelas J., Filella I., Biel C., Serrano L., Save R. (1993) The reflectance at the 950–970 nm region as an indicator of plant water status. *International journal of remote sensing*, 14, 1887–1905.

Purevdorj T.S., Tateishi R., Ishiyama T., Honda Y. (1998) Relationships between percent vegetation cover and vegetation indices. *International journal of remote sensing*, 19, 3519–3535.

Purves D.W., Lichstein J.W., Pacala S.W. (2007) Crown plasticity and competition for canopy space: a new spatially implicit model parameterized for 250 north american tree species. *PLoS ONE*, 2, e870.

Reinhardt E., Scott J., Gray K., Keane R. (2006) Estimating canopy fuel characteristics in five conifer stands in the western United States using tree and stand measurements. *Canadian Journal of Forest Research*, 36, 2803–2814.

Richardson A.J., Wiegand C.L. (1977) Distinguishing vegetation from soil background information. *Photogrammetric engineering and remote sensing*, 43, 1541–1552.

Roberts D.A., Roth K.L., Perroy R.L. (2016) Hyperspectral vegetation indices. In: Huete A., Lyon J.G., Thenkabail P.S. (eds.) *Hyperspectral Remote Sensing of Vegetation*. pp. 309–328, Boca Raton, FL: CRC Press.

Rondeaux G., Steven M., Baret F. (1996) Optimization of soil-adjusted vegetation indices. *Remote sensing of environment*, 55, 95–107.

Roujean J.L., Breon F.M. (1995) Estimating PAR absorbed by vegetation from bidirectional reflectance measurements. *Remote sensing of Environment*, 51, 375–384.

Rouse Jr J., Haas R.H., Schell J.A., Deering D.W. (1974) Monitoring vegetation systems in the Great Plains with ERTS. In: *Third ERTS Symposium*, pp. 309-317. Ed. NASA SP-351. Washington DC, USA.

Sankaran S., Khot L.R., Espinoza C.Z., *et al.* (2015) Low-altitude, high-resolution aerial imaging systems for row and field crop phenotyping: A review. *European Journal of Agronomy*, 70, 112–123.

Santos-del-Blanco L., Bonser S.P., Valladares F., Chambel M.R., Climent J. (2013) Plasticity in reproduction and growth among 52 range-wide populations of a Mediterranean conifer: adaptive responses to environmental stress. *Journal of Evolutionary Biology*, 26, 1912–1924.

Savolainen O., Pyhäjärvi T., Knürr T. (2007) Gene flow and local adaptation in trees. *Annual Review of Ecology, Evolution, and Systematics*, 38, 595–619.

Schiller G., Atzmon N. (2009) Performance of Aleppo pine (*Pinus halepensis*) provenances grown at the edge of the Negev desert: A review. *Journal of Arid Environments*, 73, 1051–1057.

Schindelin J., Arganda-Carreras I., Frise E. *et al.* (2012) Fiji: an open-source platform for biological-image analysis. *Nature Methods*, 9, 676–682.

Serra-Varela M.J., Alía R., Daniels R.R., Zimmermann N.E., Gonzalo-Jiménez J., Grivet D. (2017) Assessing vulnerability of two Mediterranean conifers to support genetic conservation management in the face of climate change. *Diversity and Distributions*, 23, 507–516.

Tang L., Shao G. (2015) Drone remote sensing for forestry research and practices. *Journal of Forestry Research*, 26, 791–797.

Tattaris M., Reynolds M.P., Chapman S.C. (2016) A direct comparison of remote sensing approaches for high-throughput phenotyping in plant breeding. *Frontiers in Plant Science*, 7, 1131.

Tognetti R., Michelozzi M., Giovannelli A. (1997) Geographical variation in water relations, hydraulic architecture and terpene composition of Aleppo pine seedlings from Italian provinces. *Tree Physiology*, 17, 241–250.

Torresan C., Berton A., Carotenuto F., Di Gennaro S.F., Gioli B., Matese A., Miglietta F., Vagnoli C., Zaldei A., Wallace L. (2017) Forestry applications of UAVs in Europe: A review. *International Journal of Remote Sensing*, 38, 2427–2447.

Vizcaíno-Palomar N., Ibáñez I., González-Martínez S.C., Zavala M.A., Alía R. (2016) Adaptation and plasticity in aboveground allometry variation of four pine species along environmental gradients. *Ecology and Evolution*, 6, 7561–7573.

Voltas J., Chambel M.R., Prada M.A., Ferrio J.P. (2008) Climate-related variability in carbon and oxygen stable isotopes among populations of Aleppo pine grown in common-garden tests. *Trees*, 22, 759–769.

Voltas J., Lucabaugh D., Chambel M.R., Ferrio J.P. (2015) Intraspecific variation in the use of water sources by the circum-Mediterranean conifer *Pinus halepensis*. *New Phytologist*, 208, 1031–1041.

Voltas J., Shestakova, T.A., Patsiou, T., di Matteo, G., Klein, T. (2018) Ecotypic variation and stability in growth performance of the thermophilic conifer *Pinus halepensis* across the Mediterranean basin. *Forest Ecology and Management*, 424, 205–215.

Vose J.M., Allen H.L. (1988) Leaf area, stemwood growth, and nutrition relationships in loblolly pine. *Forest Science*, 34, 547–563.

Weinstein A. (1989) Geographic variation and phenology of *Pinus halepensis*, *P. brutia* and *P. eldarica* in Israel. *Forest Ecology and Management*, 27, 99–108.

Weiskittel A.R., Maguire D.A. (2006) Branch surface area and its vertical distribution in coastal Douglas-fir. *Trees*, 20, 657–667.

Wong C.Y.S., Gamon J.A. (2015) The photochemical reflectance index provides an optical indicator of spring photosynthetic activation in evergreen conifers. *New Phytologist*, 206, 196–208.

Wu C., Niu Z., Tang Q., Huang W. (2008) Estimating chlorophyll content from hyperspectral vegetation indices: Modeling and validation. *Agricultural and Forest Meteorology*, 148, 1230–1241.

Xue J., Su B. (2017) Significant remote sensing vegetation indices: a review of developments and applications. *Journal of Sensors*, 2017, 1–17.

Yamazaki F., Liu W., Takasaki M. (2009) Characteristics of shadow and removal of its effects for remote sensing imagery, In: *Geoscience and Remote Sensing Symposium, IEEE*, pp. IV–426. Ed. IEEE International, IGARSS.

Yu N., Li L., Schmitz N., Tian L.F., Greenberg J.A., Diers B.W. (2016) Development of methods to improve soybean yield estimation and predict plant maturity with an unmanned aerial vehicle based platform. *Remote Sensing of Environment*, 187, 91–101.

Zarco-Tejada P., Miller J., Morales A., Berjón A., Agüera J. (2004) Hyperspectral indices and model simulation for chlorophyll estimation in open-canopy tree crops. *Remote Sensing of Environment*, 90, 463–476.

Chapter I - Tables and Figures

Table 1. Environmental and sun conditions at the moment of each flight. Air temperature (T) and relative humidity (RH) were measured in situ and used to estimate vapour pressure deficit (VPD). Azimut and sun elevation were calculated based on the position of the trial, the period of the year and the time of the flight. Sun radiation was retrieved for the time of the flight from a meteorological station located *ca.* 10 km away from the trial.

Variable	**July 2016**	**Nov. 2016**	**May 2017**
T (°C)	33.2	18.6	32.2
RH (%)	38.8	37.3	23.0
VPD (kPa)	3.1	1.3	3.7
Azimut (°)	225	207	232
Sun elevation (°)	62.8	26.3	63.0
Sun radiation (W m^{-2})	846	527	863

Table 2. Multispectral and RGB-derived vegetation indices (VIs) considered in this study. For those indices based on specific bands of the light spectrum, the formula used for calculation is reported. R indicates the reflectance in a single or in a range of wavelengths (in nm). RGB indices were calculated considering a continuous range of wavelengths, while single bands were used for multispectral VIs. The calculation of other indices that are not based on the reflectance in specific bands (Intensity, Hue, Saturation, a*, b*, u*, v* and GA) is described in the text.

Index	Descriptor	Wavelengths	Formula	Reference
Multispectral VIs				
NDVI	Leaf area	Red, NIR	$(R_{840} - R_{670})/(R_{840} + R_{670})$	Rouse *et al.*, 1973
OSAVI	Leaf area	Red, NIR	$(R_{840} - R_{670})/(R_{840} + R_{670} + 0.16)\times1.16$	Rondeaux *et al.*, 1996
RDVI	Leaf area	Red, NIR	$(R_{840} - R_{670})/(R_{840} + R_{670})^{\wedge 1/2}$	Roujean and Breon, 1995
EVI	Leaf area	Blue, Red, NIR	$2.5\times(R_{840} - R_{670})/[(R_{840} + 6\times R_{670} - 7.5\times R_{450}) + 1]$	Huete *et al.*, 2002
MCARI	Leaf chlorophyll content; leaf area	Green, Red, NIR	$[(R_{700} - R_{670})\text{-}0.2\times(R_{700} - R_{550})]\times(R_{700}/R_{670})$	Daughtry, 2000
TCARI	Leaf chlorophyll content; leaf area	Green, Red, NIR	$3\times(R_{700} - R_{670})\text{-}0.2\times(R_{700} - R_{550})\times(R_{700}/R_{670})$	Haboudane *et al.*,2002
TCARI/OSAVI	Leaf chlorophyll content	Green, Red, NIR	-	Haboudane *et al.*,2002
ARI2	Anthocyanins content	Blue, NIR	$R_{840}\times(1/R_{550} - 1/R_{700})$	Gitelson *et al.*, 2001
CRI2	Carotenoid content	Blue, NIR	$1/R_{550} - 1/R_{700}$	Gitelson *et al.*, 2002
WBI	Water content	NIR	R_{900} / R_{950}	Peñuelas *et al.*, 1993
RGB VIs				
NRGDI	Leaf area	Green, Red	$(R_{490:570} - R_{640:760})/(R_{490:570} + R_{640:760})$	Hunt *et al.*, 2005
TGI	Leaf chlorophyll content	Green, Red, Blue	$\text{-}0.5\times[(R_{665:675} - R_{475:485})\times(R_{670} - R_{550}) - (R_{665:675} - R_{445:555})\times(R_{670} - R_{480})]$	Hunt *et al.*, 2011
Intensity	-	Visible spectrum	-	Casadesús *et al.*, 2007
Hue	-	Visible spectrum	-	Casadesús *et al.*, 2007
Saturation	-	Visible spectrum	-	Casadesús *et al.*, 2007
a*	-	Visible spectrum	-	Casadesús *et al.*, 2007
b*	-	Visible spectrum	-	Casadesús *et al.*, 2007
u*	-	Visible spectrum	-	Casadesús *et al.*, 2007
v*	-	Visible spectrum	-	Casadesús *et al.*, 2007
GA	-	Visible spectrum	-	Casadesús *et al.*, 2007

Table 3. *F* statistics and *P* values of the fixed population effect of the ANOVA fitted for each vegetation index and flight.

		July 2016		Nov. 2016		May-17	
		F	***P* - value**	***F***	***P* - value**	***F***	***P* - value**
Multispectral VIs (plot)							
	NDVI	1.16	0.25	1.51	0.03	1.39	0.07
	OSAVI	1.68	0.01	1.49	0.04	1.77	<0.01
	RDVI	1.74	<0.01	1.59	0.02	1.91	<0.01
	EVI	1.83	<0.01	1.28	0.13	0.85	0.74
	MCARI	2.16	<0.01	1.74	<0.01	2.88	<0.01
	TCARI	1.86	<0.01	1.44	0.05	2.29	<0.01
	TCARI/OSAVI	1.2	0.21	1	0.48	1.27	0.13
	ARI2	1.67	0.01	1.3	0.11	1.69	<0.01
	CRI2	1.45	0.05	1.2	0.21	1.35	0.09
	WBI	1.21	0.19	1.12	0.3	1.97	<0.01
Multispectral VIs (vegetation)							
	NDVI	1.68	0.01	1.99	<0.01	1.75	<0.01
	OSAVI	2.61	<0.01	1.88	<0.01	2.41	<0.01
	RDVI	2.72	<0.01	1.95	<0.01	2.6	<0.01
	EVI	2.36	<0.01	1.93	<0.01	2.43	<0.01
	MCARI	3.26	<0.01	2.01	<0.01	3.48	<0.01
	TCARI	2.27	<0.01	1.47	0.04	2.38	<0.01
	TCARI/OSAVI	1.2	0.21	1.22	0.18	1.48	0.04
	ARI2	1.33	0.1	1.01	0.47	1.86	<0.01
	CRI2	1.12	0.29	1.05	0.41	1.69	<0.01
	WBI	1.05	0.39	1.07	0.36	2.35	<0.01
Multispectral VIs (vegetation)							
	NGRDI	1.89	<0.01	1.34	0.09	1.87	<0.01
	TGI	1.16	0.24	0.22	0.88	1.46	0.05
	Intensity	1.15	0.25	0.26	0.81	1.47	0.04
	Hue	1.96	<0.01	0.12	1.3	1.43	0.05
	Saturation	1.73	<0.01	1.34	0.09	2.01	<0.01
	a*	1.91	<0.01	1.59	0.02	2.35	<0.01
	b*	1.46	0.04	1.24	0.16	2.1	<0.01
	u*	1.61	0.02	1.53	0.03	2.3	<0.01
	v*	1.39	0.07	1.25	0.15	2.12	<0.01
	GA	2.25	<0.01	1.85	<0.01	2.25	<0.01
Vegetation cover							
		1.78	<0.01	1.56	0.02	1.49	0.04
Canopy temperature*							
		1.54	0.03	1.01	0.47	0.92	0.63

*only pixels classified as "vegetation" in July-2016 and May-2017; whole-plot temperature (all pixels) in November-2016.

Table 4. Pearson correlation coefficients between population means of vegetation indices (VI) and either vegetation cover (VC) or log-transformed stem volume (Vob). Empty cells indicate lack of population differentiation for the corresponding VI as found in the ANOVAs.

	VC			Vob		
	Jul. 16	**Nov. 16**	**May. 17**	**Jul-16**	**Nov. 16**	**May. 17**
Multispectral VIs (plot)						
NDVI	-	0.47**	-	-	0.35**	-
OSAVI	0.65**	0.63**	0.72**	0.68**	0.62**	0.59**
RDVI	0.62**	0.64**	0.72**	0.69**	0.60**	0.57**
EVI	0.54**	-	-	0.66**	-	-
MCARI	0.44**	0.55**	0.52**	0.65**	0.54**	0.35**
TCARI	0.43**	0.64**	0.34*	0.58**	0.57**	0.17
TCARI/OSAVI	-	-	-	-	-	-
ARI2	-	-	-0.31*	-	-	-0.03
CRI2	-0.32*	-	-0.41**	-0.35**	-	-0.1
WBI	-	-	-0.28*	-	-	-0.19
Multispectral VIs (vegetation)						
NDVI	0.23	0.2	0.54**	0.52**	0.41**	0.60**
OSAVI	0.33*	0.26	0.60**	0.69**	0.63**	0.58**
RDVI	0.30*	0.23	0.58**	0.69**	0.65**	0.57**
EVI	0.34*	0.28*	0.44**	0.70**	0.65**	0.39**
MCARI	0.13	0.24	0.31*	0.60**	0.57**	0.28*
TCARI	0.21	0.28*	0.22	0.62**	0.66**	0.16
TCARI/OSAVI	-	-	-0.26	-	-	-0.35**
ARI2	-	-	-0.07	-	-	0.02
CRI2	-	-	-0.32*	-	-	-0.12
WBI	-	-	-0.39**	-	-	-0.30*
RGB VIs						
NGRDI	0.57**	-	0.71**	0.47**	-	0.59**
TGI	-	-	-0.44**	-	-	-0.60**
Intensity	-	-	-0.45**	-	-	-0.62**
Hue	0.59**	-	0.05	0.53**	-	0
Saturation	0.48**	-	0.59**	0.60**	-	0.57**
a*	-0.60**	-0.50**	-0.66**	-0.51**	-0.56**	-0.49**
b*	0.55**		0.62**	0.53**	-	0.48**
u*	-0.52**	-0.46**	-0.62**	-0.44**	-0.37**	-0.44**
v*	-	-	0.62**	-	-	0.42**
GA	0.37**	0.53**	0.68**	0.51**	0.46**	0.49**

Significant correlations are indicated by * ($P < 0.05$) or ** ($P < 0.01$

Table 5. Stepwise multiple linear regression of stem volume (log-transformed) based on the different categories of vegetation indices (multispectral on the whole plot [Multispectral $_P$], multispectral on pixels containing vegetation [Multispectral $_V$], or RGB-derived) in July-2016 and May-2017. RGB indices were also combined with the two groups of multispectral indices. Only the combination showing the highest R^2 (with either multispectral indices measured on the whole plot or on pixels containing vegetation) is reported.

	Indices categories	Model	R^2	RMSE
July 2016[a]	**Multispectral $_P$**	Log(Vob) = 14.44 × OSAVI - 2.85	0.48	0.311
	Multispectral $_V$	Log(Vob) = 7.02 × OSAVI + 4.68 × EVI + 0.02 × VC - 4.09	0.50	0.314
	RGB	Log(Vob) = 15.49 × *Saturation* - 1.87	0.35	0.353
	RGB + Multispectral $_P$	Log(Vob) = 9.88 × *Saturation* + 0.30 × *u** + 18.09 × OSAVI - 8.35	0.57	0.292
July 2016 - T[b]	**Multispectral $_P$**	Log(Vob) = 6.09 × OSAVI -0.38 × T + 12.88	0.61	0.276
	Multispectral $_V$	Log(Vob) = 3.90 × EVI - 0.40 × T + 14.06	0.60	0.278
	RGB	Log(Vob) = -0.53 × T + 20.30	0.57	0.287
	RGB + Multispectral $_V$	Log(Vob) = 3.90 × EVI - 0.40 × T + 14.06	0.60	0.278
May 2017	**Multispectral $_P$**	Log(Vob) = 19.11 × OSAVI – 15.82 × MCARI 3.49 - 3.23	0.40	0.241
	Multispectral $_V$	Log(Vob) = 12.80 × NDVI + 5.21 × EVI - 11.09 × MCARI – 7.59	0.46	0.235
	RGB	Log(Vob) = 0.77 × NGRDI - 4.12 × *Intensity* + 0.57 × *b** - 1.55 × *v** - 6.15	0.57	0.210
	RGB + Multispectral $_V$	Log(Vob) = 0.71 × NGRDI - 5.98 × *Intensity* + 0.60 × *b** - 0.69 × *v** + 2.43 × GA + 11.93 × MCARI + 6.88	0.63	0.198

[a] regression performed without considering canopy temperature; [b] regression including canopy temperature

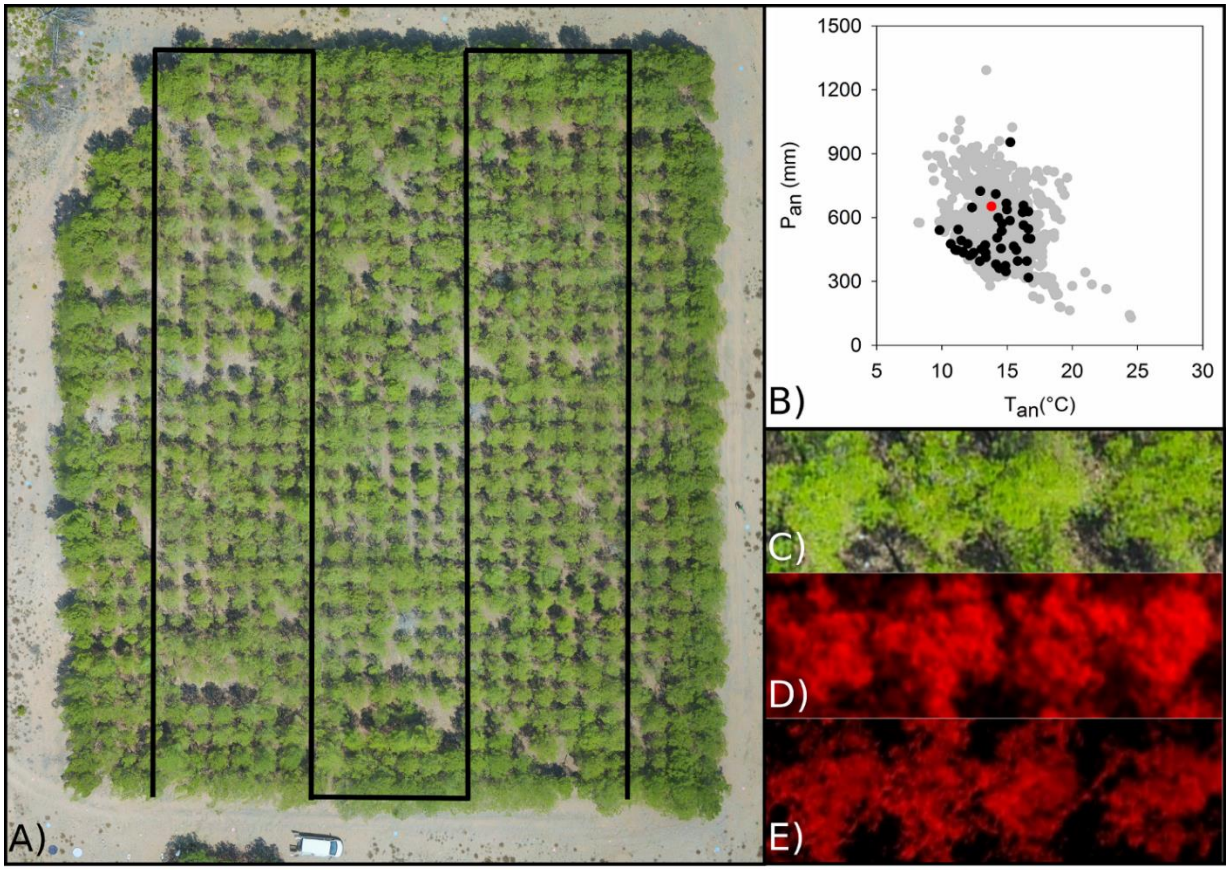

Figure 1. Aerial images of the genetic trial of *P. halepensis* considered for this study and main characteristics of the 56 populations tested. A) Aerial image of the complete trial; the black line represents the approximate trajectory followed by the UAV. B) Mean annual precipitation (P_{an}) and temperature (T_{an}) for the distribution range (EUFORGEN distribution map (http://www.euforgen.org/species/pinus-halepensis/) of *P. halepensis* (grey dots) calculated in 10' resolution grids from the WorldClim database (period 1960-1990). Temperature and precipitation of the site where the 56 populations were located at origin (black dots) and of the trial site (red dot) are shown. C) Aerial image of one experimental unit in RGB. D) Aerial image of one experimental unit as in C) in infrared (false colour). E) Aerial image of one experimental unit as in C) in infrared, but cropped for pixels containing vegetation (NDVI > 0.5

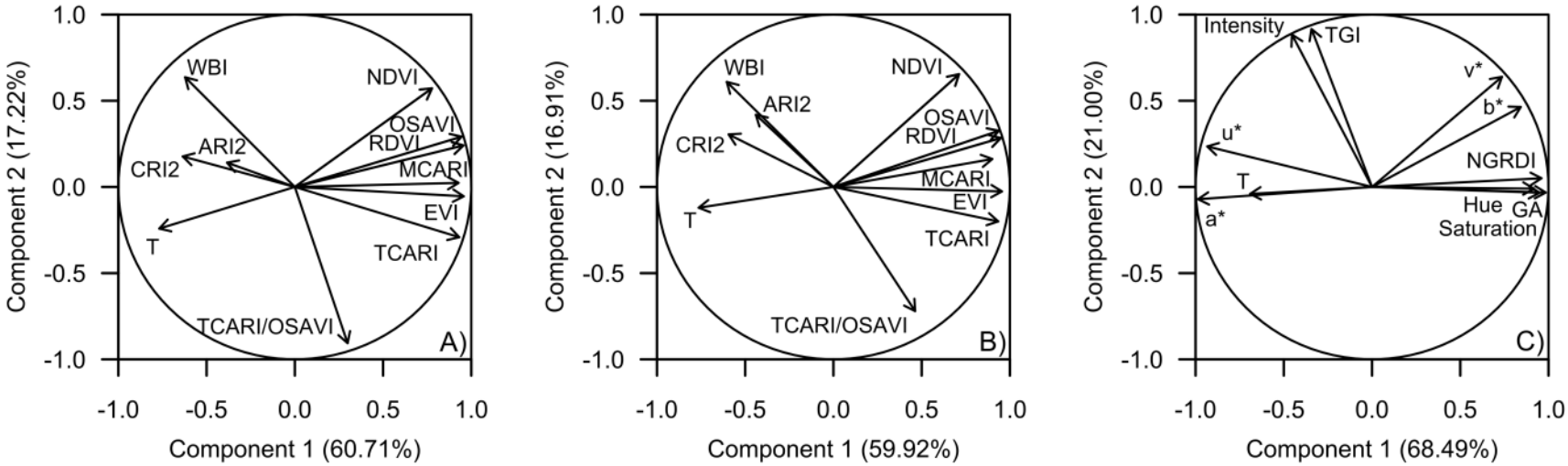

Figure 2. Component loadings of the Principal Component Analysis for multispectral indices measured on whole plot (A), multispectral indices measured on vegetation pixels only (B) and of RGB-derived indices (C) plus canopy temperature (T) measured in July-2016 based on population means. Abbreviations are as reported in the "Material and Methods" section.

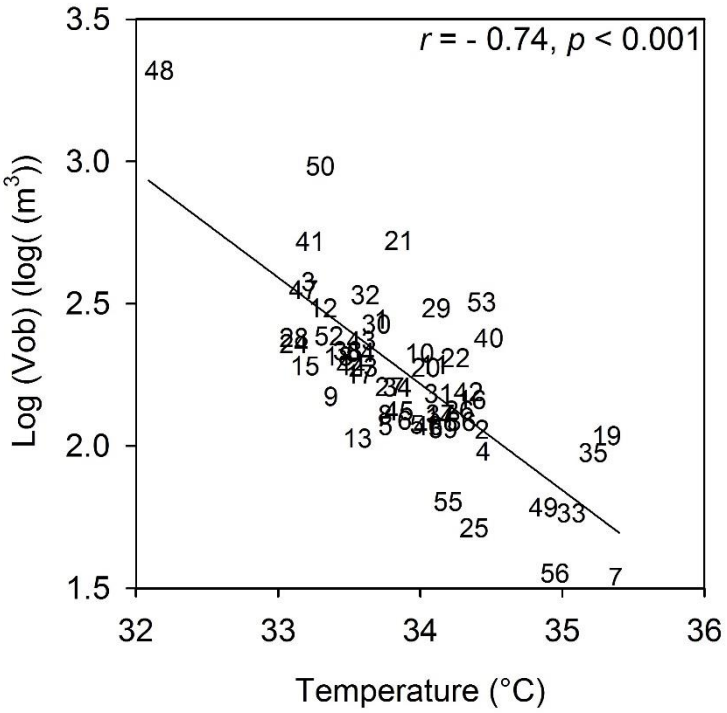

Figure 3. Correlation between canopy temperature (measured on pixels containing vegetation) and stem volume (log-transformed) calculated at the population level in July-2016. Codes represent the populations tested in the trial as in Appendix (Table S1).

Chapter I – Appendix

Table S1. Origin of the 56 *Pinus halepensis* populations tested in the genetic trial.

Population	Code	Region	Country	Latitude	Longitude
Cabanelles	1	Catalonia	Spain	42° 14' 24" N	02° 46' 48" E
Tivissa	2	Catalonia	Spain	41° 02' 60" N	00° 45' 36" E
Sant Salvador de Guardiola	3	Catalonia	Spain	41° 40' 12" N	01° 45' 36" E
Zuera	4	Ebro Depression	Spain	41° 55' 12" N	00° 55' 12" W
Valdeconcha	5	Southern Plateau	Spain	40° 26' 23" N	02° 52' 12" W
Alcantud	6	Southern Plateau	Spain	40° 33' 36" N	03° 19' 48" W
Villarejo de Salvanes	7	Southern Plateau	Spain	40° 05' 24" N	02° 18' 36" W
Cirat	8	Iberian Range	Spain	40° 02' 60" N	00° 27' 36" W
Tuejar	9	Iberian Range	Spain	39° 48' 36" N	01° 09' 36" W
Enguidanos	10	Iberian Range	Spain	39° 38' 24" N	01° 38' 60" W
Tibi	11	East Spain	Spain	38° 31' 12" N	00° 39' 00" W
Altura	12	Iberian Range	Spain	39° 47' 24" N	00° 37' 12" W
Villa de Ves	13	East Spain	Spain	39° 10' 48" N	01° 15' 00" W
Jarafuel	14	East Spain	Spain	39° 09' 36" N	01° 00' 36" W
Bicorp	15	East Spain	Spain	39° 06' 00" N	00° 51' 36" W
Commercial seed	16	East Spain	Spain	-	-
Benicassim	17	Iberian Range	Spain	40° 04' 12" N	00° 01' 48"E
Gilet	18	Iberian Range	Spain	39° 58' 12" N	03° 21' 00" W
Villajoyosa	19	East Spain	Spain	38° 29' 24" N	00° 18' 00" W
Ricote	20	N. Betic Mts	Spain	38° 08' 24" N	01° 25' 48" W
Monovar	21	N. Betic Mts	Spain	38° 22' 48" N	00° 57' 00" W
Monovar	22	N. Betic Mts	Spain	38° 23' 24" N	00° 55' 12" W
Paterna del Madera	23	N. Betic Mts	Spain	38° 37' 48" N	02° 16' 12" W
Abaran	24	N. Betic Mts	Spain	38° 16' 12" N	01° 15' 36" W
Quentar	25	S. Betic Mts	Spain	37° 31' 12" N	03° 24' 36" W
Benamaurel	26	S. Betic Mts	Spain	37° 42' 00" N	02° 44' 24" W
Velez Blanco	27	S. Betic Mts	Spain	37° 47' 24" N	02° 00' 36" W
Santiago-Pontones	28	S. Betic Mts	Spain	38° 13' 48" N	02° 28' 12" W
Lorca	29	S. Betic Mts	Spain	37° 45' 00" N	01° 57' 00" W
Alhama de Murcia	30	S. Betic Mts	Spain	37° 51' 36" N	01° 31' 48" W
Quesada	31	S. Betic Mts	Spain	37° 45' 00" N	03° 01' 12" W
Lentegi	32	South Spain	Spain	36° 49' 12" N	03° 41' 24" W
Carratraca	33	South Spain	Spain	36° 51' 00" N	04° 49' 48" W
Frigiliana	34	South Spain	Spain	36° 49' 12" N	03° 55' 12" W
Palma de Mallorca	35	Majorca	Spain	39° 53' 59" N	03° 00' 00" E
Santanyi	36	Majorca	Spain	39° 16' 48" N	03° 02' 24" E
Alcudia	37	Majorca	Spain	39° 52' 12" N	03° 10' 12" E
Calvia	38	Majorca	Spain	39° 32' 60" N	03° 08' 24" E
Marcadal, Es	39	Menorca	Spain	39° 58' 12" N	04° 10' 12" E
Migjorn Gran, Es	40	Menorca	Spain	39° 54' 36" N	04° 02' 60" E
Sant Josep de sa Talaia	41	Ibiza	Spain	38° 52' 48" N	01° 14' 24" E
Sant Josep de sa Talaia	42	Ibiza	Spain	38° 50' 24" N	01° 23' 60" E
Sant Antoni de Portmany	43	Ibiza	Spain	39° 02' 60" N	01° 19' 48" E
Valbuena de Duero	44	North. Plateu (Reforestation)	Spain	41° 39' 36" N	04° 16' 48" W
Vega de Valdetronco	45	North. Plateu (Reforestation)	Spain	41° 35' 24" N	05° 04' 48" W
Villan de Tordesillas	46	North. Plateu (Reforestation)	Spain	41° 36' 00" N	04° 55' 48" W
Istaia-eyboia	47	Greece	Greece	38° 44' 24" N	23° 29' 24" E
Amfilohia	48	Greece	Greece	38° 51' 36" N	21° 23' 24" E
Tatoi-Attica	49	Greece	Greece	38° 27' 00" N	23° 26' 60" E
Kassandra	50	Greece	Greece	40° 05' 24" N	23° 52' 48" E
Gemenos	51	France	France	43° 25' 12" N	05° 40' 12" E
Litorale tarantino	52	Italy	Italy	40° 37' 12" N	17° 06' 35" E
Gargano Monte Pucci	53	Italy	Italy	41° 53' 60" N	15° 56' 24" E
Gargano Marzini	54	Italy	Italy	41° 32' 60" N	15° 51' 36" E
Thala	55	Tunisia	Tunisia	35° 34' 12" N	08° 39' 00" E
Tabarka	56	Tunisia	Tunisia	36° 30' 00" N	09° 04' 12" E

Table S2. Mean values (±standard deviation, SD) of the populations' means for vegetation indices, vegetation cover and canopy temperature in July 2016, November 2016 and May 2017.

		July 16	November 2016	May 2017
		Mean ± SD	Mean ± SD	Mean ± SD
Multispectral VIs (plot)				
	NDVI	0.53 ± 0.02	0.68 ± 0.01	0.62 ± 0.02
	OSAVI	0.35 ± 0.02	0.44 ± 0.01	0.39 ± 0.01
	RDVI	0.26 ± 0.01	0.38 ± 0.01	0.30 ± 0.01
	EVI	0.35 ± 0.02	0.61 ± 0.04	0.42 ± 0.02
	PRI	0.16 ± 0.01	0.23 ± 0.01	0.18 ± 0.01
	MCARI	0.15 ± 0.01	0.21 ± 0.01	0.12 ± 0.01
	TCARI	0.18 ± 0.01	0.21 ± 0.01	0.15 ± 0.01
	TCARI/OSAVI	0.51 ± 0.02	0.47 ± 0.01	0.40 ± 0.01
	ARI2	0.78 ± 0.06	0.63 ± 0.05	0.56 ± 0.02
	CRI2	5.91 ± 1.07	3.63 ± 0.49	3.51 ± 0.27
	WBI	1.08 ± 0.02	0.89 ± 0.01	0.77 ± 0.01
Multispectral VIs (vegetation)				
	NDVI	0.62 ± 0.02	0.74 ± 0.01	0.68 ± 0.01
	OSAVI	0.44 ± 0.02	0.57 ± 0.02	0.48 ± 0.01
	RDVI	0.32 ± 0.01	0.44 ± 0.01	0.34 ± 0.01
	EVI	0.44 ± 0.02	0.81 ± 0.05	0.52 ± 0.02
	PRI	0.17 ± 0.00	0.24 ± 0.01	0.19 ± 0.00
	MCARI	0.19 ± 0.02	0.26 ± 0.02	0.15 ± 0.01
	TCARI	0.21 ± 0.01	0.24 ± 0.01	0.18 ± 0.01
	TCARI/OSAVI	0.49 ± 0.02	0.43 ± 0.01	0.36 ± 0.01
	ARI2	0.70 ± 0.05	0.56 ± 0.05	0.50 ± 0.02
	CRI2	4.20 ± 0.76	2.75 ± 0.43	2.71 ± 0.26
	WBI	1.08 ± 0.01	0.91 ± 0.01	0.76 ± 0.01
RGB VIs				
	NGRDI	-3.15 ± 0.64	1.48 ± 0.59	1.71 ± 0.25
	TGI	9.50 ± 0.33	9.23 ± 0.05	16.60 ± 0.49
	Intensity	0.34 ± 0.01	0.31 ± 0.01	0.54 ± 0.01
	Hue	50.26 ± 2.36	66.00 ± 1.96	72.92 ± 0.93
	Saturation	0.27 ± 0.01	0.23 ± 0.01	0.11 ± 0.01
	a*	-4.36 ± 0.8	-7.88 ± 0.74	-9.51 ± 0.60
	b*	24.36 ± 1.05	21.06 ± 1.4	20.5 ± 1.38
	u*	5.10 ± 0.85	-0.97 ± 0.58	-3.02 ± 0.30
	v*	25.99 ± 1.12	22.96 ± 1.75	26.76 ± 1.55
	GA	0.25 ± 0.06	0.57 ± 0.04	0.77 ± 0.04
Vegetation cover (%)				
		60.24 ± 4.01	60.29 ± 3.54	60.83 ± 3.43
Canopy temperature (°C)*				
		33.95 ± 0.61	18.08 ± 0.31	30.06 ± 0.46

*only pixels classified as "vegetation" in July 2016 and May 2017; whole-plot temperature (all pixels) in November 2016.

Table S3. Sperman's correlations between populations' means of VIs among flights. Empty cells indicate lack of genetic differentiation for the corresponding VI in one or both the two flights as found in the ANOVA. Significant correlations are indicated by * (p<0.05) or ** (p<0.01).

		July 16 - Nov. 16	July 16 - May 17	Nov. 16 - May 17
Multispectral VIs (plot)				
	NDVI	-	-	-
	OSAVI	0.76**	0.89**	0.78**
	RDVI	0.75**	0.88**	0.8**
	EVI	-	-	-
	MCARI	0.55**	0.77**	0.50**
	TCARI	0.43**	0.71**	0.22
	TCARI/OSAVI	-	-	-
	ARI2	-	0.59**	-
	CRI2	-	-	-
	WBI	-	-	-
Multispectral VIs (vegetation)				
	NDVI	0.71**	0.83**	0.71**
	OSAVI	0.81**	0.86**	0.81**
	RDVI	0.79**	0.84**	0.79**
	EVI	0.51**	0.69**	0.40**
	MCARI	0.64**	0.77**	0.55**
	TCARI	0.50**	0.62**	0.29*
	TCARI/OSAVI	-	-	-
	ARI2	-	-	-
	CRI2	-	-	-
	WBI	-	-	-
RGB VIs				
	NGRDI	-	0.85**	-
	TGI	-	-	-
	Intensity	-	-	-
	Hue	-	0.02	-
	Saturation	-	0.87**	-
	a*	0.70**	0.88**	0.78**
	b*	-	0.86**	-
	u*	0.52**	0.62**	0.63**
	v*	-	0.78**	-
	GA	0.52**	0.60**	0.76**
Vegetation cover				
		0.59**	0.65**	0.54**
Canopy temperature*				
		-	-	-

Table S4. Association between RGB and multispectral indices in July 2016. Significant correlations are indicated by * (p<0.05) or ** (p<0.01).

	NGRDI	TGI	Intensity	Hue	Saturation	a*	b*	u*	v*	GA
Plot										
NDVI	0.74**	-0.23*	-0.33*	0.78**	0.71**	-0.78**	0.67**	-0.74**	0.59**	0.69**
OSAVI	0.83**	-0.28*	-0.38**	0.87**	0.80**	-0.86**	0.72**	-0.82**	0.64**	0.78**
RDVI	0.83**	-0.30*	-0.40**	0.87**	0.80**	-0.86**	0.72**	-0.82**	0.63**	0.80**
EVI	0.80**	-0.25	-0.35**	0.81**	0.74**	-0.80**	0.64**	-0.77**	0.57**	0.75**
PRI	0.06	0.04	0.03	0.11	0.04	-0.09	0.10	-0.07	0.13	0.05
MCARI	0.80**	-0.25	-0.34*	0.83**	0.77**	-0.82**	0.69**	-0.77**	0.62**	0.82**
TCARI	0.72**	-0.28*	-0.36**	0.75**	0.67**	-0.72**	0.54**	-0.70**	0.48**	0.67**
TCARIOSAVI	0.06	-0.06	-0.07	0.05	0.00	-0.02	-0.08	-0.06	-0.07	0.05
ARI2	-0.21	-0.17	-0.12	-0.20	-0.10	0.20	-0.22	0.15	-0.27*	-0.12
CRI2	-0.42**	0.00	0.06	-0.42**	-0.32*	0.41**	-0.36	0.36**	-0.36**	-0.35**
WBI	-0.36**	0.30*	0.34*	-0.39**	-0.33*	0.35**	-0.17	0.40**	-0.12	-0.28*
Vegetation										
NDVI	0.65**	-0.22	-0.30*	0.68**	0.67**	-0.68**	0.61**	-0.63**	0.53**	0.75**
OSAVI	0.77**	-0.32**	-0.40**	0.81**	0.82**	-0.80**	0.71**	-0.76**	0.61**	0.85**
RDVI	0.77**	-0.32**	-0.40**	0.80**	0.81**	-0.79**	0.70**	-0.75**	0.60**	0.85**
EVI	0.73**	-0.28**	-0.36**	0.75**	0.74**	-0.75**	0.63**	-0.71**	0.54**	0.78**
PRI	-0.01	0.01	0.01	0.04	0.01	-0.03	0.04	-0.02	0.06	0.04
MCARI	0.66**	-0.21	-0.29*	0.69**	0.68**	-0.68**	0.61**	-0.62**	0.54**	0.78**
TCARI	0.65**	-0.26*	-0.33*	0.68**	0.66**	-0.66**	0.55**	-0.62**	0.48**	0.70**
TCARIOSAVI	0.17	-0.07	-0.08	0.17	0.14	-0.15	0.10	-0.15	0.09	0.16
ARI2	-0.28*	-0.06	-0.01	-0.26	-0.18	0.27*	-0.25	0.24	-0.27*	-0.22
CRI2	-0.42**	0.04	0.09	-0.42**	-0.39**	0.44**	-0.42**	0.38**	-0.40**	-0.34*
WBI	-0.41**	0.24	0.28*	-0.45**	-0.40**	0.42**	-0.30*	0.43**	-0.26	-0.29*

Table S5. Association between RGB and multispectral indices in November 2016. Significant correlations are indicated by * (p<0.05) or ** (p<0.01).

	NGRDI	TGI	Intensity	Hue	Saturation	a*	b*	u*	v*	GA
Plot										
NDVI	0.57**	0.12	0.08	0.58**	0.51**	-0.53**	0.43**	-0.62**	0.40**	0.61**
OSAVI	0.61**	0.42**	0.38**	0.61**	0.61**	-0.72**	0.69**	-0.67**	0.67**	0.71**
RDVI	0.65**	0.40**	0.35**	0.64**	0.64**	-0.74**	0.69**	-0.69**	0.66**	0.71**
EVI	0.25	0.65**	0.62**	0.28*	0.26	-0.49**	0.56**	-0.30*	0.60**	0.39**
PRI	0.15	-0.11	-0.12	0.11	0.00	0.03	-0.11	-0.12	-0.10	0.09
MCARI	0.54**	0.34*	0.31*	0.53**	0.62**	-0.63**	0.63**	-0.58**	0.60**	0.61**
TCARI	0.49**	0.56**	0.52**	0.47**	0.55**	-0.68**	0.70**	-0.51**	0.70**	0.62**
TCARIOSAVI	0.13	0.44**	0.44**	0.10	0.22	-0.31	0.38**	-0.10	0.40**	0.21
ARI2	-0.13	-0.26	-0.24	-0.14	0.03	0.07	-0.09	0.13	-0.13	-0.09
CRI2	-0.18	-0.42**	-0.40**	-0.16	-0.12	0.24	-0.32*	0.17	-0.35**	-0.19
WBI	0.30*	0.04	0.02	0.32*	0.17	-0.24	0.12	-0.34*	0.11	0.28*
Vegetation										
NDVI	0.49**	0.01	-0.02	0.51**	0.47**	-0.44**	0.36**	-0.53**	0.32*	0.46**
OSAVI	0.56**	0.22	0.18	0.59**	0.63**	-0.61**	0.58**	-0.60**	0.53**	0.57**
RDVI	0.54**	0.25	0.21	0.58**	0.62**	-0.61**	0.59**	-0.59**	0.54**	0.55**
EVI	0.35**	0.50**	0.47**	0.42**	0.44**	-0.54**	0.62**	-0.40**	0.62**	0.44**
PRI	0.02	-0.22	-0.21	-0.02	-0.18	0.22	-0.29*	0.05	-0.27*	-0.10
MCARI	0.44**	0.19	0.16	0.47**	0.61**	-0.52**	0.52**	-0.49**	0.47**	0.48**
TCARI	0.45**	0.41**	0.38**	0.51**	0.65**	-0.63**	0.66**	-0.51**	0.63**	0.55**
TCARIOSAVI	0.22	0.46**	0.45**	0.29*	0.43**	-0.44**	0.52**	-0.28*	0.52**	0.36**
ARI2	-0.09	-0.09	-0.07	-0.16	-0.01	-0.01	0.00	0.11	-0.01	-0.05
CRI2	-0.29*	-0.28*	-0.25	-0.36**	-0.34*	0.31**	-0.35**	0.32*	-0.34*	-0.31*
WBI	0.25	-0.15	-0.18	0.30*	0.11	-0.10	-0.03	-0.28*	-0.05	0.14

Table S6. Association between RGB and multispectral indices in May 2017. Significant correlations are indicated by * (p<0.05) or ** (p<0.0

	NGRDI	TGI	Intensity	Hue	Saturation	a*	b*	u*	v*	GA
Plot										
NDVI	0.80**	-0.75*	-0.77**	-0.19	0.86**	-0.81**	0.83**	-0.65**	0.80**	0.74**
OSAVI	0.90**	-0.60**	-0.62**	-0.05	0.87**	-0.91**	0.89**	-0.79**	0.88**	0.83**
RDVI	0.89**	-0.58**	-0.60**	-0.04	0.86**	-0.90**	0.89**	-0.79**	0.88**	0.83**
EVI	0.34*	-0.04	-0.04	0.08	0.33*	-0.43**	0.41**	-0.40**	0.44**	0.29*
PRI	0.62**	-0.74**	-0.77**	-0.24	0.74**	-0.63**	0.68**	-0.45**	0.63**	0.52**
MCARI	0.69**	-0.34*	-0.35**	-0.16	0.76**	-0.83**	0.85**	-0.65**	0.87**	0.66**
TCARI	0.52**	0.04	0.05	0.08	0.42**	-0.58**	0.55**	-0.53**	0.60**	0.51**
TCARIOSAVI	-0.36**	0.71**	0.74**	0.19	-0.44**	0.29	-0.32*	0.21	-0.26	-0.31*
ARI2	-0.29*	-0.26*	-0.25	-0.30*	-0.05	0.22	-0.14	0.33**	-0.17	-0.34**
CRI2	-0.49**	-0.16	-0.16	-0.33*	-0.21	0.42**	-0.33*	0.52**	-0.38**	-0.52**
WBI	-0.50**	0.03	0.03	-0.16	-0.38**	0.53**	-0.48**	0.54**	-0.51**	-0.39**
Vegetation										
NDVI	0.66**	-0.75**	-0.77**	-0.30**	0.83**	-0.73**	0.78**	-0.50**	0.74**	0.54**
OSAVI	0.79**	-0.62**	-0.65**	-0.17	0.87**	-0.86**	0.88**	-0.68**	0.85**	0.70**
RDVI	0.79**	-0.60**	-0.62**	-0.15	0.86**	-0.85**	0.87**	-0.68**	0.85**	0.69**
EVI	0.67**	-0.15	-0.17	0.27*	0.51**	-0.64**	0.57**	-0.67**	0.58**	0.64**
PRI	0.40**	-0.63**	-0.64**	-0.28**	0.56**	-0.42**	0.48**	-0.23	0.42**	0.23
MCARI	0.52**	-0.27*	-0.28*	-0.24	0.68**	-0.72**	0.76**	-0.49**	0.78**	0.50**
TCARI	0.43**	0.00	-0.00	-0.06	0.45**	-0.57**	0.57**	-0.45**	0.60**	0.48**
TCARIOSAVI	-0.18	0.57**	0.59**	0.09	-0.23	0.06	-0.09	0.04	-0.02	-0.05
ARI2	-0.15	-0.30*	-0.30**	-0.17	0.01	0.11	-0.07	0.17	-0.09	-0.25
CRI2	-0.40**	-0.10	-0.09	-0.18	-0.24	0.39**	-0.34**	0.42**	-0.37**	-0.53**
WBI	-0.60**	0.23	0.24	-0.03	-0.57**	0.67**	-0.64**	0.62**	-0.66**	-0.53**

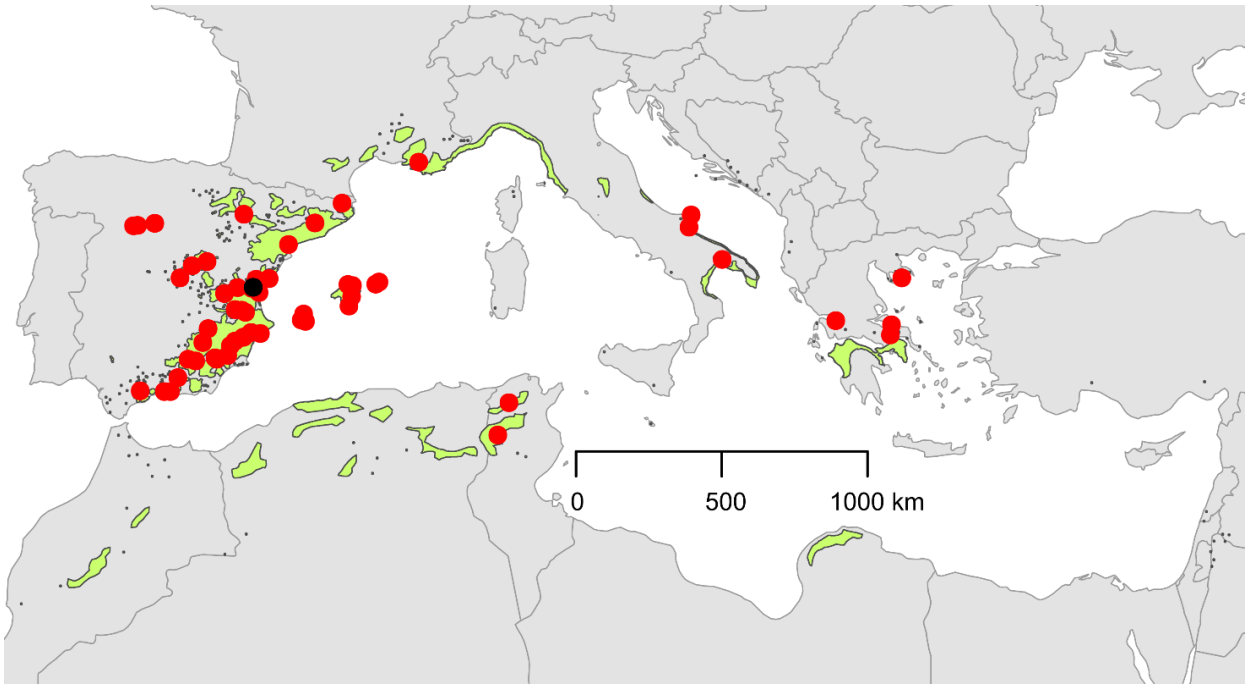

Figure S1 Geographic origin of the 56 *Pinus halepensis* populations (red dots) tested in the study site, which is indicated by a black dot and consisted of a genetic trial located in Altura (Castellon province, Spain). Green areas indicate the species range derived from the EUFORGEN distribution map (http://www.euforgen.org/species/pinus-halepensis/)

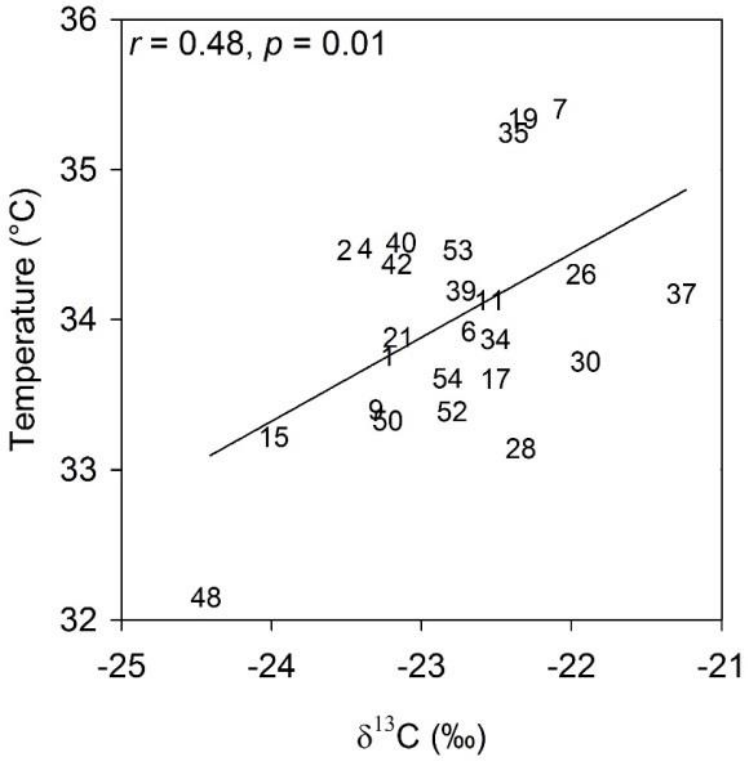

Figure S2. Association at population level between canopy temperature (measured on pixels containing vegetation) in July 2016 and carbon isotope composition of wood holocellulose as measured for a subset of 28 populations tested in the genetic trial by Voltas *et al.* (2008). Codes represent the populations tested in the trial as in Appendix (Table S1).

CHAPTER II

Phenotypic integration and life history strategies among populations of *Pinus halepensis*: an insight through Structural Equation Modeling

Filippo Santini[1,2*], José M. Climent[3], Jordi Voltas[1,2]

[1] Joint Research Unit CTFC - AGROTECNIO, Av. Alcalde Rovira Roure 191, E-25198 Lleida, Spain

[2] Department of Crop and Forest Sciences, University of Lleida, Av. Alcalde Rovira Roure 191, E-25198 Lleida, Spain

[3] INIA-CIFOR, Department of Ecology and Forest Genetics, Ctra. Coruña km 7.5, 28040 Madrid, Spain

SUMMARY

Understanding inter-population variation in the allocation of resources to specific anatomical compartments and physiological processes is crucial to disentangle adaptive patterns in forest species. This work aims at evaluating phenotypic integration and trade-offs among functional traits as determinants of life history strategies in populations of a circum-Mediterranean pine that dwells in environments where water and other resources are in limited supply. Adult individuals of 51 populations of *Pinus halepensis* grown in a common garden were characterised for 11 phenotypic traits, including direct and indirect measures of water uptake at different depths, leaf area, stomatal conductance, chlorophyll content, non-structural carbohydrates, stem diameter and tree height, age at first reproduction and cone production. The population differentiation in these traits was tested through ANOVA. The resulting populations' means were carried forward to a Structural Equation Model evaluating phenotypic integration between six latent variables (summer water uptake depth, summer transpiration, spring photosynthetic capacity, growth, reserve accumulation and reproduction). Water uptake depth and transpiration co-varied negatively among populations, as the likely result of a common selective pressure for drought resistance, while spring photosynthetic capacity was lower in populations originating from dry areas. Transpiration positively influenced growth, while growth was negatively related to reproduction and reserves among populations. Water uptake depth negatively influenced reproduction. The observed patterns indicate a differentiation in lifecycle features between fast-growing and slow-growing populations, with the latter investing significantly more in reproduction and reserves. We speculate that such contrasting strategies result from different arrays of life history traits underlying the very different ecological conditions that the Aleppo pine must face across its distribution range. These comprise, principally, drought as main stressor and fire as main ecological disturbance of the Mediterranean basin.

Keywords: evolutionary diversification; fitness; integrated phenotype; life history; *Pinus halepensis*; trade-offs; Structural Equation Modeling

INTRODUCTION

Disentangling the extent and nature of morpho-physiological adaptations is a current issue for understanding ecosystem functioning and forest dynamics in the context of global change (Guittar *et al.,* 2016; Kunstler *et al.,* 2016). Although common-garden tests have been used for a long time to characterise the genetic differentiation in functional traits for many forest species, the study of phenotypic integration for understanding adaptation syndromes has received little attention thus far (Savolainen *et al.,* 2007; Bussotti *et al.,* 2015). At the intra-specific level, phenotypic integration commonly defines the disposition of several traits to evolve jointly during the divergence of populations (i.e., evolutionary integration; Armbruster *et al.,* 2014). Indeed, the allocation of resources to a particular plant compartment or physiological process impacts on the overall carbon economy of a tree, potentially involving multiple trade-offs (Milla *et al.,* 2011). Understanding patterns of phenotypic integration is thus crucial to disentangle contrasting adaptive strategies among populations (Murren 2002).

The Aleppo pine (*Pinus halepensis* Mill.) is a widespread circum-Mediterranean gymnosperm predominantly distributed in the central-western part of the Mediterranean basin (Fady *et al.,* 2003). It is a drought-avoidant species that can be found under very contrasting ecological conditions which have shaped its current patterns of genetic variation (Serra-Varela *et al.,* 2017). Based on common-garden tests, genetic differentiation among populations has been described in life history traits such as total growth (Schiller and Atzmon, 2009; Voltas *et al.,* 2018) and reproductive allocation (Santos-del-Blanco *et al.,* 2013), and also in functional traits related to drought resistance including hydraulic conductivity (Tognetti *et al.,* 1997), needle physiology (Klein *et al.,* 2013) and water uptake patterns (Voltas *et al.,* 2015). Together with drought stress, fire has been identified as major evolutionary force in Aleppo pine. *P. halepensis* has been classified as 'fire embracer', i.e., with population resilience based on efficient post-fire recruitment after crown fires (Pausas, 2015). Differences in the frequency and intensity of forest fires across the range of *P. halepensis* have been associated with population differentiation in key traits like cone serotiny, aerial cone bank and bark thickness, and also with differences in the allocation of resources to growth or reproduction (Santos-del-Blanco *et al.,* 2013; Hernández-Serrano *et al.,* 2014; Martín-Sanz *et al.,* 2016 and submitted).

Despite the existing information about the extent of genetic (population) differentiation in functional and life history traits among populations of *P. halepensis*, little attention has been devoted to disentangle patterns of phenotypic integration in this species. For this reason, the lack of scientific background examining potential causal relations between source- and sink-related traits in Aleppo pine and other forest species does not allow delineating clear-cut hypothesis

about such genetic associations. In this study, we used Structural Equation Modeling (SEM) to investigate patterns of associations at the population level among meaningful variables describing the water and carbon economy of populations of Aleppo pine (Grace *et al.,* 2010; Fan *et al.,* 2016). The SEM approach adopted was model generating, rather than model testing, in the sense that we specified a tentative initial model which was eventually re-specified if the initial model did not fit well the experimental data or was prone to simplification. We reckon that, by using this data-driven approach, the chances to identify the true model can be limited (MacCallum 1986), leading the study from the realm of hypothesis testing to the domain of exploratory analysis (Tarka 2018). However, many causal associations underlying phenotypic integration among traits, although conceivable within the broader theoretical frame describing adaptation of Mediterranean pines, have never been evaluated in *P. halepensis* or, even, in long-lived species such as forest trees. Therefore, our conceptual model (Figure 1) is grounded on available scientific evidence and, also, on theoretical expectations.

Broadly speaking, the tree carbon economy depends on the balance between source-related processes (i.e., those influencing the amount of carbon that is available for the plant) and carbon sinks (i.e., determining the use of carbon resources) (Lacointe 2000). In a drought-avoidant conifer such as *P. halepensis*, a key source-related trait varying among populations is photosynthetic rate, which is mainly determined by stomatal regulation rather than by biochemical limitations to photosynthesis (Santini *et al.,* 2019). Some populations exhibit reduced leaf area and tight stomatal regulation as adaptations to control transpiration and water losses, hence limiting the amount of carbon fixed through photosynthesis and available for different plant compartments (Voltas *et al.,* 2008; Santini *et al.*, 2019). On the other hand, during periods of high water availability (i.e., spring) variation in photosynthetic capacity related to the needle biochemical composition may also play an important role in the carbon economy of Aleppo pine (Klein *et al.,* 2013). Populations with enhanced photosynthetic capacity may increase their carbon fixation at the beginning of the growing season, when water availability is non-limiting to photosynthesis. Another source-related variable in Mediterranean species is water uptake depth. Although a deeper water uptake may imply a greater investment in rooting depth, which is a carbon-consuming (i.e., sink) process, it is also a key determinant of water supply under drought (Eggemeyer *et al.,* 2008; Rossatto *et al.,* 2012), which may positively influence tree growth (e.g., through increased meristematic activity; Körner, 2003) or other carbon sinks. Genetic variation in source-related traits such as transpiration, photosynthetic efficiency and water uptake depth has been described among populations of *P. halepensis* as adaptive mechanisms to cope with drought stress (Voltas *et al.,* 2008; 2015; Santini *et al.,* 2019).

However, the genetic associations among these traits remain largely unexplored. As functional traits likely shaped by the same selective process (i.e., drought stress), a high phenotypic integration among these variables may have emerged linked to population differentiation (Armbruster *et al.,* 2014).

Phenotypic variation in source-related traits is therefore associated with resource availability influencing carbon sinks. Typical carbon sinks of forest trees include growth, reproduction and storage, which are determinant traits of individual fitness largely influenced by the total amount of available resources (Lacointe 2000; Ryan *et al.,* 2018). For instance, the effect of investment in root biomass or total water use on growth has been reported for several forest species (Oleksyn *et al.,* 1999; Körner, 2003; Voltas *et al.,* 2008; Klein *et al.,* 2013) including Aleppo pine, where a direct influence of an enhanced transpiration on growth has been demonstrated (Santini *et al.,* 2019). On the other hand, the direct causal effect of many source processes on carbon sinks remains largely unexplored (e.g. the effect of water uptake patterns on reproduction or reserves accumulation), especially in terms of genetic associations at the population level. Moreover, while some studies have investigated the association between pairs of source-sink processes in forest species, the influence of each source-related variable on the different carbon sinks is not easily predictable in the context of a multi-trait analysis (Granier and Vile, 2014).

A further complication arises from co-variation among plant sinks (e.g. Santos-del-Blanco *et al.,* 2012; Wiley and Helliker, 2012). In particular, growth, reproduction and storage must compete for limited carbon resources, resulting in trade-offs between resource-consuming processes. The growth *versus* reproduction trade-off is well known in forest trees, and reflects divergent adaptive strategies among populations (Obeso, 2002; Climent *et al.,* 2008; Santos-del-Blanco *et al.,* 2014). Individuals growing in unstable environments tend to invest more resources in reaching a faster sexual maturity at the expense of slower growth, and vice versa (Niklas and Enquist, 2002; Santos-del-Blanco *et al.,* 2013). Indeed, previous studies described fast-growing populations of Aleppo pine characterised by a delayed sexual maturity, in contrast to slow-growing populations which invest more resources in reproduction (Climent *et al.,* 2008). Reserve accumulation may also occur at the expense of growth, perhaps reflecting a higher resilience, as observed in populations exposed to unstable growing conditions (Wiley and Helliker, 2012; Granda and Camarero, 2017).

In this study, adult individuals of 51 population of *P. halepensis* growing in a common garden were characterised for 11 different morpho-physiological traits, which were used to derive three source-related latent variables (summer water uptake depth, summer transpiration

and spring photosynthetic efficiency) and three carbon sinks (growth, reproduction and reserves) (Figure 1). As derived by the conceptual model described above, we aim at evaluating the multivariate hypothesis of a causal influence of source-related processes on carbon sinks (model latent variables), assessing phenotypic integration (i.e., co-variation) within each group of latent variables. Specifically, we hypothesize 1) the existence of causal effects of source-related variables on each carbon sink, as suggested in the literature (e.g. Oleksyn *et al.*, 1999; Körner, 2003; Voltas *et al.*, 2008; Klein *et al.*, 2013; Santini *et al.*, 2019), 2) the presence of patterns of free covariance among source-related variables, presumably as the result of phenotypic integration influenced by common selective pressures related to water scarcity, and 3) the relevance of sizeable free covariance among carbon sinks pointing to negative associations (i.e., trade-offs) between life history traits, as the result of different patterns of resource allocation among populations (Climent *et al.*, 2008). The objective of our work is to test these hypotheses through SEM using a number of phenotypic traits that underlie the latent variables considered in the model. Aiming at producing an effective description of phenotypic integration, we also test simplified models by targeting only data-driven relevant associations among latent variables.

MATERIAL AND METHODS

Study site and plant material

The study was based on a multi-trait characterisation of adult individuals of *P. halepensis* planted in a common-garden trial located in Altura (39° 49′ 29″ N, 00° 34′ 22″ W, 640 m a.s.l.; Castellón province, eastern Spain). The trial site is representative of the average conditions in which the species can be found in the Mediterranean. The mean annual temperature is 13.8 °C, and the mean annual precipitation is 652 mm, of which 19% falls in summer (Jun. to Aug.). Mean annual potential evapotranspiration is 1115 mm. Seeds of *P. halepensis* were collected in 1995 in 56 natural populations covering most of the species' range (Figure 2; Appendix, Table S1). In each population, seeds were harvested from 20–30 trees that were spaced at least 100 m apart and planted in a forest nursery in Spain, following standard practices. In 1997, 1-year-old seedlings (16 per population) were planted systematically (2.5 × 2.5 m spacing) at the study site in four replicates following a Latinized row-column design. Four seedlings per population were planted in experimental units consisting of linear plots. A total of 896 seedlings (16 per population) were tested in the trial. Between 2004 and 2017, several field campaigns were performed to characterise the trees for different traits.

Water uptake patterns

The percentage of water taken up from two consecutive soil layers was estimated for each population in Jul. 2010. For this purpose, soil samples at two depths (0–15 cm and 15–40 cm) were systematically collected, covering all the area of the trial. One healthy and sun-exposed branch per tree was also collected from the top part of the crown and bark-peeled. Branches and soil samples were immediately frozen in dry ice and then stored at −20 °C to prevent evaporation. Water was extracted from the soil and from the xylem by cryogenic vacuum distillation as described in Otieno *et al.* (2006). Prior to water extraction, the branches sampled from trees of the same plot were pooled together. The oxygen and hydrogen isotopic composition ($\delta^{18}O$ and $\delta^{2}H$) of the soil and xylem water was determined by isotope ratio infrared spectroscopy. The relative contributions of water at 0–15 cm (TOP) and 15–40 cm (BOTTOM) to xylem water were estimated based on the isotopic composition of water through Bayesian mixing modelling. A detailed description of the procedure and the original data are reported in Voltas *et al.* (2015).

Chlorophyll content, leaf area and transpiration

Multispectral and thermal images obtained with a UAV (unmanned aerial vehicle) were used to retrieve values of vegetation indices and canopy temperature at plot level, as surrogates of leaf area, chlorophyll content and transpiration. Two flights were performed on 26 Jul. 2016 and 25 May 2017 with a Mikrokopter OktoXL (Moormerland, Germany) flying under remote control at around 100 m of altitude. A multispectral camera (MCA12; Tetracam Inc., Chatsworth, CA, US) and a thermal camera (FLIR Tau2 640; FLIR Systems, Nashua, NH, USA) were mounted, looking down, on the UAV to capture multispectral and thermal images with a resolution of 10 and 25 cm respectively. The raw photographs were combined to produce orthomosaics using a variable number of images with at least 80% overlap. The four orthomosaics (two per flight, one for multispectral and one for thermal images) that resulted from this process were used for the analyses.

The Renormalized Difference Vegetation Index (RDVI) (Roujean and Breon, 1995), the Optimized-Soil Adjusted Vegetation Index (OSAVI) (Rondeaux *et al.*, 1996) and the Transformed Chlorophyll Absorption Ratio Index (TCARI) (Haboudane *et al.*, 2002) were calculated for each pixel of single images corresponding to the experimental units. An average value per plot was obtained afterwards. Also, canopy temperature was measured from the thermal images for each pixel of a single experimental unit and used to calculate the average temperature of the plot. RDVI and OSAVI are vegetation indices based on red and near infrared (NIR) reflectance and have been used as indicators of leaf area (Roberts *et al.*, 2016; Xue and

Su, 2017). The TCARI includes also the reflectance at green wavelengths and is negatively related to leaf chlorophyll content, but it is influenced by differences in leaf area as well (Daughtry *et al.,* 2000). A better estimation of chlorophyll content in the needles can be obtained by calculating the ratio between TCARI and OSAVI (Haboudane *et al.,* 2002; Zarco-Tejada *et al.,* 2004). Thus, the TCARI/OSAVI index is negatively related to chlorophyll content. For the sake of simplicity, we multiplied this index by −1 to obtain an index that is positively related to chlorophyll content (hereafter, TCARI/OSAVI*). Canopy temperature is sensitive to changes in leaf area but it is also indicative of transpiration rates related to stomatal conductance (Gonzalez-Dugo *et al.,* 2013).

Prior to calculation of the vegetation indices and canopy temperature, a filter was applied to multispectral and thermal images to remove pixels that mainly contained soil. In the case of the multispectral images, the filter was based on the Normalized Difference Vegetation Index (NDVI; Richardson and Wiegand, 1977). In the case of thermal images, a filter based on an automatic Otsu's classification (Otsu, 1979) was applied. Only those pixels identified as vegetation were used to calculate plot-level values of RDVI, TCARI/OSAVI* and canopy temperature. A detailed account of the methodology and associated results can be found in Santini *et al.* (2019).

Non-structural carbohydrates

In Jun. and Sep. 2010, healthy and sun-exposed branches with an approximate diameter of 1 cm were collected from the top part of the crown for the analysis of non-structural carbohydrates (soluble sugars and starch) in sapwood. The analysis was performed on two different dates to characterise the accumulation of non-structural carbohydrates before (late spring) and after (early autumn) the peak period of drought stress. The branches were frozen in the field in dry ice and then dried in the laboratory. Branches collected from the same plot were bark-peeled, pooled together and finely milled. Soluble sugars were extracted from 50-mg samples with 80% ethanol in a shaking water bath at 60 °C. The concentration of soluble sugars in the supernatant obtained after centrifugation was determined colorimetrically at 490 nm using the phenol–sulphuric method described in Buysse and Merckx (1993). After ethanol extraction, the remaining sample in the undissolved precipitate was digested with an enzyme mixture containing amyloglucosidase to reduce glucose as described in Palacio *et al.* (2007). Starch concentration was determined colorimetrically using the same method as for soluble sugars. Each sample was measured twice to check for repeatability of the protocol.

Growth and reproduction

From 2001, trees were monitored across different growing seasons, and age at first female flowering (first appearing of female strobili) was recorded. In 2004 (at age 7), the number of cones per tree was measured as a surrogate of female reproduction. A detailed description of the sampling protocol and the original data are reported in Climent *et al.* (2008). In 2010 (at age 13), tree height and diameter at breast height (DBH) were registered per tree and were used as measures of tree growth. We assumed similar population rankings in tree growth from age 13 onwards, as previously observed for Aleppo pine (Sbay and Zas, 2018).

Climatic data at geographic origin of the populations

Monthly averages of precipitation and of maximum and minimum temperatures for each geographic origin were obtained for the period 1901–2016 from the CRU TS3.22 dataset (Harris *et al.*, 2014). Mean annual temperature (T_{an}), mean summer (Jun. to Aug.) temperature (T_s), mean maximum temperature of the warmest month (T_{max}), mean minimum temperature of the coldest month (T_{min}), temperature range (T_r, calculated as $T_{max} - T_{min}$), total annual precipitation (P_{an}), summer (Jun. to Aug.) precipitation (P_s) and summer to annual precipitation ratio (P_s/P_{an}) were calculated. Monthly temperatures and precipitation were used to derive the annual potential evapotranspiration (PET_{an}) according to the Hargreaves method (Hargreaves and Samani, 1982). Finally, average vapour pressure deficit (VPD) was calculated from altitude and monthly temperature and precipitation following Ferrio and Voltas (2005).

Statistical analysis

Values of cone count, age at first flowering, DBH, height, TOP, BOTTOM, soluble sugars and starch in spring and autumn, RDVI, TCARI/OSAVI* and canopy temperature were subjected to analysis of variance (ANOVA) for linear mixed-effect models in order to test for population differences. In the case of TOP, BOTTOM, OSAVI, TCARI/OSAVI*, canopy temperature, soluble sugars and starch, which were recorded at the plot level, the ANOVA consisted of population, replicate and column as fixed terms, and column by replicate interaction and row nested to replicate as random terms. In the case of cone count, age at first flowering, DBH and height, which were recorded at the tree level, an extra term accounting for intra-plot variability was included in the ANOVA. For those traits showing significant differences among populations, simple correlations between the populations' least square means and climatic conditions at origin were calculated. The populations' least square means of the different variables, as derived from the ANOVA, were used to build the Structural Equation Model and,

hence, disentangle associations among traits. Out of the initial 56 populations evaluated in the trial, 51 were used, for which records of all traits were available.

Model specification

A multivariate matrix consisting of 51 populations and 11 functional and fitness-related traits were used for SEM model fitting (Appendix, Table S2). We considered six latent variables describing key characteristics of Mediterranean forest species: water uptake depth, summer transpiration rate, spring photosynthetic capacity, reserve accumulation, growth and reproduction. Each latent variable was defined based on a set of traits as follows. First, the relative contributions of different water sources according to soil depth (TOP, BOTTOM) were considered as descriptors of the latent variable *Water uptake depth* (Voltas *et al.*, 2015). Second, the latent variable *Summer transpiration* was defined by the RDVI and also by canopy temperature, since the transpiration rate results from the combined effect of transpiring surface (i.e., leaf area) and stomatal conductance (Whitehead, 1998; Eamus *et al.*, 2000). Canopy temperature is negatively related to both leaf area and stomatal conductance, while RDVI is positively correlated with leaf area (Gonzalez-Dugo *et al.*, 2013; Roberts *et al.*, 2016; Xue and Su, 2017). Here we used RDVI and canopy temperature measured in peak summer (Jul. 2016), since canopy temperature measured in spring did not differ among populations (see 'Results' section and Santini *et al.*, 2019). On the other hand, needle chlorophyll content (as indicated by TCARI/OSAVI*) differed only in spring (May 2017), indicating population differentiation early in the growing season (see 'Results' section and Santini *et al.*, 2019). Chlorophyll content is directly related to maximum photosynthetic rate, and TCARI/OSAVI* was therefore used as an indicator for the variable *Spring photosynthetic capacity* (Gratani *et al.*, 1998; Klein *et al.*, 2013). Fourth, the latent variable *Reserves*, describing the investment in reserves, was defined by the concentration of starch and soluble sugars in branches (Hoch *et al.*, 2003). We only considered the values of soluble sugars and starch recorded in Jun., because there was no population differentiation in the case of soluble sugars and starch measured in Sep. (see 'Results' section). Fifth, we used age at first flowering and cone count as indicators of the latent variable *Reproduction*, since they are related to the precocity in reaching sexual maturity and the investment in reproductive structures (Climent *et al.*, 2008). Finally, the latent variable *Growth* was described by DBH and height measurements (Vizcaíno-Palomar *et al.*, 2016). None of the indicators had fixed path coefficient with the latent variables, with the exception of TCARI/OSAVI*.

Once the model was specified, we tested the relations between latent variables by considering all the possible free covariances among the variables within the groups of (i) source-related variables and (ii) carbon sinks. Moreover, regressions of carbon sinks on each source-related variable were included in the starting model. The starting model was thus saturated, hence testing the hypothesis of meaningful relations between all pairs of latent variables, which in some cases are grounded on existing evidences and, in others, can be theoretically conceived. After fitting the starting model, we tested simplified models in which non-relevant relations were removed either alternatively or all at once. This can be regarded as a backward strategy that corrects any possible errors of inclusion (Wheaton 1988).

Model fitting and evaluation

Prior to model fitting, the multivariate normal distribution was tested through Mardia's skewness and kurtosis tests implemented in the R package 'MVN' (Korkmaz *et al.,* 2014). The variables cone count and TOP were log-transformed to achieve multivariate normality. Model parameters were estimated through maximum likelihood which maximizes the agreement between observed and predicted variance–covariance matrices. Parameter estimation was performed in the package 'lavaan' (Rosseel, 2012) implemented in R, and the goodness of fit was evaluated through a chi-square test to check for discrepancies between the model-implied and observed matrices of variance–covariance. Several fit indices were also calculated. The Bentler's comparative fit index (CFI; Bentler, 1990) compares the proposed model with a null model in which the observed variables are uncorrelated. It ranges from 0 to 1, with values > 0.95 indicating a good fit (Hu and Bentler, 1999). The root mean square error of approximation (RMSEA; Steiger, 1990) is a measure of model misspecification, with values higher than 0.06 indicating a non-optimal model (Fan *et al.,* 1999). The standardized root mean square residual (SRMR) is a measure of the difference between the observed and the predicted matrices of correlations, and should not exceed 0.09 (Hu and Bentler, 1999). Finally, the significance of each path in the model was evaluated through a *z*-test testing the null hypothesis that the path has zero value and considering unstandardized path coefficients. A bootstrapped estimate and its associated standard error and confidence interval were also calculated for each path based on 1000 replications. This was done to check the statistical robustness of the selected model due to limited sampling size.

RESULTS

The population term in the ANOVAs was significant ($P < 0.05$) for all traits, with the exception of soluble sugars and starch concentrations measured in early autumn (Sep. 2010), canopy temperature measured in spring (May 2017) and TCARI/OSAVI* measured in peak summer (Jul. 2016). The population term for starch concentration in late spring (Jun. 2010) was marginally significant ($P = 0.12$), so we opted to include this trait in the Structural Equation Model. The associations between population means and climatic conditions at the geographic origin of the populations are reported in Table 1. In general, drier conditions at origin were associated with reduced growth, higher cone production and earlier first flowering. A lower level of chlorophyll in spring and reduced transpiration in summer were observed in populations originating from drier areas, as indicated by the associations with TCARI/OSAVI* and canopy temperature Finally, soluble sugar and starch concentrations in spring were positively correlated with temperature range and negatively associated with minimum annual temperature.

The populations' least square means derived from the ANOVAs can be found in Table S2 (Appendix). This table contains the raw values used as input for SEM model. The matrix of correlations between populations' least square means is also reported (Appendix, Table S3). A chi-square test performed on the starting SEM model was non-significant ($\chi^2 = 31.70$, $df = 30$, $P = 0.38$), indicating good agreement between the model-implied and observed variance–covariance matrices. The goodness-of-fit statistics showed optimal values (CFI = 0.99, RMSEA = 0.03, SRMR = 0.07). On the other hand, a number of regression coefficients between latent variables were not significant. The path coefficients of the starting model are reported in Figure S1 and Table S4 (Appendix). We simplified this model by excluding all non-significant relations. The variance–covariance matrix implied by the simplified model still showed good agreement with the observed matrix, as indicated by the chi-square test ($\chi^2 = 35.84$, $df = 35$, $P = 0.43$). The goodness-of-fit statistics also indicated a good overall fit (CFI = 1.00, RMSEA = 0.02, SRMR = 0.09). A Likelihood-Ratio test performed on these two models was non-significant, suggesting that the simplified model fitted the data as well as the complex model.

The standardized path coefficients of the simplified model (obtained by re-scaling the selected traits and latent variables to unit variance) are shown in Figure 3. The non-standardized coefficients, including standard errors, *z*-tests and confidence intervals, are reported in Table 2. In general, the selected traits were good indicators of latent variables at the population level, with absolute standardized path coefficients exceeding 0.80. The only exception was starch concentration, which showed a relatively low coefficient (0.52) with the latent variable *Reserves*. Significant covariation emerged between source latent variables, and also between sink latent

variables (Figure 3; Table 2). *Water uptake depth* and *Summer transpiration* were negatively related, suggesting that populations having enhanced transpiration in summer used comparatively less water from deeper soil layers. The variable *Spring photosynthetic capacity* was positively related to *Summer transpiration*, indicating a tendency of populations with a higher photosynthetic capacity in spring to show enhanced transpiration in summer. *Spring photosynthetic capacity* was also negatively associated with *Water uptake depth*, although this relation was only marginally significant. Among the sink variables, *Growth* and *Reproduction* and *Growth* and *Reserves* were negatively related. Associations between source and sink variables were relevant in some instances. In particular, *Reproduction* was negatively influenced by *Water uptake depth* and by *Spring photosynthetic capacity*, *Reserves* was positively dependent on *Spring photosynthetic capacity*, and *Growth* was positively influenced by *Summer transpiration*. A marginally (positive) influence of *Spring photosynthetic capacity* on *Growth* was also observed. This relation was kept in the model since its removal penalized goodness-of-fit statistics. The bootstrapped estimates of the path coefficients in the simplified model were similar to those obtained through maximum likelihood (Table S5). While the model explained about 65% of the latent variable *Growth*, it explained poorly the variance of the latent variables *Reproduction* and *Reserves* (Figure 3), as indicated by low R^2 values.

DISCUSSION

Population differentiation in functional traits

This study combined population records of meaningful morpho-physiological traits of *P. halepensis* derived from different published and unpublished studies performed in a representative common-garden experiment (Climent *et al.*, 2008; Voltas *et al.*, 2008, 2015; Santini *et al.*, 2019). In *P. halepensis*, population differentiation in water uptake patterns, leaf physiology, canopy architecture, growth and reproduction has been thoroughly described in relation to the relevance of local adaptation, particularly in terms of drought resistance (Climent *et al.*, 2008; Voltas *et al.*, 2008; Klein *et al.*, 2013; Santos-del-Blanco *et al.*, 2013; Santini *et al.*, 2019). In addition to such differences, we also report on the extent of population differentiation in reserve accumulation, a feature not previously investigated for this species. The investment in reserves may represent a demanding carbon sink that can ensure survival in periods of potential carbon starvation, which in the Mediterranean region corresponds to the peak of summer in concord with the highest drought severity (Wiley and Helliker, 2012; García de la Serrana *et al.*, 2015). However, only soluble sugars concentration measured in spring clearly differed among populations. In particular, enhanced concentration was related to continentality (i.e., temperature

range) and negatively associated with minimum temperatures at the geographic origin of the populations, indicating an influence of winter harshness on the accumulation of spring reserves (Hoch *et al.*, 2003). This finding suggests that the accumulation of reserves does not play a relevant role in determining adaptation to drought in *P. halepensis*. In this regard, Klein *et al.* (2014a) found a very small variation in non-structural carbohydrates accumulated in branches of individuals of *P. halepensis* exposed to different drought treatments. However, the accumulation of reserves in anatomical compartments other than branches (i.e., roots or main trunk) may be important in providing resources during periods of carbon starvation (Hoch *et al.*, 2003).

Contrasting life history strategies among populations of *P. halepensis*

The saturated SEM model described the nature of phenotypic integration adequately, as indicated by goodness-of-fit statistics (Fan *et al.*, 2016), but some of the hypothesized relations between latent variables resulted statistically irrelevant. Thus, the selected simplified model was considered a parsimonious representation of the existing association patterns among traits underlying the true model. It should be noticed, however, that this model is one of the possible theoretical models that is consistent with our dataset, and no sufficient theoretical background is still available for a strictly confirmatory theory testing using SEM.

Notably, the simplified SEM model revealed that the three source-related traits (i.e., summer water uptake depth, transpiration in summer, and spring photosynthetic capacity) were highly integrated. Transpiration divergence among populations co-varied with water uptake depth in summer. However, these two traits were negatively related, which indicates that a shallower water uptake is associated with enhanced transpiration – in terms of higher stomatal conductance and/or larger total leaf area – under moderately water-limited conditions (e.g., those encountered in the common-garden test). Under drought stress, a deeper water uptake is expected to ensure water supply, thus sustaining higher stomatal conductance and a greater transpiring surface (Eggemeyer *et al.*, 2008; Rossatto *et al.*, 2012). *P. halepensis* is known to rely on deep water sources to overcome drought periods (Voltas *et al.*, 2015), but genetic differences in the depth of water uptake are indicative of variation in the investment in roots among populations of this species (Klein *et al.*, 2014b; Voltas *et al.*, 2015). The associations with climatic conditions at origin revealed that populations from (i.e., likely adapted to) drought-prone areas tend to invest more resources in a deeper rooting system and, simultaneously, reduce summer transpiration by physiological (i.e., reduced stomatal conductance) and anatomical (i.e., reduced total leaf area) adaptations (Otieno *et al.*, 2006). These results point to water uptake depth and transpiration as

functionally related traits whose population covariation has been likely shaped by such common selective pressure (Armbruster and Schwaegerle, 1996).

Similarly, spring photosynthetic capacity was negatively related to access to deeper water pools and positively associated with summer transpiration. The TCARI/OSAVI* index measured in spring (i.e., indicative of photosynthetic capacity) was negatively associated with potential evapotranspiration and VPD at origin. These findings indicate that populations originating from drought-prone areas are characterised by a reduced photosynthetic capacity in spring along with reduced summer transpiration and a deeper water uptake. In turn, they confirm previous evidence of higher spring chlorophyll content in needles of *P. halepensis* populations originating from Greece, which are among the populations experiencing the wettest growing conditions at origin among those considered in our study (Klein *et al.,* 2013). We hypothesize that *P. halepensis* populations originating from mesic conditions (i.e., characterised by lower water uptake depth and higher summer transpiration) have developed more efficient photosynthetic machinery in spring, when photosynthesis may be light- rather than water-limited in Mediterranean ecosystems (Flexas *et al.,* 2014). In this regard, other traits related to photosynthetic capacity (i.e., photosynthetic pigments) have been found to be relatively constant in summer – when water availability is expected to limit photosynthesis across the whole species' range – across populations of *P. halepensis* (Santini *et al.,* 2019).

Significant associations emerged between source-related variables and carbon sinks, although these associations explained a relatively low variance of reproductive and storage patterns. On the other hand, they explained *ca.* 65% of the variation in growth among populations, indicating a good SEM predictive ability of carbon allocation patterns to stem biomass. Indeed, a strong, positive intra-specific association was observed between summer transpiration and growth, confirming that carbon assimilation in Aleppo pine depends more on total needle area and stomatal regulation than on photosynthetic capacity (Voltas *et al.,* 2008). The results of our model indicate that populations originating from conditions enabling higher water use and, therefore, higher transpiration can sustain a higher growth (Fardusi *et al.,* 2016).

Contrarily to growth, reproduction and reserve accumulation were not directly related to summer transpiration, suggesting that differences in summer carbon fixation among populations do not elicit changes in these alternative sinks. On the other hand, a strong and negative covariation between reproduction and growth was noticeable. A high investment in primary and secondary growth for populations of this species is coupled with delayed sexual maturity or low cone yield (Climent *et al.,* 2008; Santos-del-Blanco *et al.,* 2013). This realization emphasises the evolutionary divergence in growth and reproduction as functionally opposed life history traits in

P. halepensis, and points to contrasting population strategies in the allocation of resources to such fundamental processes. Indeed, trade-offs in resource allocation to reproduction or growth are well known in forest species (Obeso, 2002). This differentiation has been linked to particular life history strategies related to growth conditions (Niklas and Enquist, 2002). In general, individuals growing in unstable environments tend to invest more resources in reaching sexual maturity faster at the expense of lower vegetative growth, and vice versa (Santos-del-Blanco *et al.*, 2013).

In Mediterranean forests, fire has been identified as a primary source of ecological instability that acts as evolutionary force in pine species (Pausas, 2015). Differences in the frequency and intensity of forest fires across the range of *P. halepensis* may produce greater investment in reproduction in some populations, in contrast to those exposed to less recurrent fire disturbances (Hernández-Serrano *et al.*, 2014; Martín-Sanz *et al.*, 2016). In this regard, our results indicate that populations showing higher primary and secondary growth, low cone yield and delayed reproduction are those originating from more humid geographic origins, where fire occurrence is expected to be lower (Oliveira *et al.*, 2012). Moreover, a high investment in the rooting system at the population level is obtained at the expense of reduced reproduction, but does not seem to affect growth directly (Voltas *et al.*, 2015). Similarly to growth, a high investment in the root system is typical of trees characterised by a long lifespan, which is evolutionarily relevant in stable environments (Strauss and Ledig, 1985). On the other hand, some populations show reduced root investment coupled with early reproduction, which is indicative of a short lifespan. In these populations, recurrent ecological disturbances such as forest fires may have induced the development of such a strategy (Pausas, 2015). Other fire-related traits such as bark thickness have also been associated with different life strategies in *P. halepensis* (Martín-Sanz *et al.*, submitted) and in other Mediterranean conifers (Resco de Dios *et al.*, 2018).

Alongside reproduction, reserves are a third important sink component which may compete with growth in the carbon economy of a tree (Hoch *et al.*, 2003; Körner, 2003). Broadly speaking, two different models have been proposed to describe the competition between investment in growth and reserves in trees (Wiley and Helliker, 2012): 1) forest species can invest carbon in growth and then use the residual resources to produce reserves (passive accumulation), or 2) they can actively withdraw resources to grow in order to accumulate reserves (active accumulation). Our data reveal intra-specific covariation between growth and reserves, which points to an active model of carbon accumulation in *P. halepensis*.

Spring photosynthetic capacity was the only source-related trait affecting all sink-related traits simultaneously. However, these relations were generally weaker than other source-sink relationships. Specifically, a positive association between photosynthetic capacity and growth emerged, even if much less relevant than the association between summer transpiration and growth. This finding suggests that enhanced spring photosynthetic capacity results in greater allocation of resources to growth in this species (Klein *et al.*, 2013), although a feedback of sink activity on source activity, signalled through the phloem, may also play an important role (Körner, 2014). A positive association between spring photosynthetic capacity and reserve accumulation also emerged from the model, which indicates that photosynthetic products from enhanced spring photosynthesis are (partially) invested in carbon reserves. On the other hand, the negative association between photosynthetic capacity and reproduction might be a consequence of the strong trade-off between reproduction and growth rather than from a direct causal effect. In this regard, the associations between spring photosynthetic capacity and either reproduction or reserves were of the same magnitude, but of opposite sign. Since no significant free co-variance was found between these carbon sinks, this finding indicates that an increase in spring photosynthetic capacity results in an increase of reserves coupled with an equivalent decrease (in terms of carbon resources) of reproduction.

CONCLUSIONS

This work provides strong insights into the array of life history strategies that are found range-wide in *P. halepensis*. Although additional data are needed to validate our findings or test alternative models through SEM, this study is the first, at the best of our knowledge, to deeply explore patterns of phenotypic integration among a representative number of populations of a widespread pine. The development of complex adaptive syndromes, in which functionally related traits show high phenotypic covariation among populations, has been linked to selective processes (Armbruster and Schwaegerle, 1996). Contrasting selective pressures are likely at the origin of the phenotypic covariation observed among source-related traits, for which a functional integration related to drought adaptation can be postulated. Across the range of the species, fast-growing populations showing high photosynthetic capacity in spring sharply contrast with slow-growing populations having a favourable expression of functional traits related to drought resistance (i.e., deeper rooting system and reduced summer transpiration). These complementary strategies are indicative of evolutionary divergence for the species. On the other hand, the trade-offs that emerged among sink-related traits may be explained in the light of differences in fire regimes, which influence the ecological stability of Mediterranean environments. Slow-growing

populations allocate more resources to faster reproduction and to greater accumulation of reserves, which are strategies that have been linked to highly unstable environments characterised by recurrent, intense and widespread forest fires (Niklas and Enquist, 2002; Körner, 2003; Wiley and Helliker, 2012; Pausas, 2015).

ACKNOWLEDGMENTS

We acknowledge P. Sopeña and M.J. Pau for technical assistance.

AUTHOR CONTRIBUTIONS

J.V. and F.S. conceived and designed the research. F.S., J.M.C., and J.V. collected the data; F.S. analysed the data; F.S. and J.V. wrote the manuscript, with contributions from J.M.C.

REFERENCES

Armbruster W.S., Schwaegerle K.E. (1996) Causes of covariation of phenotypic traits among populations. *Journal of Evolutionary Biology*, 9, 261–276.

Armbruster W.S., Pelabon C., Bolstad G.H., Hansen T.F. (2014) Integrated phenotypes: understanding trait covariation in plants and animals. *Philosophical Transactions of the Royal Society B: Biological Sciences*, 369, 20130245–20130245.

Bentler P.M. (1990) Comparative fit indexes in structural models. *Psychological Bulletin*, 107, 238.

Bussotti F., Pollastrini M., Holland V., Brüggemann W. (2015) Functional traits and adaptive capacity of European forests to climate change. *Environmental and Experimental Botany*, 111, 91–113.

Buysse J.A.N., Merckx R. (1993) An improved colorimetric method to quantify sugar content of plant tissue. *Journal of Experimental Botany*, 44, 1627–1629.

Climent J., Prada M.A., Calama R., Chambel M.R., de Ron D.S., Alia R. (2008) To grow or to seed: ecotypic variation in reproductive allocation and cone production by young female Aleppo pine (*Pinus halepensis*, Pinaceae). *American Journal of Botany*, 95, 833–842.

Daughtry C.S.T., Walthall C.L., Kim M.S., De Colstoun E.B., McMurtrey J.E. III. (2000) Estimating corn leaf chlorophyll concentration from leaf and canopy reflectance. *Remote Sensing of Environment*, 74, 229–239.

Eamus D, O'Grady AP, Hutley L. 2000. Dry season conditions determine wet season water use in the wet–tropical savannas of northern Australia. *Tree Physiology*, 20, 1219–1226.

Eggemeyer K.D., Awada T., Harvey F.E., Wedin D.A., Zhou X., Zanner C.W. (2008) Seasonal changes in depth of water uptake for encroaching trees *Juniperus virginiana* and *Pinus ponderosa* and two dominant C4 grasses in a semiarid grassland. *Tree Physiology*, 29, 157–169.

Fady B., Semerci H., Vendramin G.G. (2003) EUFORGEN Technical Guidelines for genetic conservation and use for Aleppo pine (*Pinus halepensis*) and Brutia pine (*Pinus brutia*). International Plant Genetic Resources Institute, Rome, Italy

Fan X., Thompson B., Wang L. (1999) Effects of sample size, estimation methods, and model specification on structural equation modeling fit indexes. *Structural Equation Modeling*, 6, 56–83.

Fan Y., Chen J., Shirkey G. *et al.* (2016) Applications of structural equation modeling (SEM) in ecological studies: an updated review. *Ecological Processes*, 5, 19.

Fardusi M.J., Ferrio J.P., Comas C., Voltas J., Resco de Dios V., Serrano L. (2016) Intra-specific association between carbon isotope composition and productivity in woody plants: a meta-analysis. *Plant Science*, 251, 110–118.

Ferrio J.P., Voltas J. (2005) Carbon and oxygen isotope ratios in wood constituents of *Pinus halepensis* as indicators of precipitation, temperature and vapour pressure deficit. *Tellus B*, 57, 164–173.

Flexas J., Díaz-Espejo A., Gago J. *et al.* (2014) Photosynthetic limitations in Mediterranean plants: a review. *Environmental and Experimental Botany*, 103, 12–23.

García de la Serrana R., Vilagrosa A., Alloza J.A. (2015) Pine mortality in southeast Spain after an extreme dry and warm year: interactions among drought stress, carbohydrates and bark beetle attack. *Trees*, 29, 1791–1804.

Gonzalez-Dugo V., Zarco-Tejada P., Nicolás E. *et al.* (2013) Using high resolution UAV thermal imagery to assess the variability in the water status of five fruit tree species within a commercial orchard. *Precision Agriculture*, 14, 660–678.

Grace J.B., Anderson T.M., Olff H., Scheiner S.M. (2010) On the specification of structural equation models for ecological systems. *Ecological Monographs*, 80, 67–87.

Granda E., Camarero J.J. (2017) Drought reduces growth and stimulates sugar accumulation: new evidence of environmentally driven non-structural carbohydrate use. *Tree Physiology*, 37, 997-1000.

Granier C., Vile D. (2014) Phenotyping and beyond: modelling the relationships between traits. *Current Opinion in Plant Biology*, 18, 96–102.

Gratani L., Pesoli P., Crescente M.F. (1998) Relationship between photosynthetic activity and chlorophyll content in an isolated *Quercus ilex* L. tree during the year. *Photosynthetica*, 35, 445–451.

Guittar J., Goldberg D., Klanderud K., Telford R.J., Vandvik V. (2016) Can trait patterns along gradients predict plant community responses to climate change? *Ecology*, 97, 2791–2801.

Haboudane D., Miller J.R., Tremblay N., Zarco-Tejada P.J., Dextraze L. (2002) Integrated narrow-band vegetation indices for prediction of crop chlorophyll content for application to precision agriculture. *Remote Sensing of Environment*, 81, 416–426.

Hargreaves G.H., Samani Z.A. (1982) Estimating potential evapotranspiration. *Journal of the Irrigation and Drainage Division*, 108, 225–230.

Harris I.P.D.J., Jones P.D., Osborn T.J., Lister D.H. (2014) Updated high-resolution grids of monthly climatic observations–the CRU TS3. 10 Dataset. *International Journal of Climatology*, 34, 623–642.

Hernández-Serrano A., Verdú M., Santos-del-Blanco L., Climent J.M., González-Martínez S.C., Pausas J.G. (2014) Heritability and quantitative genetic divergence of serotiny, a fire-persistence plant trait. *Annals of Botany*, 114, 571–577.

Hoch G., Richter A., Körner C. (2003) Non-structural carbon compounds in temperate forest trees. *Plant, Cell and Environment*, 26, 1067–1081.

Hu L., Bentler P.M. (1999) Cutoff criteria for fit indexes in covariance structure analysis: conventional criteria versus new alternatives. *Structural Equation Modeling*, 6, 1–55.

Klein T., Di Matteo G., Rotenberg E., Cohen S., Yakir D. (2013) Differential ecophysiological response of a major Mediterranean pine species across a climatic gradient. *Tree Physiology*, 33, 26–36.

Klein T., Hoch G., Yakir D., Körner C. (2014a) Drought stress, growth and nonstructural carbohydrate dynamics of pine trees in a semi-arid forest. *Tree Physiology*, 34, 981–992.

Klein T., Rotenberg E., Cohen-Hilaleh E. *et al.* (2014b) Quantifying transpirable soil water and its relations to tree water use dynamics in a water-limited pine forest. *Ecohydrology*, 7, 409–419.

Korkmaz S., Goksuluk D., Zararsiz G. (2014) MVN: an R Package for assessing multivariate normality. *The R Journal*, 6, 151-162.

Körner C. (2003) Carbon limitation in trees. *Journal of Ecology*, 91, 4–17.

Körner C. (2014) Paradigm shift in plant growth control. *Current Opinion in Plant Biology*, 25, 107–114.

Kunstler G., Falster D., Coomes D.A. *et al.* (2016) Plant functional traits have globally consistent effects on competition. *Nature*, 529, 204–207.

Lacointe A. (2000) Carbon allocation among tree organs: a review of basic processes and representation in functional-structural tree models. *Annals of Forest Science*, 5, 521-533.

MacCallum R.C. (1986) Specification searches in covariance structure modeling. *Psycholgical bulletin*, 100, 107–120.

Martín-Sanz R.C., Santos-del-Blanco L., Notivol E., Chambel M.R., San-Martin R., Climent J.M. (2016) Disentangling plasticity of serotiny, a key adaptive trait in a Mediterranean conifer. *American Journal of Botany*, 103, 1582–1591.

Martín-Sanz R.C., San-Martin R., Poorter H., Vázquez A., Climent J.M. How does environment affect the relative and absolute allocation to bark in a Mediterranean conifer? *Frontiers in Plant Science* submitted.

Milla R., Reich P.B. (2011) Multi-trait interactions, not phylogeny, fine-tune leaf size reduction with increasing altitude. *Annals of Botany*, 107, 455–465.

Murren C.J. (2002) Phenotypic integration in plants. *Plant Species Biology*, 17, 89–99.

Niklas K.J., Enquist B.J. (2002) On the vegetative biomass partitioning of seed plant leaves, stems, and roots. *The American Naturalist*, 159, 482–497.

Obeso J.R. (2002) The costs of reproduction in plants. *New Phytologist*, 155, 321–348.

Oleksyn J., Reich P.B., Chalupka W., Tjoelker M.G. (1999) Differential above- and below-ground biomass accumulation of European *Pinus sylvestris* populations in a 12-year-old provenance experiment. *Scandinavian Journal of Forest Research*, 14, 7–17.

Oliveira S., Oehler F., San-Miguel-Ayanz J., Camia A., Pereira J.M. (2012) Modeling spatial patterns of fire occurrence in Mediterranean Europe using Multiple Regression and Random Forest. *Forest Ecology and Management*, 275, 117–129.

Otieno D.O., Kurz-Besson C., Liu J. *et al.* (2006) Seasonal variations in soil and plant water status in a *Quercus suber* L. stand: roots as determinants of tree productivity and survival in the Mediterranean-type ecosystem. *Plant and Soil*, 283, 119–135.

Otsu N. (1979) A threshold selection method from gray-level histograms. *IEEE Transactions on Systems, Man, and Cybernetics*, 9, 62–66.

Palacio S., Maestro M., Montserrat-Martí G. (2007) Seasonal dynamics of nonstructural carbohydrates in two species of Mediterranean sub-shrubs with different leaf phenology. *Environmental and Experimental Botany*, 59, 34–42.

Pausas J.G. (2015) Evolutionary fire ecology: lessons learned from pines. *Trends in Plant Science*, 20, 318–324.

Resco de Dios V., Arteaga C., Hedo J., Gil-Pelegrín E., Voltas J. (2018) A trade-off between embolism resistance and bark thickness in conifers: are drought and fire adaptations antagonistic? *Plant Ecology and Diversity*, 11, 253-258.

Richardson A.J., Wiegand C.L. (1977) Distinguishing vegetation from soil background information. *Photogrammetric Engineering and Remote Sensing*, 43, 1541–1552.

Roberts D.A., Roth K.L., Perroy R.L. (2016) Hyperspectral vegetation indices. In: Huete A., Lyon J.G., Thenkabail P.S. (eds.) *Hyperspectral Remote Sensing of Vegetation*. pp. 309–328, Boca Raton, FL: CRC Press.

Rondeaux G., Steven M., Baret F. (1996) Optimization of soil-adjusted vegetation indices. *Remote Sensing of Environment*, 55, 95–107.

Rossatto D.R., de Carvalho Ramos Silva L., Villalobos-Vega R., Sternberg L.D.S.L., Franco A.C. (2012) Depth of water uptake in woody plants relates to groundwater level and vegetation structure along a topographic gradient in a neotropical savanna. *Environmental and Experimental Botany*, 77, 259–266.

Rosseel Y. (2012) lavaan: an R package for structural equation modeling and more Version 0.5-12 (BETA). *Journal of Statistical Software*, 48, 1–36.

Roujean J-L., Breon F-M. (1995) Estimating PAR absorbed by vegetation from bidirectional reflectance measurements. *Remote Sensing of Environment*, 51, 375–384.

Ryan M.G., Oren R., Waring R.H. (2018) Fruiting and sink competition. *Tree physiology*, 38, 1261–1266

Santini F., Kefauver S.C., Resco de Dios V., Araus J.L., Voltas J. (2019) Using unmanned aerial vehicle based multispectral, RGB and thermal imagery for phenotyping of forest genetic trials: a case study in *Pinus halepensis*. *Annals of Applied Biology,* 174, 262-276.

Santos-del-Blanco L., Climent J., González-Martínez S.C., Pannell J.R. (2012) Genetic differentiation for size at first reproduction through male versus female functions in the widespread Mediterranean tree *Pinus pinaster*. *Annals of Botany,* 110, 1449–1460.

Santos-del-Blanco L., Bonser S.P., Valladares F., Chambel M.R., Climent J. (2013) Plasticity in reproduction and growth among 52 range-wide populations of a Mediterranean conifer: adaptive responses to environmental stress. *Journal of Evolutionary Biology,* 26, 1912–1924.

Santos-del-Blanco L., Climent J. (2014) Costs of female reproduction in a conifer tree: a whole-tree level assessment. *Journal of Ecology,* 102, 1310–1317.

Savolainen O., Pyhäjärvi T., Knürr T. (2007) Gene flow and local adaptation in trees. *Annual Review of Ecology, Evolution, and Systematics,* 38, 595–619.

Sbay H., Zas R. (2018) Geographic variation in growth, survival, and susceptibility to the processionary moth (*Thaumetopoea pityocampa* Dennis and Schiff.) of *Pinus halepensis* Mill. and *P. brutia* Ten.: results from common gardens in Morocco. *Annals of Forest Science,* 75, 69.

Schiller G., Atzmon N. (2009) Performance of Aleppo pine (*Pinus halepensis*) provenances grown at the edge of the Negev desert: a review. *Journal of Arid Environments,* 73, 1051–1057.

Serra-Varela M.J., Alía R., Daniels R.R., Zimmermann N.E., Gonzalo-Jiménez J., Grivet D. (2017) Assessing vulnerability of two Mediterranean conifers to support genetic conservation management in the face of climate change. *Diversity and Distributions,* 23, 507–516.

Steiger J.H. (1990) Structural model evaluation and modification: an interval estimation approach. *Multivariate Behavioral Research,* 25, 173–180.

Strauss S.H., Ledig F.T. (1985) Seedling architecture and life history evolution in pines. *The American Naturalist,* 125, 702–715.

Tarka P. (2018) An overview of structural equation modeling: its beginnings, historical development, usefulness and controversies in the social sciences. *Quality and Quantity,* 52, 313–354.

Tognetti R., Michelozzi M., Giovannelli A. (1997) Geographical variation in water relations, hydraulic architecture and terpene composition of Aleppo pine seedlings from Italian provinces. *Tree Physiology,* 17, 241–250.

Vizcaíno-Palomar N., Ibáñez I., González-Martínez S.C., Zavala M.A., Alía R. (2016) Adaptation and plasticity in aboveground allometry variation of four pine species along environmental gradients. *Ecology and Evolution,* 6, 7561–7573.

Voltas J., Chambel M.R., Prada M.A., Ferrio J.P. (2008) Climate-related variability in carbon and oxygen stable isotopes among populations of Aleppo pine grown in common-garden tests. *Trees,* 22, 759–769.

Voltas J., Lucabaugh D., Chambel M.R., Ferrio J.P. (2015) Intraspecific variation in the use of water sources by the circum-Mediterranean conifer *Pinus halepensis*. *New Phytologist,* 208, 1031–1041.

Voltas J., Shestakova T.A., Patsiou T., di Matteo G., Klein T. (2018) Ecotypic variation and stability in growth performance of the thermophilic conifer *Pinus halepensis* across the Mediterranean basin. *Forest Ecology and Management,* 424, 205–215.

Wheaton B. (1988) Assessment of fit in overidentified models with latent variables. In: Long, JS (ed.) Common problems/poor solutions: avoiding error in quantitative research. Sage Publications, Beverly Hills

Whitehead D. (1998) Regulation of stomatal conductance and transpiration in forest canopies. *Tree Physiology,* 18, 633–644.

Wiley E., Helliker B. (2012) A re-evaluation of carbon storage in trees lends greater support for carbon limitation to growth: letters. *New Phytologist*, 195, 285–289.

Xue J., Su B. (2017) Significant remote sensing vegetation indices: a review of developments and applications. *Journal of Sensors*, 2017, 1–17.

Zarco-Tejada P., Miller J., Morales A., Berjón A., Agüera J. (2004) Hyperspectral indices and model simulation for chlorophyll estimation in open-canopy tree crops. *Remote Sensing of Environment*, 90, 463–476.

Chapter II - Tables and Figures

Table 1. Pearson's correlations between population means of the 11 phenotypic traits considered (i.e. as described in "Material and Methods" section) and climatic conditions at origin. Significant correlations are indicated by * ($P < 0.05$) or ** ($P < 0.01$). Marginally significant correlations ($P < 0.1$) are indicated by $^{+}$.

	T_{an}	T_s	T_{max}	T_{min}	T_r	P_{an}	P_s	P_s/P_{an}	PET_{an}	VPD
BOTTOM	0.03	0.05	0.20	0.02	0.09	−0.07	−0.21	−0.20	0.22	0.19
TOP	0.02	−0.03	−0.22	0.06	−0.17	0.19	0.21	0.16	−0.26^{+}	−0.22
Height	0.12	0.02	−0.35*	0.13	−0.30*	0.05	0.23	0.19	−0.33*	−0.20
DBH	0.09	0.01	−0.26^{+}	0.07	−0.20	−0.11	0.09	0.09	−0.21	−0.11
Soluble sugars	−0.31*	−0.18	0.08	−0.32*	0.33*	0.00	0.09	0.18	0.05	−0.13
Starch	−0.24^{+}	−0.16	0.13	−0.27*	0.31*	−0.21	−0.18	−0.03	0.11	0.02
RDVI	−0.17	−0.08	−0.09	−0.23	0.16	−0.17	0.06	0.14	−0.06	−0.09
TCARI/OSAVI*	−0.37**	−0.33*	−0.26^{+}	−0.33*	0.15	0.16	0.36*	0.39**	−0.36*	−0.40**
Canopy T	0.23	0.28*	0.31*	0.22	−0.03	0.10	−0.23	−0.31*	0.20	0.23
Age first flowering	0.07	−0.09	−0.33	0.13	−0.29*	0.10	0.21	0.19	−0.30*	−0.24
Cone count	0.08	0.24^{+}	0.39	0.05	0.17	0.06	−0.26^{+}	−0.32*	0.32*	0.27*

T_{an} annual temperature; T_s summer temperature (Jun. to Aug.); T_{max} mean maximum temperature of the warmest month; T_{min} mean minimum temperature of the coldest month; T_r range of annual temperature; P_{an} annual precipitation; P_s summer precipitation (Jun. to Aug.); PET_{an} annual potential evapotranspiration; VPD mean vapour pressure deficit.

Table 2. Parameter estimates of the Structural Equation Model. The variables are described in "Material and Methods" section. The estimated non-standardized coefficients are reported. The *z*-statistic corresponds to the estimate divided by its standard error. The *p*-value is calculated by evaluating the *z*-statistic under a standard normal distribution. CI indicates the 95% confidence intervals (lower and upper).

Left variable	Operator	Right variable	Estimate	SE	*z*-value	*p*-value	CI (lower)	CI (upper)
Growth	=~	DBH	1.00	0.00	-	-	1.00	1.00
Growth	=~	Height	1.23	0.09	12.01	0.00	1.05	1.42
Reproduction	=~	Cone Count	1.00	0.00	-	-	1.00	1.00
Reproduction	=~	Age First Flowering	−0.95	0.18	−5.35	0.00	−1.30	−0.60
Water uptake depth	=~	Bottom	1.00	0.00	-	-	1.00	1.00
Water uptake depth	=~	Top	−0.80	0.10	−8.17	0.00	−0.99	−0.61
Summer transpiration	=~	RDVI	1.00	0.00	-	-	1.00	1.00
Summer transpiration	=~	Canopy T	−3.66	0.51	−7.28	0.00	−4.67	−2.69
Reserves	=~	Soluble sugars	1.00	0.00	-	-	1.00	1.00
Reserves	=~	Starch	0.91	0.37	2.46	0.01	0.18	1.63
Photos. capacity	=~	TCARI/OSAVI*	1.00	0.00	-	-	1.00	1.00
Water uptake depth	~~	Photos. capacity	0.00	0.00	−1.94	0.05	0.00	0.00
Summer transpiration	~~	Photos. capacity	0.00	0.00	2.03	0.04	0.00	0.00
Water uptake depth	~~	Summer transpiration	0.00	0.00	1.82	0.07	0.00	0.00
Reproduction	~	Summer transpiration	−0.14	0.05	−2.88	0.00	−0.24	−0.05
Reproduction	~	Water uptake depth	−0.99	0.45	-2.23	0.03	−1.87	−0.12
Reproduction	~	Photos. capacity	2.03	0.31	6.57	0.00	1.42	2.64
Growth	~	Summer transpiration	0.51	0.28	1.75	0.08	−0.60	1.07
Growth	~	Water uptake depth	3.18	1.43	2.22	0.03	0.37	5.99
Growth	~	Photos. capacity	0.00	0.00	−2.76	0.01	0.00	0.00
Reserves	~	Summer transpiration	−0.01	0.00	−2.93	0.00	0.00	0.00
Reserves	~	Water uptake depth	1.00	0.00	-	-	1.00	1.00
Reserves	~	Photos. capacity	1.23	0.09	12.01	0.00	1.05	1.42
Growth	~~	Reproduction	1.00	0.00	-	-	1.00	1.00
Reproduction	~~	Reserves	−0.95	0.18	−5.35	0.00	−1.30	−0.60
Growth	~~	Reserves	1.00	0.00	-	-	1.00	1.00

=~ latent variable; ~ regressed on; ~~ covariance

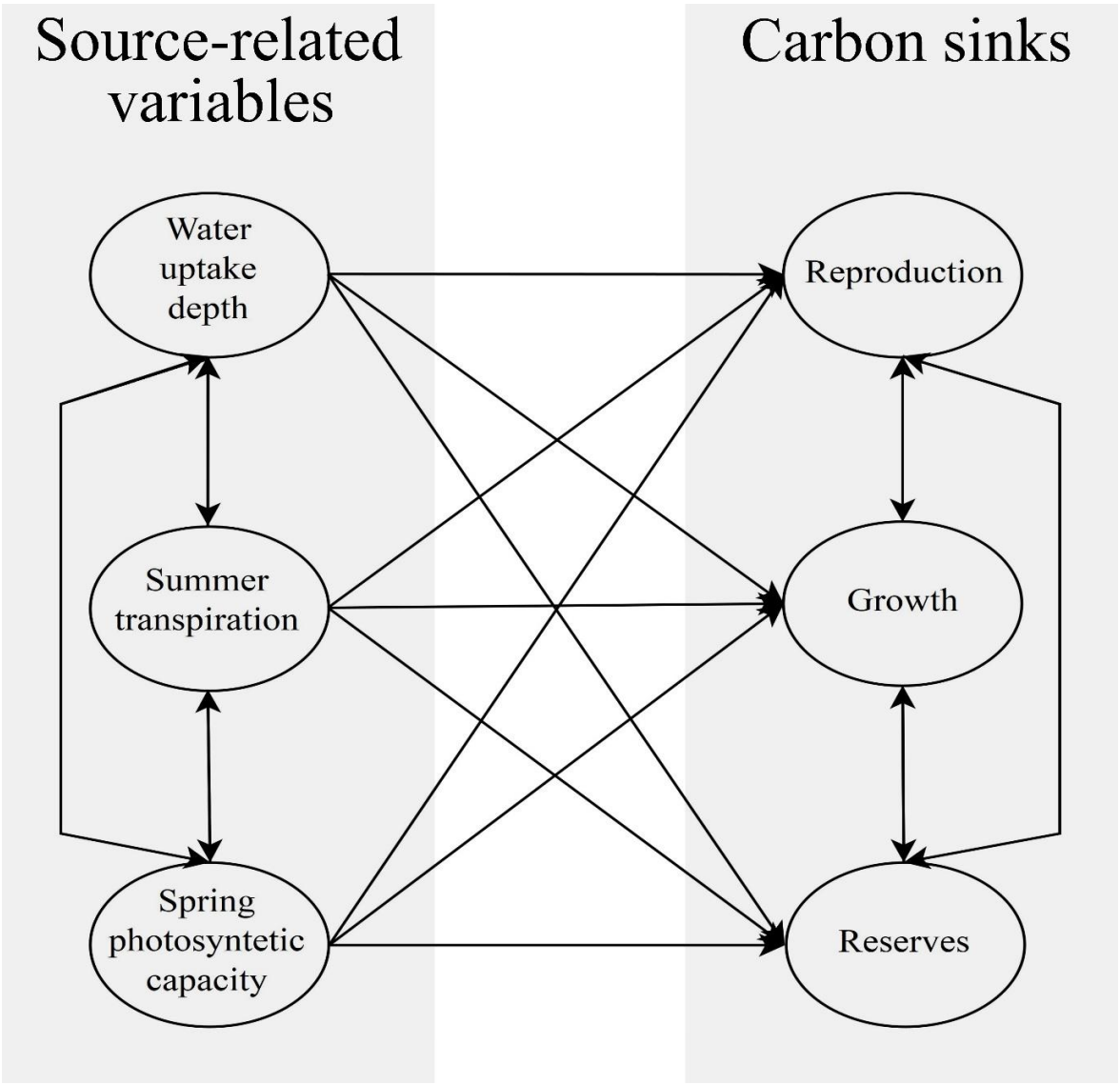

Figure 1. Starting Structural Equation Model. Directional arrows between latent variables indicate regression, while double arrows indicate covariance.

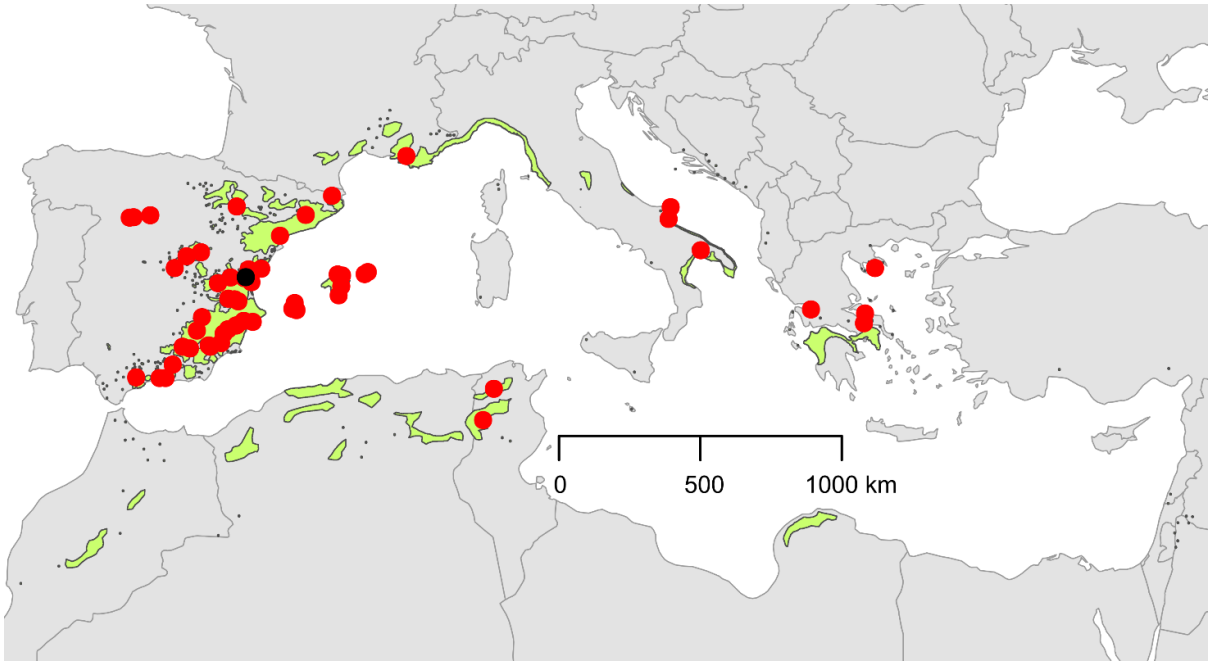

Figure 2. Geographic origin of the 56 *Pinus halepensis* populations (red dots) used in this study and tested in the genetic trial (black dot). Green areas indicate the species range derived from the EUFORGEN distribution map (http://www.euforgen.org/species/pinus-halepensis/).

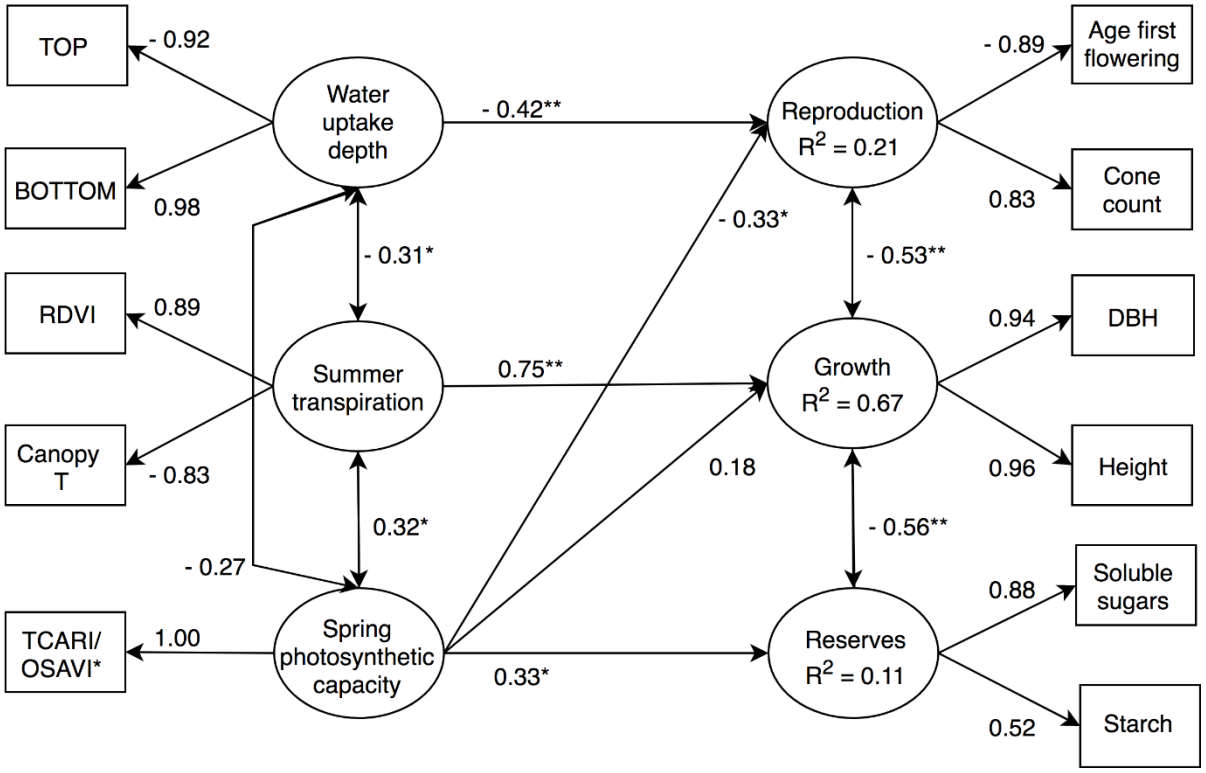

Figure 3. Final Structural Equation Model. Square nodes denote observed variables, while latent variables are represented by circles. Directional arrows between latent variables indicate regressions, while double arrows indicate covariance. The standardized path coefficients are reported, as well as R^2 values for sink variables significantly explained by source-related variable(s). Significant path coefficients are indicated by * ($P < 0.05$) or ** ($P < 0.01$) according to *z*-tests performed on unstandardized coefficients (Table 2).

Chapter II - Appendix

Table S1. Origin of the 56 *Pinus halepensis* populations tested in the genetic trial.

Population	Region	Country	Latitude	Longitude
Cabanelles	Catalonia	Spain	42° 14' 24" N	02° 46' 48" E
Tivissa	Catalonia	Spain	41° 02' 60" N	00° 45' 36" E
Sant Salvador de Guardiola	Catalonia	Spain	41° 40' 12" N	01° 45' 36" E
Zuera	Ebro Depression	Spain	41° 55' 12" N	00° 55' 12" W
Valdeconcha	Southern Plateau	Spain	40° 26' 23" N	02° 52' 12" W
Alcantud	Southern Plateau	Spain	40° 33' 36" N	03° 19' 48" W
Villarejo de Salvanes	Southern Plateau	Spain	40° 05' 24" N	02° 18' 36" W
Cirat	Iberian Range	Spain	40° 02' 60" N	00° 27' 36" W
Tuejar	Iberian Range	Spain	39° 48' 36" N	01° 09' 36" W
Enguidanos	Iberian Range	Spain	39° 38' 24" N	01° 38' 60" W
Tibi	East Spain	Spain	38° 31' 12" N	00° 39' 00" W
Altura	Iberian Range	Spain	39° 47' 24" N	00° 37' 12" W
Villa de Ves	East Spain	Spain	39° 10' 48" N	01° 15' 00" W
Jarafuel	East Spain	Spain	39° 09' 36" N	01° 00' 36" W
Bicorp	East Spain	Spain	39° 06' 00" N	00° 51' 36" W
Commercial seed	East Spain	Spain	-	-
Benicassim	Iberian Range	Spain	40° 04' 12" N	00° 01' 48"E
Gilet	Iberian Range	Spain	39° 58' 12" N	03° 21' 00" W
Villajoyosa	East Spain	Spain	38° 29' 24" N	00° 18' 00" W
Ricote	N. Betic Mts	Spain	38° 08' 24" N	01° 25' 48" W
Monovar	N. Betic Mts	Spain	38° 22' 48" N	00° 57' 00" W
Monovar	N. Betic Mts	Spain	38° 23' 24" N	00° 55' 12" W
Paterna del Madera	N. Betic Mts	Spain	38° 37' 48" N	02° 16' 12" W
Abaran	N. Betic Mts	Spain	38° 16' 12" N	01° 15' 36" W
Quentar	S. Betic Mts	Spain	37° 31' 12" N	03° 24' 36" W
Benamaurel	S. Betic Mts	Spain	37° 42' 00" N	02° 44' 24" W
Velez Blanco	S. Betic Mts	Spain	37° 47' 24" N	02° 00' 36" W
Santiago-Pontones	S. Betic Mts	Spain	38° 13' 48" N	02° 28' 12" W
Lorca	S. Betic Mts	Spain	37° 45' 00" N	01° 57' 00" W
Alhama de Murcia	S. Betic Mts	Spain	37° 51' 36" N	01° 31' 48" W
Quesada	S. Betic Mts	Spain	37° 45' 00" N	03° 01' 12" W
Lentegi	South Spain	Spain	36° 49' 12" N	03° 41' 24" W
Carratraca	South Spain	Spain	36° 51' 00" N	04° 49' 48" W
Frigiliana	South Spain	Spain	36° 49' 12" N	03° 55' 12" W
Palma de Mallorca	Majorca	Spain	39° 53' 59" N	03° 00' 00" E
Santanyi	Majorca	Spain	39° 16' 48" N	03° 02' 24" E
Alcudia	Majorca	Spain	39° 52' 12" N	03° 10' 12" E
Calvia	Majorca	Spain	39° 32' 60" N	03° 08' 24" E
Marcadal, Es	Menorca	Spain	39° 58' 12" N	04° 10' 12" E
Migjorn Gran, Es	Menorca	Spain	39° 54' 36" N	04° 02' 60" E
Sant Josep de sa Talaia	Ibiza	Spain	38° 52' 48" N	01° 14' 24" E
Sant Josep de sa Talaia	Ibiza	Spain	38° 50' 24" N	01° 23' 60" E
Sant Antoni de Portmany	Ibiza	Spain	39° 02' 60" N	01° 19' 48" E
Valbuena de Duero	North. Plateu (Reforestation)	Spain	41° 39' 36" N	04° 16' 48" W
Vega de Valdetronco	North. Plateu (Reforestation)	Spain	41° 35' 24" N	05° 04' 48" W
Villan de Tordesillas	North. Plateu (Reforestation)	Spain	41° 36' 00" N	04° 55' 48" W
Istaia-eyboia	Greece	Greece	38° 44' 24" N	23° 29' 24" E
Amfilohia	Greece	Greece	38° 51' 36" N	21° 23' 24" E
Tatoi-Attica	Greece	Greece	38° 27' 00" N	23° 26' 60" E
Kassandra	Greece	Greece	40° 05' 24" N	23° 52' 48" E
Gemenos	France	France	43° 25' 12" N	05° 40' 12" E
Litorale tarantino	Italy	Italy	40° 37' 12" N	17° 06' 35" E
Gargano Monte Pucci	Italy	Italy	41° 53' 60" N	15° 56' 24" E
Gargano Marzini	Italy	Italy	41° 32' 60" N	15° 51' 36" E
Thala	Tunisia	Tunisia	35° 34' 12" N	08° 39' 00" E
Tabarka	Tunisia	Tunisia	36° 30' 00" N	09° 04' 12" E

Table S2. Populations' least square means of the eleven phenotypic traits derived from the ANOVA. This matrix was used as input for the structural equation modelling, with the exclusion of the following populations: Tivissa, Monovar, Valbuena de Duero, Vega de Valdetronco and Villan de Tordesillas. Prior to fit the model, the variable height was scaled by 1000, the variables cone count and DBH were scaled by 100 and the variables age at first flowering and canopy temperature were scaled by 10 to make the magnitude of the variances comparable to the other variables. Top and cone count were also log-transformed to reach a multivariate normal distribution.

Population	Bottom	Top	Height	DBH	SS	ST	RDVI	TCARI/ OSAVI*	T	Aff	CC
Cabanelles	0.31	0.23	548.88	29.73	0.64	1.68	0.32	-0.37	33.75	6.38	7.72
Tivissa	-	-	484.96	23.88	0.86	1.95	0.31	-0.36	34.46	5.96	5.24
Sant Salvador de Guardiola	0.37	0.1	571.03	29.45	0.78	1.34	0.32	-0.36	33.24	6.41	6.5
Zuera	0.41	0.14	452.32	23.6	1.32	2.06	0.31	-0.34	34.47	6.02	13.86
Valdeconcha	0.49	0.06	504.5	26.18	0.85	2.1	0.33	-0.34	33.78	6.33	7.3
Alcantud	0.57	0.03	484.54	26.1	0.95	2.45	0.32	-0.36	33.92	6.49	9.09
Villarejo de Salvanes	0.43	0.11	403.8	18.11	0.94	1.91	0.3	-0.37	35.4	6.01	17.15
Cirat	0.29	0.27	482.08	25.09	1.15	2.19	0.32	-0.36	33.78	5.91	11.42
Tuejar	0.39	0.12	524.78	28.46	1.09	2.29	0.33	-0.36	33.4	6.81	7.86
Enguidanos	0.51	0.09	525.17	29.52	1.02	2.01	0.32	-0.33	34.02	6.27	8.38
Tibi	0.46	0.06	521.42	26.21	0.73	2.01	0.31	-0.36	34.12	6.47	9.32
Altura	0.33	0.22	499.86	30.77	0.88	2.1	0.33	-0.37	33.34	5.73	14.12
Villa de Ves	0.1	0.44	527.28	26.21	0.66	1.76	0.33	-0.36	33.58	5.77	11.62
Jarafuel	0.37	0.09	515.27	27.15	0.69	2.03	0.31	-0.36	34.16	6.03	18.77
Bicorp	0.41	0.19	506.52	27.28	1.02	1.9	0.33	-0.37	33.21	5.72	17.66
Commercial seed	0.44	0.12	505.26	26.86	0.81	2.09	0.29	-0.36	34.39	5.68	21.14
Benicassim	0.54	0.06	507.81	27.29	0.89	2.01	0.31	-0.37	33.6	6.94	7.3
Gilet	0.46	0.04	537.96	28.88	0.84	1.91	0.31	-0.37	33.45	5.93	14.35
Villajoyosa	0.48	0.06	513.21	27.64	0.72	1.88	0.31	-0.39	35.34	5.99	7
Ricote	0.29	0.33	525.88	29.21	0.69	2.04	0.32	-0.38	34.07	5.55	18.74
Monovar	-	-	562.88	33.5	0.66	1.81	0.33	-0.36	33.88	6.28	14.22
Monovar II	0.33	0.17	543.5	29.65	0.75	1.69	0.32	-0.36	34.27	6.32	12.53
Paterna del Madera	0.43	0.09	517.41	29.78	1	1.99	0.32	-0.36	33.62	5.96	12.02
Abaran	0.31	0.18	536.5	29.61	0.72	1.73	0.33	-0.38	33.14	6.12	8.15
Quentar	0.47	0.11	419.38	23.04	1	1.94	0.31	-0.35	34.41	5.94	23.24
Benamaurel	0.46	0.07	468.82	24.46	0.87	2.4	0.31	-0.38	34.3	5.83	6.95
Velez Blanco	0.5	0.09	530.99	27.36	0.87	1.72	0.33	-0.36	33.81	6.44	9.06
Santiago-Pontones	0.5	0.05	539.27	28.67	0.91	1.92	0.33	-0.35	33.14	5.79	24.34
Lorca	0.46	0.1	501.45	31.34	0.91	2.11	0.33	-0.36	34.14	5.82	15.82
Alhama de Murcia	0.39	0.12	493.27	29.18	0.9	2.19	0.32	-0.37	33.72	5.78	15.47
Quesada	0.47	0.09	506.88	27.52	0.69	1.9	0.31	-0.36	34.16	5.96	26.94
Lentegi	0.54	0.04	537.82	30.78	0.92	2.12	0.34	-0.39	33.64	5.77	14.54
Carratraca	0.34	0.24	443.01	21.27	0.79	2.06	0.31	-0.38	35.09	5.51	36.85
Frigiliana	0.38	0.11	521.76	29.07	0.97	1.73	0.31	-0.37	33.86	6.64	11.85
Palma de Mallorca	0.44	0.11	469.39	25.38	0.79	1.99	0.28	-0.36	35.24	6.89	4.75
Santanyi	0.62	0.03	506.73	24.11	0.79	1.84	0.31	-0.35	34.32	6.53	8.98
Alcudia	0.79	0.04	506.58	25.27	0.67	1.88	0.31	-0.38	34.17	7	7.94
Calvia	0.19	0.36	534.64	29.11	1	2.08	0.31	-0.35	33.51	6.32	10.8
Marcadal, Es	0.36	0.16	499.71	26.01	0.97	1.95	0.31	-0.37	34.19	5.51	23.74
Migjorn Gran, Es	0.16	0.4	550.96	28.12	0.84	2.21	0.3	-0.33	34.51	5.71	13.89
Sant Josep de sa Talaia	0.5	0.02	584.7	35.29	0.81	1.78	0.33	-0.35	33.25	6.84	6.68
Sant Josep de sa Talaia	0.48	0.06	510.37	28.15	0.91	1.93	0.31	-0.37	34.37	6.88	5.99
Sant Antoni Portmany	0.54	0.03	525.57	27.74	0.79	1.89	0.32	-0.37	33.61	6.74	7.08
Valbuena de Duero	0.52	0.03	533.48	28.39	0.82	2.04	0.34	-0.36	33.54	-	-
Vega de Valdetronco	0.48	0.08	506.68	26.4	0.72	1.58	0.31	-0.35	33.88	-	-
Villan de Tordesillas	0.4	0.12	473.88	26.38	0.77	2.06	0.33	-0.38	34.08	-	-
Istaia-eyboia	0.53	0.05	559.53	35.05	0.88	1.88	0.34	-0.36	33.21	6.39	12.22
Amfilohia	0.24	0.28	697.55	43.04	0.75	1.43	0.38	-0.34	32.09	6.05	9.03
Tatoi-Attica	0.41	0.13	472.3	21.08	1.17	2.25	0.32	-0.38	34.89	6.18	6.24
Kassandra	0.31	0.25	668.66	38.51	1.04	1.61	0.34	-0.34	33.32	6.24	6
Gemenos	0.41	0.13	521.88	25.24	0.66	1.36	0.3	-0.38	34.05	5.87	13.9
Litorale tarantino	0.13	0.39	499.37	28.96	0.74	1.63	0.35	0.36	33.38	5.26	3.56
Gargano Monte Pucci	0.34	0.21	609.53	31.7	0.77	1.93	0.33	0.35	34.46	6.55	2.57
Gargano Marzini	0.19	0.31	546.29	30.67	0.94	2.13	0.34	0.35	33.6	6.56	2.99
Thala	0.52	0.05	423.25	20.59	1.14	2.01	0.32	0.37	34.22	5.2	3.39
Tabarka	0.44	0.11	416.25	18.82	0.68	1.66	0.29	0.4	34.97	5.35	3.47

Top (%); Bottom (%); T canopy temp. (°C); SS soluble sugars, ST starch (% of dry mass; Jun. 2010); DBH diameter at breast height (cm); Height (cm); Aff age first flowering (years); CC cone count

Table S3. Matrix of correlations calculated at population level between the least square means of the eleven phenotypic traits derived from the ANOVA.

	Bottom	**Top**	**Height**	**DBH**	**SS**	**ST**	**RDVI**	**TCARI/ OSAVI***	**T**	**Aff**	**CC**
Bottom	1.00	-0.91	-0.27	-0.24	0.05	0.14	-0.33	-0.26	0.20	0.35	-0.22
Top	-0.91	1.00	0.23	0.19	-0.08	-0.10	0.31	0.26	-0.16	-0.35	0.24
Height	-0.27	0.23	1.00	0.91	-0.23	-0.41	0.65	0.38	-0.65	0.31	-0.38
DBH	-0.24	0.19	0.91	1.00	-0.13	-0.29	0.72	0.38	-0.72	0.24	-0.29
SS	0.05	-0.08	-0.23	-0.13	1.00	0.45	0.05	0.31	-0.01	-0.03	-0.02
ST	0.14	-0.10	-0.41	-0.29	0.45	1.00	-0.21	0.06	0.28	-0.02	0.03
RDVI	-0.33	0.31	0.65	0.72	0.05	-0.21	1.00	0.28	-0.74	-0.03	-0.02
TCARI/OSAVI*	-0.26	0.26	0.38	0.38	0.31	0.06	0.28	1.00	-0.28	0.21	-0.14
T	0.20	-0.16	-0.65	-0.72	-0.01	0.28	-0.74	-0.28	1.00	-0.10	0.13
Aff	0.35	-0.35	0.31	0.24	-0.03	-0.02	-0.03	0.21	-0.10	1.00	-0.75
CC	-0.22	0.24	-0.38	-0.29	-0.02	0.03	-0.02	-0.14	0.13	-0.75	1.00

Bottom (%); Top (%); T canopy temperature (°C); SS soluble sugars (% of dry mass; June 2010); ST starch (% of dry mass; 2010); DBH diameter at breast height (cm); Height (cm); Aff age at first flowering (years); CC cone count

Table S4. Parameter estimates of the starting SEM. The non-standardized coefficients are reported. The *z*-statistic corresponds to the estimate divided by its standard error. The *p*-value is calculated by evaluating the *z*-statistic under a standard normal distribution. CI indicates the 95% confidence intervals (lower and upper).

Left variable	Operator	Right variable	Estimate	SE	*z*-value	*p*-value	CI (lower)	CI (upper)
Growth	=~	DBH	1.00	0.00	-	-	1.00	1.00
Growth	=~	Height	1.23	0.09	13.86	0.00	1.06	1.41
Reproduction	=~	Cone Count	1.00	0.00	-	-	1.00	1.00
Reproduction	=~	Age First Flowering	-0.99	0.18	-5.60	0.00	-1.33	-0.64
Water uptake depth	=~	Bottom	1.00	0.00	-	-	1.00	1.00
Water uptake depth	=~	Top	-0.83	0.09	-9.05	0.00	-1.00	-0.65
Summer transpiration	=~	RDVI	1.00	0.00	-	-	1.00	1.00
Summer transpiration	=~	Canopy T	-3.67	0.51	-7.23	0.00	-4.65	-2.66
Reserves	=~	Soluble sugars	1.00	0.00	-	-	1.00	1.00
Reserves	=~	Starch	1.04	0.36	2.92	0.00	0.34	1.75
Photos. capacity	=~	TCARI/OSAVI*	1.00	0.00	-	-	1.00	1.00
Water uptake depth	~~	Photos. capacity	0.00	0.00	-1.84	0.07	0.00	0.00
Summer transpiration	~~	Photos. capacity	0.00	0.00	2.03	0.04	0.00	0.00
Water uptake depth	~~	Summer transpiration	0.00	0.00	-2.00	0.05	0.00	0.00
Reproduction	~	Summer transpiration	-0.29	0.47	-0.62	0.54	-1.19	0.62
Reproduction	~	Water uptake depth	-0.17	0.06	-2.99	0.00	-0.28	-0.06
Reproduction	~	Photos. capacity	-0.96	0.45	2.12	0.03	-1.84	-0.07
Growth	~	Summer transpiration	2.22	0.38	5.81	0.00	1.47	2.97
Growth	~	Water uptake depth	0.01	0.04	0.29	0.80	-0.06	0.08
Growth	~	Photos. capacity	0.47	0.31	1.52	0.11	0.78	6.71
Reserves	~	Summer transpiration	-1.03	1.60	-0.64	0.52	-4.14	2.10
Reserves	~	Water uptake depth	0.18	0.18	1.04	0.30	-0.16	0.53
Reserves	~	Photos. capacity	3.74	1.51	2.47	0.01	0.78	6.71
Growth	~~	Reproduction	0.00	0.00	-2.59	0.01	0.00	0.00
Reproduction	~~	Reserves	0.00	0.00	1.19	0.23	0.00	0.00
Growth	~~	Reserves	-0.01	0.00	-2.90	0.00	-0.01	0.00

=~ latent variable; ~ regressed on; ~~ covariance

Table S5. Bootstrapped estimates parameter of the simplified SEM. The non-standardized coefficients are reported. The *z*-statistic corresponds to the estimate divided by its standard error. The *p*-value is calculated by evaluating the *z*-statistic under a standard normal distribution. CI indicates the 95% confidence intervals (lower and upper).

Left variable	Operator	Right variable	Estimate	SE	*z*-value	*p*-value	CI (lower)	CI (upper)
Growth	=~	DBH	1.00	0.00	-	-	1.00	1.00
Growth	=~	Height	1.24	0.09	13.09	0.00	1.05	1.42
Reproduction	=~	Cone Count	1.00	0.00	-	-	1.00	1.00
Reproduction	=~	Age First Flowering	-0.95	0.18	-5.35	0.00	-1.29	-0.60
Water uptake depth	=~	Bottom	1.00	0.00	-	-	1.00	1.00
Water uptake depth	=~	Top	-0.80	0.09	-8.16	0.00	-0.99	-0.61
Summer transpiration	=~	RDVI	1.00	0.00	-	-	1.00	1.00
Summer transpiration	=~	Canopy T	-3.68	0.51	-7.28	0.00	-4.67	-2.69
Reserves	=~	Soluble sugars	1.00	0.00	-	-	1.00	1.00
Reserves	=~	Starch	0.90	0.37	2.42	0.02	0.17	1.63
Photos. capacity	=~	TCARI/OSAVI*	1.00	0.00	-	-	1.00	1.00
Water uptake depth	~~	Photos. capacity	0.00	0.00	-1.92	0.05	0.00	0.00
Summer transpiration	~~	Photos. capacity	0.00	0.00	2.03	0.04	0.00	0.00
Water uptake depth	~~	Summer transpiration	0.00	0.00	-1.82	0.07	0.00	0.00
Reproduction	~	Summer transpiration	-0.14	0.05	-2.86	0.00	-0.24	-0.05
Reproduction	~	Water uptake depth	-0.99	0.44	2.22	0.03	-1.87	-0.12
Reproduction	~	Photos. capacity	2.03	0.31	6.57	0.00	1.43	2.64
Growth	~	Summer transpiration	0.50	0.29	1.75	0.08	-0.06	1.07
Growth	~	Water uptake depth	3.18	1.44	2-22	0.03	0.37	5.99
Growth	~	Photos. capacity	0.00	0.00	-2.75	0.00	0.00	0.00
Reserves	~	Summer transpiration	-0.01	0.00	-2.93	0.00	-0.00	0.00
Reserves	~	Water uptake depth	1.00	0.00	-	-	1.00	1.00
Reserves	~	Photos. capacity	1.24	0.09	13.09	0.00	1.05	1.42
Growth	~~	Reproduction	1.00	0.00	-	-	1.00	1.00
Reproduction	~~	Reserves	-0.95	0.18	-5.35	0.00	-1.29	-0.60
Growth	~~	Reserves	1.00	0.00	-	-	1.00	1.00

=~ latent variable; ~ regressed on; ~~ covariance

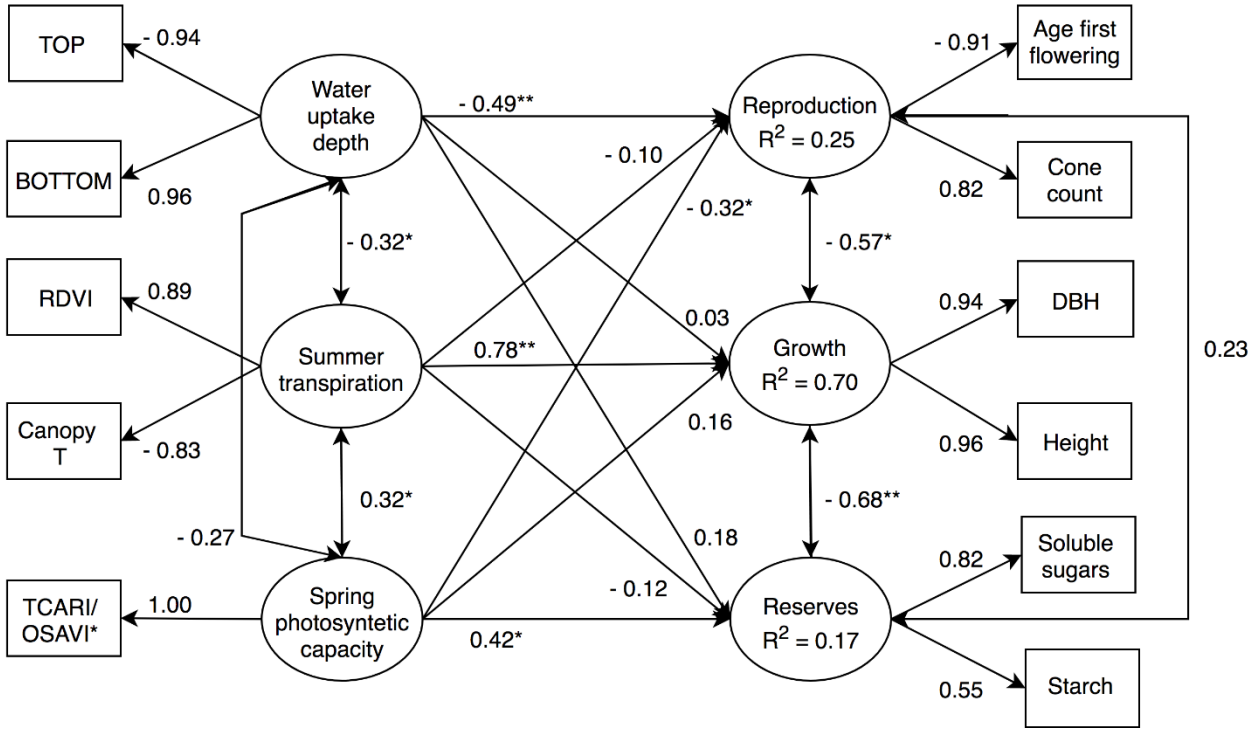

Figure S1. Path coefficients of the starting model

CHAPTER III

Bridging the genotype-phenotype gap for a Mediterranean pine through automatic crown segmentation and multispectral imagery

SUMMARY

The wide availability of genomic information coupled with the development of high-throughput phenotyping techniques provides the potential to study the genomic bases of phenotypic differentiation in trees. In this study, we developed an automatic methodology based on Unmanned Aerial Vehicle (UAV) imagery for deriving tree-level phenotypes of adult individuals of *Pinus halepensis* (Mill.) growing in a common garden located in Altura, eastern Spain. A single flight was performed in July 2016 to retrieve RGB, multispectral and thermal images of the trial. A dense 3D point cloud was obtained from RGB images and was used to estimate tree height and crown area and for automatic canopy segmentation. The segmented crowns were combined with multispectral and thermal orthomosaics to retrieve individual records of vegetation indices and canopy temperature as surrogates of leaf area, photosynthetic pigments and leaf water concentration and total transpiration. Thereafter, a genome-wide association study (GWAS) was performed to analyse the association between phenotypic records of 375 individuals with genomic variation at 235 Single Nucleotide Polymorphism (SNPs) loci derived from the species transcriptome. Phenotypic differentiation in several traits was associated with genomic variation in different SNPs located in genes encoding for proteins involved in a wide-range of processes. Growth traits were associated with variation in 12 SNPs, mainly located in genes involved in cellulose and carbohydrates metabolism. Transpiration and water concentration in the leaves were associated with variation in genes encoding for proteins involved in stomata dynamics. Variation in leaves pigments and leaf area was associated with 11 SNPs located in genes whose protein products were mainly involved in plant signalling and peroxisomes metabolisms. The phenotypic variance explained by single SNPs was generally low (1-9%). However, a multi-locus association test revealed that a combination of several SNPs explained up to 24% of variation in height, indicating a polygenic control of growth traits. This study provided a first insight into the genomic mechanisms of phenotypic variation in a wide-spread Mediterranean conifer, highlighting the feasibility of combining cost-effective genotyping tools with high-throughput phenotyping obtained with UAVs to narrow the genotype-phenotype knowledge gap in forest species.

Keywords: Aleppo pine; Genomics; GWAS; Remote Sensing; SNPs; UAV

INTRODUCTION

The rapid development of high-throughput genotyping technologies together with advances in phenomics related to the availability of non-destructive phenotyping tools has narrowed the prevailing knowledge gap between genes and phenotypes (Houle *et al.,* 2010; Großkinsky *et al.,* 2015). Nowadays, hundreds of individuals can be characterised at an increasing number of genetic markers covering large part of the genome, resulting in thriving amount of genome-wide association studies (GWAS) aiming at understanding the genetic basis of phenotypic differentiation by linking individual genotypes to phenotypes (Lobos *et al.,* 2017). In forest species, the common approach relies on the characterisation of individuals growing in common garden experiments, in which numerous trees can be grown in semi-natural environments to remove the effects of growing conditions on phenotypic variation (McKown *et al.,* 2014; Baison *et al.,* 2019). Combining the information derived from accurate phenotyping performed in common gardens with genomic scan at hundreds of loci can result in an effective methodology to study the genetic basis of adaptation in forest species (de Villemereuil *et al.,* 2016).

To this end the following two requisites are necessary. First, genome-wide sets of molecular markers should be available for the selected species in order to gain information on the number of loci which could contribute to phenotypic differentiation (Grattapaglia and Resende, 2011). This issue has been progressively solved from the turn of this century. Once available only for few model organisms, sets of molecular markers putatively under selection are now available also for non-model species such as forest trees (Khan and Korban, 2012; Jaramillo-Correa *et al.,* 2015). The second issue is related to difficulties in obtaining phenotypic information of a representative number of trees, particularly in the case of adult individuals (Ludovisi *et al.*, 2017). Indeed, with the exception of simple measurements of growth traits, trees are difficult to characterise for meaningful anatomical and physiological traits with standard phenotyping approaches. As a possible solution to this issue, Unmanned Aerial Vehicles (UAV) imagery is emerging as an effective high-throughput phenotyping tool to indirectly infer variation in traits such as leaf gas exchange and crown anatomy in common garden experiments of forest trees (Santini *et al.,* 2019). High-resolution remote sensing data coupled with efficient algorithms for automatic crown identification represent a powerful tool for individual tree phenotyping (Wallace *et al.,* 2016; Santini *et al.,* 2019).

Aleppo pine (*Pinus halepensis* Mill.) is a drought-avoidant species representing the most widespread conifer of the Mediterranean basin. Common garden experiments have revealed a wide differentiation among populations of this species in traits such as aerial growth (Schiller

and Atzmon, 2009; Voltas *et al.,* 2018), phenology (Klein *et al.,* 2013), water uptake patterns (Voltas *et al.,* 2015), hydraulic conductivity (Tognetti *et al.,* 1997) and reproductive effort (Climent *et al.,* 2008). However, the genetic basis of this variation remains largely unexplored. Recently, a set of Single Nucleotide Polymorphisms (SNPs) markers derived from the species transcriptome have been developed for *P. halepensis* (Pinosio *et al.,* 2014). A GWAS based on these markers has provided the first insights into the genetic basis of variation in traits including growth, reproduction, water use efficiency and wood anatomy among Aleppo pine individuals (Rodríguez Quilón, 2017). A complication derives from the complex neutral genetic structure of this species, which have been shaped by past population dynamics and makes difficult the identification of loci associated with phenotypic differentiation (Yu *et al.,* 2006; Serra-Varela *et al.,* 2017). Indeed, recent studies have identified a strong genetic structure separating western and central-Eastern Mediterranean populations, with further subdivisions among each group (Ruiz Daniels *et al.,* 2018).

In this study, we combined genotypic information obtained in a common garden of adult individuals of *P. halepensis* with phenotypic data derived at tree level using UAV-derived remote sensing data. We aimed at describing the genetic control of variation in traits that, partially due to phenotyping difficulties, are uncommonly considered in genotype-phenotype association studies. Specifically, the objective of this study were 1) to develop a straightforward methodology for deriving tree-level information of growth traits, vegetation indices, photosynthetic pigments concentration and whole tree transpiration, 2) to identify phenotypic associations among these traits, 3) to identify putative genes underlying the variation in such traits and test for a multi-genic control of phenotypic variation and 4) to estimate the proportion of variation in phenotypes explained by genotypes. Due to the set of markers used, which were derived from putative genes related to different stress responses (Pinosio *et al.,* 2014), we expected to identify a significant number of genotype-phenotype associations.

MATERIALS AND METHODS

Study site and plant material

The study was carried out on adult individuals of Aleppo pine growing in a common garden experiment in Altura (39°49′29″N, 00°34′22″W, 640 m a.s.l.; Castellón province, eastern Spain). Seeds from 56 natural population of *P. halepensis* covering a large part of the species range were collected in 1995 and planted in a forest nursery in Spain (Table 1; Appendix, Figure S1). In 1997, one year old seedlings were planted systematically (2.5 × 2.5 m spacing) at the study site in experimental units consisting of linear plots of four seedlings. Four replicates were established

following a Latinised row-column design for a total of 896 seedlings (16 per population) tested in the trial. Height and diameter at breast height (DBH) were measured per tree in 2010 (at age 13).

UAV flight

A single flight was performed at noon on 26th July 2016 using a Mikrokopter OktoXL (Moormerland, Germany) flying under remote control at around 100 m of altitude. The UAV was equipped with three different cameras that were mounted down-looking in consecutive flights. First, a multispectral camera (MCA12; Tetracam Inc., Chatsworth, CA, US) was operated to capture 15.6-megapixel images in 10 wavelengths (450 ± 40, 550 ± 10, 570 ± 10, 670 ± 10, 700 ± 10, 720 ± 10, 840 ± 10, 860 ± 10, 900 ± 20, 950 ± 40 nm) in the visible and near infrared (NIR) regions of the spectrum. Second, RGB images were obtained using a Mirrorless Interchangeable Lens Camera (Lumix GX7; Panasonic, Osaka, Japan). Finally, a FLIR (Tau2 640; FLIR Systems, Nashua, NH, USA) thermal camera was employed for the acquisition of thermal images. For a detailed description of image acquisition, see Santini *et al.* (2019).

Image processing and crown segmentation

The workflow that we followed to derive individual-level phenotypes data is schematised in Figure 1. Two orthomosaics (one multispectral and one thermal) were obtained from raw multispectral and thermal images using the Agisoft PhotoScan Professional software (Agisoft LLC, St. Petersburg, Russia). The geographical coordinates of four ground control points were obtained with 1 meter accuracy using a GPS device (Juno 5B, Trimble Inc., Sunnyvale, USA) and were used for georeferencing the orthomosaics.

RGB images were analysed through structure-from-motion (SfM) photogrammetry in the software Agisoft PhotoScan Professional to obtain a georeferenced 3D dense point cloud of the common garden, in which the height of each point is expressed in meters above sea level. The software FUSION (Mcgaughey, 2014) was employed to classify vegetation and soil points of the dense point cloud, and a digital terrain model (DTM) was obtained thereafter. Subsequently, the dense point cloud and the DTM were combined in FUSION to obtain a normalized point cloud, in which the height of each point is expressed in meter above ground. Finally, we obtained a canopy height model (CHM) from the normalized point cloud using the function grid_canopy implemented in the package lidR (Roussel *et al.*, 2018) of the R environment

The CHM was used to identify treetops using an algorithm based on local maximum filter (Popescu and Wynne, 2004) implemented in the function tree_detection in the R package lidR

(Roussel *et al.,* 2018). The height of each treetop was retrieved from the CHM as an imagery-derived estimation of tree height (H_{UAV}). Finally, single crowns were segmented (i.e. outlined) in the CHM using the function mcws in the ForestTools package (Plowright 2018), which performs a watershed segmentation (Meyer and Beucher 1990) guided by the locations of the treetops. Tree crown area was calculated as the projection of the outlined crown on the ground. Crown area was considered as a surrogate of DBH (Lockhart *et al.,* 2005).

The accuracy of tree identification was visually checked in the software QGIS (version 3.6; QGIS Development Team, 2019) and the crowns of the misidentified trees were manually identified. The result of this process was a total 806 georeferenced crown shapes (discarding dead trees), which were used to crop corresponding images from multispectral and thermal orthomosaics. Therefore, two images of the crown (one multispectral and one thermal) were obtained for each of the 806 trees of the common garden and used to calculate tree-level vegetation indices and canopy temperature.

Vegetation indices and canopy temperature

From multispectral images, several vegetation indices (Table 2) were calculated for each pixel of a single image corresponding to a particular tree crown. An average value was obtained afterwards for each of the indices per each image. Indices related to leaf area were calculated, including the Normalised Difference Vegetation Index (NDVI), the Optimised Soil Adjusted Vegetation Index (OSAVI), the Re-normalized Difference Vegetation Index (RDVI) and the Enhanced Vegetation Index (EVI). Additionally, the Modified Chlorophyll Absorption Reflectance Index (MCARI) and the Transformed Chlorophyll Absorption Ratio Index (TCARI) were calculated. The latter indices are related to both leaf area and chlorophyll concentration (Daughtry *et al.,* 2000). The ratio between TCARI and OSAVI (TCARI/OSAVI index) was calculated as a better estimate of chlorophyll concentration free of the effect of leaf area (Zarco-Tejada *et al.,* 2004). Finally, the Carotenoid Reflectance Index 2 (CRI2), the Anthocyanin Reflectance Index 2 (ARI2) and the Water Band Index (WBI) were calculated to investigate other photosynthetic pigments and the water concentration of needles. Finally, thermal images were used to retrieve crown-level estimates of canopy temperature.

Genotyping

A subset of 375 individuals belonging to 28 out of the 52 tested populations was used for genetic analysis (Table 1). First, they were genotyped at eight simple sequence repeats (SSRs) loci: epi3 (Budde *et al.,* 2014), FRPP94 and ITPH4516 (Mariette *et al.,* 2001), NZPR544 and B4F08

(Guevara *et al.,* 2005), pEST2669 and pEST8 (Steinitz *et al.,* 2011) and PtTX3030 and PtTX3116 (González-Martínez *et al.,* 2004). A detailed description of SSR amplification is reported in (Ruiz Daniels *et al.,* 2018).

Additionally, the same subset of individuals was genotyped at 294 SNPs using a 384-plex SNP assay with Illumina VeraCode Technology, as described in details in Pinosio *et al.* (2014). The SNPs included loci derived from the transcriptome of *P. halepensis* and from re-sequenced loci firstly identified in loblolly pine, thus comprising candidate genes related to wood anatomy, growth, phenology and to a wide-range of stress responses.

Statistical analysis

Phenotypic data

To validate the imagery-derived estimations of growth traits, H_{UAV} and crown area were compared by simple correlations to ground-based measurements of height and DBH. In order to remove the effect of non-uniform growing conditions on phenotypic records in the common garden, tree-level estimates of H_{UAV}, crown area, vegetation indices and canopy temperature were subjected to mixed-model ANOVA. The ANOVA consisted of column and replicate as fixed terms and column by replicate interaction, row nested to replicate and column by replicate by row interaction as random terms. The tree-level residuals of this model are individuals' phenotypic data which retains only genotypic variation (i.e., they are free of environmental effects related to the trial design). For this reason, they were used for genotype-phenotype association analysis (see below). These residuals were also used as input for a PCA analysis, with the objective of summarizing the information retrieved by vegetation indices and to analyse tree-level associations among traits. To this end, the loadings of H_{UAV}, crown area, vegetation indices and canopy temperature were plotted for the first two components of the PCAs.

SSRs data

Individuals' genotypes at SSRs loci were used to calculate individuals' relatedness. For this purpose, a kinship matrix was obtained from SSRs in the software SpaGeDi 1.3 (Hardy and Vekemans, 2015) using the kinships coefficient developed by Loiselle *et al.* (1995). In addition, the genetic structure of the populations was inferred using the Bayesian clustering method implemented in STRUCTURE (Pritchard *et al.,* 2000). At this purpose, STRUCTURE was run varying the numbers of possible genetic clusters (K) from one to ten, and each K was replicated ten times. Each run consisted of 1×10^5 burn-in iterations and 1×10^6 data collection iterations. The different runs for the same K were then averaged using the software CLUMPP (Jakobsson

and Rosenberg, 2007). The most likely K was selected calculating an empirical statistic, ΔK, based on the second derivative of the likelihood of K (Evanno *et al.,* 2005). Since including a reliable genetic structure is crucial to avoid false positives in the following GWAS, the genetic structure obtained through Bayesian clustering was evaluated with an independent approach. At this purpose, Principals Coordinates Analysis (PCoA) were calculated on a matrix of pair-wise genetic distances (G'_{ST}) between populations and the first two components were plotted to summarise the relations between populations. Both the calculation of genetic distances and PCoA were carried out using the program GenAlEx (Peakall and Smouse, 2006).

GWAS

A GWAS was performed to test for the association between genotypes at single locus and each phenotypic trait (i.e. H_{UAV}, crown area, canopy temperature and each vegetation index). We used the residuals obtained from the ANOVA as phenotypes, which were associated with genotypes at 235 SNPs out of the 384-plex assay. These 235 SNPs where those showing high quality genotypes and a frequency of the minor allele >0.05.

For the association analysis, a mixed linear model (MLM) was fitted independently for each pair of SNP and phenotypic trait following the procedure of Yu *et al.* (2006) implemented in Tassel 5.0 (Bradbury *et al.,* 2007). The probability of membership of each individual to each genetic cluster detected from clustering analysis (see "results") was included to avoid false positive associations related to large-scale genetic structure. Moreover, the kinship matrix was also included in the model, to control for finest genetic structure (Yu *et al.,* 2006). After the MLMs were fitted, a correction for multiple testing was performed on the *p*-values using the false discovery rate method (Storey and Tibshiriani, 2003) implemented in R qvalue package (Storey *et al.*, 2019).

SNPs loci for which significant association emerged with traits were annotated from homology with other plant species. For this purpose, the DNA sequence of the SNP locus was compared with the reference proteins (refseq_protein) database using the blastx tool (https://blast.ncbi.nlm.nih.gov/Blast.cgi?LINK_LOC=blasthomeandPAGE_TYPE=BlastSearchandPROGRAM=blastx). For those SNPs that were successfully annotated, the molecular and biological functions of the homologous protein, if available, were retrieved using the Uniprot database (https://www.uniprot.org/).

Multi-locus association tests

GWAS tests for significant contributions of single locus to trait variation, but it does not provide an estimate for the total number of loci contributing to phenotypic variation. Therefore, the number of SNPs explaining trait variation and the overall phenotypic variance explained by combinations of SNPs were estimated using a Bayesian variable selection regression model (BVSR) implemented in the software *pimass* (Guan and Stephens, 2011). This implements an iterative process in which at each steps a liner model is fitted where phenotype is determined by a subset of SNPs. In each iteration, each SNP may be kept, added or removed from the model, with SNPs with strongest associations with the phenotype added to the model with highest probability. The total number of SNPs contributing to the phenotype and the percentage of variation explained (PVE) is calculated at each iteration and defines the posterior distributions on these parameters. For each trait (i.e. H_{UAV}, crown area, canopy temperature and each vegetation indices), *pimass* was run with 1×10^5 iterations after a burn-in period of 10,000 iterations. The number of SNPs contributing to the phenotype and PVE were recorded every 10th iteration. The median values and 95% equal tail probability credible intervals of the number of SNPs contributing to the phenotype and of PVE were calculated from the posterior distribution of these parameters per each trait. Since *pimass* does not implement a correction for genetic structure, before running the program a different ANOVA was performed on the raw phenotypic data. The model consisted of column and replicate as fixed terms and column by replicate interaction, row nested to replicate and column by replicate by row interaction as random terms. In addition, the probabilities to belong to the two genetic clusters emerged by STRUCTURE (see "results" section) were included as covariates. The residuals of this ANOVA, which are phenotypic data corrected for genetic structure and free of environmental effects related to trial design, were used as phenotypes for the BVSR.

RESULTS

Canopy segmentation and PCA analysis

A total of 736 trees (92%) were successfully identified through automatic canopy segmentation, while 67 trees were not recognized by the segmentation algorithm and were manually identified. Moreover, 13 false identification of trees happened. Based on the detected treetops and tree crowns, individual records of H_{UAV}, crown area, vegetation indices and canopy temperature were successfully obtained for the 806 individuals of the common garden. H_{UAV} correlated with ground-based height measurements at tree-level ($r=0.81$, $p<0.001$), indicating a reliable imagery-

derived estimation of tree height. Crown area correlated with ground-measured DBH ($r=0.68$, $p<0.001$).

The PCA loadings revealed relationships among vegetation indices (Figure 2). Indices related to leaf area (i.e., NDVI, RDVI and OSAVI) grouped together in the plot of loadings, being unrelated to TCARI/OSAVI (informative of chlorophyll content). MCARI, EVI and TCARI grouped with NDVI, OSAVI and RDVI, but closer to TCARI/OSAVI. WBI (informative of water concentration), ARI2 (informative of anthocyanin concentration) and CRI2 (informative carotenoid concentration) were less explained by the first two PCA dimensions and were negatively associated with TCARI/OSAVI. Canopy temperature was negatively associated with H_{UAV} and crown area, which were in turn positively related to indices describing leaf area. However, canopy temperature, H_{UAV} and crown area were poorly represented in the first two axes of the PCA (Figure 2).

Neutral genetic data

All the SSRs loci resulted polymorphic, with a mean number of allele per locus of 3.07 across populations. The Bayesian clustering performed on SSRs genotypes indicated that the most probable number of clusters was two (Appendix, Figure S2). In this scenario, Eastern Mediterranean populations comprising individuals from the Iberian Peninsula and the Balearic islands were separated from central Mediterranean ones (i.e. Greek, Italian and Tunisian), even if one Tunisian populations showed a higher degree of admixture (Figure 3). Possible clustering also emerged at K=4 or K=7, but with a lower probability than the K=2 scenario (Appendix, Figure S2). However, considering four or seven genetic clusters did not result in clear geographical distinction between genetic groups. Moreover, the scenario with two main genetic clusters was confirmed by PCoA performed on a matrix of populations' genetic distances (Figure S3). The first two axis of the PCoA identified a clear clustering in the two above-mentioned groups. Probabilities of individual assignment to the two clusters at K=2 were then used for correcting genotypic-phenotypic associations to avoid false positives.

GWAS

GWAS revealed twelve significant associations between SNPs and growth traits (i.e. H_{UAV} and crown area) with a p-value$< 10^{-3}$ (Table 3). H_{UAV} resulted associated with 10 markers, which explained between 5% and 10% of the variance. Two SNPs were associated with crown area, explaining 5% of the phenotypic variance.

Sixteen associations emerged between SNPs and vegetation indices (Table 3). Among those, seven associations occurred with indices related to leaf area, five with WBI (indicative of leaf water concentration), two with CRI2 (indicative of carotenoid concentration) and one with ARI2 (indicative of anthocyanin concentration). These associations explained a small proportion of phenotypic variance (range 3.5% - 5.5%). No associations emerged with TCARI/OSAVI (indicative of chlorophyll concentration). Finally, one SNP was associated with canopy temperature, explaining *ca.* 4% of the variance.

Some SNPs resulted associated with more than one trait (Table 3). SNP 91 was associated with EVI (indicative of leaf area) and WBI (indicative of leaf water content), and SNP 108 was associated with H_{UAV}, EVI and WBI. SNP 133 was associated with H_{UAV} and WBI, while SNP 241 was associated with EVI and MCARI. Finally, SNP 273 and SNP 350 were associated with H_{UAV} and EVI simultaneously.

Most SNPs for which significant associations emerged resulted annotated in known genes (Table 3). For some of the annotated markers, it was possible to retrieve the molecular and biological functions of the homologous protein, which are reported in Table 4.

Multi-locus association test

The multi-locus association test performed through BVSR revealed that combinations of the 235 SNPs explained a relatively high proportion of variance of H_{UAV} (Table 5). The median value of PVE was 24% and the median number of SNPs explaining the variation was 94. On the other hand, only 7% of the variance of crown area was explained by a combination of SNPs. Similarly, PVE was low in the case of the traits derived from remote sensing data, ranging between 1% and 4% for most traits. In addition, the number of SNPs contributing to variation was generally low, and for many traits the 95% confidence interval included the value of only one SNP explaining phenotypic variation. As exceptions, a relatively higher PVE was found for the vegetation indices EVI (8%) and WBI (7%). In these cases, a slightly higher number of SNPs was included in the models (Table 5).

DISCUSSION

Canopy segmentation and recovery of phenotypic information

Developing cost and time effective phenotyping approaches is fundamental for understanding the genetic basis of phenotypic differentiation (Lobos *et al.*, 2017). In this regard, canopy segmentation based on RGB-derived dense point clouds is being increasingly used for the estimation of growth traits in natural forests and fruit orchards (Wallace *et al.*, 2016; Weiss and

Baret, 2017). Several studies have shown that this approach – based on inexpensive devices – can provide accurate estimations comparable to those obtained with more expensive and complex technologies such as light detection and ranging (LIDAR) (Zarco-Tejada *et al.,* 2014; Wallace *et al.,* 2016). Our study is, to the best of our knowledge, the first one to have applied automatic canopy segmentation in a common garden of a forest species. This approach resulted effectively and highly precise to provide tree-level estimations of growth-related traits. Particularly, UAV-derived height estimation highly agreed with ground-based measurement, while crown area is a good surrogate of stem diameter, as reported elsewhere (Lockhart *et al.,* 2005; Filipescu *et al.,* 2012). Moreover, automatic identification of crown areas allowed retrieving tree-level values of vegetation indices as surrogates of meaningful morpho-physiological traits that are uncommonly recorded with standard phenotyping techniques. In a previous study performed in the same common garden, vegetation indices and canopy temperature derived at plot level were used to investigate inter-population differentiation in vegetation characteristics (Santini *et al.,* 2019). The present study provided more detailed information (i.e., tree-level *vs*. plot-level), which, besides being appropriate for the analysis of inter-population differentiation, is also suitable for genotype-phenotype association studies and for the assessment of trade-offs and trait associations at the individual level.

In this regard, PCA analysis revealed a strong association between indices related to leaf area, canopy temperature and above-ground growth traits. Trees having high leaf area and reduced canopy temperature (i.e. indicative of a higher transpiration) showed a high growth, indicated by increased height and crown area. These results confirm the strong dependence of growth to variation in photosynthetic surface and total transpiration in *P. halepensis* under drought conditions (Voltas *et al.,* 2008; Santini *et al.,* 2019). On the other hand, variation in leaf biochemistry seemed not to affect tree growth (Santini *et al.,* 2019).

Association genetics of vegetation properties

The genome-wide association study revealed a number of SNPs significantly associated with phenotypic variation in vegetation indices. Since linkage disequilibrium usually decays rapidly in conifers (De La Torre *et al.,* 2014, Plomion *et al.,* 2016), these SNPs are likely quantitative trait nucleotides (i.e. single polymorphism influencing phenotype) or are located in close proximity to the causative polymorphisms. Several relevant SNPs were annotated with known proteins, even though in some cases a correct annotation was not possible. This may be partially due to the relatively scarce information on conifer genomes that is available to date, which emphasises the need of further studies to characterise tree genomes (De La Torre *et al.,* 2014).

However, the identified associations provided a first insight into the genetic basis of phenotypic variation in *P. halepensis*.

In the case of vegetation indices related to leaf area, two of the identified SNPs were annotated to known proteins characterised in other species. SNP 151 is found in a gene encoding for PEX11C protein involved in peroxisome metabolism. Peroxisomes are cellular organelles which mediate many essential biochemical processes including lipids mobilization, photorespiration, metabolism of plant hormones, metabolism of reactive oxygen species and, also, photomorphogenesis (Hu, 2007; Kaur and Hu, 2013). SNP 273 is found in a gene encoding for cellulose synthase. This is part of a family of genes with a crucial role in cell wall synthesis and organization, influencing several plant processes (Richmond and Somerville, 2000). In this regard, variation in the same SNP is also associated with lignin metabolism in *P. halepensis* (Rodríguez-Quilón, 2017).

No significant associations emerged with vegetation indices related to needle chlorophyll content. This may be due to the weak differentiation in chlorophyll concentration in this species for this trait (Santini *et al.,* 2019). On the other hand, four SNPs were associated with carotenoids or anthocyanins content. Three of these (61, 204 and 258) were correctly annotated. SNPs 204 and 258 are located in genes encoding for proteins involved in auxin transport and auxin-mediated signalling, while the protein associated with SNP 61 is involved in pathogen resistance. The WBI index, indicative of leaf water concentration, was associated with five different SNPs, but only one was located in a gene of known function. SNP 133 is located in a gene coding for a protein of the polygalacturonase family, which are involved in pectine degradation influencing cell wall construction, differentiation, maturation and degradation (Yang *et al.,* 2018). Specifically, SNP 133 is located in a gene encoding the polygalacturonase isoform X3, which has been widely studied in the model plant *Arabidopsis*. In this species, polygalacturonase isoform X3 protein influences tissue development and is involved in stomatal dynamics of mature leaves, which might explain the association found with leaf water concentration (Rui *et al.,* 2017).

In the case of canopy temperature, only SNP 140 resulted associated with phenotypic variation. This SNP was correctly annotated with a Rac-like GTP binding protein characterised in *Picea mariana* (Perry and Bousquet, 1998). GTP binding proteins are a wide family of proteins which have been studied for a long time for their role in plant signalling (Terryn *et al.,* 1993). These proteins are known for their interactions with plant hormones, their role in regulation of organogenesis and their involvement in various stress and defence responses (Ma, 2007). In this regard, it is interestingly to note that some GTP-binding proteins are involved in stomatal closure

induced by abscisic acid, which might influence plant transpiration as indicated by canopy temperature (Lemichez, 2001). Indeed, differences in summer canopy temperature are indicative of variation in stomatal conductance across individuals (Gonzalez-Dugo *et al.,* 2013; Santini *et al.,* 2019).

However, all these SNPs had small effects on phenotypes, explaining less than 6% of the variation in vegetation indices or canopy temperature. Several studies have reported that in forest species the genetic variation in single markers accounts for a small proportion of phenotypic variance (Eckert *et al.,* 2009; Prunier *et al.,* 2013; Baison *et al.,* 2019). Indeed, many adaptive traits are likely under a polygenic control, suggesting that many loci with relatively small effects might affect their variation (White *et al.*, 2007; Savolainen *et al.,* 2007). However, the proportion of traits` variance explained by genetic effects did not increase significantly using multi-locus association tests. In the best cases, combinations of SNPs explained only around 8% of variance in vegetation indices. We speculate that the low proportion of variance explained may be related to the relatively low number of markers used, an issue that stresses the importance of relying on arrays of markers covering the largest possible part of the genome (Resende *et al.,* 2012). However, a high level of phenotypic variance is rarely explained by genetic variation even in studies performed in model organisms whose genomes have been well characterised and for which dense and genome-wide sets of molecular markers are available (Manolio *et al.,* 2009). This issue, known as "missing hereditability", suggests that phenotypic variation may be broadly influenced by largely unknown underlying factors such as epistatic interactions or epigenetic modifications of genes expression (Manolio *et al.,* 2009; Trerotola *et al.,* 2015).

Association genetics of growth traits

GWAS also identified twelve SNPs significantly associated to crown area and UAV-derived tree height, explaining a proportion of variance (5-10%) slightly higher than in the case of associations with vegetation indices and canopy temperature. This discrepancy and the higher number of associations may be related to the higher quality of growth data, which could be retrieved from UAV-imagery with less noise than indirect information obtained through vegetation indices, leading to a more accurate genotype-phenotype association. However, it should also be noticed that a number of interacting processes including, among others, cell division and expansion, meristematic activity, phenology and stress responses concur to determine the complexity of growth traits. Growth is undoubtedly controlled by a multitude of genetic processes, a fact that supports the high number of detected associations (Grattapaglia *et al.,* 2009). In this regard, the growth-associated SNPs that could be correctly annotated included

genomic regions encoding for a disparate number of proteins. Differences in crown area were associated with variation in a gene encoding for a trehalose-phosphatase (SNP 2), which is involved in several signalling pathways and in plant development (Ponnu *et al.,* 2011). Notably, studies performed in *Arabidopsis* have demonstrated the role of trehalose-phosphatase in the regulation of cell shape, with significant implication in plant architecture that might explain the association of this SNP with crown area (Chary *et al.,* 2008). In the case of tree height, significant associations were found with genes encoding for calcium-dependent kinase (SNP 159) involved in plant responses to endogenous and environmental cues (Romeis, 2001), for a GDP-mannose pyrophosporylase (SNP340) involved in ascorbic acid metabolism (Keller *et al.,* 1999), and for the aforementioned polygalacturonase (SNP 133) and cellulose synthase (SNP 273).

These evidences suggest that the genetic control of complex trait such as growth is associated with a large number of interacting genes with very diverse functions. Moreover, the single contribution of many other genes to a complex trait such as growth may be too small to be detected by GWAS (Resende *et al.,* 2017). In this regard, the multi-locus analysis revealed that a significantly larger proportion (i.e. 24% on average) of height variation could be explained by evaluating several SNPs at time. This result indicated that association analysis carried out considering a larger number of markers at the same time could explain a significant variation of individuals' complex traits in forest species (Savolainen *et al.,* 2007; Grattapaglia *et al.,* 2009).

Pleiotropy

In our study, some SNPs showed significant associations with multiple correlated traits, a possible indication of pleiotropic effects with genes influencing different traits simultaneously (Wu *et al.,* 2000). However, these SNPs likely concur to determine only one of the traits, showing multiple associations because of correlated traits. For example, three SNPs (108, 273 and 350) resulted associated with both height and indices related to leaf area. However, aerial growth and photosynthetic surface described by vegetation indices resulted associated in *P. halepensis*, both at tree (this study) and at population level (Santini *et al.,* 2019). On the other hand, SNPs 133 and 350 were associated both with height and WBI, two traits which were not correlated among individuals. In this case, the association of the markers with more than one trait could be indicative of true pleiotropy, with genes in which these SNPs are located influencing both leaf water content and tree growth together.

Conclusions

In this study, we developed a straightforward workflow for automatic phenotyping of trees growing in a common garden. In the era of genomics, the ability of retrieving meaningful phenotypic information with time and cost effective approaches allows to characterise the genetic basis of fundamental evolutionary processes involved in phenotypic differentiation of non-model organisms (Großkinsky *et al.*, 2015). Indeed, our study provided an important insight on the molecular processes controlling phenotypic differentiation in a widespread conifer. Undoubtedly, the scope of our inferences could be broadened by using a significantly larger number of markers and individuals. Although strong evidences explaining how variation at the cellular and tissue level is coordinated with changes at the whole-organism level are still lacking, our results highlight the potential of widely available new technologies to fill the gap between genetic differentiation and individual phenotypes (Houle *et al.*, 2010).

REFERENCES

Baison J., Vidalis A., Zhou L., *et al.* (2019) Genome-wide association study identified novel candidate loci affecting wood formation in Norway spruce. *The Plant Journal*. doi: 10.1111/tpj.14429

Bradbury P.J., Zhang Z., Kroon D.E., Casstevens T.M., Ramdoss Y., Buckler E.S. (2007) TASSEL: software for association mapping of complex traits in diverse samples. *Bioinformatics*, 23, 2633–2635.

Budde K.B., Heuertz M., Hernández-Serrano A., Pausas J.G., Vendramin G.G., Verdú M., González-Martínez S.C. (2014) *In situ* genetic association for serotiny, a fire-related trait, in Mediterranean maritime pine (*Pinus pinaster*). *New Phytologist*, 201, 230–241.

Chary S.N., Hicks G.R., Choi Y.G., Carter D., Raikhel N.V. (2008) Trehalose-6-phosphate synthase/phosphatase regulates cell shape and plant architecture in *Arabidopsis*. *Plant Physiology*, 146, 97–107.

Climent J., Prada M.A., Calama R., Chambel M.R., de Ron D.S., Alía R. (2008) To grow or to seed: ecotypic variation in reproductive allocation and cone production by young female Aleppo pine (*Pinus halepensis*, Pinaceae). *American Journal of Botany*, 95, 833–842.

Daughtry C.S.T., Walthall C.L., Kim M.S., De Colstoun E.B., McMurtrey J.E. (2000) Estimating corn leaf chlorophyll concentration from leaf and canopy reflectance. *Remote sensing of Environment*, 74, 229–239.

De La Torre A.R., Birol I., Bousquet J. *et al.* (2014) Insights into conifer giga-genomes. *Plant Physiology*, 166, 1724–1732.

de Villemereuil P., Gaggiotti O.E., Mouterde M., Till-Bottraud I. (2016) Common garden experiments in the genomic era: new perspectives and opportunities. *Heredity*, 116, 249–254.

Eckert A.J., Bower A.D., Wegrzyn J.L., Pande B., Jermstad K.D., Krutovsky K. V, St Clair J.B., Neale D.B. (2009) Association genetics of coastal Douglas fir (*Pseudotsuga menziesii* var. *menziesii*, Pinaceae). I. Cold-hardiness related traits. *Genetics*, 182, 1289–302.

Evanno G., Regnaut S., Goudet J. (2005) Detecting the number of clusters of individuals using the software structure: a simulation study. *Molecular Ecology*, 14, 2611–2620.

Filipescu C.N., Groot A., MacIsaac D.A., Cruickshank M.G., Stewart J.D. (2012) Prediction of diameter using height and crown attributes: a case study. *Western Journal of Applied Forestry*, 27, 30–35.

Gitelson A.A., Merzlyak M.N., Chivkunova O.B. (2001) Optical properties and nondestructive estimation of anthocyanin content in plant leaves. *Photochemistry and Photobiology*, 74, 38–45.

Gitelson A.A., Zur Y., Chivkunova O.B., Merzlyak M.N. (2002) Assessing carotenoid content in plant leaves with reflectance spectroscopy. *Photochemistry and Photobiology*, 75, 272–281.

Gonzalez-Dugo V., Zarco-Tejada P., Nicolás E., Nortes P.A., Alarcón J.J., Intrigliolo D.S., Fereres E. (2013) Using high resolution UAV thermal imagery to assess the variability in the water status of five fruit tree species within a commercial orchard. *Precision Agriculture*, 14, 660–678.

González-Martínez S.C., Robledo-Arnuncio J.J., Collada C., Díaz A., Williams C.G., Alía R., Cervera M.T. (2004) Cross-amplification and sequence variation of microsatellite loci in Eurasian hard pines. *Theoretical and Applied Genetics*, 109, 103–111.

Grattapaglia D., Plomion C., Kirst M., Sederoff R.R. (2009) Genomics of growth traits in forest trees. *Current Opinion in Plant Biology*, 12, 148–56.

Grattapaglia D., Resende M.D.V. (2011) Genomic selection in forest tree breeding. *Tree Genetics and Genomes*, 7, 241–255.

Großkinsky D.K., Svensgaard J., Christensen S., Roitsch T. (2015) Plant phenomics and the need for physiological phenotyping across scales to narrow the genotype-to-phenotype knowledge gap. *Journal of Experimental Botany*, 66, 5429–5440.

Guan Y., Stephens M. (2011) Bayesian variable selection regression for genome-wide association studies and other large-scale problems. *The Annals of Applied Statistics*, 5, 1780–1815.

Guevara M.A., Chagne D., Almeida M.H. *et al.* (2005) Isolation and characterisation of nuclear microsatellite loci in *Pinus pinaster* Ait. *Molecular Ecology Notes*, 5, 57–59.

Haboudane D., Miller J.R., Tremblay N., Zarco-Tejada P.J., Dextraze L. (2002) Integrated narrow-band vegetation indices for prediction of crop chlorophyll content for application to precision agriculture. *Remote Sensing of Environment*, 81, 416–426.

Hardy O., Vekemans X. (2015) SPAGeDi 1.5. a program for spatial pattern analysis of genetic diversity. Eds. Université Libre de Bruxelles, Brussells, Belgium.

Houle D., Govindaraju D.R., Omholt S. (2010) Phenomics: the next challenge. *Nature Reviews Genetics*, 11, 855–866.

Huete A., Didan K., Miura T., Rodriguez E.P., Gao X., Ferreira L.G. (2002) Overview of the radiometric and biophysical performance of the MODIS vegetation indices. *Remote Sensing of Environment*, 83, 195–213.

Hu J. (2007) Plant peroxisome multiplication: highly regulated and still enigmatic. *Journal of Integrative Plant Biology*, 49, 1112–1118.

Jakobsson M., Rosenberg N.A. (2007) CLUMPP: a cluster matching and permutation program for dealing with label switching and multimodality in analysis of population structure. *Bioinformatics*, 23, 1801–1806.

Jaramillo-Correa J.P., Prunier J., Vázquez-Lobo A., Keller S.R., Moreno-Letelier A. (2015) Molecular signatures of adaptation and selection in forest trees. In *Advances in Botanical Research*, pp. 265–306. Elsevier.

Kaur N, Li J., Hu J. (2013) Peroxisomes and photomorphogenesis. In Luis A., Rio D. (eds.) *Peroxisomes and their key role in cellular signaling and metabolism*, pp. 195-211. Eds. Springer, Dordrecht.

Keller R., Renz F.S.A, Kossmann J. (1999) Antisense inhibition of the GDP-mannose pyrophosphorylase reduces the ascorbate content in transgenic plants leading to developmental changes during senescence. *The Plant Journal*, 19, 131–141.

Khan M.A., Korban, S.S. (2012) Association mapping in forest trees and fruit crops. *Journal of Experimental Botany*, 63, 4045-4060.

Klein T., Di Matteo G., Rotenberg E., Cohen S., Yakir D. (2013) Differential ecophysiological response of a major Mediterranean pine species across a climatic gradient. *Tree Physiology*, 33, 26–36.

Lemichez E. (2001) Inactivation of AtRac1 by abscisic acid is essential for stomatal closure. *Genes and Development*, 15, 1808–1816.

Lobos G.A., Camargo A.V., del Pozo A., Araus J.L., Ortiz R., Doonan J.H. (2017) Editorial: plant phenotyping and phenomics for plant breeding. *Frontiers in Plant Science*, 8.

Lockhart B.R., Jr R.C.W., Smith K.M. (2005) Crown radius and diameter at breast height relationships for six bottomland hardwood species. *Journal of the Arkansas Academy of Science*, 59, 110-115

Loiselle B.A., Sork V.L., Nason J., Graham C. (1995) Spatial genetic structure of a tropical understory shrub, P*sychotria officinalis* (Rubiaceae). *American Journal of Botany*, 82, 1420–1425.

Ludovisi R., Tauro F., Salvati R., Khoury S., Mugnozza Scarascia G., Harfouche A. (2017) UAV-Based thermal imaging for high-throughput field phenotyping of black poplar response to drought. *Frontiers in Plant Science*, 8.

Ma Q.-H. (2007) Small GTP-binding proteins and their functions in plants. *Journal of Plant Growth Regulation*, 26, 369–388.

Manolio T.A., Collins F.S., Cox N.J., Goldstein D.B. *et al.* (2009) Finding the missing heritability of complex diseases. *Nature*, 461, 747–753.

Mariette S., Chagné D., Decroocq S., Vendramin G.G., Lalanne C., Madur D., Plomion C. (2001) Microsatellite markers for *Pinus pinaster* Ait. *Annals of Forest Science*, 58, 203–206.

McGaughey R.J. (2012) FUSION/LDV: Software for LiDAR data analysis and visualization—V3. 10. In *USDA Forest Service* (p. 168). Pacific Northwest Research Station, Portland, OR US.

McKown A.D., Klápště J., Guy R.D. *et al.* (2014) Genome-wide association implicates numerous genes underlying ecological trait variation in natural populations of *Populus trichocarpa*. *New Phytologist*, 203, 535–553.

Meyer F, Beucher S (1990) Morphological segmentation. *Journal of Visual Communication and Image Representation*, 1, 21-46.

Peakall R.O.D., Smouse P.E. (2006) GENALEX 6: genetic analysis in Excel. Population genetic software for teaching and research. *Molecular Ecology Notes*, 6, 288-295.

Peñuelas J., Filella I., Biel C., Serrano L., Save R. (1993) The reflectance at the 950–970 nm region as an indicator of plant water status. *International Journal of Remote Sensing*, 14, 1887–1905.

Perry D.J, Bousquet J. (1998). Sequence-tagged-site (STS) markers of arbitrary genes: development, characterisation and analysis of linkage in black spruce. *Genetics*, 149, 1089-1098.

Pinosio S., González-Martínez S.C., Bagnoli F. *et al.* (2014) First insights into the transcriptome and development of new genomic tools of a widespread circum-Mediterranean tree species, *Pinus halepensis* Mill. *Molecular Ecology Resources*, 14, 846–856.

Plomion C., Bartholomé J., Lesur I. *et al.* (2016) High-density SNP assay development for genetic analysis in maritime pine (*Pinus pinaster*). *Molecular Ecology Resources*, 16, 574–587.

Plowright A. (2018) Foresttools: analyzing remotely sensed forest data. *R Package Version 0.2.0*.

Ponnu J., Wahl V., Schmid M. (2011) Trehalose-6-Phosphate: connecting plant metabolism and development. *Frontiers in Plant Science*, 2.

Popescu S.C., Wynne R.H. (2004) Seeing the trees in the forest. *Photogrammetric Engineering and Remote Sensing*, 70, 589-604.

Pritchard J.K., Stephens M., Donnelly P. (2000) Inference of population structure using multilocus genotype data. *Genetics*, 155, 945-959.

Prunier J., Pelgas B., Gagnon F., Desponts M., Isabel N., Beaulieu J., Bousquet J. (2013) The genomic architecture and association genetics of adaptive characters using a candidate SNP approach in boreal black spruce. *BMC Genomics*, 14, 368.

QGIS Development Team (2019) QGIS Geographic Information System. Open Source Geospatial Foundation Project. http://qgis.osgeo.org

Resende M.D.V., Resende M.F.R., Sansaloni C.P. *et al.* (2012) Genomic selection for growth and wood quality in Eucalyptus: capturing the missing heritability and accelerating breeding for complex traits in forest trees. *New Phytologist*, 194, 116–128.

Resende R.T., Resende M.D.V., Silva F.F., Azevedo C.F., Takahashi E.K., Silva-Junior O.B., Grattapaglia D. (2017) Regional heritability mapping and genome-wide association identify loci for complex growth, wood and disease resistance traits in *Eucalyptus*. *New Phytologist*, 213, 1287–1300.

Richmond, T.A., Somerville C.R. (2000) The cellulose synthase superfamily. *Plant Physiology*, 124, 495-498.

Rodríguez Quilón I. (2017) Ecological and association genetics in two Mediterranean pine species. Doctoral dissertation, Universitad Politécnica de Madrid.

Rondeaux G., Steven M., Baret F. (1996) Optimization of soil-adjusted vegetation indices. *Remote Sensing of Environment*, 55, 95–107.

Roujean J.L., Breon F.M. (1995) Estimating PAR absorbed by vegetation from bidirectional reflectance measurements. *Remote Sensing of Environment*, 51, 375–384.

Rouse Jr J., Haas R.H., Schell J.A., Deering D.W. (1974) Monitoring vegetation systems in the Great Plains with ERTS. In: *Third ERTS Symposium*, pp. 309-317. Ed. NASA SP-351. Washington DC, USA.

Roussel J.R., Auty, D. (2018) lidR: Airborne LiDAR data manipulation and visualization for forestry applications. *R package version 1.0. 0*.

Romeis T. (2001) Calcium-dependent protein kinases play an essential role in a plant defence response. *The EMBO Journal*, 20, 5556–5567.

Rui Y., Xiao C., Yi H., Kandemir B., Wang J.Z., Puri V.M., Anderson C.T. (2017) Polygalacturonase involved in expansion3 functions in seedling development, rosette growth, and stomatal dynamics in *Arabidopsis thaliana*. *The Plant Cell*, 29, 2413–2432.

Ruiz Daniels R., Taylor R.S., Serra-Varela M.J., Vendramin G.G., González-Martínez S.C., Grivet D. (2018) Inferring selection in instances of long-range colonization: The Aleppo pine (*Pinus halepensis*) in the Mediterranean Basin. *Molecular Ecology*, 27, 3331–3345.

Santini F., Kefauver S.C., Resco de Dios V., Araus J.L., Voltas J. (2019) Using unmanned aerial vehicle-based multispectral, RGB and thermal imagery for phenotyping of forest genetic trials: A case study in *Pinus halepensis*. *Annals of Applied Biology*, 174, 262–276.

Savolainen O., Pyhäjärvi T., Knürr T. (2007) Gene flow and local adaptation in trees. *Annual Review of Ecology, Evolution, and Systematics*, 38, 595–619.

Serra-Varela M.J., Alía R., Daniels R.R., Zimmermann N.E., Gonzalo-Jiménez J., Grivet D. (2017) Assessing vulnerability of two Mediterranean conifers to support genetic conservation management in the face of climate change. *Diversity and Distributions*, 23, 507–516.

Schiller G., Atzmon N. (2009) Performance of Aleppo pine (*Pinus halepensis*) provenances grown at the edge of the Negev desert: A review. *Journal of Arid Environments*, 73, 1051–1057.

Steinitz O., Troupin D., Vendramin G.G., Nathan R. (2011) Genetic evidence for a Janzen-Connell recruitment pattern in reproductive offspring of *Pinus halepensis* trees: genetic evidence for Janzen-Connell effect. *Molecular Ecology*, 20, 4152–4164.

Storey J.D., Tibshirani R. (2003) Statistical significance for genomewide studies. *Proceedings of the National Academy of Sciences*, 100, 9440-9445.

Storey J.D., Bass A.J., Dabney A., Robinson D. (2019). qvalue: Q-value estimation for false discovery rate control. *R package version 2.16.0*

Terryn N., Van Montagu M., Inzé, D. (1993) GTP-binding proteins in plants. *Plant Molecular Biology*, 22, 143-152.

Tognetti R., Michelozzi M., Giovannelli A. (1997) Geographical variation in water relations, hydraulic architecture and terpene composition of Aleppo pine seedlings from Italian provinces. *Tree Physiology*, 17, 241-250.

Trerotola M., Relli V., Simeone P., Alberti S. (2015) Epigenetic inheritance and the missing heritability. *Human Genomics*, 9, 17.

Voltas J., Chambel M.R., Prada M.A., Ferrio J.P. (2008) Climate-related variability in carbon and oxygen stable isotopes among populations of Aleppo pine grown in common-garden tests. *Trees*, 22, 759–769.

Voltas J., Lucabaugh D., Chambel M.R., Ferrio J.P. (2015) Intraspecific variation in the use of water sources by the circum-Mediterranean conifer *Pinus halepensis*. *New Phytologist*, 208, 1031–1041.

Voltas J., Shestakova T.A., Patsiou T., di Matteo G., Klein T. (2018) Ecotypic variation and stability in growth performance of the thermophilic conifer *Pinus halepensis* across the Mediterranean basin. *Forest Ecology and Management*, 424, 205–215.

Wallace L., Lucieer A., Malenovský Z., Turner D., Vopěnka P. (2016) Assessment of forest structure using two uav techniques: a comparison of airborne laser scanning and structure from motion (SfM) point clouds. *Forests*, 7, 62.

Weiss M., Baret F. (2017) Using 3D point clouds derived from UAV RGB imagery to describe vineyard 3D macro-structure. *Remote Sensing*, 9, 111.

White T.L., Adams W.T., Neale D.B. (2007) Forest genetics. Eds. CABI. Cambridge, MA.

Wu, R., Zeng, Z. B., McKeand, S. E., and O Malley, D. M. (2000). The case for molecular mapping in forest tree breeding. *Plant Breeding Reviews*, *19*, 41-68.

Yang Y., Yu Y., Liang Y., Anderson C.T., Cao J. (2018) A profusion of molecular scissors for pectins: classification, expression, and functions of plant polygalacturonases. *Frontiers in Plant Science*, 9, 1208.

Yu J., Pressoir G., Briggs W.H. *et al.* (2006) A unified mixed-model method for association mapping that accounts for multiple levels of relatedness. *Nature Genetics*, 38, 203–208.

Zarco-Tejada P., Miller J., Morales A., Berjón A., Agüera J. (2004) Hyperspectral indices and model simulation for chlorophyll estimation in open-canopy tree crops. *Remote Sensing of Environment*, 90, 463–476.

Zarco-Tejada P.J., Diaz-Varela R., Angileri V., Loudjani P. (2014) Tree height quantification using very high resolution imagery acquired from an unmanned aerial vehicle (UAV) and automatic 3D photo-reconstruction methods. *European Journal of Agronomy*, 55, 89–99.

Chapter III - Tables and Figure

Table 1. Geographic origin of the 56 *Pinus halepensis* populations tested in this study. Underlined populations represent the subset used for genotpying.

Population	Code	Region	Country	Latitude	Longitude
Cabanelles	CAB	Catalonia	Spain	42° 14' 24" N	02° 46' 48" E
Tivissa	TIV	Catalonia	Spain	41° 02' 60" N	00° 45' 36" E
Sant Salvador de Guardiola	GUA	Catalonia	Spain	41° 40' 12" N	01° 45' 36" E
Zuera	ZUE	Ebro Depression	Spain	41° 55' 12" N	00° 55' 12" W
Valdeconcha	VAL	Southern Plateau	Spain	40° 26' 23" N	02° 52' 12" W
Alcantud	ALC	Southern Plateau	Spain	40° 33' 36" N	03° 19' 48" W
Villarejo de Salvanes	COT	Southern Plateau	Spain	40° 05' 24" N	02° 18' 36" W
Cirat	CIR	Iberian Range	Spain	40° 02' 60" N	00° 27' 36" W
Tuejar	TUE	Iberian Range	Spain	39° 48' 36" N	01° 09' 36" W
Enguidanos	ENG	Iberian Range	Spain	39° 38' 24" N	01° 38' 60" W
Tibi	TIB	East Spain	Spain	38° 31' 12" N	00° 39' 00" W
Altura	CUC	Iberian Range	Spain	39° 47' 24" N	00° 37' 12" W
Villa de Ves	VES	East Spain	Spain	39° 10' 48" N	01° 15' 00" W
Jarafuel	JAR	East Spain	Spain	39° 09' 36" N	01° 00' 36" W
Bicorp	BIC	East Spain	Spain	39° 06' 00" N	00° 51' 36" W
Commercial seed	LIN	East Spain	Spain	-	-
Benicassim	BIM	Iberian Range	Spain	40° 04' 12" N	00° 01' 48"E
Gilet	GIL	Iberian Range	Spain	39° 58' 12" N	03° 21' 00" W
Villajoyosa	VIL	East Spain	Spain	38° 29' 24" N	00° 18' 00" W
Ricote	RIC	N. Betic Mts	Spain	38° 08' 24" N	01° 25' 48" W
Monovar	MNV	N. Betic Mts	Spain	38° 22' 48" N	00° 57' 00" W
Monovar II	MVA	N. Betic Mts	Spain	38° 23' 24" N	00° 55' 12" W
Paterna del Madera	PAT	N. Betic Mts	Spain	38° 37' 48" N	02° 16' 12" W
Abaran	ABA	N. Betic Mts	Spain	38° 16' 12" N	01° 15' 36" W
Quentar	QUE	S. Betic Mts	Spain	37° 31' 12" N	03° 24' 36" W
Benamaurel	BEN	S. Betic Mts	Spain	37° 42' 00" N	02° 44' 24" W
Velez Blanco	VEL	S. Betic Mts	Spain	37° 47' 24" N	02° 00' 36" W
Santiago-Pontones	SAN	S. Betic Mts	Spain	38° 13' 48" N	02° 28' 12" W
Lorca	LOR	S. Betic Mts	Spain	37° 45' 00" N	01° 57' 00" W
Alhama de Murcia	ESP	S. Betic Mts	Spain	37° 51' 36" N	01° 31' 48" W
Quesada	QUD	S. Betic Mts	Spain	37° 45' 00" N	03° 01' 12" W
Lentegi	LEN	South Spain	Spain	36° 49' 12" N	03° 41' 24" W
Carratraca	CAR	South Spain	Spain	36° 51' 00" N	04° 49' 48" W
Frigiliana	FRI	South Spain	Spain	36° 49' 12" N	03° 55' 12" W
Palma de Mallorca	PMC	Majorca	Spain	39° 53' 59" N	03° 00' 00" E
Santanyi	SAV	Majorca	Spain	39° 16' 48" N	03° 02' 24" E
Alcudia	CUD	Majorca	Spain	39° 52' 12" N	03° 10' 12" E
Calvia	GAL	Majorca	Spain	39° 32' 60" N	03° 08' 24" E
Marcadal	COT	Menorca	Spain	39° 58' 12" N	04° 10' 12" E
Migjorn Gran	ATA	Menorca	Spain	39° 54' 36" N	04° 02' 60" E
Sant Josep de sa Talaia	HOR	Ibiza	Spain	38° 52' 48" N	01° 14' 24" E
Sant Josep de sa Talaia	SAL	Ibiza	Spain	38° 50' 24" N	01° 23' 60" E
Sant Antoni de Portmany	BAL	Ibiza	Spain	39° 02' 60" N	01° 19' 48" E
Valbuena de Duero	BUE	Northern Plateu (Reforestation)	Spain	41° 39' 36" N	04° 16' 48" W
Vega de Valdetronco	VEG	Northern Plateu (Reforestation)	Spain	41° 35' 24" N	05° 04' 48" W
Villan de Tordesillas	VIE	Northern Plateu (Reforestation)	Spain	41° 36' 00" N	04° 55' 48" W
Istaia-eyboia	IST	Greece	Greece	38° 44' 24" N	23° 29' 24" E
Amfilohia	ANF	Greece	Greece	38° 51' 36" N	21° 23' 24" E
Tatoi-Attica	TAT	Greece	Greece	38° 27' 00" N	23° 26' 60" E
Kassandra	KAS	Greece	Greece	40° 05' 24" N	23° 52' 48" E
Gemenos	GEM	France	France	43° 25' 12" N	05° 40' 12" E
Litorale tarantino	TAR	Italy	Italy	40° 37' 12" N	17° 06' 35" E
Gargano Monte Pucci	PUC	Italy	Italy	41° 53' 60" N	15° 56' 24" E
Gargano Marzini	MAR	Italy	Italy	41° 32' 60" N	15° 51' 36" E
Thala	THA	Tunisia	Tunisia	35° 34' 12" N	08° 39' 00" E
Tabarka	TAB	Tunisia	Tunisia	36° 30' 00" N	09° 04' 12" E

Table 2. Vegetation indices (VIs) considered in this study. R indicates the reflectance in a single wavelength (in nm).

Index	Descriptor	Wavelengths	Formula	Reference
NDVI	Leaf area	Red, NIR	$(R_{840} - R_{670})/(R_{840} + R_{670})$	Rouse *et al.,* 1973
OSAVI	Leaf area	Red, NIR	$(R_{840} - R_{670})/(R_{840} + R_{670} + 0.16)\times 1.16$	Rondeaux *et al.,* 1996
RDVI	Leaf area	Red, NIR	$(R_{840} - R_{670})/(R_{840} + R_{670})^{\wedge 1/2}$	Roujean and Breon, 1995
EVI	Leaf area	Blue, Red, NIR	$2.5\times(R_{840} - R_{670})/[(R_{840} + 6\times R_{670} - 7.5\times R_{450}) + 1]$	Huete *et al.,* 2002
MCARI	Leaf chlorophyll content; leaf area	Green, Red, NIR	$[(R_{700} - R_{670})\text{-}0.2\times(R_{700} - R_{550})]\times(R_{700}/R_{670})$	Daughtry, 2000
TCARI	Leaf chlorophyll content; leaf area	Green, Red, NIR	$3\times(R_{700} - R_{670})\text{-}0.2\times(R_{700} - R_{550})\times(R_{700}/ R_{670})$	Haboudane *et al.*,2002
TCARI/OSAVI	Leaf chlorophyll content	Green, Red, NIR	-	Haboudane *et al.*,2002
ARI2	Anthocyanins content	Blue, NIR	$R_{840}\times(1/R_{550} - 1/R_{700})$	Gitelson *et al.,* 2001
CRI2	Carotenoid content	Blue, NIR	$1/R_{550} - 1/R_{700}$	Gitelson *et al.,* 2002
WBI	Water content	NIR	R_{900} / R_{950}	Peñuelas *et al.,* 1993

Table 3. Results of the GWAS. The SNPs associated with traits with *p*-value < 10^{-3} are reported, together with the corrected *q*-value and the percentage of variance explained (PVE). For those SNPs that could be annotated, the best annotation obtained with blastx is reported.

Trait	Indicator	Marker	*p*-value	*q*-value	PVE	Best blastx	Species	Annotation
Leaf area								
	EVI	SNP108	3.26E-04	0.01	4.26	TKS08810.1	*Populus alba*	DNAJ heat shock N-terminal domain-containing protein
	EVI	SNP241	8.33E-04	0.01	3.75	MF394470.1	*Pinus pinaster*	SP_COC_1_1 hypothetical protein
	EVI	SNP273	5.56E-04	0.01	4.64	AAQ63936.1	*Pinus radiata*	Cellulose synthase
	EVI	SNP350	2.37E-04	0.01	4.43	AEX11975.1	*Pinus taeda*	Hypothetical protein
	EVI	SNP91	5.98E-04	0.01	4.60	-	-	-
	MCARI	SNP241	7.16E-04	0.07	3.52	MF394470.1	*Pinus pinaster*	SP_COC_1_1 hypothetical protein
	TCARI	SNP151	5.98E-04	0.07	4.54	XP_023633255.1	*Capsella rubella*	Peroxisomal membrane protein 11C
Photosynthetic pigments								
	ARI2	SNP258	5.89E-04	0.14	4.87	XP_024991722.1	*Cynara cardunculus*	Auxin efflux carrier component 7-like
	CRI2	SNP201	8.28E-04	0.06	3.95	-	-	-
	CRI2	SNP204	1.39E-04	0.03	4.96	XP_021596589.1	*Manihot esculenta*	Auxin-binding protein ABP19a-like
	CRI2	SNP67	4.58E-04	0.05	5.00	XP_026443681.1	*Papaver somniferum*	Leaf rust 10 disease-resistance locus receptor R-LIKE 1.5
Water concentration								
	WBI	SNP108	7.03E-04	0.02	4.07	TKS08810.1	*Populus alba*	DNAJ heat shock N-terminal domain-containing protein
	WBI	SNP133	4.90E-04	0.02	4.28	XP_028226388.1	*Glicine soja*	Probable polygalacturonase isoform X3
	WBI	SNP265	3.59E-04	0.02	4.46	-	-	-
	WBI	SNP350	1.89E-04	0.02	4.82	AEX11975.1	*Pinus taeda*	Hypothetical protein
	WBI	SNP91	3.80E-04	0.02	5.15	-	-	-
Canopy T								
	T	SNP140	8.98E-04	0.11	4.34	AF051223.1	*Picea mariana*	Rac-like GTP binding protein
Growth traits								
	Crown Area	SNP2	5.17E-04	0.05	4.94	PON68114.1	*Trema orientalis*	Trehalose-phosphatase
	Crown Area	SNP9	2.51E-04	0.05	5.38	ATP65499.1	*Pinus pinaster*	Hypothetical protein
	H_{UAV}	SNP350	1.25E-07	1.25E-06	10.03	AEX11975.1	*Pinus taeda*	Hypothetical protein
	H_{UAV}	SNP108	2.25E-05	7.83E-05	6.64	TKS08810.1	*Populus alba*	DNAJ heat shock N-terminal domain-containing protein
	H_{UAV}	SNP18	2.82E-05	7.83E-05	7.39	-	-	-
	H_{UAV}	SNP133	3.13E-05	7.83E-05	6.43	XP_028226388.1	*Glicine soja*	Probable polygalacturonase isoform X3
	H_{UAV}	SNP159	6.24E-05	1.25E-04	6.85	ACJ09662.1	*Cupressus sempervirens*	Putative calcium-dependent protein kinase
	H_{UAV}	SNP206	3.50E-04	5.00E-04	5.70	-	-	-
	H_{UAV}	SNP340	3.50E-04	5.00E-04	5.70	ABR15469.1	*Pinus taeda*	GDP-mannose pyrophosporylase
	H_{UAV}	SNP273	4.59E-04	5.22E-04	5.52	AAQ63936.1	*Pinus radiata*	Cellulose synthase
	H_{UAV}	SNP250	4.70E-04	5.22E-04	5.50	-	-	-
	H_{UAV}	SNP217	8.81E-04	8.81E-04	5.08	AHG95199.1	*Pinus mugo*	Hypotetical protein Pr2_23

Table 4. Molecular and biological function of the annotated SNPs for which the functions of the corresponding protein is known.

Trait	Indicator	Marker	Annotation	Molecular Function	Biological Function
Leaf area					
	EVI	SNP273	Cellulose synthase	Cellulose synthase (UDP-forming); metal ion binding	Cellulose biosynthetic process; cell wall organization
	TCARI	SNP151	Peroxisomal membrane protein 11C	Identical protein binding	Peroxisome fission; peroxisome organization; regulation of eproxisome size
Photosynthetic pigments					
	ARI2	SNP258	Auxin efflux carrier component 7-like	-	Auxin-activated signaling pathway; transmembrane transport
	CRI2	SNP204	Auxin-binding protein ABP19a-like	Manganese ion binding; nutrient reservoir activity	auxin-activated signaling pathway
	CRI2	SNP67	Leaf rust 10 disease-resistance locus receptor R-LIKE 1.5	ATP binding; polysaccharide binding; protein serine/threonine kinase activity	-
Water concentration					
	WBI	SNP133	Probable polygalacturonase isoform X3	Polygalacturonase activity	carbohydrate metabolic process; cell wall organization
Canopy T					
	T	SNP140	Rac-like GTP binding protein	Gtpase activity; gtpase binding	Small gtpase mediated signal transduction
Growth traits					
	Crown Area	SNP2	Trehalose-phosphatase	Catalytic activity	trehalose biosynthetic process
	H_{UAV}	SNP133	Probable polygalacturonase isoform X3	Polygalacturonase activity	carbohydrate metabolic process; cell wall organization
	H_{UAV}	SNP159	Putative calcium-dependent protein kinase	Calcium ion binding; kinase activity	-
	H_{UAV}	SNP340	GDP-mannose pyrophosporylase	Nucleotidyltransferase activity	Biosynthetic process
	H_{UAV}	SNP273	Cellulose synthase	Cellulose synthase (UDP-forming); metal ion binding	Cellulose biosynthetic process; cell wall organization

Table 5 Results of the multi-locus association analysis. For each trait, the median value across 100,000 iterations is reported for the percentage of variance explained (PVE) and the number of SNPs involved. The 95% confidence interval is also reported.

Trait	**Indicator**	**PVE**			**Number of SNPs**		
		Median	**95%down**	**95%up**	**Median**	**95%down**	**95%up**
Leaf area							
	NDVI	0.9	0.1	4.4	3	1	29
	OSAVI	1.5	0.1	6.7	5	1	221
	RDVI	2.1	0.1	8.1	12	1	98
	EVI	8.4	1.7	17.9	90	3	225
	MCARI	2.7	0.2	9.4	32	1	190
	TCARI	4.4	0.5	11.8	51	2	158
Photosynthetic pigments							
	TCARI/OSAVI	1.4	0.1	6.4	5	1	184
	ARI2	1.9	0.1	7.4	8	1	64
	CRI2	2.4	0.1	9.0	10	1	134
Water concentration							
	WBI	6.9	1.2	15.7	33	3	220
Canopy temperature							
	T	3.6	0.1	13.5	18	1	207
Growth traits							
	Crown area	6.8	0.9	14.7	18	2	93
	H_{UAV}	23.6	15.6	31.6	94	22	228

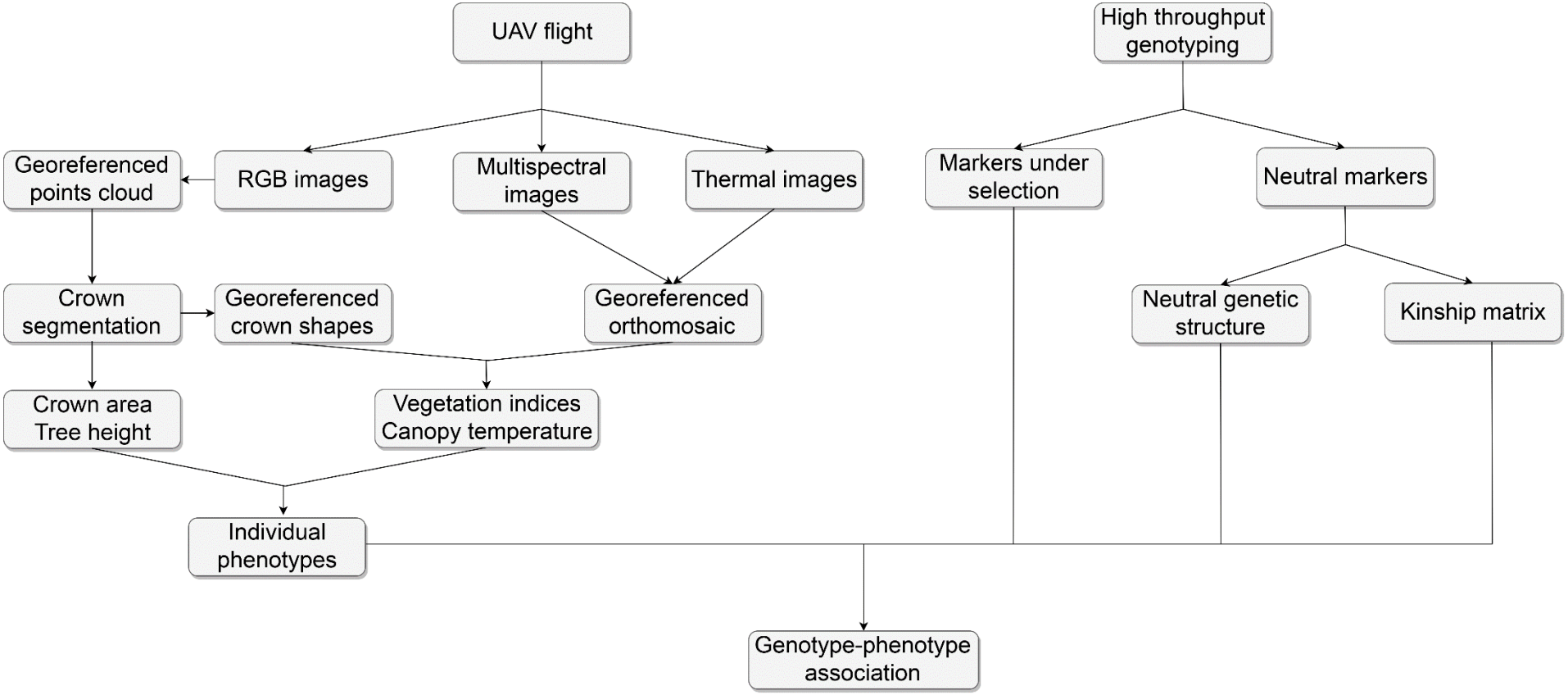

Figure 1. Flowchart showing the different steps followed to carry out the study of association genetics in *P. halepensis*.

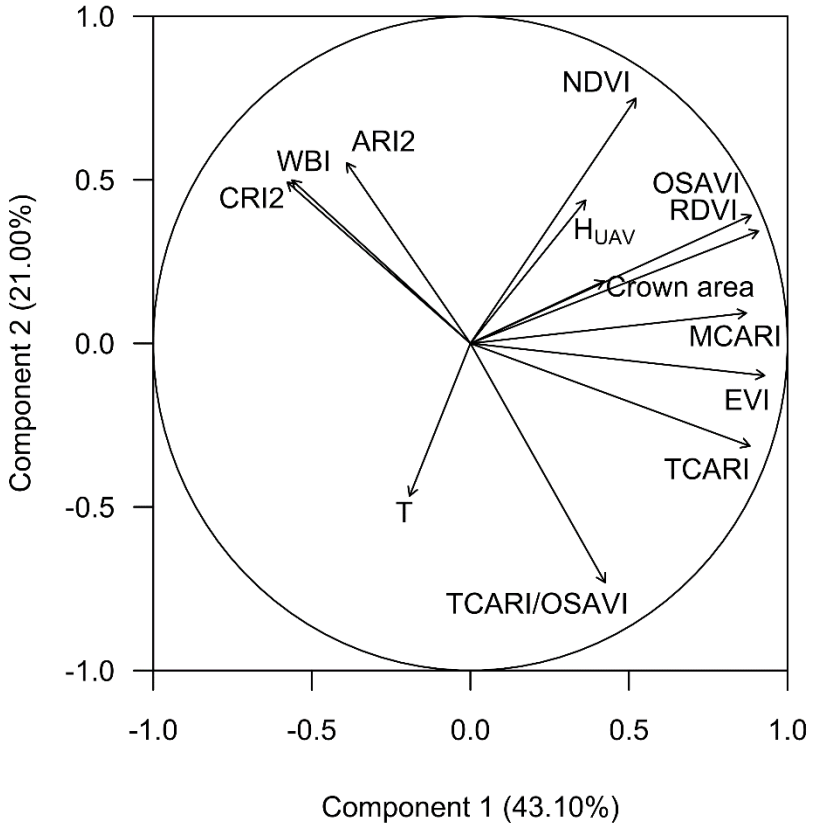

Figure 2. Plot of the loadings of the first two PCA axes describing the relations between UAV-derived growth traits, vegetation indices and canopy temperature.

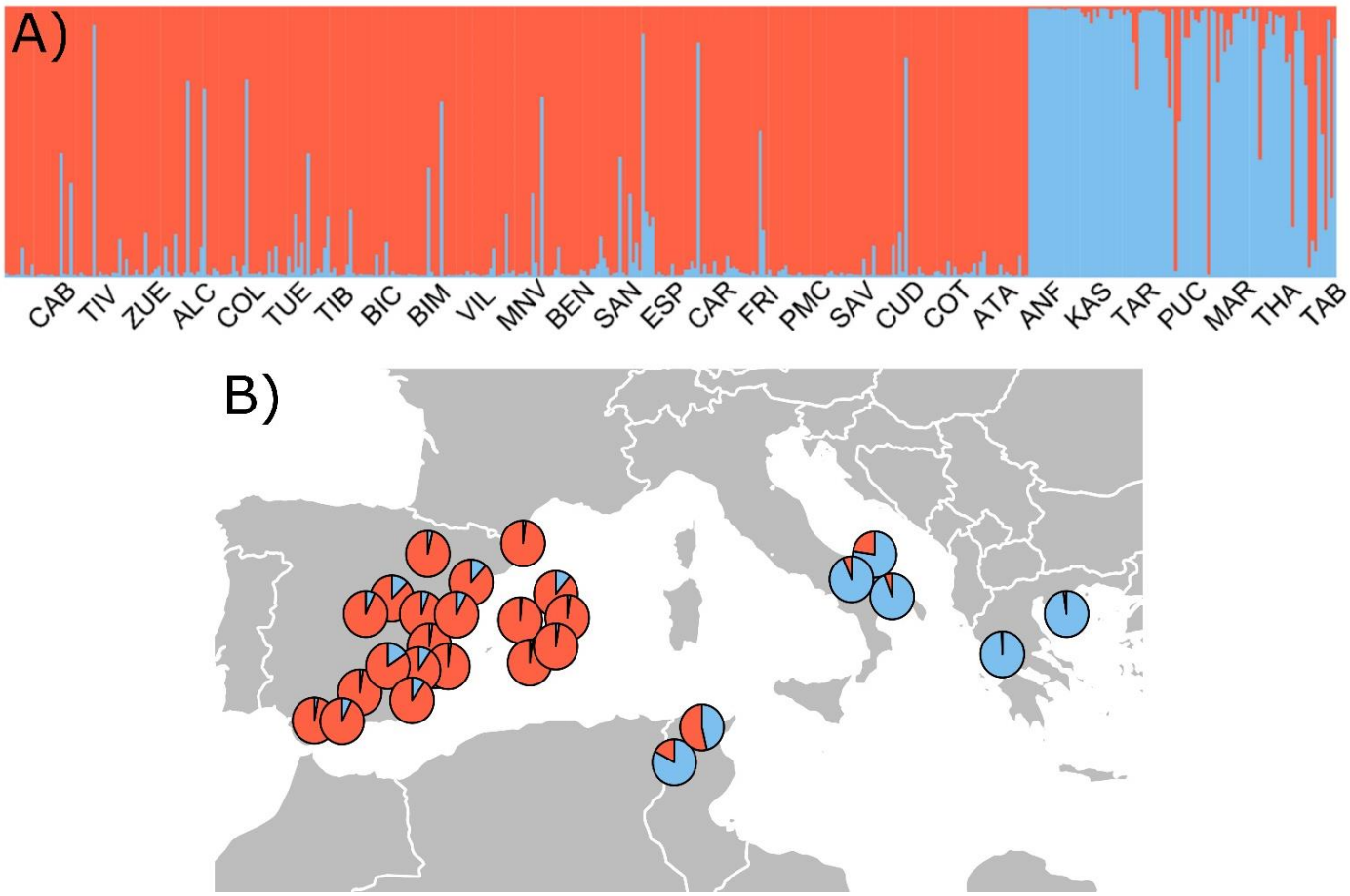

Figure 3 A) Bar plot showing results of the assignment test with K=2 for the 375 genotyped individuals. Each individual is represented by a vertical line divided into 2 coloured segments representing the probabilities that the individual is assigned to the group comprising western (in red) or central-eastern (in blue) Mediterranean populations. Population tags are reported in Table 1. B) Pie charts showing the percentage of assignment to the two groups in each population. The charts are plotted on the actual geographic coordinates of the populations.

Chapter III - Appendix

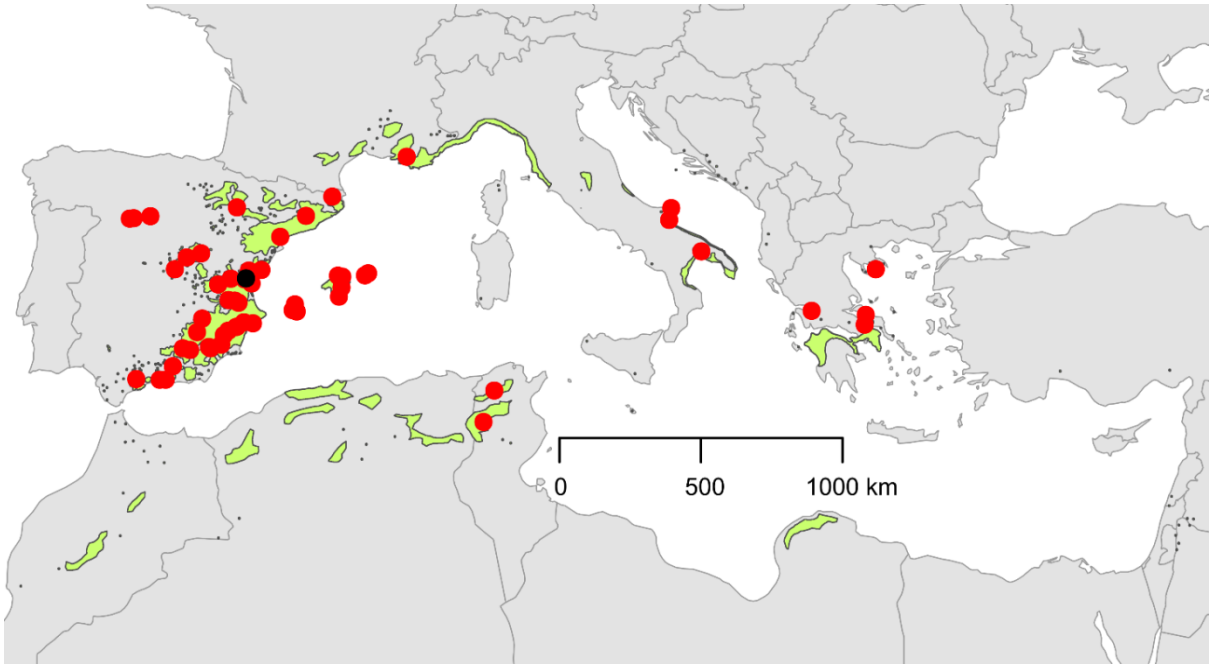

Fig S1. Geographic locations of the populations tested (red dots) in the common garden (black dot). The distribution range of the species according to the EUFORGEN distribution map is also reported (green colour).

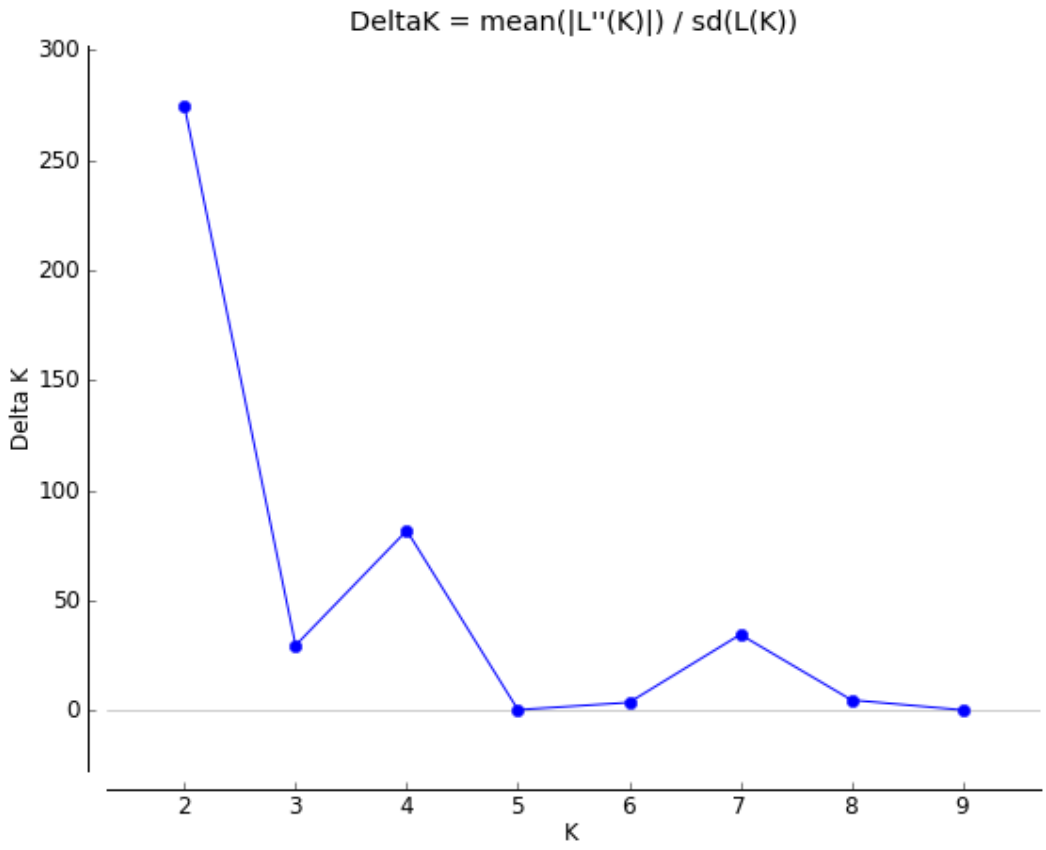

Fig S2. *ΔK* results from STRUCTURE analysis.

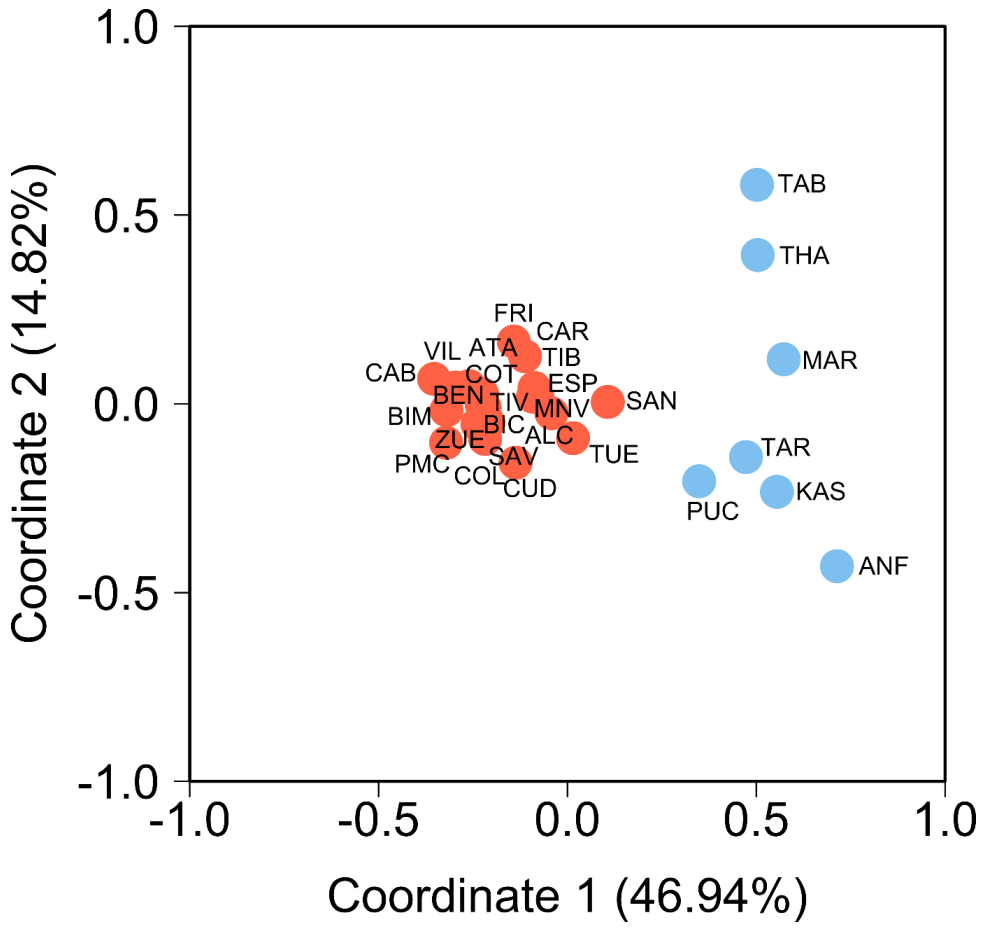

Fig S3 Plot of first and second coordinates of PCoA performed on a matrix of genetic distances between populations. The colours correspond to the two genetic groups identified by cluster analysis. Populations' codes are reported in Table 1.

CHAPTER IV

Morpho-physiological variability of *Pinus nigra* populations reveals climate-driven local adaptation but weak water use differentiation

Filippo Santini[1,2*], Luis Serrano[1,2], Shawn Carlisle Kefauver[3,4], Mamun Abdullah-Al[2], Mònica Aguilera[1,2], Ester Sin[2], Jordi Voltas[1,2]

[1]Joint Research Unit CTFC - AGROTECNIO, Av. Alcalde Rovira Roure 191, E-25198 Lleida, Spain;

[2]Department of Crop and Forest Sciences, University of Lleida, Av. Alcalde Rovira Roure 191, E-25198 Lleida, Spain;

[3]AGROTECNIO (Center for Research in Agrotechnology), Av. Alcalde Rovira Roure 191, E-25198 Lleida, Spain;

[4]Integrative Crop Ecophysiology Group, Plant Physiology Section, Faculty of Biology, University of Barcelona, E-08028 Barcelona, Spain.

SUMMARY

Disentangling patterns of intra-specific changes in morpho-physiological traits is crucial for understanding the capacity of tree populations to cope with human-induced environmental changes. This study combined well-established phenotyping techniques and unmanned aerial vehicle (UAV) imagery to characterise the extent of intra-specific variation for an array of meaningful traits among 18 populations of *Pinus nigra* growing in a common-garden experiment in central Spain, subject to summer drought. Data for eight traits describing above-ground growth, intrinsic water-use efficiency, water uptake patterns and reserve accumulation were obtained for 210 adult individuals belonging to the subspecies *laricio*, *calabrica*, *nigra* and *salzmanii*. UAV imagery was used to derive seven vegetation indices describing canopy structure and photosynthetic pigments. A strong inter-population differentiation arising from adaptation to cold and continental conditions at the geographical origin of the populations was found for growth traits, reserve accumulation, chlorophyll concentration and leaf surface area. Fast-growing populations, originating from milder climates, emerged in contrast to slow-growing populations, originating from colder and more continental areas of the species range. The latter were characterised by higher leaf chlorophyll concentration and higher investment in reserves. Inter-population variation was highly structured at the subspecies level. Subspecies *laricio* and *calabrica* were characterised by a higher growth investment, but diverged in relative radial to primary growth allometry, whereas subspecies *nigra* and *salzmanii* showed the highest investment in reserves. Importantly, variation of traits related to water economy was negligible, both at the population and subspecies level, indicating that Mediterranean populations of *P. nigra* may lack specific adaptation to drought stress. These results provided valuable information in forecasting the performance of this species in the context of climate change. Specifically, they anticipated the potential vulnerability of Mediterranean populations of *P. nigra* to future reduction in water availability.

Keywords: carbon isotopes; common garden; European black pine; non-structural carbohydrates; remote sensing; Unmanned Aerial Vehicle

INTRODUCTION

Ongoing environmental changes driven by human-induced global warming are affecting the distribution and composition of forests (Chen *et al.,* 2011). In this current situation, intra-specific variation is a crucial factor determining the capacity of populations of forests species to cope with such changes (Hampe and Petit, 2005; Alberto *et al.,* 2013). Selective pressures varying at geographical scales combine with population dynamics to determine the extent of trait variability (Violle *et al.,* 2012). These processes result in diverging phenotypes which often show local adaptation, thus reflecting their capacity to thrive under particular environments. Therefore, disentangling the adaptive potential of forest species according to intra-specific variation in morphology, physiology and phenology is a current issue for forecasting the fate of tree populations under future conditions (Díaz *et al.,* 2016, Guittar *et al.,* 2016, Kunstler *et al.,* 2016).

Common-garden experiments have been long established with the general aim of testing intra-specific patterns of phenotypic traits in forest species (Mátyás 1996; Bussotti *et al.,* 2015; de Villemereuil *et al.,* 2016). In the case of Mediterranean pines such as *Pinus halepensis* (e.g., Santos-del-Blanco *et al.,* 2013, Voltas *et al.,* 2015) or *Pinus pinaster* (e.g. Correia *et al.,* 2008; Santos-del-Blanco *et al.,* 2012), well-established phenotyping techniques have been applied to characterise variation in growth, reproduction, storage and water use strategies, among other characteristics. In addition, remote sensing information retrieved from unmanned aerial vehicles (UAVs) has recently been proposed as a valuable source in characterising vegetation properties (e.g., leaf area and photosynthetic pigments) among populations of forest species (Ludovisi *et al.,* 2017, Santini *et al.,* 2019a).

The European black pine (*Pinus nigra* Arnold) is a widespread conifer, playing an important ecological role in mid-altitude Mediterranean forests and in temperate woodlands of central-eastern Europe. It can be found from the Iberian Peninsula through the central and eastern parts of the Mediterranean basin to Turkey, including the Italian and Balkan peninsulas (Isajev *et al.,* 2004). Scattered populations are also present in North Africa and central-eastern Europe (Caudullo *et al.,* 2017). As a result of its ecological flexibility, this species has been used extensively in reforestation and land rehabilitation, resulting in the presence of introduced populations within and outside its natural distribution range (Vallauri *et al.,* 2002: Enescu *et al.,* 2016), where planted forests provide fundamental services such as erosion prevention and soil stabilization (Burylo *et al.,* 2009). Moreover, *P. nigra* has been proposed as a candidate species for assisted migration in central Europe, where it may be used to replace indigenous species in the context of ongoing climate change (Thiel *et al.,* 2012). Due to its ecological and economic

importance, previous research has been performed aimed to disentangle intra-specific patterns of growth variation (Roman-Amat and Arbez, 1985; Varelides *et al.,* 2001).

However, extensive characterisation of population differentiation is still lacking for key physiological traits of *P. nigra*, and the limited information available has largely been collected at the juvenile stage (e.g., Kreyling *et al.,* 2012, Topacoglu, 2013). Existing evidence from common-garden experiments indicates genetic differences related to cold resistance (Varelides *et al.,* 2001; Kreyling *et al.,* 2012) and adaptation to different soil conditions (Varelides *et al.,* 2001). On the other hand, there is no clear evidence for specific adaptation to drought stress (Thiel *et al.,* 2012, Matías *et al.,* 2017, Fkiri *et al.,* 2018). The few existing studies that have investigated adaptive patterns to drought in *P. nigra* have not included populations originating from the driest part of the species range, the Iberian and Anatolia peninsulas (e.g., Thiel *et al.,* 2012). The intra-specific taxonomic structure of *P. nigra* is also inconsistent (Giovannelli *et al.,* 2019). Five subspecies are traditionally recognised based on morphological and molecular differences (Isajev *et al.,* 2004, Caudullo *et al.,* 2017). *P. nigra* subsp. *salzmannii* (Dunal) Franco covers large areas of the Iberian Peninsula and southern France. *P. nigra* subsp. *nigra* (Hoss) is found from the Central Apennines to northern Greece, through the eastern Alps and the Balkan Peninsula. *P. nigra* subsp. *pallasiana* (Lamb.) covers over 2.5 million ha of Greece and Turkey. *P. nigra* subsp. *dalmatica* (Vis.) Franco is found with relict populations on a few islands along the Croatian coast (Isajev *et al.,* 2004). Finally, *P. nigra* subsp. *laricio* (Poiret) is present in Corsica and southern Italy, though these Italian populations are sometimes classified as a different subspecies (*Pinus nigra* subsp. *calabrica* Murray; Fineschi, 1984).

In this study, we combined well-established phenotypic techniques and UAV-derived remote sensing data to characterise morpho-physiological traits of adult individuals of *P. nigra* growing in a common-garden experiment, aiming at disentangling the adaptive strategies adopted by populations of this species. Specifically, the study: i) tested for intra-specific differentiation in growth, reserve accumulation, canopy structure and physiology (water-use efficiency and water uptake, water potential and photosynthetic pigments); ii) evaluated associations between traits across populations; and iii) related variation in such phenotypic traits to environmental conditions at the geographic origin of the populations. We hypothesised extensive genetic variation related to growth and cold adaptation, reflecting different ecological strategies (Kreyling *et al.,* 2012b). In addition, although existing evidence points to a lack of intra-specific variation for drought resistance (Lebourgeois *et al.,* 1998, Thiel *et al.,* 2012), we expected a sizeable differentiation in traits related to water use, since our study included populations from areas subject to pervasive drought stress (Martín-Benito *et al.,* 2013). The

implications that could be derived from the observed genetic patterns were also discussed in the context of climate change.

MATERIAL AND METHODS

Study site and plant material

The study was carried out in a common-garden experiment located in Valsaín (Segovia province, Central Spain), which consisted of adult individuals of *P. nigra*. (Figure 1, Table 1). The trial site is characterised by a period of drought in the summer (Figure 1a), and is drier than the average conditions under which the species is found (Figure 1b). Seeds belonging to the subspecies *salzmannii*, *nigra,* and *laricio* were collected in 1995 from 18 populations representative of a large part of the geographic range of the species (Figure 1, Table 1). Two of the sampled populations, initially included in the subspecies *laricio*, originated from southern Italy and were alternatively classified as subspecies *calabrica*. For each population, seeds were harvested from 20-30 trees spaced at least 100 m apart and planted in a forest nursery in Spain, following standard practises. In 1996, 800 one-year-old seedlings generated from these seeds were planted systematically (4.0 × 1.5 m spacing) at the study site in twelve replicates, following a randomised complete block design. For each replicate, four seedlings per population were planted in experimental units consisting of rectangular plots. In winter 2016, the trial was systematically thinned to reduce the density of trees, with two out of four trees being felled in each unit.

Two sampling events were performed in July 2017 and July 2018, at ages 22 years and 23 years, respectively. Trait phenotyping (as described below) was performed on 210 trees in six out of the 12 original replicates showing homogenous growing conditions. Each population was present in each of the six replicates. As an exception, water potential and remote sensing data were collected in two or three out of the six chosen replicates, respectively (see below for details). Mortality at sampling was very low, at 4% of the original trees.

Water uptake patterns

The isotopic composition of xylem water was analysed to investigate differences in water uptake among populations in summer. On 19th July 2017, one healthy and sun-exposed branch of about 2─3 cm diameter was collected per tree from the top part of the crown with a telescopic lopper, and was bark-peeled. Branches were immediately frozen in dry ice and then stored at -20 °C to prevent evaporation. Xylem water was extracted by cryogenic vacuum distillation, as described by Martín-Gómez *et al.* (2015). The oxygen and hydrogen isotopic composition ($\delta^{18}O$ and $\delta^{2}H$)

of xylem water was determined by isotope ratio infrared spectroscopy using a Picarro L2120-*i* $\delta D/\delta^{18}O$ isotopic water analyser, coupled to an A0211 high precision vaporizer (Picarro Inc., Sunnyvale, CA, USA).

Non-structural carbohydrates

The same branches used for the analysis of isotope composition of xylem water were analysed for non-structural carbohydrates. Wood was fine milled with a MM301 mixer mill (Retsch, Haan, Germany) and soluble sugars were extracted from 50 mg samples with 80% ethanol in a shaking water bath at 60 °C. The concentration of soluble sugars in the supernatant obtained after centrifugation was determined colourimetrically at 490 nm, using the phenol-sulphuric method described by Buysse and Merckx (1993). After ethanol extraction, the remaining undissolved precipitate was digested with amyloglucosidase to reduce starch to glucose, as described by Palacio *et al.* (2007). The resulting glucose was measured by the method of Buysse and Merckx (1993), from which the original starch concentration was determined.

Carbon isotope composition of wood α-cellulose

The carbon isotope composition ($\delta^{13}C$) of wood α-cellulose was analysed as a surrogate of intrinsic water-use efficiency (WUE_i; Farquhar *et al.*, 1989). On 19th July 2017, one wood core was extracted per tree using an increment borer. Tree rings were visually cross-dated, and those corresponding to the period 2008─2015 were pooled together for carbon isotope analysis. The pooled rings were milled to a fine powder with a MM301 mixer mill (Retsch, Haan, Germany) and α-cellulose was purified according to Ferrio and Voltas (2005). Samples underwent combustion using a Flash EA-1112 elemental analyser interfaced with a Finnigan MAT Delta C isotope ratio mass spectrometer (Thermo Fisher Scientific Inc., MA, USA). Carbon isotope composition ($\delta^{13}C$) was calculated as:

$$\delta^{13}C\ (‰) = (R_{sample} / R_{standard} - 1) \times 1000 \quad (1)$$

where R_{sample} and $R_{standard}$ are the isotope ratios ($^{13}C/^{12}C$) of the sample and of the Vienna Pee Dee Belemnite (VPDB) standard, respectively.

Stem water potential

On 19th July 2017, 34 trees were sampled in two adjacent replicates for the determination of stem water potential. The sampled trees belonged to eight of the populations tested and comprised the

four subspecies. A healthy branch was sampled from the top part of the tree's crown and water potential was measured with a Scholander pressure chamber. Water potential was determined at pre-dawn (06.00 AM solar time) and mid-day (01.00 PM solar time).

Vegetation indices

Multispectral images obtained with an UAV were used to retrieve vegetation indices as surrogates of leaf area, photosynthetic pigments and leaf water concentration at the tree level. At noon on 10th July 2018, one flight was performed at an altitude of around 50 m with a MK OktoXL 6S12 (Mikrokopter, Moormerland, Germany), equipped with a MCA12 multispectral camera (Tetracam Inc., Chatsworth, CA, US) capturing images at six wavelengths (550 ± 10, 670 ± 10, 700 ± 10, 840 ± 10, 900 ± 20, 950 ± 40 nm) in the visible and near-infrared (NIR) regions of the spectrum. An orthomosaic image of the common-garden was produced from 80 raw photographs with at least 80% overlap, employing Agisoft PhotoScan Professional software (Agisoft LLC, St. Petersburg, Russia). Unfortunately, the quality of the orthomosaic image only allowed retrieval of valid records from the first three replicates of the common garden. Ninety-nine tree crowns were visually identified and manually cropped from the orthomosaic using QGIS software (version 3.6; QGIS Development Team, 2019). Several vegetation indices were calculated for each pixel of a single image corresponding to a particular tree crown (Table 2). From these, an average value was obtained for each of the indices per tree, as is indicated below.

The normalised difference vegetation index (NDVI) and optimised soil adjusted vegetation index (OSAVI) are vegetation indices based on red and NIR reflectance which have been widely used as indicators of leaf area index (Rondeaux *et al.,* 1996; Roberts *et al.,* 2016, Xue and Su, 2017). The transformed chlorophyll absorption ratio index (TCARI) also includes reflectance in the green wavelength and is negatively related to leaf chlorophyll concentration; however, it might also be influenced by changes in leaf area (Daughtry *et al.,* 2000). Thus, the ratio between TCARI and OSAVI (TCARI/OSAVI index; Haboudane *et al.,* 2002) was calculated as a better proxy of chlorophyll concentration. Since TCARI and TCARI/OSAVI are expected to be negatively related to chlorophyll concentration (Zarco-Tejada *et al.,* 2004), their opposite values (TCARI* and TCARI/OSAVI*) were used to obtain indices positively associated with chlorophyll concentration. Alternative indices related to other leaf pigments are carotenoid reflectance index 2 (CRI2; Gitelson *et al.,* 2002) and anthocyanin reflectance index 2 (ARI2; Gitelson *et al.,* 2001), while water band index (WBI; Peñuelas *et al.,* 1993) is associated with the water content of leaves. Prior to calculation of vegetation indices, pixels having NDVI <0.5, which were considered to contain mainly soil, were filtered and not used in the derivation

of vegetation indices at the tree crown level (Richardson and Wiegand, 1977; Santini *et al.*, 2019a).

To confirm some of the information contained in the vegetation indices, needles were collected as a sub-sample of 39 trees in the first two blocks at the same time of the flight, from which the chlorophyll concentration was determined. A variable number (5─8) of 1-year old needles were sampled from the top part of the crown and were immediately frozen in dry ice. In the laboratory, needles were chopped into 1 mm segments, and 15 mg of this material was incubated in 95% ethanol at 65 °C for 8 hours. The absorbance of the solution was then measured at 649 and 664 nm with a UV-1600PC spectrophotometer (VWR^{TM}, Lutterworth, UK), and used to obtain total chlorophyll concentrations as reported by Minocha *et al.* (2009). Chlorophyll records were compared with vegetation indices through simple correlation.

Growth records

On 20th July 2018, height and diameter at breast height (DBH) were measured for each tree using telescopic measuring sticks and tapes, respectively. The ratio between height and DBH (height/DBH) was also calculated as a measure of slenderness.

Climate data

The WorldClim database (Hijmans *et al.,* 2005) was used to retrieve long-term (1960─1990) monthly averages of precipitation, and maximum and minimum temperatures of each geographic origin of the populations. Data were used to determine the total annual precipitation (P_a), summer (June to August) precipitation (P_s), summer to annual precipitation ratio (P_s /P_a), mean annual temperature (T_a), mean summer temperature (T_s), minimum temperature of the coldest month (T_{min}) and maximum temperature of the warmest month (T_{max}). The temperature range (T_r) was also calculated as the difference between T_{max} and T_{min}. Annual potential evapotranspiration (PET_a) was derived from monthly temperatures according to the Hargreaves method (Hargreaves and Samani 1982), and the P_a/PET_a ratio was calculated as indicator of aridity.

Statistical analysis

Values of DBH, height, height/DBH, $\delta^{13}C$ in α-cellulose, $\delta^{18}O$ and $\delta^{2}H$ in xylem water, stem water potential, soluble sugars and starch in branches, NDVI, OSAVI, TCARI*, TCARI/OSAVI*, ARI2, CRI2 and WBI were subjected to analysis of variance (ANOVA) for linear mixed-effects models in order to test for population differences. ANOVA had population and replicate as fixed terms, and population by replicate interaction and tree within experimental

unit as random terms. A second ANOVA was also run to test for differences among subspecies. The model consisted of subspecies, populations nested to subspecies and replicate as fixed terms, and populations nested to subspecies by replicate interaction and tree within experimental units as random terms. Two variants were considered for analysis at the subspecies level, which included either three subspecies (subsp. *salzmannii*, *nigra* and *laricio*) or four subspecies, where the subspecies *laricio* was split into two groups as Corsican (subsp. *laricio*) and southern Italy populations (subsp. *calabrica*). The least squares means of subspecies were compared using Tukey's honestly significant difference (HSD) test.

When significant population effects emerged from ANOVA, correlations between environmental conditions at their origins and the populations' least square means were calculated for the corresponding traits. This analysis tested for the adaptive significance of genetic variation as linked to the environmental conditions at origin. Alternative correlations were calculated that excluded the effect of subspecies from the relations between population's means and conditions at origin. For this purpose, residuals of populations' least square means, obtained after correcting for subspecies effects through ANOVA, were correlated to environmental conditions at origin. Population #16, originating from Austria, was excluded from these analyses because we were not confident about the exact geographic coordinates of this population.

Finally, principal component analysis (PCA) was performed on the means of populations for those traits that differed among populations: DBH, height, height/DBH, NDVI, OSAVI, TCARI*, TCARI/OSAVI* and starch concentration. PCA loadings for these traits were plotted to summarise the associations between different traits across populations. The PCA scores of the 18 populations were also plotted to investigate population groupings due to phenotypic differentiation. All statistical analyses were performed in SAS/STAT (ver. 9.4, SAS Inc., Cary, NC, USA).

RESULTS

Genetic variation

The population term in the ANOVA was significant for many traits ($p < 0.05$), indicating the presence of intra-specific genetic differentiation (Table 3). Specifically, growth traits (DBH, height and height/DBH), starch concentration and some vegetation indices (NDVI, OSAVI, TCARI* and TCARI/OSAVI*) varied significantly among populations. In contrast, sugar concentration and ARI2, CRI2 and WBI indices did not show significant population differences. Similarly, population differentiation was not found for isotopic traits (xylem water isotopes and α-cellulose $\delta^{13}C$). Mean water potential of trees was -0.68 ± 0.11 MPa (mean ± SD) at pre-dawn

and -1.83 ± 0.19 MPa at mid-day, indicating a moderate drought stress at the sampling time in summer 2017. However, differences of stem water potential among populations were not significant (Appendix, Table S1). Simple correlations between vegetation indices and chlorophyll concentration, calculated at the tree level, revealed that TCARI* and TCARI/OSAVI* were related to chlorophyll concentration (r = 0.39 and r = 0.41, respectively; $p < 0.05$). By contrast, associations between chlorophyll concentration and NDVI, OSAVI, ARI2, CRI2 and WBI were not significant.

Significant variation among subspecies was found for height, DBH, height/DBH, starch concentration, NDVI and OSAVI, but not for TCARI* and TCARI/OSAVI*. Moreover, DBH, height/DBH, NDVI, OSAVI, TCARI* and TCARI/OSAVI* also differed among populations within subspecies (Appendix, Table S2). After splitting the subspecies *laricio* into two groups, Corsican (*P. nigra laricio*) and south Italian populations (*P. nigra calabrica*), the differentiation at the subspecies level became more evident (Table 3). Specifically, a significant differentiation also emerged for TCARI* and TCARI/OSAVI*, while the variation among populations within each subspecies became non-significant for most traits, except NDVI, OSAVI, TCARI* and TCARI/OSAVI* (Table 3). The WBI index, indicative of water content in needles, also marginally differed among subspecies ($p = 0.08$). Considering the four subspecies, *laricio* and *calabrica* showed a larger height compared to *nigra* and *salzmannii* (range = 7.71–9.00 m; Figure 2a). In addition, *P. nigra calabrica* showed the largest DBH (range = 14.1–17.7 cm; Figure 2a), while *P. nigra laricio* had a higher height/DBH ratio than the other subspecies (range = 51.5–63.5; Figure 2b). Subspecies *nigra* and *salzmannii* accumulated more starch than *calabrica* and *laricio* (range = 1.19–1.83%; Figure 2b). Subspecies *laricio* showed the lowest NDVI, indicating a reduced leaf area compared to other subspecies (range = 0.75–0.79; Figure 2c) and also a reduced chlorophyll concentration, i.e., a more negative TCARI* and TCARI/OSAVI* (Figure 2c). By contrast, no significant differentiation emerged for sugar concentration, ARI2 and CRI2 indices, isotopic traits and water potential among subspecies or among populations within subspecies, either when considering the grouping of three or four subspecies.

Association with climate conditions at origin of populations

At the population level, significant associations involving a number of traits were found with climatic conditions at their origins (Figure 3a). Height and height/DBH were negatively correlated with temperature range (T_r), indicating that populations from more continental areas (i.e. experiencing higher temperature fluctuations through the year) exhibited reduced growth and slenderness. Height/DBH was also positively associated with P_a/PET_a, indicating a higher

slenderness in populations originating from more humid areas. Conversely, starch concentration was negatively associated with P_a/PET_a and positively related to T_r. TCARI/OSAVI* and TCARI* correlated with the minimum temperature of the coldest month (T_{min}), indicating higher chlorophyll in summer for populations experiencing harsher winters at origin. Finally, NDVI and OSAVI correlated positively with the ratio of summer to annual precipitation, while TCARI* was positively related to annual precipitation. DBH did not correlate with any climatic factor at origin.

Most correlations were driven by subspecies differentiation in growing conditions at origin. Indeed, when correlations involving populations' means corrected for subspecies effects were calculated, most significant associations vanished (Fig 3b). However, NDVI was still correlated with summer precipitation. Moreover, a positive (although weak) correlation emerged between TCARI/OSAVI* and annual temperature, while height was negatively related to altitude.

Principal component analysis

The PCA loadings revealed distinct associations between physiological and growth traits across populations (Figure 4a). Specifically, height and starch concentration were negatively associated ($r = -0.57$, $p < 0.01$), with starch concentration being in turn associated with TCARI/OSAVI* ($r = 0.48$, $p < 0.04$). NDVI and OSAVI were positively related to DBH ($r \geq 0.50$, $p < 0.05$). Height/DBH was negatively related to DBH, NDVI and OSAVI ($r \leq -0.56$, $p < 0.05$), but it was unrelated to height.

The PCA scores clearly distinguished *P. nigra salzmannii* and *P. nigra nigra*, with populations from each subspecies forming a different group (Figure 4b). Populations of *P. nigra laricio* also formed two different groups (Figure 4b). Those originating from Corsica (#13, #14 and #15) grouped together well apart from the remaining *P. nigra* populations, while those from southern Italy (#12 and #13) clustered with the *P. nigra salzmannii* populations, well apart from those originating in Corsica.

DISCUSSION

Taxonomic differentiation in Pinus nigra: the case of subspecies laricio

The taxonomy of *P. nigra* is highly debated, and alternative classifications have been proposed based on genetic and phenotypic information (Isajev *et al.*, 2004, Enescu *et al.*, 2016, Giovanelli *et al.*, 2019). In the current study, growth traits, vegetation properties and reserve accumulation discriminated between subspecies *salzmannii*, *nigra* and *laricio*. In particular, results indicated

superior growth performance of *laricio* populations, although they differed for some traits, with southern Italian populations showing higher DBH, lower slenderness (i.e. low height/DBH) and higher chlorophyll concentration than Corsican populations. This result confirmed previous evidences reporting Corsican populations having greater apical dominance than south Italian populations (Roman-Amat and Arbez, 1985; Varelides *et al.,* 2001), which were characterised by a greater secondary growth. Such differences in growth allometry and chlorophyll concentration (i.e. photosynthetic potential) likely underlie the presence of adaptive variability within the *laricio* group (Fineschi, 1984).

Sizeable population variation in growth and storage

Our study emphasised the existence of intra-specific differentiation in above-ground growth in populations of European black pine. Fast primary growth provides an evolutionary advantage in optimal environments, in which trees are subjected to increased competition for light (King, 1990; Falster and Westoby, 2003). We found a greater allocation to primary growth for subspecies originating from climates that experienced less fluctuating and generally milder conditions. On the other hand, high stem slenderness resulting from enhanced vertical growth might affect tree stability through greater exposure to mechanical stresses related to wind or snow coverage (Peltola, 2006). In a mountain species, such as *P. nigra*, snow damage can produce evolutionary divergence in terms of changes in allometry among populations (Martín-Alcón *et al.,* 2010). Our data showed that stem slenderness was higher for populations subjected to warmer winters, in which snowfall is likely reduced. In addition, height was negatively associated with altitude regardless of subspecies.

Starch accumulation also differed among populations, and was positively associated with temperature range at origin. The accumulation of non-structural carbohydrates is related to individual resilience, since storage can ensure survival in periods of carbon starvation, thus affecting trees' ability to cope with stringent growing conditions (Hoch *et al.,* 2003). However, reserve accumulation can impact on other sink processes, due to limited carbon availability (Palacio *et al.,* 2014, Santini *et al.,* 2019b). In this regard, a low primary growth was associated with a high starch concentration, which may assist slow-growing populations in tolerating harsher and more fluctuating climatic conditions. Even if other factors such as phenology or reproduction might influence growth of *P. nigra* populations (Climent *et al.,* 2013), this result suggested an active accumulation of carbon reserves, which might at least partially be obtained at the expense of growth (Wiley and Helliker, 2012, Santini *et al.,* 2019b). This effect was highly structured at the sub-species level, with *laricio* and *calabrica* experiencing faster growth and, in

turn, lower starch accumulation than *nigra* and *salzmannii*. These findings suggest divergent evolutionary strategies related to intra-annual climatic instability (Niklas and Enquist, 2002). Unfortunately, our results did not allow to clearly distinguishing the relative contributions of winter harshness, summer high temperatures and drought in shaping these adaptations. Indeed, growth traits and starch accumulation were associated to extreme temperatures and aridity conditions, suggesting combined effects of these factors on determining the extent of genetic differences in tree performance.

Population differences in vegetation indices

The association between TCARI or TCARI/OSAVI and chlorophyll concentration confirmed the effectiveness of both indices in estimating photosynthetic capacity, as reported elsewhere (Zarco-Tejada *et al.,* 2004; Roberts *et al.,* 2016). Variation in these indices pointed to genetic differentiation in leaf-level carbon fixation. Summer photosynthetic capacity, as described by vegetation indices, was negatively associated with minimum temperature at origin. Indeed, a higher chlorophyll concentration is typically found in tree populations limited by low temperature or light availability (e.g., Oleksyn *et al.*, 1998). In this regard, the lowest chlorophyll concentration was found in the subspecies *laricio*, whose populations were characterised by the highest minimum winter temperature at origin. However, TCARI and TCARI/OSAVI were not directly related to growth (i.e., DBH or height) across populations. Instead, they were positively associated with starch concentration, indicating that populations with higher needle chlorophyll tend to accumulate more reserves. It can be hypothesised that cold winters, high intra-annual temperature fluctuations and summer drought have acted as selective factors prioritizing photosynthetic capacity and storage at the expense of above-ground growth (Armbruster and Schwaegerle, 1996; Kreyling *et al.*, 2012b).

NDVI and OSAVI were associated with water availability at origin. As expected, these indices did not correlate well with chlorophyll concentration. Instead, they have been widely used as surrogates of total leaf area (Roberts *et al.*, 2016, Santini *et al.*, 2019a). Leaf area is a key determinant of water loss through transpiration, and populations originating from dry areas could show enhanced water conservation through reduced leaf area as strategy to cope with drought (Otieno *et al.*, 2005, Santini *et al.*, 2019a). On the other hand, a reduced leaf area entails a low potential for carbon fixation, which may impact on tree sinks such as growth or storage. In particular, leaf area (as described by NDVI and OSAVI) was positively associated with DBH in our study, indicating a larger secondary growth of populations showing larger photosynthetic surface, as previously described for the xeric *P. halepensis* (Santini *et al.*, 2019a). Conversely,

the lack of association between leaf area and starch accumulation implied that a greater photosynthetic surface does not directly result in higher reserve accumulation.

Lack of intra-specific variation in traits related to water use

Our work included *P. nigra* populations originating from Mediterranean areas in which summer drought is expected to limit performance (Martín-Benito *et al.,* 2013). Moreover, growing conditions at the trial site were characterised by a period of summer drought and were drier than those at the origin sites of most populations tested (*cf.* Figure 1). In this regard, *P. nigra* has been shown to drastically reduce stomatal conductance at mid-day water potentials between -2.06 and -1.6 MPa (Froux *et al.,* 2005), which are values similar to those measured in the common garden in summer 2017. This confirms that pines were subjected to drought stress. For this reason, population differences in growth and storage at the trial site may indicate intra-specific variation in pine performance under drought conditions. However, only a multi-environment trial exposing the same populations to variable levels of water availability can provide unequivocal information on intra-specific growth patterns as related to drought intensity.

Importantly, intra-specific variation for physiological traits related to water use and drought resistance (e.g. $\delta^{13}C$, xylem water isotopes, water potential) was absent in our common-garden experiment. Inter-population differentiation in $\delta^{13}C$ (a surrogate of intrinsic water-use efficiency) has been described in other Mediterranean pines such as *P. halepensis* and *P. pinaster*, indicating divergent stomatal regulation as a response to limited water availability (Voltas *et al.,* 2008; Aranda *et al.,* 2010). By contrast, the lack of genetic variability in intrinsic water-use efficiency of *P. nigra* agrees with the case of Iberian populations of the Eurosiberian pine *P. sylvestris* (Santini *et al.,* 2018). Similarly, the absence of genetic variation in the isotope composition of xylem water suggests lack of differentiation in rooting patterns, at least for the conditions of the common-garden experiment. This attribute is used to determine genetic differences in water uptake depth and root investment under drought stress (Voltas *et al.,* 2015). Altogether, these evidences indicated that selective pressures for deeper rooting or tighter stomatal regulation were not relevant in explaining different adaptive syndromes for this species (Lebourgeois *et al.,* 1998, Thiel *et al.,* 2012). Our findings are consistent with previous studies involving a more limited array of populations, which recognize an overall moderate drought resistance in *P. nigra* but weak intra-specific differentiation in drought responses (Lebourgeois *et al.,* 1998; Thiel *et al.,* 2012; Fkiri *et al.,* 2018). This is likely indicative of a weaker role of drought as driver of adaptive variation in *P. nigra* compared with winter temperatures and continentality (Varelides *et al.,* 2001; Kreyling *et al.,* 2012b). However, more research should

involve populations from the eastern Mediterranean basin and monitor alternative surrogates of drought resistance, such as hydraulic conductivity. Another factor not considered in our study was soil type, which might influence the ability of some populations to cope with reduced water availability (Roman-Amat and Arbez, 1985; Varelides *et al.,* 2001).

Implications in the context of climate change

The aforementioned results suggested that Mediterranean populations of European black pine lack variation in physiological adaptation to drought (Thiel *et al.,* 2012). Therefore, adaptive potential may be absent to cope with future environmental changes in the Mediterranean region. Coupled with existing evidences of drought-induced decline and pest susceptibility of some Mediterranean populations, our work highlights the vulnerability of *P. nigra* in the context of climate change (Linares and Tiscar 2010, Matias *et al.,* 2017). It also points to the absence of specifically suited populations for assisted migration where this species could replace local trees, such as native conifers and *Quercus spp.,* as climate warms and dries (Isajev *et al.*, 2004, Thiel *et al.,* 2012, Matias *et al.,* 2017). Even so, *P. nigra* is a Mediterranean species showing an overall higher drought resistance than central European species adapted to cold-continental climates (Isajev *et al.,* 2004, Thiel *et al.,* 2012). In this regard, a major limitation for introducing European black pine out of its normal range is frost damage, reducing its suitability for colder climates (Varelides *et al.,* 2001). For this reason, populations of European black pine originating from Austria and the Balkan Peninsula (i.e., the subspecies *nigra*), with higher resistance to low temperatures, have traditionally been used for reforestation in central Europe (Isajev *et al.,* 2004, Kreyling *et al.,* 2012). This current study supports this approach, indicating specific adaptation to cold conditions for this subspecies (i.e., higher reserves and photosynthetic capacity), though with indistinct drought resistance traits.

Conclusions

In summary, this study disentangled intra-specific differentiation for key morpho-physiological traits that could explain local adaptation in *P. nigra*, providing insight into patterns of evolutionary divergence in populations of this species. This is likely the first study in which such information have been extensively retrieved for adult individuals of European black pine, and highlights the effectiveness of combining well-established and newly developed phenotyping techniques in characterising forest genetic trials (Santini *et al.,* 2019a). The information that can be gathered with this approach is fundamental to forecast the performance of ecologically-important species in the context of climate change (Alberto *et al.,* 2013; Bussotti *et al.,* 2015).

Indeed, the weak or absent differentiation observed for many traits mainly related to water economy suggest that Mediterranean populations of European black pine may lack specific adaptation to cope with rapid human-induced environmental changes such as reduced water availability (Linares and Tiscar, 2010, Matias *et al.*, 2017). Additional efforts should aim at characterising other traits relevant to drought adaptation and involve eastern Mediterranean populations for in-field evaluation, preferably in multi-environment trials.

ACKNOWLEDGMENTS

We acknowledge P. Sopeña and M.J. Pau for technical assistance.

AUTHOR CONTRIBUTIONS

J.V. and F.S. conceived and designed the research. F.S., L.S., S.C.K., E.S., and J.V. collected the data; F.S., L.S., M.A.A. and M.A. analysed the data; F.S. and J.V. wrote the manuscript, with contributions from the other authors.

REFERENCES

Alberto F.J., Aitken S.N., Alía R., González-Martínez S.C., Hänninen H., Kremer A., Lefèvre F., Lenormand T., Yeaman S., Whetten R., Savolainen O. (2013) Potential for evolutionary responses to climate change - evidence from tree populations. *Global Change Biology*, 19, 1645–1661.

Aranda I., Alía R., Ortega U., Dantas Â.K., Majada J. (2010) Intra-specific variability in biomass partitioning and carbon isotopic discrimination under moderate drought stress in seedlings from four *Pinus pinaster* populations. *Tree Genetics and Genomes*, 6, 169–178.

Armbruster W.S., Schwaegerle K.E. (1996) Causes of covariation of phenotypic traits among populations. *Journal of Evolutionary Biology*, 9, 261–276.

Burylo M., Rey F., Roumet C., Buisson E., Dutoit T. (2009) Linking plant morphological traits to uprooting resistance in eroded marly lands (Southern Alps, France). *Plant and Soil*, 324, 31–42.

Bussotti F., Pollastrini M., Holland V., Brüggemann W. (2015) Functional traits and adaptive capacity of European forests to climate change. *Environmental and Experimental Botany*, 111, 91–113.

Buysse J., Merckx R. (1993) An improved colorimetric method to quantify sugar content of plant tissue. *Journal of Experimental Botany*, 44, 1627–1629.

Caudullo G., Welk E., San-Miguel-Ayanz J. (2017) Chorological maps for the main European woody species. *Data in Brief*, 12, 662–666.

Chen I.-C., Hill J.K., Ohlemuller R., Roy D.B., Thomas C.D. (2011) Rapid range shifts of species associated with high levels of climate warming. *Science*, 333, 1024–1026.

Climent J., Chambel M.R., Santos del Blanco L., Martínez Valcuende L., Alía R. (2013) Esclareciendo la variación adaptativa entre subespecies y procedencias de *Pinus nigra* Arnold. In: 6 Congreso Forestal Español. Sociedad Espanola de Ciencias Forestales. https://www.congresoforestal.es/actas/doc/6CFE/6CFE01-194.pdf

Correia I., Almeida M.H., Aguiar A., Alía R., David T.S., Pereira JS. (2008). Variations in growth, survival and carbon isotope composition ($\delta^{13}C$) among *Pinus pinaster* populations of different geographic origins. *Tree Physiology*, 28, 1545-1552.

Daughtry C.S.T., Walthall C.L., Kim M.S., Brown de Colstoun E., McMurtrey III J.E. (2000) Estimating corn leaf chlorophyll concentration from leaf and canopy reflectance. *Remote Sensing of Environment*, 74, 229–239.

de Villemereuil P., Gaggiotti O.E., Mouterde M., Till-Bottraud I. (2016) Common garden experiments in the genomic era: new perspectives and opportunities. *Heredity*, 116: 249.

Díaz S., Kattge J., Cornelissen J.H.C., *et al.* (2016) The global spectrum of plant form and function. *Nature*, 529, 167–171.

Enescu C.M., de Rigo D., Caudullo G., Mauri A., Houston Durrant T. (2016) *Pinus nigra* in Europe: distribution, habitat, usage and threats. In: San-Miguel-Ayanz J., de Rigo D., Caudullo G., Houston Durrant T., Mauri A. (eds) European atlas of forest tree species. Publ Off EU, Luxembourg, pp 126–127.

Falster D.S., Westoby M. (2003) Plant height and evolutionary games. *Trends in Ecology and Evolution*, 18, 337–343.

Farquhar G.D., Ehleringer J.R., Hubick K.T. (1989) Carbon isotope discrimination and photosynthesis. *Annual Review of Plant Physiology and Plant Molecular Biology*, 40, 503–537.

Ferrio J.P., Voltas J. (2005) Carbon and oxygen isotope ratios in wood constituents of *Pinus halepensis* as indicators of precipitation, temperature and vapour pressure deficit. *Tellus B*, 57, 164–173.

Fkiri S., Guibal F., Fady B., El Khorchani A., Khaldi A., Khouja M.L., Nasr Z. (2018). Tree-rings to climate relationships in nineteen provenances of four black pines sub-species (*Pinus nigra* Arn.) growing in a common garden from Northwest Tunisia. *Dendrochronologia*, 50, 44-51.

Fineschi S. (1984) Determination of the Origin of an Isolated Group of Trees of *Pinus nigra* through Enzyme Gene Markers. *Silvae Genetica*, 33, 169–172.

Froux F., Ducrey M., Dreyer E., Huc R. (2005) Vulnerability to embolism differs in roots and shoots and among three Mediterranean conifers: consequences for stomatal regulation of water loss?. *Trees*, 19, 137-144.

Giovannelli G., Scotti-Saintagne C., Scotti I., Roig A., Spanu I., Vendramin G.G., Guibal F., Fady B. (2019) The genetic structure of the European black pine (*Pinus nigra* Arnold) is shaped by its recent Holocene demographic history. Supplementary files. *bioRxiv*. Available at: http://biorxiv.org/lookup/doi/10.1101/535591

Gitelson A.A., Merzlyak M.N., Chivkunova O.B. (2001) Optical properties and nondestructive estimation of anthocyanin content in plant leaves. *Photochemistry and Photobiology*, 74, 38–45.

Gitelson A.A., Zur Y., Chivkunova O.B., Merzlyak M.N. (2002) Assessing carotenoid content in plant leaves with reflectance spectroscopy. *Photochemistry and Photobiology*, 75, 272–281.

Guittar J., Goldberg D., Klanderud K., Telford R.J., Vandvik V. (2016) Can trait patterns along gradients predict plant community responses to climate change? *Ecology*, 97, 2791–2801.

Haboudane D., Miller J.R., Tremblay N., Zarco-Tejada P.J., Dextraze L. (2002) Integrated narrow-band vegetation indices for prediction of crop chlorophyll content for application to precision agriculture. *Remote Sensing of Environment*, 81, 416–426.

Hargreaves G.H., Samani Z.A. (1982) Estimating potential evapotranspiration. *Journal of the Irrigation and Drainage Division*, 108, 225–230.

Hampe A., Petit R.J. (2005) Conserving biodiversity under climate change: the rear edge matters: Rear edges and climate change. *Ecology Letters*, 8, 461–467.

Hijmans R.J., Cameron S.E., Parra J.L., Jones P.G., Jarvis A. (2005) Very high resolution interpolated climate surfaces for global land areas. *International Journal of Climatology: A Journal of the Royal Meteorological Society*, 25, 1965–1978.

Hoch G., Richter A., Korner Ch. (2003) Non-structural carbon compounds in temperate forest trees. *Plant, Cell and Environment*, 26, 1067–1081.

Isajev V., Fady B., Semerci H., Andonovski V. (2004) EUFORGEN Technical Guidelines for genetic conservation and use for European European black pine (*Pinus nigra*). International Plant Genetic Resources Institute, Rome, Italy.

King D.A. (1990) The Adaptive Significance of Tree Height. *The American Naturalist*, 135, 809–828.

Kreyling J., Wiesenberg G.L.B., Thiel D., Wohlfart C., Huber G., Walter J., Jentsch A., Konnert M., Beierkuhnlein C. (2012) Cold hardiness of Pinus nigra Arnold as influenced by geographic origin, warming, and extreme summer drought. *Environmental and Experimental Botany*, 78, 99–108.

Kunstler G., Falster D., Coomes D.A., *et al.* (2016) Plant functional traits have globally consistent effects on competition. *Nature*, 529, 204–207.

Lebourgeois F., Lévy G., Aussenac G., Clerc B., Willm F. (1998) Influence of soil drying on leaf water potential, photosynthesis, stomatal conductance and growth in two European black pine varieties. *Annals of Forest Sciences*, 55, 287–299.

Linares J.C., Tiscar P.A. (2010) Climate change impacts and vulnerability of the southern populations of *Pinus nigra* subsp. salzmannii. *Tree Physiology*, 30, 795–806.

Ludovisi R., Tauro F., Salvati R., Khoury S., Mugnozza Scarascia G., Harfouche A. (2017) UAV-Based Thermal Imaging for High-Throughput Field Phenotyping of Black Poplar Response to Drought. *Frontiers in Plant Science*, 8.

Martín-Alcón S., González-Olabarría J., Coll L. (2010) Wind and snow damage in the Pyrenees pine forests: effect of stand attributes and location. *Silva Fennica*, 44, 399-410.

Martin-Benito D., Beeckman H., Cañellas I. (2013) Influence of drought on tree rings and tracheid features of Pinus nigra and Pinus sylvestris in a mesic Mediterranean forest. *European Journal of Forest Research*, 132, 33–45.

Martín-Gómez P., Barbeta A., Voltas J., Peñuelas J., Dennis K., Palacio S., Dawson T.E., Ferrio J.P. (2015) Isotope-ratio infrared spectroscopy: a reliable tool for the investigation of plant-water sources? *New Phytologyst*, 207, 914–927.

Matías L., Castro J., Villar-Salvador P., Quero J.L., Jump A.S. (2017) Differential impact of hotter drought on seedling performance of five ecologically distinct pine species. *Plant Ecology*, 218, 201–212.

Mátyás C. (1996) Climatic adaptation of trees: rediscovering provenance tests. *Euphytica*, 92, 45–54.

Minocha R., Martinez G., Lyons B., Long S. (2009) Development of a standardized methodology for quantifying total chlorophyll and carotenoids from foliage of hardwood and conifer tree species. *Canadian Journal of Forest Research*, 39, 849–861.

Niklas K.J., Enquist B.J. (2002) On the vegetative biomass partitioning of seed plant leaves, stems, and roots. *The American Naturalist*, 159, 482–497.

Oleksyn J., Modrzynski J., Tjoelker M.G., Z.ytkowiak R., Reich P.B., Karolewski P. (1998) Growth and physiology of Picea abies populations from elevational transects: common garden evidence for altitudinal ecotypes and cold adaptation. *Functional Ecology*, 12, 573–590.

Otieno D.O., Schmidt M.W.T., Adiku S., Tenhunen J. (2005) Physiological and morphological responses to water stress in two Acacia species from contrasting habitats. *Tree physiology*, 25, 361–371.

Palacio S., Maestro M., Montserrat.Martí G. (2007) Seasonal dynamics of non-structural carbohydrates in two species of mediterranean sub-shrubs with different leaf phenology. *Environmental and Experimental Botany*, 59, 34–42.

Palacio S., Hoch G., Sala A., Körner C., Millard P. (2014) Does carbon storage limit tree growth? *New Phytologist*, 201, 1096–1100.

Peltola H.M. (2006) Mechanical stability of trees under static loads. *American Journal of Botany*, 93, 1501–1511.

Peñuelas J., Filella I., Biel C., Serrano L., Save R. (1993) The reflectance at the 950–970 nm region as an indicator of plant water status. *International Journal of Remote Sensing*, 14, 1887–1905.

QGIS Development Team (2019) QGIS Geographic Information System. Open Source Geospatial Foundation Project. http://qgis.osgeo.org

Richardson A.J., Wiegand C.L. (1977) Distinguishing vegetation from soil background information. *Photogrammetric Engineering and Remote Sensing*, 43, 1541–1552.

Roberts D.A., Roth K.L., Perroy R.L. (2016) Hyperspectral vegetation indices. In: Huete A., Lyon J.G., Thenkabail P.S. (eds.) *Hyperspectral Remote Sensing of Vegetation*. pp. 309–328, Boca Raton, FL: CRC Press.

Roman-Amat B., Arbez M. (1985) Pins laricio de Corse et de Calabre : quelles provenances choisir ? Le point sur les expériences comparatives de l'I.N.R.A. *Revue Forestière Française*, 377.

Rondeaux G., Steven M., Baret F. (1996) Optimization of soil-adjusted vegetation indices. *Remote Sensing of Environment*, 55, 95–107.

Rouse Jr J., Haas R.H., Schell J.A., Deering D.W. (1974) Monitoring vegetation systems in the Great Plains with ERTS. In: *Third ERTS Symposium*, pp. 309-317. Ed. NASA SP-351. Washington DC, USA.

Santini F., Ferrio J.P., Hereş A.-M., Notivol E., Piqué M., Serrano L., Shestakova T.A., Sin E., Vericat P., Voltas J. (2018) Scarce population genetic differentiation but substantial spatiotemporal phenotypic variation of water-use efficiency in Pinus sylvestris at its western distribution range. *European Journal of Forest Research*, 137, 863–878.

Santini F., Kefauver S.C., Resco de Dios V., Araus J.L., Voltas J. (2019a) Using unmanned aerial vehicle-based multispectral, RGB and thermal imagery for phenotyping of forest genetic trials: A case study in *Pinus halepensis*. *Annals of Applied Biology*, 174, 262-276

Santini F., Climent J.M., Voltas J. (2019b). Phenotypic integration and life history strategies among populations of *Pinus halepensis*: an insight through structural equation modelling. *Annals of Botany*. doi: 10.1093/aob/mcz088

Santos-del-Blanco L., Climent J., González-Martínez S.C., Pannell J.R. (2012). Genetic differentiation for size at first reproduction through male versus female functions in the widespread Mediterranean tree *Pinus pinaster*. *Annals of Botany*, 110, 1449-1460.

Santos-del-Blanco L., Bonser S.P., Valladares F., Chambel M.R., Climent J. (2013) Plasticity in reproduction and growth among 52 range-wide populations of a Mediterranean conifer: adaptive responses to environmental stress. *Journal of Evolutionary Biology*, 26, 1912–1924.

Thiel D., Nagy L., Beierkuhnlein C., Huber G., Jentsch A., Konnert M., Kreyling J. (2012) Uniform drought and warming responses in *Pinus nigra* provenances despite specific overall performances. *Forest Ecology and Management*, 270, 200–208.

Topacoglu O. (2013). Genetic diversity among populations in European black pine (*Pinus nigra* Arnold. subsp. *pallasiana* (Lamb.) Holmboe) seed stands in Turkey. *Bulgarian Journal of Agricultural Scienc*e, 19, 1459-1464.

Vallauri D.R., Aronson J., Barbéro M. (2002) An analysis of forest restoration 120 years after reforestation on badlands in the southwestern Alps. *Restoration Ecology*, 10, 16–26.

Varelides C., Brofas G., Varelides Y. (2001) Provenance variation in *Pinus nigra* at three sites in Northern Greece. *Annals of Forest Science*, 58, 893–900.

Violle C., Enquist B.J., McGill B.J., Jiang L., Albert C.H., Hulshof C., Jung V., Messier J. (2012) The return of the variance: intraspecific variability in community ecology. *Trends in Ecology and Evolution*, 27, 244–252.

Voltas J., Chambel M.R., Prada M.A., Ferrio J.P. (2008) Climate-related variability in carbon and oxygen stable isotopes among populations of Aleppo pine grown in common-garden tests. *Trees*, 22, 759–769.

Voltas J., Lucabaugh D., Chambel M.R., Ferrio J.P. (2015) Intraspecific variation in the use of water sources by the circum-Mediterranean conifer *Pinus halepensis*. *New Phytologist*, 208, 1031–1041.

Wiley E., Helliker B. (2012) A re-evaluation of carbon storage in trees lends greater support for carbon limitation to growth. *New Phytologyst*, 195, 285–289.

Xue J., Su B. (2017) Significant remote sensing vegetation indices: a review of developments and applications. *Journal of Sensors*, 2017, 1–17.

Zarco-Tejada P.J., Miller J.R., Morales A., Berjón A., Agüera J. (2004) Hyperspectral indices and model simulation for chlorophyll estimation in open-canopy tree crops. *Remote Sensing of Environment*, 90, 463–476.

Chapter IV- Tables and Figure

Table 1. Geographic origin and environmental conditions of the 18 populations of *P. nigra* tested in the common-garden experiment. The site location and the growing conditions of the common garden are also reported.

Code	Population	Country	Lat	Lon	Subspecies	Altitude (m a.s.l.)	P_a (mm)	P_s (mm)	P_s/P_a	T_a (°C)	T_s (°C)	T_{max} (°C)	T_{min} (°C)	T_r (°C)	PET_a (mm)	P_a/PET_a
1	Ena	Spain	42º 31' 15" N	0º 45' 15" E	*salzmannii*	920	800	171	0.21	9.21	16.37	23.37	-2.08	25.44	877	0.91
2	Solsonés	Spain	42º 02' 33" N	1º 31' 37" E	*salzmannii*	645	711	201	0.28	12.14	19.75	26.03	0.90	25.13	913	0.78
3	Cuenca	Spain	39º 59' 59" N	2º 03' 13" E	*salzmannii*	995	521	92	0.18	11.55	20.33	29.75	-1.75	31.50	1099	0.47
4	Los Palancares	Spain	40º 01' 34" N	1º 58' 34" W	*salzmannii*	1220	559	106	0.19	10.31	19.14	28.30	-2.68	30.98	1041	0.54
5	Los Cadorzos	Spain	39º 50' 29" N	2º 00' 31" W	*salzmannii*	765	441	87	0.20	12.95	21.04	27.89	1.13	26.75	1015	0.43
6	Navahondona	Spain	37º 54' 60" N	2º 54' 25" W	*salzmannii*	1390	595	61	0.10	11.61	20.75	30.69	-1.32	32.01	1123	0.53
7	Paterna del Madera	Spain	38º 34' 42" N	2º 19' 05" W	*salzmannii*	1125	495	67	0.13	12.34	21.24	30.74	-0.67	31.41	1137	0.44
8	Cazorla-Alcaraz	Spain	38º 13' 60" N	2º 37' 60" W	*salzmannii*	1330	561	66	0.12	11.61	20.64	30.46	-1.41	31.87	1120	0.50
9	Huéscar	Spain	37º 56' 55" N	2º 34' 48" W	*salzmannii*	1795	700	91	0.13	9.29	18.44	28.39	-3.53	31.92	1040	0.67
10	Gagniéres	South France	44º 06' 60" N	4º 17' 00" E	*salzmannii*	280	770	142	0.18	12.39	20.37	27.83	0.24	27.59	971	0.79
11	Grancia	South Italy	39º 24' 59" N	16º 35' 09" E	*laricio/calabrica*	1495	858	96	0.11	8.50	16.07	20.84	-0.93	21.76	686	1.25
12	Macchia della Tavola	South Italy	39º 22' 20" N	16º 35' 18" E	*laricio/calabrica*	1545	858	95	0.11	8.27	15.77	20.57	-1.21	21.78	680	1.26
13	Noceta	France (Corsica)	42º 09' 60" N	9º 11' 00" E	*laricio*	685	725	74	0.10	12.10	18.84	23.45	3.25	20.21	728	1.00
14	Sorba	France (Corsica)	42º 07' 60" N	9º 12' 00" E	*laricio*	1030	777	86	0.11	10.39	17.28	21.68	1.70	19.97	656	1.18
15	Ghisoni	France (Corsica)	42º 04' 60" N	9º 12' 00" E	*laricio*	700	717	72	0.10	12.07	18.83	23.40	3.28	20.12	721	0.99
16	Parabluberg	Austria	46º 53' 39" N	13º 24' 16" E	*nigra*	-	-	-	-	-	-	-	-	-	-	-
17	Milea	Greece	39º 45' 55" N	21º 11' 41" E	*nigra*	1110	914	111	0.12	9.65	18.26	26.62	-3.47	30.09	983	0.93
18	Villetta Barrea	Central Italy	41º 46' 60" N	13º 46' 03" E	*nigra*	1360	805	151	0.19	8.36	16.40	22.31	-2.18	24.49	742	1.08
-	Common garden	Spain	40º 50' 42" N	4º 00' 52" W	-	920	505	81	0.16	10.50	19.09	26.89	-1.33	28.22	993	0.51

P_a, annual precipitation; P_s, summer (June to August) precipitation; T_a, annual temperature; T_s, summer temperature; T_{max}, mean maximum temperature of the warmest month; T_{min}, mean minimum temperature of the coldest month; T_r, T_{max} - T_{min}..

Table 2. Vegetation indices (VIs) considered in this study based on reflectance at different wavelengths. R indicates the reflectance at a single wavelength (in nm).

Index	Descriptor	Wavelengths	Formula	Reference
NDVI	Leaf area	Red, NIR	$(R_{840} - R_{670})/(R_{840} + R_{670})$	Rouse *et al.,* 1973
OSAVI	Leaf area	Red, NIR	$(R_{840} - R_{670})/(R_{840} + R_{670} + 0.16)\times1.16$	Rondeaux *et al.,* 1996
TCARI	Leaf chlorophyll content; leaf area	Green, Red, NIR	$3\times(R_{700} - R_{670})-0.2\times(R_{700} - R_{550})\times(R_{700}/ R_{670})$	Haboudane *et al.*,2002
TCARI/OSAVI	Leaf chlorophyll content	Green, Red, NIR	-	Haboudane *et al.*,2002
TCARI*	Leaf chlorophyll content; leaf area	Green, Red, NIR	- TCARI	-
TCARI/OSAVI*	Leaf chlorophyll content	Green, Red, NIR	-TCARI/OSAVI	-
ARI2	Anthocyanins content	Blue, NIR	$R_{840}\times(1/R_{550} - 1/R_{700})$	Gitelson *et al.,* 2001
CRI2	Carotenoid content	Blue, NIR	$1/R_{550} - 1/R_{700}$	Gitelson *et al.,* 2002
WBI	Water content	NIR	R_{900} / R_{950}	Peñuelas *et al.,* 1993

Table 3. Populations and subspecies effects of the mixed model analysis of variance for 15 morpho-physiological traits and vegetation indices considered in this study. The population effect was split into subspecies and a population within subspecies terms. This table reports the model considering four subspecies, *salzmannii*, *nigra*, *laricio* and *calabrica*.

Source of variation	**Num. df**	**Morphophysiological traits**															
		DBH		**Height**		**Height / DBH**		**cellulose $\delta^{13}C$**		**xylem $\delta^{2}H$**		**xylem $\delta^{18}O$**		**% Sugar**		**% Starch**	
		F-value	*P>F*	*F*-value	*P>F*	*F*-value	*P>F*	*F*-value	*P>F*	*F*-value	*P>F*	*F*-value	*P>F*	*F*-value	*P>F*	*F-value*	*P>F*
Population	17	2.87	< 0.01	2.52	< 0.01	5.13	< 0.01	0.68	0.82	0.76	0.72	0.94	0.52	0.89	0.58	1.80	0.05
Subspecies	3	5.57	< 0.01	6.07	< 0.01	12.36	< 0.01	0.16	0.92	2.09	0.11	1.32	0.27	2.51	0.06	5.46	< 0.01
Population (subspecies)	14	0.84	0.65	1.00	0.46	0.73	0.76	0.80	0.67	0.61	0.85	0.79	0.67	0.50	0.93	0.83	0.63
		Vegetation indices															
		NDVI		**OSAVI**		**TCARI***		**TCARI/OSAVI***		**ARI2**		**CRI2**		**WBI**			
		F-value	*P>F*	*F*-value	*P>F*	*F*-value	*P>F*	*F*-value	*P>F*	*F*-value	*P>F*	*F*-value	*P>F*	*F*-value	*P>F*		
Population	17	2.65	< 0.01	2.34	0.02	2.47	< 0.01	2.27	< 0.01	1.11	0.39	0.89	0.58	1.14	0.49		
Subspecies	3	4.27	0.01	2.55	0.08	6.44	< 0.01	6.93	< 0.01	2.27	0.10	1.30	0.29	2.52	0.08		
Population (subspecies)	14	2.08	0.05	1.91	0.07	1.90	0.04	1.67	0.08	0.84	0.62	0.87	0.59	0.61	0.83		

df, degrees of freedom; DBH, diameter at breast height; NDVI, normalised difference vegetation index; OSAVI, optimised soil adjusted vegetation index; TCARI, transformed chlorophyll absorption ratio index; ARI2, anthocyanin reflectance index 2; CRI2, carotenoid reflectance index 2; WBI, water band index

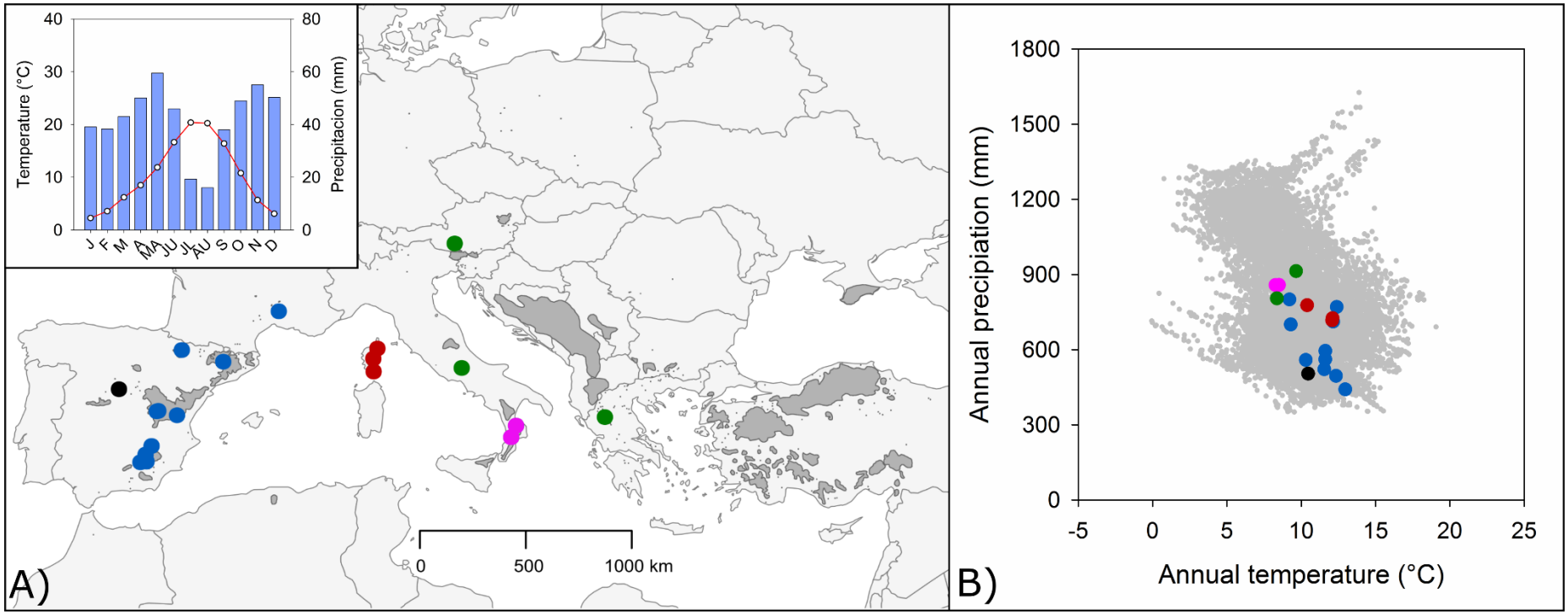

Figure 1. A) Geographical origin of the 18 populations of *P. nigra* tested in the common-garden experiment, classified in the subspecies *salzmannii* (blue dots), *nigra* (green dots), *laricio* (i.e., populations from Corsica; red dots) and *calabrica* (i.e., populations from southern Italy, alternatively classified with those from Corsica in the subspecies *laricio*; pink dots). The common-garden site is indicated by a black dot, while the species range according to the European forest genetic resources programme (EUFORGEN) distribution map (http://www.euforgen.org/species/pinus-nigra/) is reported in grey. The insert reports monthly average values of temperature and precipitation for the trial site, calculated from the WorldClim database for 1960─1990. B) Mean annual precipitation and temperature for the distribution range (according to EUFORGEN) for *P. nigra* (grey circles), calculated in 10' resolution grids from the WorldClim database for 1960─1990. Temperature and precipitation of the trial site and each population tested are indicated.

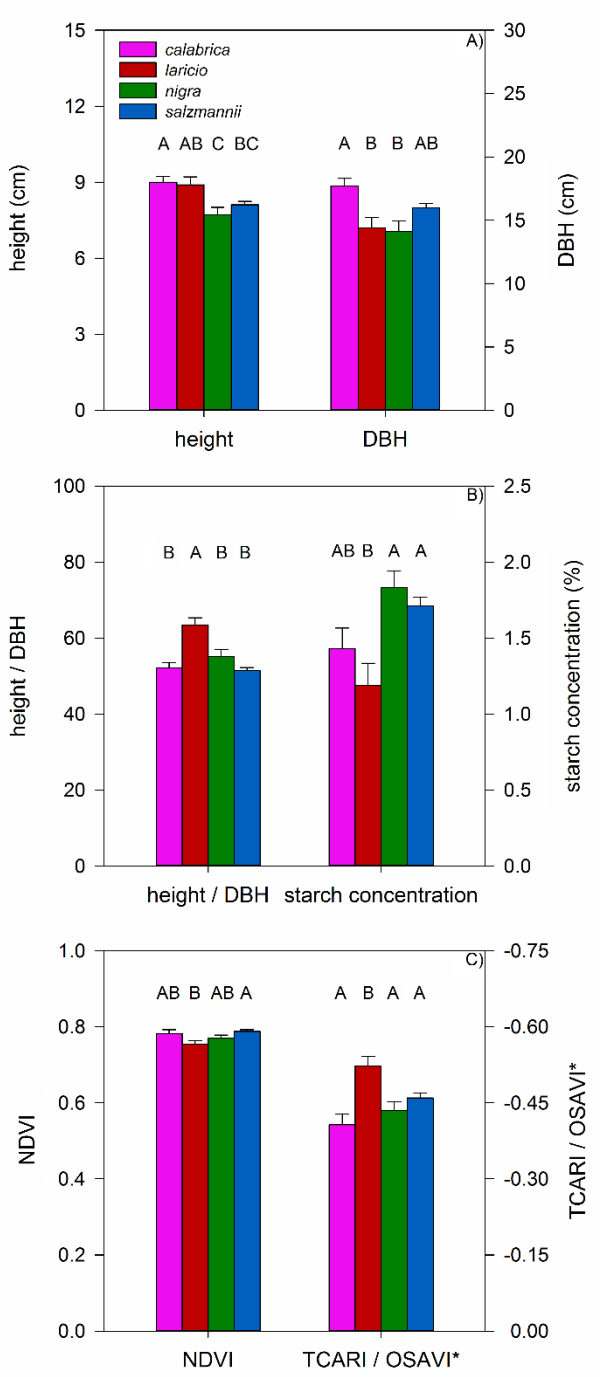

Figure 2. Subspecies least squares means for A) height and DBH, B) height/DBH and starch concentration, and C) NDVI and TCARI/OSAVI*. Significant differences among subspecies according to Tukey's test are indicated by letters. In the case of TCARI/OSAVI*, more negative values of the index indicate a lower chlorophyll content. DBH, diameter at breast height; NDVI, normalised difference vegetation index; OSAVI, optimised soil adjusted vegetation index; TCARI, transformed chlorophyll absorption ratio index.

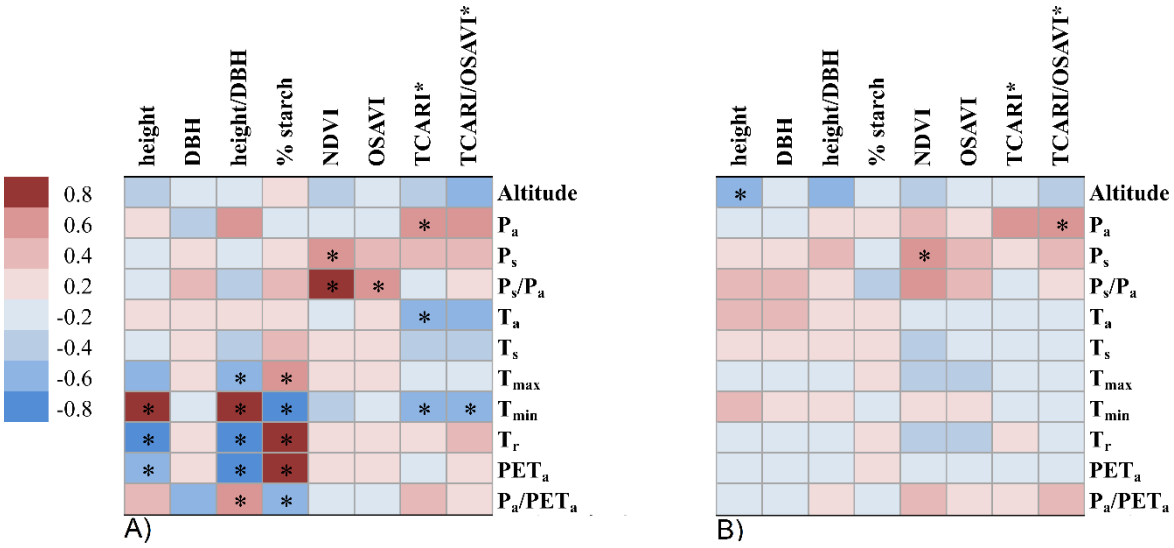

Figure 3. Simple correlations between A) population means or B) population means corrected for the effect of subspecies of eight morpho-physiological traits and environmental factors at the origin of the populations. Significant correlations are indicated by an asterisk. DBH, diameter at breast height; NDVI, normalised difference vegetation index; OSAVI, optimised soil adjusted vegetation index; TCARI, transformed chlorophyll absorption ratio index; P_a, annual precipitation; P_s, summer (June to August) precipitation; T_a, annual temperature; T_s, summer temperature; T_{max}, mean maximum temperature of the warmest month; T_{min}, mean minimum temperature of the coldest month; T_r, T_{max} - $T_{min.}$; PET_a, annual potential evapotranspiration.

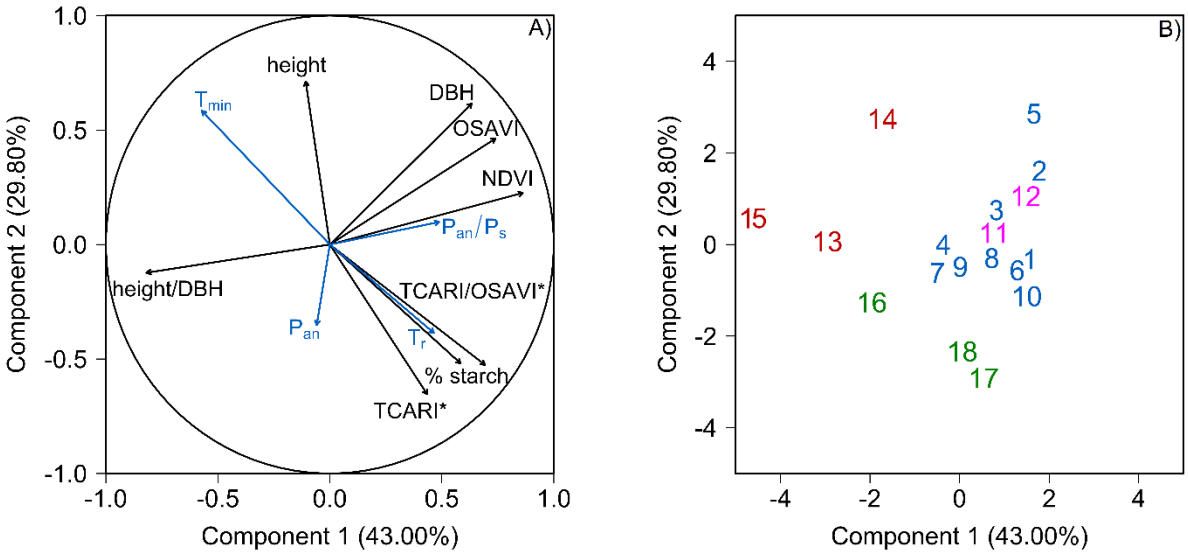

Figure 4. Principal component analysis plots. A) Loadings of the eight traits considered (black arrows). Four supplementary variables (i.e., not considered in the PCA calculations) representing climatic conditions at the geographical origin of the populations were passively introduced in the graph (blue arrows). Other climatic variables were not included for the sake of clarity. B) Population scores of the first two principal components (codes as in Table 1). Colours indicate the different subspecies: *calabrica* (pink), *laricio* (red), *nigra* (green), and *salzmannii* (blue). DBH, diameter at breast height; NDVI, normalised difference vegetation index; OSAVI, optimised soil adjusted vegetation index; TCARI, transformed chlorophyll absorption ratio index.

Chapter IV- Appendix

Table S1. Populations and subspecies effects of the mixed model analysis of variance for water potential measured at pre-dawn and mid-day in a subset of 34 trees.

Source of variation	Num. df	Water potential Pre-dawn		Water potential Mid-day	
		F-value	*P>F*	*F*-value	*P>F*
Population	8	0.81	0.62	0.84	0.60
[a]Subspecies	3	0.89	0.49	0.69	0.58
[a]Population[subspecies]	5	0.74	0.61	0.93	0.51

		Water potential Pre-dawn		Water potential Mid-day	
		F-value	*P>F*	*F*-value	*P>F*
Population	8	0.81	0.62	0.84	0.60
[b]Subspecies	2	0.72	0.64	1.04	0.47
[b]Population[subspecies]	6	1.03	0.41	0.25	0.78

[a]Model with four subspecies (*calabrica, laricio, nigra* and *salzmannii*)
[b]Model with three subspecies (*laricio, nigra* and *salzmannii*)

Table S2. Populations and subspecies effects of the mixed model analysis of variance for 15 morpho-physiological traits and vegetation indices considered in this study. The population term was split in a subspecies and in a population within subspecies terms. This table report the model considering three subspecies (i.e. *salzmannii*, *nigra* and *laricio*).

Source of variation	**Num. df**	**Morphophysiological traits**															
		DBH		**Height**		**Height / DBH**		**$\delta^{13}C$**		**$\delta^{2}H$**		**$\delta^{18}O$**		**% Sugar**		**% Starch**	
		F-value	*P>F*	*F*-value	*P>F*	*F*-value	*P>F*	*F*-value	*P>F*	*F*-value	*P>F*	*F*-value	*P>F*	*F*-value	*P>F*	*F-value*	*P>F*
Population	17	2.52	<0.01	5.13	<0.01	0.68	0.82	0.76	0.72	0.94	0.52	0.89	0.58	0.89	0.58	1.8	0.05
Subspecies	3	10.57	<0.01	23.45	<0.01	0.18	0.84	2.92	0.06	1.92	0.15	2.24	0.12	2.51	0.06	4.06	0.02
Population[subspecies]	14	1.1	0.37	2.79	<0.01	0.74	0.73	0.61	0.86	0.76	0.72	0.31	0.98	0.50	0.93	0.48	0.93
		Vegetation indices															
		NDVI		**OSAVI**		**TCARI***		**TCARI/OSAVI***		**ARI2**		**CRI2**		**WBI**			
		F-value	*P>F*	*F*-value	*P>F*	*F*-value	*P>F*	*F*-value	*P>F*	*F*-value	*P>F*	*F*-value	*P>F*	*F*-value	*P>F*		
Population	17	2.65	<0.01	2.34	0.02	2.47	<0.01	2.27	<0.01	1.11	0.39	0.89	0.58	1.14	0.49		
Subspecies	3	4.61	0.02	3.30	0.05	2.19	0.12	1.80	0.17	1.89	0.17	0.85	0.44	2.72	0.08		
Population[subspecies]	14	2.29	0.03	1.98	0.06	2.55	<0.01	2.57	<0.01	0.97	0.51	0.91	0.57	0.73	0.73		

CHAPTER V

Scarce population genetic differentiation but substantial spatiotemporal phenotypic variation of water-use efficiency in *Pinus sylvestris* at its western distribution range

F. Santini[a], J.P. Ferrio[b,c], A-M. Hereş[d,e], E. Notivol[c], M. Piqué[f], L. Serrano[a], T.A. Shestakova[a,g], E. Sin[a], P. Vericat[f], J. Voltas[a*]

[a] Department of Crop and Forest Sciences – AGROTECNIO Center, University of Lleida, Avda. Alcalde Rovira Roure 191, E-25198 Lleida, Spain.

[b] Aragon Agency for Research and Development (ARAID), E-50018 Zaragoza, SPAIN

[c] Forest Resources Unit, Agrifood Research and Technology Centre of Aragón (CITA), Avda. Montañana 930, E-50059 Zaragoza, SPAIN

[d] Department of Forest Sciences, Transilvania University of Brasov, Sirul Beethoven -1, 500123 Brasov, Romania

[e] BC3 - Basque Centre for Climate Change, Scientific Campus of the University of the Basque Country, 48940 Leioa, Spain

[f] Sustainable Forest Management Unit, Forest Sciences Centre of Catalonia (CTFC), Ctra. Sant Llorenç de Morunys km. 2, E-25280 Solsona, Spain

[g] Siberian Federal University, L. Prushinskoy st, 2, Krasnoyarsk, Russia

SUMMARY

Water and carbon fluxes in forests are largely related to leaf gas exchange physiology varying across spatiotemporal scales and modulated by plant responses to environmental cues. We quantified the relevance of genetic and phenotypic variation of intrinsic water-use efficiency (WUE_i, ratio of net photosynthesis to stomatal conductance of water) in *Pinus sylvestris* L. growing in the Iberian Peninsula as inferred from tree-ring carbon isotopes. Inter-population genetic variation, evaluated in a provenance trial comprising Spanish and German populations, was low and relevant only at continental scale. In contrast, phenotypic variation, evaluated in natural stands (at spatial level) and by tree-ring chronologies (at temporal inter-annual level), was important and ten- and three-fold larger than the population genetic variance, respectively. These results points to preponderance of plastic responses dominating variability in WUE_i for this species. Spatial phenotypic variation in WUE_i correlated negatively with soil depth ($r= -0.66$; $p<0.01$), while temporal phenotypic variation was mainly driven by summer precipitation. At the spatial level, WUE_i could be scaled-up to ecosystem-level WUE derived from remote sensing data by accounting for soil water holding capacity ($r= 0.63$; $p<0.01$). This outcome demonstrates a direct influence of the variation of leaf-level WUE_i on ecosystem water and carbon balance differentiation. Our findings highlight the contrasting importance of genetic variation (negligible) and plastic responses in WUE_i (with changes of up to 50% among sites) on determining carbon and water budgets at stand and ecosystem scales in a widespread conifer such as *Pinus sylvestris*.

Keywords: genetic variation; phenotypic plasticity; *Pinus sylvestris*; remote sensing; tree rings; water-use efficiency

INTRODUCTION

The carbon and water cycles on Earth are coupled with the composition and functioning of forest ecosystems (Pan *et al.,* 2011; Ukkola *et al.,* 2016). Forests represent a net sink of 1.1×10^{15} g of carbon per year (Pan *et al.,* 2011) and contribute to *ca*. 56% of terrestrial evapotranspiration (Schlesinger and Jasechko, 2014). Ecosystem water-use efficiency (WUE), defined as the ratio between gross primary productivity and evapotranspiration, is a key characteristic determining the carbon and water balance of forests. Spatial heterogeneity, temporal fluctuations and their interactions over a broad spectrum of scales determine the multifaceted variability of WUE (e.g. Saurer *et al.,* 2014). In order to monitor climate-vegetation feedbacks, an in-depth understanding of factors and processes that determine variation of WUE has become an urgent priority in ecology and biogeosciences (Keenan *et al.,* 2013; Knauer *et al.,* 2016).

Attempts to relate ecosystem WUE to leaf-level plant responses are pursued by the estimation of intrinsic water-use efficiency (WUE_i), or the ratio of net photosynthesis to stomatal conductance of water. The diffusion equation [$WUE_i = A/g_s = (C_a - C_i)/1.6$] links carbon assimilation rate (A) to stomatal conductance (g_s) to the difference in atmospheric (C_a) and inner leaf (C_i) CO_2 concentration, irrespective of atmospheric water demand (Farquhar *et al.,* 1989a). Detailed information on leaf-level physiology can be gained through the analysis of stable isotopes in tree rings (McCarroll and Loader 2004). Particularly, the ratio of the heavy to light carbon isotopes ($^{13}C/^{12}C$) depends on factors affecting CO_2 uptake, being directly related to WUE_i (Farquhar *et al.,* 1989b). Alternatively, eddy covariance fluxes, remote sensing data and dynamic global vegetation models provide estimates of WUE at ecosystem scale (e.g. Frank *et al.,* 2015; Dekker *et al.,* 2016).

The spatiotemporal dynamics of WUE are conditional to the functional characteristics of the vegetation and, particularly, of the dominant tree species as fundamental component of forests. In this regard, it is expected that WUE_i fluctuations of a prevailing tree species could be a determinant factor of WUE variation, hence strongly influencing water and carbon economy of the whole ecosystem. Quantifying the spatial and temporal dimensions of the variation of a functional characteristic such as WUE_i in forest trees is experimentally challenging. Trees can respond to changes in the environment through phenotypic plasticity, i.e. the array of phenotypes that an individual shows in response to different growing conditions (Nicotra *et al.,* 2010). Phenotypic plasticity allows plants to adjust their functional traits to environmental changes, up to a level in which the extent of plastic responses (or range of potential acclimation) does not suffice to cope with substantial variations in external factors (Bussotti *et al.,* 2015). Concurrently, different selective pressures may also engender variation in functional traits within the genetic

pool of a species through localised selection of genotypes that perform better under particular conditions (i.e. genetic adaptation, Alberto *et al.,* 2013). Intra-specific phenotypic variation of a functional trait is thus the result of the co-occurring effects of phenotypic plasticity and genetic adaptation, which have been long proposed as partially independent mechanisms shaping plants' responses to the environment (Bradshaw, 1965).

So far, a comprehensive investigation of the magnitude of phenotypic variation and its components (spatiotemporal and genetic) is mostly lacking for WUE_i, even for widely distributed tree species. The analysis of genotype by environment interaction in multi-environment trials (i.e. the assessment of the performance of individuals in common gardens across different environments) is well suited to this task, but their availability in forest trees is limited and their records are often extremely unbalanced, which further complicates partitioning such effects in a straightforward manner.

In this study, we focus on Scots pine (*Pinus sylvestris* L.), the most widespread conifer of the Northern Hemisphere. Scots pine is found under very diverse climatic conditions and ecological habitats from Boreal forests at high latitudes to Alpine biomes and meso-Mediterranean areas at mid-latitudes, with some populations at the trailing edge of distribution (e.g., Mediterranean basin) subjected to chronic summer drought (Irvine *et al.,* 1998; Sánchez-Salguero *et al.,* 2015). As most pines, Scots pine is considered a drought-avoidant and isohydric species (Irvine *et al.,* 1998), that is, prone to close stomata under water shortage to maintain approximately constant leaf water potentials. During the last decades, the southernmost populations of this species have experienced drought-induced decline in growth and die-back episodes (Hereş *et al.,* 2012; Camarero *et al.,* 2018). Data derived from common garden experiments indicate the existence of inter-population genetic differentiation in traits such as nutrient acquisition (Oleksyn *et al.,* 2003), phenology (Notivol *et al.*, 2007), survival (Benito-Garzón *et al.,* 2011) or carbon allocation (Bachofen *et al.,* 2018). Some evidences also suggest specific adaptation of southern populations to drought (Taeger *et al.,* 2013; Matías *et al.,* 2014). In addition to genetic differentiation, phenotypic plasticity drives variation in traits such as hydraulic conductivity (Irvine *et al.,* 1998), radial growth and carbon isotope composition (Eilmann *et al.,* 2010), and gas exchange physiology (Feichtinger *et al.,* 2017) in this species.

Despite the wealth of information on functional traits for *P. sylvestris*, little is known about how phenotypic variation of WUE_i is structured for this species. A few studies based on carbon isotopes have investigated the relevance of genetic variation of WUE_i through common garden tests and clone bank experiments (Palmroth *et al.,* 1999; Brendel *et al.,* 2002), finding low intra-specific genetic variation for this trait. However, these studies did not include

populations from the trailing edge of distribution of the species, where trees are subjected to frequent summer droughts (Sánchez-Salguero *et al.,* 2015). A persistent selective pressure on water conservation might have led to an appreciable population genetic differentiation in WUE_i. Conversely, Brendel *et al.* (2002) concluded that the main source of phenotypic variation of WUE_i is related to a plastic response of individuals to climate, as expected for a species with high stomatal sensitivity to water shortage (Irvine *et al.,* 1998), which can be found across a vast array of conditions and environments. However, the magnitude and relevance of the spatial and temporal components of phenotypic variation remain unclear. Several studies have characterised temporal variation of WUE_i in *P. sylvestris* (e.g. Andreu-Hayles *et al.*, 2011; Voltas *et al.,* 2013), but mainly focusing on the long-term consequences of rising atmospheric CO_2 and climate on tree performance rather than on interpreting the relevance of temporal variation in relation to spatial and genetic effects.

Here, we use carbon isotope discrimination ($\Delta^{13}C$) in tree rings sampled in a provenance trial and in natural stands of *P. sylvestris* aiming at quantifying the importance of inter-population genetic variation of WUE_i in relation to the overall spatiotemporal phenotypic variation of the species near its south-western distribution limit (Pyrenees range, north-eastern Iberian Peninsula). Our main objective is to understand how phenotypic variation in carbon assimilation rate and stomatal conductance is structured in a widespread conifer and to identify the external drivers of such changes. We hypothesize that: 1) the inter-population genetic variation of WUE_i is of little relevance for *P. sylvestris* owing to a reduced selective pressure towards water conservation as compared with other pine species that are more xeric and, therefore, subjected to extreme and recurrent drought events (e.g. *Pinus halepensis* [Voltas *et al.,* 2008]); and 2) the spatiotemporal phenotypic variation of WUE_i is of comparatively much more relevance than the extent of population genetic differentiation, mainly owing to the relevance of plastic effects for this functional trait. To better understand how leaf-level responses of a dominant tree species may contribute to the overall water and carbon balance in conifer forests, WUE_i records of phenotypic variation obtained across natural stands are compared to several indicators of ecosystem-level WUE derived from satellite data. In this way, we evaluate the feasibility of upscaling tree-ring-based high-resolution spatial estimates of WUE_i over the whole forest stand.

MATHERIAL AND METHODS

Provenance trial

A provenance trial located in Aragüés del Puerto (NE Iberian Peninsula; 42°44'N, 00°37'W, 1350 m a.s.l.) and comprising sixteen Spanish and six German populations (Figure 1a; Appendix,

Table S1) was sampled to quantify the importance of inter-population genetic differentiation of WUE_i for the species. The mean annual temperature at the site is 7.4°C and the mean annual precipitation is 1086 mm (Figure 1a), of which *ca*. 22% fall in summer (1960-1990 period) (WorldClim database; Hijmans *et al.,* 2005). The trial has optimal growing conditions for this species in the Iberian Peninsula, and can be considered representative of the average (albeit slightly warmer) climate conditions encountered by *P. sylvestris* across Europe (Figure 1b). Two-years-old seedlings were planted in 1992 according to a randomized complete block design with four replicates. Each replicate plot consisted of 16 trees of the same population, spaced 2.5 × 2.5 m, resulting in square-shaped experimental units.

The Spanish populations are representative of the species distribution in the Iberian Peninsula (south-western edge of its present range). The German populations are distributed across the country (i.e. approximately the centre of the European distribution range for this species) and were chosen to compare their performance against those of the Spanish populations (for further details see Alía *et al.,* 2001) (Figure 1b). At age 20 (year 2010), survival rate (%) per replicate plot was recorded and height and diameter at breast height (DBH) were measured using telescopic measuring sticks and tapes respectively. Mean tree-ring width (TRW) of each tree was estimated as the radius divided by age. At age 25 (year 2015), wood cores were sampled at 1.3 m using 5-mm Pressler increment borers. We selected two adjacent blocks having relatively uniform growing conditions and a total of six trees per population were sampled (i.e. three trees per block). Tree rings were visually cross-dated and rings corresponding to the 2005-2014 period were pooled together and used for carbon isotope analysis.

Natural stands

The spatial extent of phenotypic variation in WUE_i, which comprises genetic variation and phenotypic plasticity, was evaluated in natural stands of *P. sylvestris*. The sampling sites consisted of 30 unmanaged, monospecific and even-aged stands located in the central and eastern Pyrenees mountains (north-eastern Iberian Peninsula) (Figure 1a; Appendix, Table S2). The stands cover a wide range of local climatic, physiographic and edaphic conditions (Figure 1b; Appendix, Table S2). These stands are supposed to share adaptive characteristics as they belong to two neighbouring Spanish provenance regions (or adaptive units in which phenotypically or genetically similar stands are found; European Council Directive 1999/105/EC). Each stand was characterised for the following features: elevation, slope, hillslope position (footslope, backslope or shoulder) and aspect, carbonate content in soil, stand density, stand basal area and soil depth (maximum dig depth before finding a compact rock layer). The Harmonized World Soil

Database (FAO, 2009) classifies the soils of the stands as humic or calcaric cambisols with a resolution of 1 km^2. Soil texture is relatively uniform among sites (range = 37-42% sand, 23-44% silt and 19-36% clay).

Wood cores were sampled at 1.3 m using 5-mm Pressler increment borers in (2008) A variable number of representative trees (two to ten) were taken per stand (tree age = 68±18 years; mean ± SD). Tree rings were visually cross-dated and tree age was calculated. The rings corresponding to the period of 2000-2007 were identified and used to estimate mean tree-ring width (TRW) for a representative number of years. These rings were then pooled together and used for carbon isotope analysis. Height and DBH of sampled trees were also measured.

Tree-ring chronologies

At temporal level, the magnitude of phenotypic variation was evaluated in two representative sites (Arcalís, 42°22'N, 01°11'E, 1150 m a.s.l.; Seira, 42°31'N, 0°23'E, 1538 m a.s.l.) out of the 30 sites comprising the sampled region (Figure 1a; Appendix, Table S2). Tree-ring chronologies were built in these sites for further carbon isotopes analysis. Arcalís is drier and warmer compared with Seira (Figure 1b) and is located in an area where recent die-off episodes have been observed (Hereş *et al.*, 2012). Wood cores were sampled from 40 and 20 representative, adult and healthy trees in Arcalís and Seira respectively. Tree rings were cross-dated and TRW was measured using WinDENDRO^{TM} (Regent Instruments Inc., Ville de Québec, Canada) with a resolution of 0.01 mm. The accuracy of cross-dating was checked with the COFECHA program (Holmes, 1983). The quality of the resulting chronologies was evaluated by calculating the expressed population signal (EPS) statistic, which resulted adequate (>0.85) for the study period (1975-2009). Individual rings from a subset of ten cores in Arcalís and five cores in Seira were separated with a scalpel under a binocular microscope to carry out carbon isotope analysis with annual resolution. Approximately the last 30 rings (corresponding to 1975-2008 for Arcalís and 1980-2009 for Seira) were used for isotopic analysis to avoid juvenile imprints on the carbon isotope signature (tree age = 68±19 and 66±11 years in Arcalís and Seira respectively; mean ± SD).

Carbon isotope analysis and leaf-level intrinsic water-use efficiency

Wood samples (i.e. pooled rings from the provenance trial and sampled sites, annual rings from tree-ring chronologies) were milled to a fine powder with a mixer mill (Retsch MM301, Haan, Germany) and purified to α-cellulose following Ferrio and Voltas (2005). An aliquot of 0.9-1.1 mg of α-cellulose was weighted and encapsulated into tin capsules that underwent combustion

using a Flash EA-1112 elemental analyser interfaced with a Finnigan MAT Delta C isotope ratio mass spectrometer (Thermo Fisher Scientific Inc., MA, USA). Carbon isotope composition ($\delta^{13}C$) was calculated as:

$$\delta^{13}C\ (‰) = (R_{sample} / R_{standard} - 1) \times 1000 \quad (1)$$

where R_{sample} and $R_{standard}$ are the isotope ratios ($^{13}C/^{12}C$) of the sample and of the Vienna Pee Dee Belemnite (VPDB) standard respectively.

The $\delta^{13}C$ values were then used to estimate carbon isotope discrimination ($\Delta^{13}C$) following Farquhar *et al.* (1989b):

$$\Delta^{13}C\ (‰) = (\delta^{13}C_a - \delta^{13}C_s)/(1 + \delta^{13}C_s/1000) \quad (2)$$

where $\delta^{13}C_a$ and $\delta^{13}C_s$ are the carbon isotope composition of atmospheric CO_2 and sample respectively. $\delta^{13}C_a$ was inferred by interpolating a range of data from Antarctic ice-core records, as described by Ferrio *et al.* (2005). According to these records, the $\delta^{13}C_a$ value applied to α-cellulose $\delta^{13}C$ was -8.20‰ (provenance trial samples; 2005-2014 period), -8.09‰ (sampled sites; 2000-2007 period) and ranged between -7.30‰ and -8.23‰ (annually-resolved tree rings; 1975-2009 period).

$\Delta^{13}C$ is proportional to the ratio of intercellular (C_i) to atmospheric (C_a) CO_2 concentrations in C3 plants as follows:

$$\Delta^{13}C\ (‰) \approx a + (b - a) \times (C_i/C_a) \quad (3)$$

where *a* is the fractionation during diffusion through stomata (~4.4‰) and *b* is the fractionation due to carboxylation by Rubisco (~27‰) (Farquhar *et al.*, 1989b). The previous equation is valid for the primary photosynthetic assimilates, but it does not consider further fractionation occurring downstream from photosynthesis to α-cellulose formation (Gessler *et al.*, 2014). Indeed, leaves are usually less enriched in ^{13}C than wood α-cellulose. To estimate $\Delta^{13}C$ at the leaf level, we added a value of +2.1‰ to our α-cellulose $\Delta^{13}C$ values, as average difference between leaf $\Delta^{13}C$ and α-cellulose $\Delta^{13}C$ reported by Frank *et al.* (2015). We assumed near-constancy of differences between chloroplastic and intercellular CO_2 concentration at the intra-specific level and a linear relationship between g_s and internal conductance in response to varying

water availability. Anyhow, the high internal conductance of *Pinus sylvestris* suggests low mesophyll limitations of photosynthesis (Vernomann-Jürgenson *et al.*, 2017).

WUE_i was obtained from leaf-level $\Delta^{13}C$ according to Farquhar *et al.* (1989b):

$$WUE_i = (C_a \times (b - \Delta^{13}C)) / (1.6 \times (b - a)) \quad (4)$$

C_a was obtained from National Oceanic and Atmospheric Administration (NOAA) Earth System Research Laboratory data (http://www.esrl.noaa.gov/). We considered the average C_a corresponding to the time period of the analysed tree rings (ten years for the provenance trial, eight years for the sampled sites and annually-resolved values for characterising temporal variation). Further analyses were performed using leaf-level WUE_i estimates.

Climate data

Long-term (1960-1990) averages of precipitation, maximum and minimum temperatures were obtained on a monthly basis from the WorldClim database with a resolution of 1 km^2 (Hijmans *et al.*, 2005). They were used to infer mean annual temperature (T_{an}), total annual precipitation (P_{an}) and summer (June to August) precipitation (P_s) of each geographic origin of populations evaluated at the provenance trial (Table S1) and of each natural stand (Table S2). Annual potential evapotranspiration (PET_{an}) was derived from monthly temperatures and precipitation according to the Hargreaves method (Hargreaves and Samani, 1982). Climate at the Spanish provenances is in general less humid than that of German provenances. Particularly, Spanish populations originated from climates having a significantly lower P_s (143±49 mm *vs*. 242±89 mm respectively; mean ± SD), lower P_s to P_{an} ratio (0.19±0.16 *vs*. 0.32±0.21) and higher PET_{an} (880±69 mm *vs*. 762±62 mm) than their German counterparts ($p<0.05$; two-tailed *t*-tests). In comparison, the climate conditions in the provenance trial are intermediate between those typical of German and Spanish populations (P_s=238 mm, P_s to P_{an} ratio=0.22, PET_{an}=747 mm).

Precipitation, temperature and the Standardised Precipitation-Evapotranspiration Index (SPEI) corresponding to the site chronologies were obtained on a monthly basis from the CRU TS3.22 dataset (Harris *et al.*, 2014). CRU TS3.22, despite its lower spatial resolution compared with WorldClim, provides yearly records of monthly climate data suitable to investigate relationships between climate and annually-resolved WUE_i estimates of chronologies. The climate records, available on a 0.5º latitude/longitude grid for global land areas, covered the period in which annual estimates of WUE_i were available (1975-2008 for Arcalís, 1980-2009 for Seira).

Statistical analyses

The magnitudes of population genetic differentiation and phenotypic variation (spatial and temporal) in WUE_i were quantified independently using the three different sources of data: provenance trial for population differentiation, natural stands for spatial variation, and tree-ring chronologies for temporal variation. To this end, we used linear mixed-effects or random-effects models through restricted maximum likelihood (REML) (see below for a detailed description for each data source). The significance of variance components of random effects was evaluated through likelihood ratio tests. These models were fitted using SAS/STAT (ver. 9.4, SAS Inc., Cary, NC, USA). The suitability of analysis of variance (ANOVA) was evaluated through normal quantile plots of the residuals (Appendix, Figure S1).

Provenance trial

The provenance trial was subjected to mixed-effects analysis of variance (ANOVA) with a fixed block effect, a random population effect, a random block × population interaction (intra-block error) and a random variation of trees within a plot (intra-plot error or residual). The random population term provided an estimate for the variance component associated to inter-population genetic variation in WUE_i. This term was further partitioned into a fixed term accounting for differences between large regions (or countries of origin, Germany *vs*. Spain) and a random effect quantifying the variation among populations nested to country of origin. This was done in order to determine the extent by which population genetic differentiation for the trait could be attributed to differences between contrasting ecoregions. An equivalent procedure was also applied to tree height, mean TRW and survival (expressed in per cent values on a plot basis). In this last case, an angular transformation was used to achieve normality.

Natural stands

A full random-effects ANOVA was fitted to WUE_i and TRW records of the sampling sites testing for significant variation among stands. The stand (site) effect was declared as random and the associated variance component was used as an estimate of the spatial dimension of phenotypic variation for these traits. The random variation of trees within a site was used as residual or error term. We used simple correlations to test for the effects of physiography, climate and soil characteristics on site WUE_i and TRW. The associations between WUE_i, TRW and height, and the effect of tree age on WUE_i and TRW were also tested at tree level by simple correlations.

Tree-ring chronologies

WUE_i and TRW time series of the site chronologies showed long-term trends (Figure S2). For the purpose of studying high-frequency variation in WUE_i, estimates were re-calculated considering an average C_a value for a 30-year period instead of using annually-resolved C_a records. In this way, the direct effect of CO_2 fertilization enhancing WUE_i over time was eliminated from the temporal trend. For the same purpose, TRW was investigated by high-pass filtering using cubic smoothing splines with 50% frequency cut-off at 15 years (ARSTAN program; Cook and Krusic, 2005). The resulting WUE_i time series (C_a-constant WUE_i) and the residuals of TRW splines (TRW_{res}) were assumed to be free of increased atmospheric CO_2 concentration and ontogenic effects, thus retaining primarily inter-annual variation. Thus, only the fraction of temporal variation associated to climate effects was presumably quantified by mixed-effects ANOVAs. These models consisted of a fixed site chronology effect and random year, random year by site interaction and random tree-within-site effects. The random year by tree-within-site interaction was used as a residual term. The variance component for the year effect was taken as an estimate of the temporal dimension of phenotypic variation for these traits. Indexed TRW records (TRW_i) were obtained by applying an autoregressive model to each TRW_{res} series in order to remove the autocorrelation related to the growth of previous year and later calculating the ratio of observed to predicted values of the cubic splines. Bootstrapped correlations between annual C_a-constant WUE_i or TRW_i and monthly climate factors (precipitation, temperature and SPEI) from the October of the previous year to September of the ring year were calculated using the software DendroClim (Biondi and Waikul, 2004). Statistical significance of correlations was estimated by drawing 1000 bootstrapped samples with replacement from the initial data set.

Ecosystem water-use efficiency

We correlated our estimates of leaf-level WUE_i of the natural stands with four ecosystem-level indicators of water-use efficiency. Ecosystem water-use efficiency (EWUE) is a common indicator calculated as the ratio between ecosystem gross primary productivity (GPP) and its associated evapotranspiration (ET) (Huang *et al.*, 2015). Soil water-use efficiency (SWUE) is a recently proposed indicator calculated as the ratio between GPP and soil water content (SWC) (He *et al.*, 2017). We took advantage of available high-resolution (1 km^2) remote sensing data to calculate the two indices for each sampled site. Mean GPP and ET data for the period of 2000-2014 were derived from Moderate Resolution Imaging Spectroradiometer (MODIS) on board NASA's Terra satellite, available at https://daacmodis.ornl.gov/data.html. Mean SWC for the

period of 2010-2016 was derived from the ESA's Soil Moisture and Ocean Salinity (SMOS) mission data, downscaled at 1 km^2 resolution as described in Merlin *et al.* (2013). SWC data are available at http://cp34-bec.cmima.csic.es/data/data-access/. We also calculated an "inherent" WUE (IWUE) multiplying EWUE by the average vapour pressure deficit (VPD) estimated at each site. IWUE accounts for atmospheric water demand and it better approximates WUE_i compared with EWUE (Beer *et al.*, 2009). Average VPD was calculated from altitude and monthly temperature and precipitation following Ferrio and Voltas (2005). As SWC is given in relative units as m^3 of water per m^3 of soil, we estimated the total amount of water available along the soil profile by multiplying SWC by soil depth at the site level. We then recalculated SWUE as the ratio between GPP and the corrected (total) SWC (SWUE'). Finally, we correlated leaf-level WUE_i with EWUE, SWUE, IWUE or SWUE' across sites.

RESULTS

Inter-population genetic variation inferred from the provenance trial

We found low inter-population genetic variation for WUE_i and radial growth in *P. sylvestris* as indicated by small and poorly estimated variance components of population effects, which were non-significant (Table 1). However, when the population effect was partitioned into a fixed effect accounting for differences between countries of origin and a remaining random population effect, significant differences in WUE_i emerged between Spanish and German populations ($p<0.05$). In particular, German populations showed a 3.2% higher WUE_i than Spanish populations (Figure 2). On the other hand, there were no significant differences in TRW between countries (Figure 2), but Spanish populations showed a significantly lower tree height than German ones (9.12±0.27 m *vs*. 10.84±0.28 m respectively; mean ± SE) and experienced lower mortality (11.2±0.05% *vs*. 19.2±0.12 % respectively).

Spatial phenotypic variation inferred from natural stands

The spatial phenotypic variation for WUE_i was highly significant and *ca*. ten-fold higher than the magnitude of inter-population genetic variation estimated at the provenance trial (Table 1). WUE_i varied across sites between 85.26 µmol CO_2 mol^{-1} H_2O (Vallfogona) and 113.01 µmol CO_2 mol^{-1} H_2O (Estamariu II), which translated into a relative maximum WUE_i difference of 33% among stands. Mean TRW varied between 0.51 mm (Valls de Valira II) and 2.51 mm (Gombreny), which translated into a relative maximum TRW difference of *ca*. 400% among stands. The spatial component of phenotypic variation for TRW was highly significant and about five-fold higher than that of inter-population genetic variation (Table 1).

WUE_i did not correlate with any physiographic, climatic or edaphic characteristic across stands (Table S3). The only exception was soil depth, which was negatively associated with WUE_i (Figure 3a). WUE_i did not correlate with TRW across stands (Figure 3b). On the other hand, TRW was negatively correlated with the ratio of summer to total precipitation, with annual potential evapotranspiration and with stand density (Appendix, Table S3). At tree level, we did not find significant relationships between WUE_i and age or height, but TRW was negatively associated with tree age (Appendix, Table S3).

Temporal phenotypic variation inferred from tree-ring chronologies

WUE_i increased significantly over the last 30 years, with similar rates in Arcalís and Seira (Figure S2). Particularly, WUE_i was 17% (Arcalís) and 11% (Seira) higher in the period of 2004-2008 than at the beginning of the 1980s (1980-1984 period). Due to the positive effect of increased atmospheric CO_2 concentration on WUE_i over time, the temporal (year) variance calculated through annually-resolved C_a values was much higher than the inter-population genetic variance (over ten-fold higher) and slightly higher than the spatial phenotypic variance (Appendix, Table S4). Instead, the high-frequency signal of time-varying WUE_i was estimated using an average C_a value over the 30 year study period (1975-2008 in Arcalís and 1980-2009 in Seira). After recalculation, the increasing trend disappeared in Seira (Appendix, Figure S2). The resulting C_a-constant mean WUE_i over the study period was 77.79 µmol CO_2 mol^{-1} H_2O in Seira and 85.00 µmol CO_2 mol^{-1} H_2O in Arcalís and the temporal phenotypic variance became four-fold lower (9.57 *vs*. 40.77 (µmol CO_2 mol^{-1} $H_2O)^2$) and only marginally significant (p=0.11). Also, it was about four-fold lower than the magnitude of spatial variation but still three-fold higher than the magnitude of inter-population genetic variation (Table 1). The variance component of year by site (spatiotemporal) interaction was not significant and had about the same magnitude of the variance component of population (genetic) effects found in the provenance trial (Table 1).

TRW showed a significant increase over time in Seira, but a significant decrease in Arcalís (Appendix, Figure S2). The common temporal variance estimated across sites on non-detrended (absolute) TRW records was negligible, but the magnitude of year by site interactions was very relevant (higher than that of inter-population genetic variation and of spatial phenotypic variation) (Table S4). After high-pass filtering, the common temporal variance for TRW_{res} became sizeable (0.04 ± 0.02 mm^2) and the variance associated with year by site interaction took a comparable value (Table 1). In this regard, the temporal component of phenotypic variation for TRW_{res} was similar to that of inter-population genetic variation (Table 1).

The relationships between C_a-constant WUE_i or TRW_i and monthly climatic variables are summarized in Figure 4. In Seira, C_a-constant WUE_i correlated positively with March precipitation and negatively with summer (June and August) precipitation and SPEI drought index. At this site, TRW_i correlated negatively with October temperature and positively with November temperature and August precipitation and SPEI. In Arcalís, C_a-constant WUE_i correlated negatively with spring to early-summer precipitation and SPEI (April and June) and positively with July temperature. It also showed a strong negative correlation with winter (previous December and current January) precipitation, SPEI and temperature. TRW_i correlated positively with January SPEI and April temperature, and with precipitation and SPEI in May-June.

Ecosystem-level WUE

The average ecosystem WUE (EWUE) estimated for the period of 2000-2014 varied between 2.17 g C mm^{-1} H_20 (Seira) and 3.66 g C mm^{-1} H_20 (Sant Llorenç) across sites. Alternatively, the average soil WUE (SWUE) varied between 12.63 g C kg^{-1} H_2O (Espot) and 19.68 g C kg^{-1} H_2O (St. Joan Abadesses) across sites. Neither EWUE nor SWUE correlated with leaf-level WUE_i (Figure 5a,b). IWUE (i.e. EWUE corrected by atmospheric water demand) varied between 11.02 g C hPa mm^{-1} H_2O (Seira) and 23.00 g C hPa mm^{-1} H_2O (Sant Llorenç). IWUE did not correlate with leaf-level WUE_i (Figure 5c). The modified SWUE values taking into account soil depth at the stand level, that is, accounting for the total amount of water potentially available along the soil profile, varied between 19.44 g C kg^{-1} H_2O (Espot) and 76.48 g C kg^{-1} H_2O (St. Joan Abadesses). In this case, a significant positive correlation was found between SWUE' and WUE_i (Figure 5d).

DISCUSSION

The extent of genetic and phenotypic variation of WUE_i in *Pinus sylvestris*

Phenotypic diversity in functional traits, including intra-specific genetic variation and phenotypic plasticity, is called upon to play a central role in assisting forest populations to withstand future environmental conditions (Nicotra *et al.*, 2010; Alberto *et al.*, 2013; Bussotti *et al.*, 2015). Our results demonstrate very limited genetic divergence in WUE_i among *P. sylvestris* populations of the western part of the species distribution, in line with previous studies reporting lack of genetic differences in $\Delta^{13}C$ in adult trees among populations of this species (Palmroth *et al.*, 1999; Brendel *et al.*, 2002). *P. sylvestris* is not subjected to pervasive droughts and, thus, selective pressure towards a strong stomatal regulation of water losses may be irrelevant to shape

physiological adaptations among populations for this species (Matías *et al.,* 2017). In comparison, other European pines thriving in Mediterranean regions and exposed to substantial water shortage, such as *Pinus pinaster* or *P. halepensis*, are known to bear a large intra-specific genetic variation in WUE_i (Voltas *et al.,* 2008; Aranda *et al.,* 2010). Specifically, Voltas *et al.* (2008) reported differences of *ca*. 26 µmol CO_2 mol^{-1} H_2O among populations of the drought-avoidant *P. halepensis*, which is almost three-fold higher than the range we estimated for *P. sylvestris* (*ca*. 10 µmol CO_2 mol^{-1} H_2O). However, our results are not conclusive of lack of intra-specific genetic variation in WUE_i in *P. sylvestris*. Indeed, they do not allow for an assessment of intra-population genetic variation in relation to that present among populations. Such a comparison would require testing the performance of different progenies within each population in a provenance/progeny trial, which is currently unavailable at the south-western distribution range of *P. sylvestris*.

On the other hand, we could identify a significant, albeit low, genetic differentiation in WUE_i after grouping populations according to their country of origin, which might suggest a role of selection on functional traits that contribute to WUE_i (i.e. assimilation rate and stomata control), but only at large (i.e. continental) scales. Particularly, German populations showed increased WUE_i coupled with a greater height growth compared with Spanish populations. This outcome agrees with an indirect evidence of genetic differentiation in WUE_i reported in *P. sylvestris* at the seedling stage for a subset of European populations (Bachofen *et al.,* 2018). These results may indicate improved carbon uptake through photosynthesis as mechanism enhancing WUE_i at the genetic level (and hence, primary growth) for this species (Fardusi *et al.,* 2016).

We estimated for a small Scots pine area (~5,000 km^2) a phenotypic variation of WUE_i over ten-fold larger than the extent of variation related to inter-population genetic differentiation for two major European regions occupying together over 800,000 km^2. Phenotypic variation in natural stands is the result of the interacting effects of genetic variation and phenotypic plasticity, but our approach could not directly disentangle the relative importance of these two components. Despite this caveat, results from the provenance trial suggests lack of relevant population differentiation in WUE_i continent-wide for *P. sylvestris*, making unlikely the presence of a significant inter-population differentiation at the much smaller scale of the sampled natural stands. In this regard, two populations evaluated in the provenance trial, Morrano and Pobla de Lillet (Table S1), which originated from the area where the 30 natural stands were sampled, did not differ in terms of WUE_i (89.09±2.46 µmol mol^{-1} *vs*. 91.14±2.62 µmol mol^{-1}), TRW (3.32±0.26 mm *vs*. 3.47±0.26 mm) and height (8.67±0.74 m *vs*. 8.41±0.74 m). This observation

supports a lack of genetic differentiation among stands for the study traits. Although it can be argued that our results do not quantify within-population genetic variation in WUE_i, the sampling strategy adopted in the natural stands, consisting of a number of representative trees sampled per site, buffered possible genetic differences among trees. Therefore, the reported phenotypic variation among natural stands is most probably indicative of plastic responses to divergent growing conditions. The large phenotypic plasticity for *P. sylvestris* is somewhat expected since pines are known to be extremely plastic organisms (e.g. Tapias *et al.*, 2004), and suggests that Scots pine performance is primarily modulated by plastic responses in functional characteristics such as WUE_i (Feichtinger *et al.*, 2017), rather than by genetic adaptation. Other drought-related traits such as leaf-to-sapwood area ratio (Martínez-Vilalta *et al.*, 2009) or wood anatomy (Eilmann *et al.*, 2009; Martín *et al.*, 2010) also show high plasticity in *P. sylvestris*.

Notably, climate characteristics did not correlate with WUE_i across stands, despite the sampled sites differed considerably in terms of total precipitation, evapotranspiration and summer drought intensity. As a comparison, Ferrio and Voltas (2005) found that WUE_i negatively correlated with annual precipitation across an aridity gradient of the xeric *P. halepensis* in eastern Iberian Peninsula. Coupling our data with those from Ferrio and Voltas (2005), a decay pattern of plastic WUE_i responses to annual precipitation is evident across species (Figure 6). The environmental conditions in which these two isohydric pines overlap in the Iberian Peninsula (~800 mm of annual precipitation) roughly agree with the threshold at which WUE_i (and stomatal sensitivity) becomes unresponsive to precipitation (Figure 6) or water deficit (Figure 6 insert), as observed for *P. halepensis* (del Castillo *et al.*, 2015). Within such a continuous distribution of pines, precipitation would mainly drive phenotypic variation of WUE_i in *P. halepensis*, while *P. sylvestris* would be found in conditions where precipitation is no longer a fundamental determinant of spatial variation in gas exchange.

Instead, the driving force of phenotypic variation in WUE_i for *P. sylvestris* was the amount of water available to roots, as indicated by the negative relationship between soil depth and WUE_i. Because of methodological difficulties, the study of rooting patterns for elucidating adaptations to edaphic conditions is a much less explored field of research compared with the analysis of above-ground tree characteristics. However, the distribution of water along the soil profile is known to be extremely relevant in modulating plastic responses of forest trees to drought (Lebourgeois *et al.*, 2010; Song *et al.*, 2015; Voltas *et al.*, 2015). Song *et al.* (2015) found a lower increase of WUE_i under drought stress in old plantations of *P. sylvestris* compared to young stands, and explained the difference as a higher rooting depth of older trees and, therefore, an easier access to deep water sources. In our case, the depth of rooting zone, which

can be regarded as proxy of water holding capacity, seems a critical characteristic for *P. sylvestris* growing at its south-western distribution edge (Mellert *et al.,* 2017). However, other soil factors such as nutrient availability and its interactions with climate may also determine changes in WUE_i across sites, hence warranting further examination (Silva *et al.,* 2015).

WUE_i increased over the last 30 years by 11% and 17% at the mesic (Seira) and xeric site (Arcalís) respectively. These rates are consistent with previous results reporting similar WUE_i increments in European forests (Saurer *et al.,* 2014) and in other *P. sylvestris* stands from the Iberian Peninsula (Andreu-Hayles *et al.,* 2011; Voltas *et al.,* 2013). After reappraising WUE_i for constant C_a, we observed increases over time only at Arcalís, indicating that warming-induced drought effects may effectively contribute to long-term WUE_i changes in drought-prone areas for this species. In fact, most sampling sites of the central and eastern Pyrenees showed higher mean WUE_i than Arcalís over the same period (93 µmol CO_2 mol^{-1} H_2O) (*cf.* Figure 3a), which suggests that water availability is the most limiting factor for regional tree performance. It can therefore be hypothesised that a long-term temporal variation of WUE_i related to increasing drought effects (Shestakova *et al.,* 2017) may be common to most *P. sylvestris* stands of the region.

The lack of interaction between spatial and temporal plastic responses in terms of WUE_i anticipates the existence of common temporal patterns across sampling sites. Although this point would need further assessment, the fact that Arcalís and Seira shared the dependence of WUE_i on summer precipitation indicates a predominant role of summer water availability influencing inter-annual variation of WUE_i. However, WUE_i was also negatively correlated with winter precipitation at the xeric site (Arcalís), which can be interpreted as the effect of groundwater recharge on tree performance during the growing season (Shestakova *et al.,* 2014). Indeed, water stress could be delayed or supressed during the growing season in years with important snow coverage, resulting in low WUE_i. Thus, our results suggest that soil water plays an important role in modulating inter-annual variation of WUE_i, at least at the xeric site, which is supportive of a strong dependence of spatial variation of WUE_i on soil depth for *P. sylvestris*.

Inter-population genetic differentiation and phenotypic variation of radial growth

The extent of phenotypic variation and the magnitude of inter-population genetic differentiation in WUE_i were compared with those of radial growth as indicator of overall performance in forest trees. Tree growth is indeed influenced by many biotic, abiotic and stand (local) factors, but climate plays a major role in driving growth variation in *P. sylvestris* (Matías and Jump, 2012; Sánchez-Salguero *et al.,* 2015). A large body of literature is available about radial growth

responses of *P. sylvestris* to climatic factors. Broadly speaking, the phenotypic variation in radial growth is predominantly driven by drought at the southern edge of the species distribution (Camarero *et al.*, 1998; Matías and Jump, 2012) and by low temperatures in boreal latitudes (Grace and Norton, 1990; Persson and Beuker, 1997; Matías and Jump, 2012). However, there is less clear-cut information quantifying the contribution of plastic and genetic responses to this variation. In our study, we estimated the amount of inter-population genetic variation in radial growth to be about one-fifth and one-half the spatial and temporal phenotypic variation respectively. As for the case of WUE_i, this finding suggests preponderance of plastic variation (especially at spatial level) over population differentiation in radial growth, but with smaller differences compared with those of WUE_i.

Upscaling WUE_i to the ecosystem level

In order to understand the relevance of leaf-level WUE_i in determining ecosystem-level WUE, we attempted at scaling up our long-term spatial WUE_i estimates based on tree rings (2000-2007 period) using remote sensing data. This could be undertaken owing to comparatively homogeneous stand conditions across sites. Indeed, the sampled forests were mature, even-aged and unmanaged, with large basal areas and crown covers exceeding 65%, hence suggesting comparable leaf area indices (Whitehead, 1978).

In the present work, we used high resolution (~1 km^2) estimates of GPP and ET derived from MODIS satellite data, which are considered reliable at large (i.e. regional or continental) scales. The use of MODIS GPP and ET at local (i.e. site) scale is instead more problematic. However, reliable site-level estimates of MODIS GPP and ET have been reported in evergreen-needle forests similar to our stands (Turner *et al.*, 2006a; Turner *et al.*, 2006b; Kim *et al.*, 2012; Cristiano *et al.*, 2015). Anyhow, absolute values of productivity and evapotranspiration have relatively little importance in the present study, since our purpose was to assess variation in carbon-water balance among stands. In this regard, a bias in GPP or ET estimations, if present, would likely be consistent across sites due to homogenous vegetation type and stand structure.

Our estimates of ecosystem WUE (EWUE) varied considerably among stands and were similar to the values reported for evergreen-needle forests derived from either flux tower measurements (Tang *et al.*, 2014) or remote sensing data (He *et al.*, 2017). It should be noted, however, that EWUE is not able to directly catch the influence of available soil water on ecosystem performance, which was instead the primary driver of variation in WUE_i along the study area. He *et al.* (2017) proposed a new indicator (SWUE, or ratio of gross productivity to soil water content) to potentially improve the information on how ecosystems use available

water. In the present study, SWUE was calculated from remotely sensed data of soil water content (SWC) previously validated for the north-eastern Iberian Peninsula (Merlin *et al.,* 2013). The derived SWUE values were much higher than those reported by He *et al.* (2017). The authors found an average SWUE of 3.4 g C kg^{-1} H_2O for evergreen-needle forests, while our values varied between 12.63 and 19.68 g C kg^{-1} H_2O. Such discordance may be related to the very large difference in data resolution (1 km^2 in this work compared with ~ 600 km^2 in He *et al.,* 2017), which may have influenced site-level SWUE estimation. This issue, however, would require specific attention that is beyond the scope of our study.

Neither EWUE nor SWUE were related to variation in WUE_i among stands. At ecosystem level, a better approximation of WUE_i may be obtained by correcting EWUE for atmospheric water demand (i.e. inherent WUE, IWUE) (Beer *et al.,* 2009). However, IWUE neither correlated with WUE_i. On the other hand, when SWUE was corrected to account for soil depth, the resulting SWUE' significantly correlated with WUE_i ($p<0.01$), indicating a tight relation between leaf-level physiology and gross productivity per unit of water available in the soil. This outcome suggests that the range of variation in leaf-level WUE_i, as inferred from tree rings, can be upscaled to the ecosystem level if accounting for soil water holding capacity *via* soil depth. Indeed, many studies have demonstrated the influence of soil water availability on canopy conductance, an effect that is remarkably similar across tree species (e.g. Granier *et al.,* 2000). Our finding suggests a direct influence of the plastic variation of WUE_i of a major forest species in determining water and carbon balances at ecosystem level. On the other hand, local factors controlling WUE_i (such as rooting depth) must be taken into account when scaling up from leaf to ecosystem WUE.

Conclusions

The accurate prediction of water-use efficiency changes in forests is crucial to understand how climate change will affect terrestrial carbon and water balances. While the two components – genetic and plastic– of phenotypic variation of WUE_i can potentially influence ecosystem WUE, our results point to a minor role of genetic differentiation in the variation of WUE_i in *P. sylvestris*. Instead, a maximum 33%–difference in WUE_i among stands indicates a strong spatial divergence in the water and carbon economy of pinewoods in a small area of *ca*. 5000 km^2. We also showed that long-term spatial differentiation in ecosystem WUE can be directly coupled to carbon uptake and stomatal responses for closed forest canopies in an isohydric species such as *P. sylvestris*. The key role of soil water holding capacity modulating WUE at both leaf and ecosystem levels, at least in *P. sylvestris*, emphasises the necessity to incorporate belowground information when

forecasting forest responses to climate (Ostle *et al.,* 2009; van der Putten *et al.,* 2013). Although the importance of inter-population genetic variation of WUE_i seems marginal for understanding *P. sylvestris* responses to global changes, this observation could not hold true for other widespread isohydric pines (e.g. *P. halepensis* or *Pinus pinaster*) in which strong genetic variation for this trait is acknowledged (Voltas *et al.,* 2008; Aranda *et al.,* 2010). Altogether, accurate predictions of global change impacts on forests should consider potential additive effects of genetic variation and phenotypic plasticity in modulating phenotypic variation in functional traits such as WUE_i, as well as their interactions (Benito-Garzón *et al.,* 2011; Klein *et al.,* 2013).

ACKNOWLEDGEMENTS

We acknowledge P. Sopeña and M.J. Pau for technical assistance and V. Muñoz, M. Sala and A. Teixidó for field sampling.

AUTHOR CONTRIBUTIONS

J.V. and F.S. conceived and designed the research. F.S., A.M.H., E.N., M.P., L.S., E.S., P.V. and J.V. collected the data; F.S., J.P.F., T.S. and J.V. analysed the data; F.S. and J.V. wrote the manuscript, with contributions from the other authors.

REFERENCES

Alberto F.J., Aitken S.N., Alía R., *et al.* (2013) Potential for evolutionary responses to climate change–evidence from tree populations. *Global Change Biology*, 19, 1645-1661.

Alía R., Moro-Serrano J., Notivol E. (2001) Genetic variability of Scots pine (*Pinus sylvestris*) provenances in Spain: growth traits and survival. *Silva Fennica*, 35,27–38.

Andreu-Hayles L., Planells O., Gutiérrez E., Muntan E., Helle G., Anchukaitis K.J., Schleser G.H. (2011) Long tree-ring chronologies reveal 20th century increases in water-use efficiency but no enhancement of tree growth at five Iberian pine forests. *Global Change Biology*, 17, 2095–2112.

Aranda I., Alía R., Ortega U., Dantas Â.K., Majada J. (2010) Intra-specific variability in biomass partitioning and carbon isotopic discrimination under moderate drought stress in seedlings from four *Pinus pinaster* populations. *Tree Genetics and Genomes*, 6,169–178.

Bachofen C., Moser B., Hoch G., Ghazoul J., Wohlgemuth T. (2018). No carbon "bet hedging" in pine seedlings under prolonged summer drought and elevated CO_2. *Journal of Ecology*, 106, 31-46.

Beer C., Ciais P., Reichstein M., et al (2009) Temporal and among-site variability of inherent water use efficiency at the ecosystem level. *Global Biogeochemical Cycles*, 23, GB2018.

Benito-Garzón M., Alía R., Robson M., Zavala M.A. (2011) Intra-specific variability and plasticity influence potential tree species distributions under climate change. *Global Ecology and Biogeography*, 20, 766-778.

Biondi F., Waikul K. (2004) DENDROCLIM2002: a C++ program for statistical calibration of climate signals in tree-ring chronologies. *Computers and Geosciences*, 30, 303–311.

Bradshaw A.D. (1965) Evolutionary significance of phenotypic plasticity in plants. *Advances in Genetics*, 13, 115–155.

Brendel O., Handley L., Griffiths H. (2002) Differences in $\delta^{13}C$ and diameter growth among remnant Scots pine populations in Scotland. *Tree Physiology*, 22, 983–992.

Bussotti F., Pollastrini M., Holland V., Brüggemann W. (2015) Functional traits and adaptive capacity of European forests to climate change. *Environmental and Experimental Botany*, 111, 91–113.

Camarero J.J., Guerrero-Campo J., Gutiérrez E. (1998) Tree-ring growth and structure of *Pinus uncinata* and *Pinus sylvestris* in the Central Spanish Pyrenees. *Arctic and Alpine Research*, 30, 1–10.

Camarero J.J., Gazol A., Sangüesa-Barreda G., *et al.* (2018) Forest growth responses to drought at short-and long-term scales in Spain: squeezing the stress memory from tree rings. *Frontiers in Ecology and Evolution*, 6, 9.

Cook E.R., Krusic P.J. (2005) Program ARSTAN: a tree-ring standardization program based on detrending and autoregressive time series modeling, with interactive graphics. Lamont-Doherty Earth Observatory, Columbia University, Palisades, NY.

Cristiano P.M., Campanello P.I., Bucci S.J., *et al.* (2015) Evapotranspiration of subtropical forests and tree plantations: a comparative analysis at different temporal and spatial scales. *Agricoltural and Forest Meteorology*, 203, 96-106.

Dekker S.C., Booth B.B., Cox P.M. (2016) Spatial and temporal variations in plant water-use efficiency inferred from tree-ring, eddy covariance and atmospheric observations. *Earth System Dynamics Discussions*, 7, 525–533.

del Castillo J., Voltas J., Ferrio J.P. (2015) Carbon isotope discrimination, radial growth, and NDVI share spatiotemporal responses to precipitation in Aleppo pine. *Trees*, 29, 223–233.

Eilmann B., Zweifel R., Buchmann N., Fonti P., Rigling A. (2009) Drought-induced adaptation of the xylem in Scots pine and pubescent oak. *Tree Physiology*, 29, 1011-1020.

Eilmann B., Buchmann N., Siegwolf R., Saurer M., Rigling P.C. (2010) Fast response of Scots pine to improved water availability reflected in tree-ring width and $\delta^{13}C$. *Plant, Cell and Environment*, 33, 1351-1360.

FAO/IIASA/ISRIC/ISS-CAS/JRC (2009) Harmonized World Soil Database (version 1.1). FAO, Rome, Italy and IIASA, Laxenburg, Austria

Fardusi M.J., Ferrio J.P., Comas C., Voltas J., de Dios V.R., Serrano L. (2016) Intra-specific association between carbon isotope composition and productivity in woody plants: A meta-analysis. *Plant Science*, 251, 110–118.

Farquhar G.D., Ehleringer J.R., Hubick K.T. (1989a) Carbon isotope discrimination and photosynthesis. *Annual Review of Plant Biology*, 40, 503–537.

Farquhar G.D., Hubick K.T., Condon A.G., Richards R.A. (1989b) Carbon isotope fractionation and plant water-use efficiency. In: Rundel PW, Ehleringer JR, Nagy KA (eds.) *Stable Isotopes in Ecological Research*. Springer, New York, pp 21-40.

Feichtinger L.M., Siegwolf R.T.W., Gessler A., Buchmann N., Lévesque M., Rigling A. (2017) Plasticity in gas-exchange physiology of mature Scots pine and European larch drive short- and long-term adjustments to changes in water availability. *Plant, Cell and Environment*, 40, 1972–1983.

Ferrio J.P., Araus J.L., Buxó R., Voltas J., Bort J. (2005) Water management practices and climate in ancient agriculture: inferences from the stable isotope composition of archaeobotanical remains. *Vegetation History and Archaeobotany*, 14, 510–517.

Ferrio J.P., Voltas J. (2005) Carbon and oxygen isotope ratios in wood constituents of *Pinus halepensis* as indicators of precipitation, temperature and vapour pressure deficit. *Tellus b*, 57, 164–173.

Frank D.C., Poulter B., Saurer M., *et al.* (2015) Water-use efficiency and transpiration across European forests during the Anthropocene. *Nature Climate Change*, 5, 579-583.

Gessler A., Ferrio J.P., Hommel R., Treydte K., Werner R.A., Monson R.K. (2014) Stable isotopes in tree rings: towards a mechanistic understanding of isotope fractionation and mixing processes from the leaves to the wood. *Tree Physiology*, 34, 796–818.

Grace J., Norton D.A. (1990) Climate and growth of *Pinus sylvestris* at its upper altitudinal limit in Scotland: evidence from tree growth-rings. *Journal of Ecology*, 78, 601–610.

Granier A., Loustau D., Bréda N. (2000) A generic model of forest canopy conductance dependent on climate, soil water availability and leaf area index. *Annals of Forest Science*, 57, 755–765.

Hargreaves G.H., Samani Z.A. (1982) Estimating potential evapotranspiration. *Journal of the Irrigation and Drainage Division*, 108, 225–230.

Harris I.P.D.J., Jones P.D., Osborn T.J., Lister D.H. (2014) Updated high-resolution grids of monthly climatic observations – the CRU TS3.10 Dataset. *International Journal of Climatology*, 34, 623–642.

He B., Wang H., Huang L., Liu J., Chen Z. (2017) A new indicator of ecosystem water use efficiency based on surface soil moisture retrieved from remote sensing. *Ecological Indicators*, 75, 10–16.

Hereş A-M., Martínez-Vilalta J., López B.C. (2012) Growth patterns in relation to drought-induced mortality at two Scots pine (*Pinus sylvestris* L.) sites in NE Iberian Peninsula. *Trees*, 26, 621–630.

Hereş A-M., Voltas J., López B.C., Martínez-Vilalta J. (2014) Drought-induced mortality selectively affects Scots pine trees that show limited intrinsic water-use efficiency responsiveness to raising atmospheric CO_2. *Functional Plant Biology*, 41, 244–256.

Hijmans R.J., Cameron S.E., Parra J.L., Jones P.G., Jarvis A. (2005) Very high resolution interpolated climate surfaces for Glob land areas. *International Journal of Climatology*, 25, 1965–1978.

Holmes R.L. (1983) Computer-assisted quality control in tree-ring dating and measurement. *Tree-Ring Bulletin*, 43, 69–78.

Huang M., Piao S., Sun Y., *et al.* (2015) Change in terrestrial ecosystem water-use efficiency over the last three decades. *Global Change Biology*, 21, 2366–2378.

Irvine J., Perks M.P., Magnani F., Grace J. (1998) The response of *Pinus sylvestris* to drought: stomatal control of transpiration and hydraulic conductance. *Tree Physiology*, 18, 393–402.

Keenan T.F., Hollinger D.Y., Bohrer G., Dragoni D., Munger J.W., Schmid H., Richardson A.D. (2013) Increase in forest water-use efficiency as atmospheric carbon dioxide concentrations rise. *Nature*, 499, 324–327.

Kim H.W., Hwang K., Mu Q., Lee S.O., Choi M. (2012) Validation of MODIS 16 Glob terrestrial evapotranspiration products in various climates and land cover types in Asia. *KSCE Journal of Civil Engineering*, 16, 229-238.

Klein T., Di Matteo G., Rotenberg E., Cohen S., Yakir D. (2013) Differential ecophysiological response of a major Mediterranean pine species across a climatic gradient. *Tree Physiology*, 33, 26–36.

Knauer J., Zaehle S., Reichstein M., Medlyn B.E., Forkel M., Hagemann S., Werner C. (2016) The response of ecosystem water-use efficiency to rising atmospheric CO_2 concentrations: sensitivity and large-scale biogeochemical implications. *New Phytologyst*, 213, 1654–1666.

Lebourgeois F., Rathgeber C.B., Ulrich E. (2010) Sensitivity of French temperate coniferous forests to climate variability and extreme events (*Abies alba*, *Picea abies* and *Pinus sylvestris*). *Journal of Vegetation Science*, 21, 364–376.

Martín J.A., Esteban L.G., de Palacios P., García-Fernández F. (2010) Variation in wood anatomical traits of *Pinus sylvestris* L. between Spanish regions of provenance. *Trees*, 24, 1017-1028.

Martínez-Vilalta J., Cochard H., Mencuccini M., *et al.* (2009) Hydraulic adjustment of Scots pine across Europe. *New Phytologyst*, 184, 353-364.

Matías L., Jump A.S. (2012) Interactions between growth, demography and biotic interactions in determining species range limits in a warming world: the case of *Pinus sylvestris*. *Forest Ecology and Management*, 282, 10-22.

Matías L., González-Díaz P., Jump A.S. (2014) Larger investment in roots in southern range-edge populations of Scots pine is associated with increased growth and seedling resistance to extreme drought in response to simulated climate change. *Environmental and Experimetnal Botany*, 105, 32–38.

Matías L., Castro J., Villar-Salvador P., Quero J.L., Jump A.S. (2017) Differential impact of hotter drought on seedling performance of five ecologically distinct pine species. *Plant Ecology*, 218, 201–212.

McCarroll D., Loader N.J. (2004) Stable isotopes in tree rings. *Quaternary Science Reviews*, 23, 771–801.

Mellert K.H., Lenoir J., Winter S., *et al.* (2017) Soil water storage appears to compensate for climatic aridity at the xeric margin of European tree species distribution. *European Journal of Forest Research*, 137, 79-92.

Merlin O., Escorihuela M.J., Mayoral M.A., Hagolle O., Al Bitar A., Kerr Y. (2013) Self-calibrated evaporation-based disaggregation of SMOS soil moisture: An evaluation study at 3km and 100m resolution in Catalunya, Spain. *Remote Sensing of Environment*, 130, 25-38.

Nicotra A.B., Atkin O.K., Bonser S.P., *et al.* (2010) Plant phenotypic plasticity in a changing climate. *Trends in Plant Science*, 15, 684-692.

Notivol E., Garcia-Gil M.R., Alía R., Savolainen O. (2007) Genetic variation of growth rhythm traits in the limits of a latitudinal cline in Scots pine. *Canadian Journal of Forest Research*, 37, 540–551.

Oleksyn J., Reich P.B., Zytkowia R., Karolewski P., Tjoelker M.G. (2003) Nutrient conservation increases with latitude of origin in European *Pinus sylvestris* populations. *Oecologia*, 136, 220–235.

Ostle N.J., Smith P., Fisher R., *et al.* (2009) Integrating plant–soil interactions into global carbon cycle models. *Journal of Ecolgy*, 97, 851-863.

Palmroth S., Berninger F., Nikinmaa E., Lloyd J., Pulkkinen P., Hari P. (1999) Structural adaptation rather than water conservation was observed in Scots pine over a range of wet to dry climates. *Oecologia*, 121, 302–309.

Pan Y., Birdsey R.A., Fang J.m *et al.* (2011) A large and persistent carbon sink in the world's forests. *Science*, 333, 988-993.

Persson B., Beuker E. (1997) Distinguishing between the effects of changes in temperature and light climate using provenance trials with *Pinus sylvestris* in Sweden. *Canadian Journal of Forest Research*, 27, 572-579.

Sánchez-Salguero R., Camarero J.J., Hevia A., *et al.* (2015) What drives growth of Scots pine in continental Mediterranean climates: drought, low temperatures or both? *Agricoltural and Forest Meteorology*, 206, 151-162.

Saurer M., Spahni R., Frank D.C., *et al.* (2014) Spatial variability and temporal trends in water-use efficiency of European forests. *Global Change Biology*, 20, 3700-3712.

Schlesinger W.H., Jasechko S. (2014) Transpiration in the global water cycle. *Agricoltural and Forest Meteorology*, 189, 115–117.

Shestakova T.A., Aguilera M., Ferrio J.P., Gutiérrez E., Voltas J. (2014) Unravelling spatiotemporal tree-ring signals in Mediterranean oaks: a variance-covariance modelling approach of carbon and oxygen isotope ratios. *Tree Physiology*, 34, 819–838.

Shestakova T.A., Camarero J.J., Ferrio J.P., Knorre A.A., Gutiérrez E., Voltas J. (2017) Increasing drought effects on five European pines modulate $\Delta^{13}C$–growth coupling along a Mediterranean altitudinal gradient. *Functional Ecology*, 31, 1359–1370

Silva L.C., Gómez-Guerrero A., Doane T.A., Horwath W.R. (2015) Isotopic and nutritional evidence for species- and site-specific responses to N deposition and elevated CO_2 in temperate forests. *Journal of Geophysical Research: Biogeosciences*, 120, 1110–1123.

Song L., Zhu J., Li M., Yan Q. (2015) Intrinsic water use efficiency in wet and dry years at young and old plantations of *Pinus sylvestris* var. *mongolica* in semiarid China. *Journal of Forest Research*, 20, 263-271.

Taeger S., Fussi B., Konnert M., Menzel A. (2013) Large-scale genetic structure and drought-induced effects on European Scots pine (*Pinus sylvestris* L.) seedlings. *European Journal of Forest Research*, 132, 481–496.

Tang X., Li H., Desai A.R. (2014) How is water-use efficiency of terrestrial ecosystems distributed and changing on Earth? *Scientific Reports*, 4, 7483.

Tapias R., Climent J., Pardos J.A., Gil L. (2004) Life histories of Mediterranean pines. *Plant Ecology*, 171, 53–68.

Turner D.P., Ritts W.D., Cohen W.B., *et al.* (2006a) Evaluation of MODIS NPP and GPP products across multiple biomes. *Remote Sensing of Environment*, 102, 282-292.

Turner D.P., Ritts W.D., Zhao M., *et al.* (2006b) Assessing interannual variation in MODIS-based estimates of gross primary production. *IEEE Transactions on Geoscience and Remote Sensing*, 44, 1899-1907.

Ukkola A.M., Keenan T.F., Kelley D.I., Prentice I.C. (2016) Vegetation plays an important role in mediating future water resources. *Environmental Research Letters*, 11, 094022.

van der Putten W.H., Bardgett R.D., Bever J.D., *et al.* (2013) Plant–soil feedbacks: the past, the present and future challenges. *Journal of Ecology*, 101, 265-276.

Vernomann-Jürgenson L-L., Tosens T., Laanisto L., Niinemets U. (2017) Extremely thick cell walls and low mesophyll conductance: welcome to the world of ancient living! *Journal of Experimental Botany*, 68, 1639-1653.

Voltas J., Camarero J.J., Carulla D., Aguilera M., Ortiz A., Ferrio J.P. (2013) A retrospective, dual-isotope approach reveals individual predispositions to winter-drought induced tree dieback in the southernmost distribution limit of Scots pine. *Plant, Cell and Environment*, 36, 1435–1448.

Voltas J., Chambel M.R., Prada M.A., Ferrio J.P. (2008) Climate-related variability in carbon and oxygen stable isotopes among populations of Aleppo pine grown in common-garden tests. *Trees*, 22, 759–769.

Voltas J., Lucabaugh D., Chambel M.R., Ferrio J.P. (2015) Intraspecific variation in the use of water sources by the circum-Mediterranean conifer *Pinus halepensis*. *New Phytologyst*, 208, 1031–1041.

Whitehead D. (1978) The estimation of foliage area from sapwood basal area in Scots pine. *Forestry*, 51, 137–149.

Chapter V - Tables and Figures

Table 1. Linear mixed-effects models for intrinsic water-use efficiency (WUE_i) and tree-ring width (TRW). Data were obtained from the provenance trial of Aragüés del Puerto, a set of 30 natural stands located in the central and eastern Pyrenees mountains and two tree-ring chronologies from the same area. For chronologies, variance components were estimated based on C_a-constant WUE_i values or high-pass filtered TRW residuals (TRW_{res}). Only the random effects of the models are shown.

	Source of variation	Variance component	% of total variance	Chi-Square value[a]	Likelihood ratio test (*p*-value)[a]
WUE_i					
Provenance trial					
	Population	3.38±3.73[b]	11.20	0.87	p=0.35
	Population×Block	4.14±4.50	13.73	1.14	p=0.28
	Residual	22.68±3.87	75.07		
Natural stands					
	Site	34.47±12.37[c]	50.77	38.63	p<0.01
	Residual	33.42±5.41	49.23		
Chronologies					
	Tree [Site]	20.53±8.40	40.65	52.45	p<0.01
	Year	9.57±5.27[d]	18.94	2.45	p=0.11
	Year×Site	3.69±3.26[e]	7.30	3.52	p=0.06
	Residual	16.72±2.34	33.11		
TRW					
Provenance trial					
	Population	0.03±0.02[b]	3.97	3.70	p=0.05
	Population×Block	0.07±0.02	10.31	32.81	p<0.01
	Residual	0.58±0.03	85.72		
Natural stands					
	Site	0.15±0.05[c]	54.27	31.67	p<0.01
	Residual	0.13±0.02	45.73		
Chronologies					
	Tree [Site]	0.00±0.00	0.00	0.00	p=1.00
	Year	0.04±0.02[d]	10.11	7.64	p<0.01
	Year×Site	0.03±0.01[e]	7.30	30.66	p<0.01
	Residual	0.32±0.01	82.59		

[a] Test for the null hypothesis of variance component being equal to 0; [b] estimate of inter-population genetic variation; [c] estimate of spatial phenotypic variation; [d] estimate of temporal phenotypic variation; [e] estimate of spatiotemporal phenotypic variation

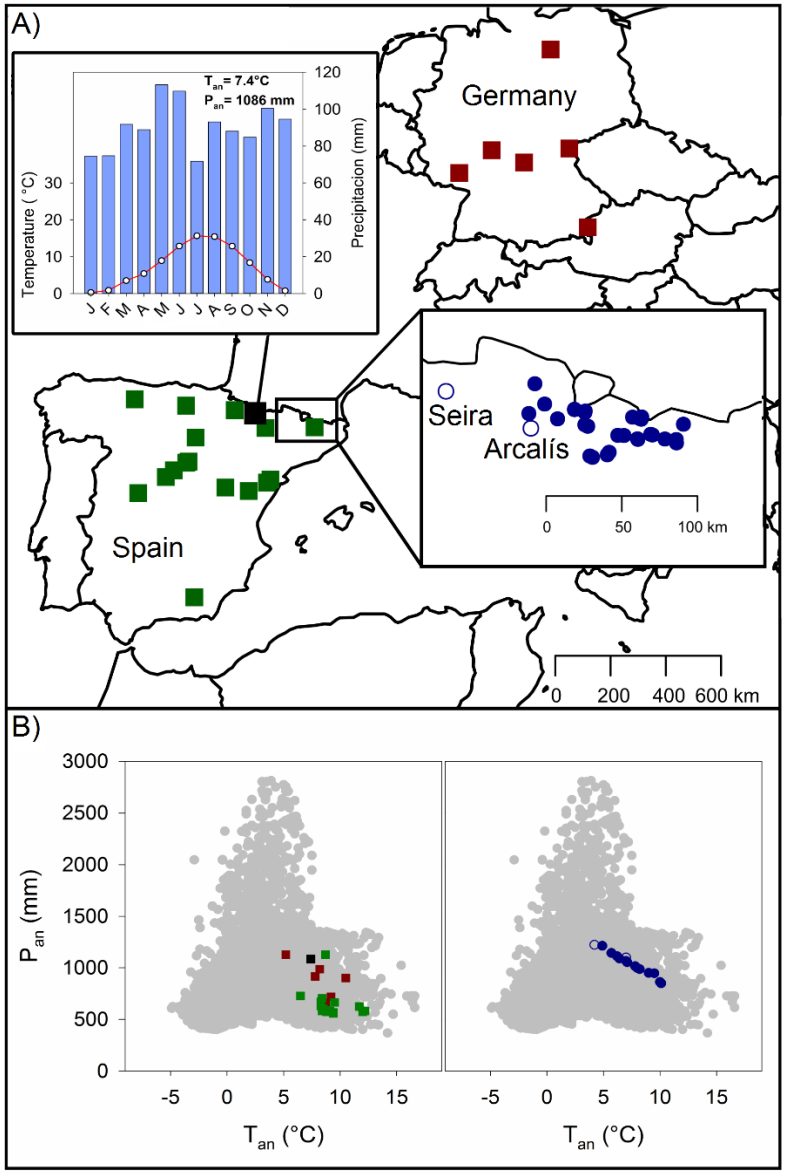

Figure 1. (A) Location of the provenance trial (Aragüés del Puerto, Spanish Pyrenees) (black square) and geographic origin of the German (green squares) and Spanish (red squares) populations evaluated in the trial. The climograph of the trial site is also included (left insert). The right insert shows the study area in which the natural stands (blue circles) were sampled. Sites chosen to build temporal chronologies (Arcalís and Seira) are indicated with empty blue circles in the right insert. (B) Mean annual precipitation and temperature for the distribution range of *P. sylvestris* in Europe (grey circles) calculated in 10' resolution grids from the WorldClim database (period 1960-1990). The species range is derived from the EUFORGEN distribution map (http://www.euforgen.org/species/pinus-sylvestris). Temperature and precipitation of the trial site (black square), of German and Spanish sites of origin (red and green squares), of natural stands (blue circles) and of two chronologies sites (open blue circles) are shown

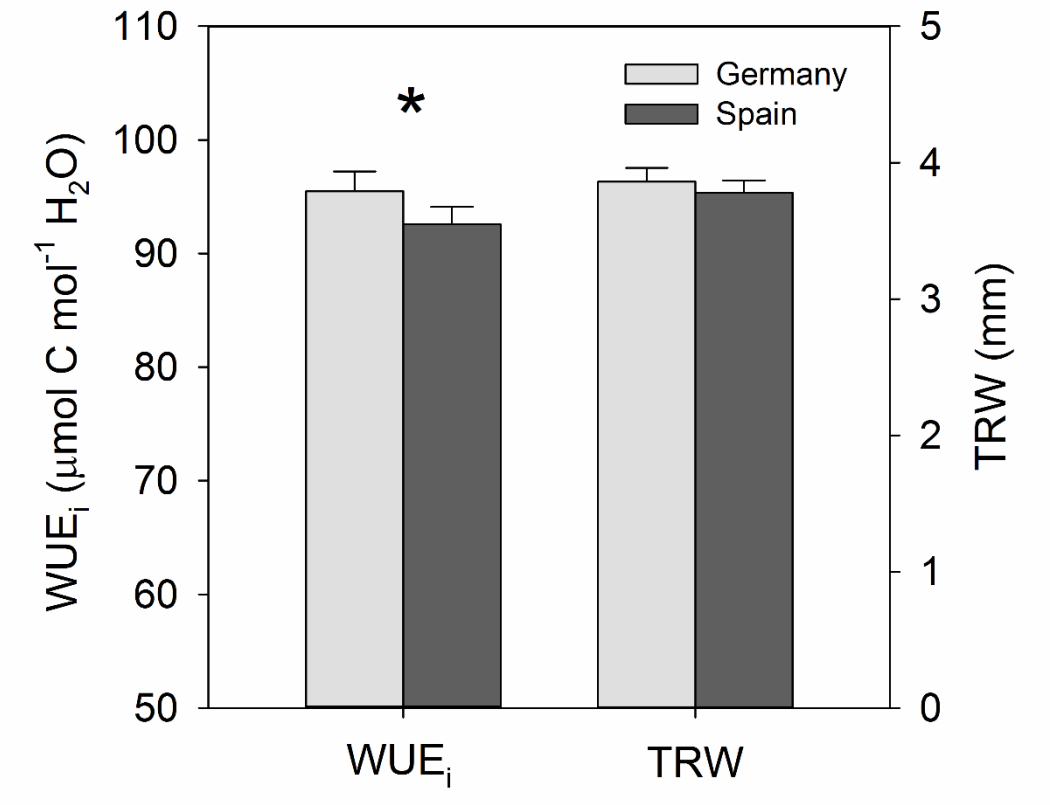

Figure 2. Mean intrinsic water-use efficiency (WUE_i) and tree-ring width (TRW) of Spanish and German populations of the provenance trial. Error bars indicate standard errors. The asterisk indicates a statistically significant difference at $p < 0.05$

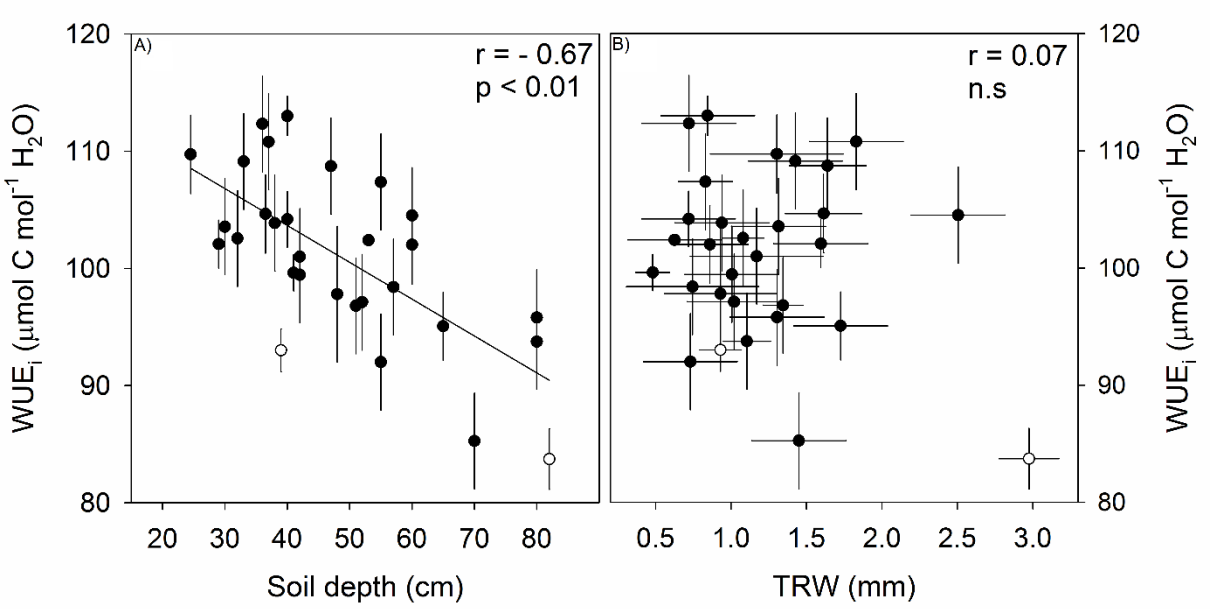

Figure 3. A) Relationships between intrinsic water-use efficency (WUE_i) and soil depth and B) between WUE_i and tree-ring width (TRW) (B) in the 30 natural stands composing the study area. Each dot indicates one particular stand. Open dots indicate the two sites where temporal chronologies were available. Error bars indicate standard errors

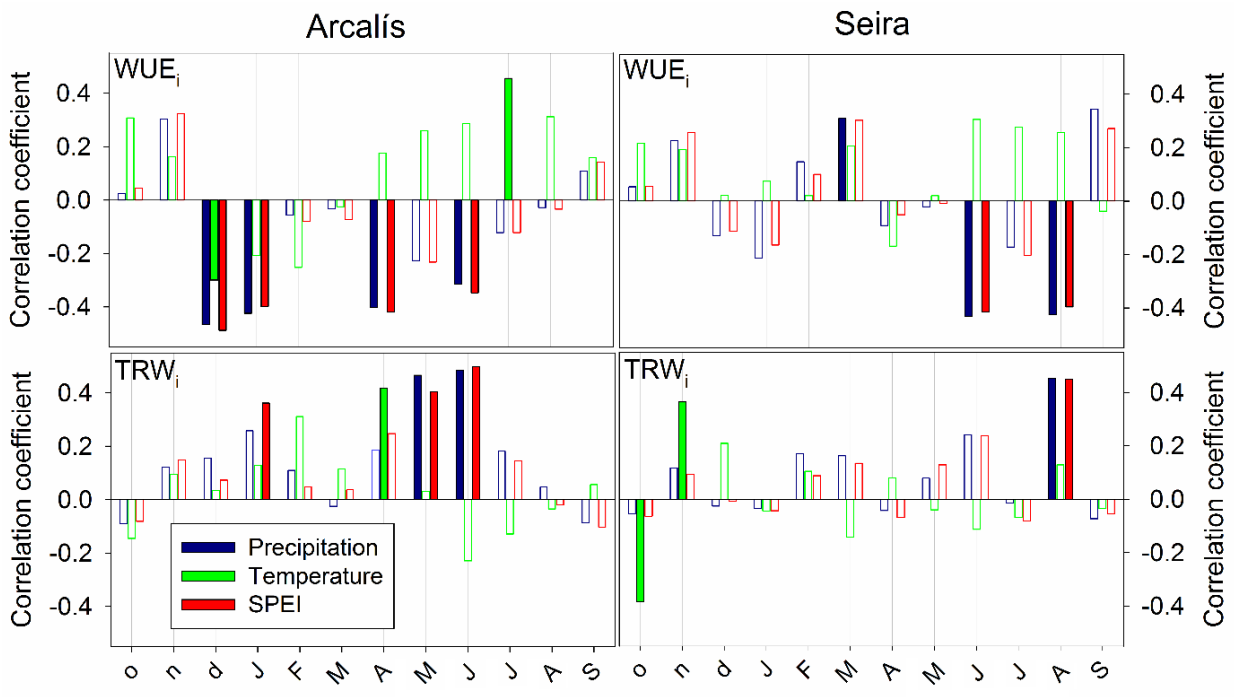

Figure 4. Bootstrapped correlations between intrinsic water-use efficiency (WUE_i, top panels) or indexed tree-ring width (TRW_i, bottom panels) and precipitation, temperature and SPEI drought index in Arcalís (1975-2008 period) and Seira (1980-2009 period). Correlations were calculated on a monthly basis from October of the previous year to September of the current year. Filled bars represent significant correlations

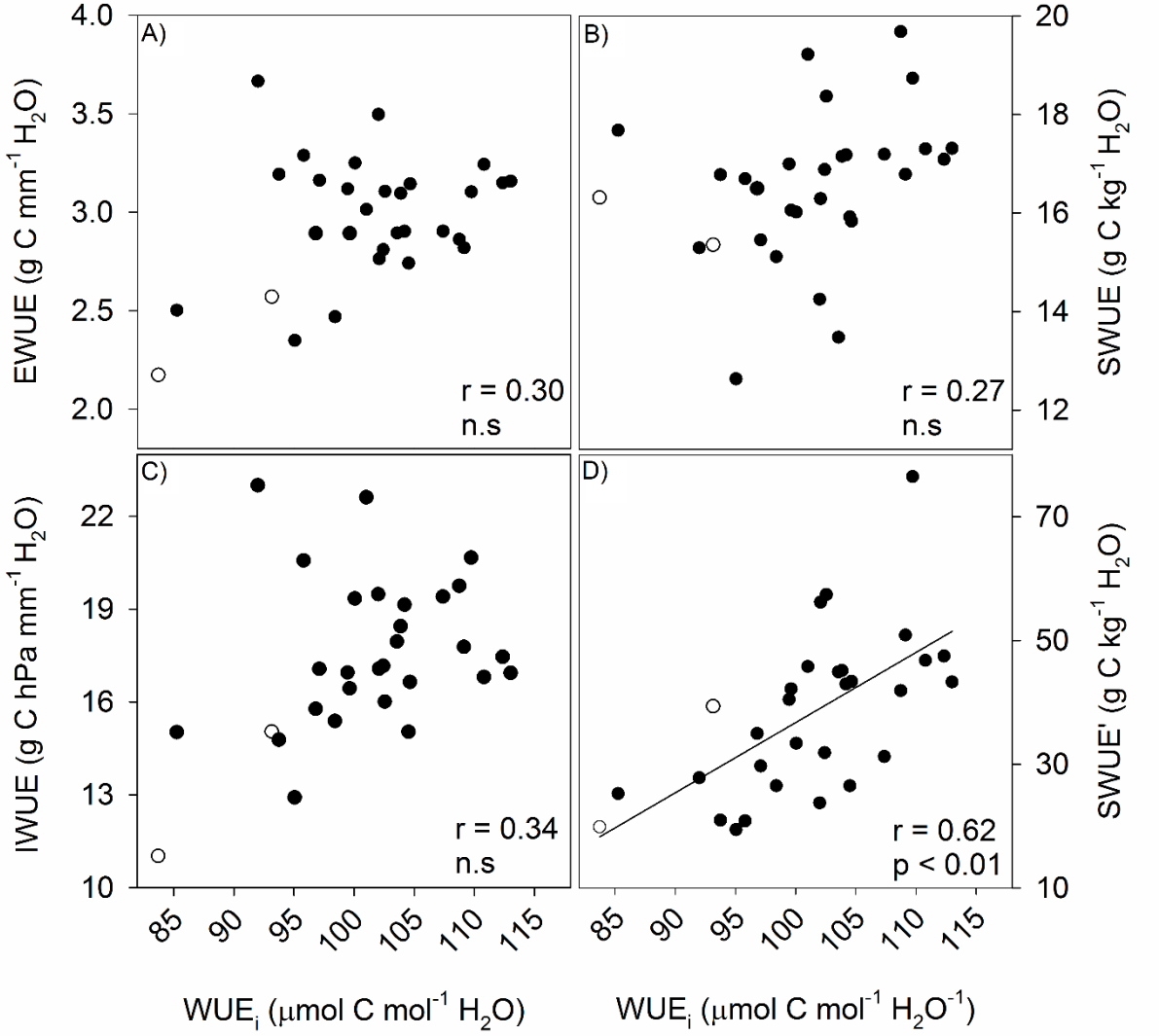

Figure 5. Relationships between WUE_i and A) ecosystem water-use efficiency (EWUE), B) soil water-use efficiency (SWUE), C) inherent water-use efficiency (IWUE) and D) soil water-use efficiency corrected for soil depth (SWUE') in the 30 natural stands composing the study area. Each dot indicates one particular stand. Open dots indicate the two sites where temporal chronologies were available

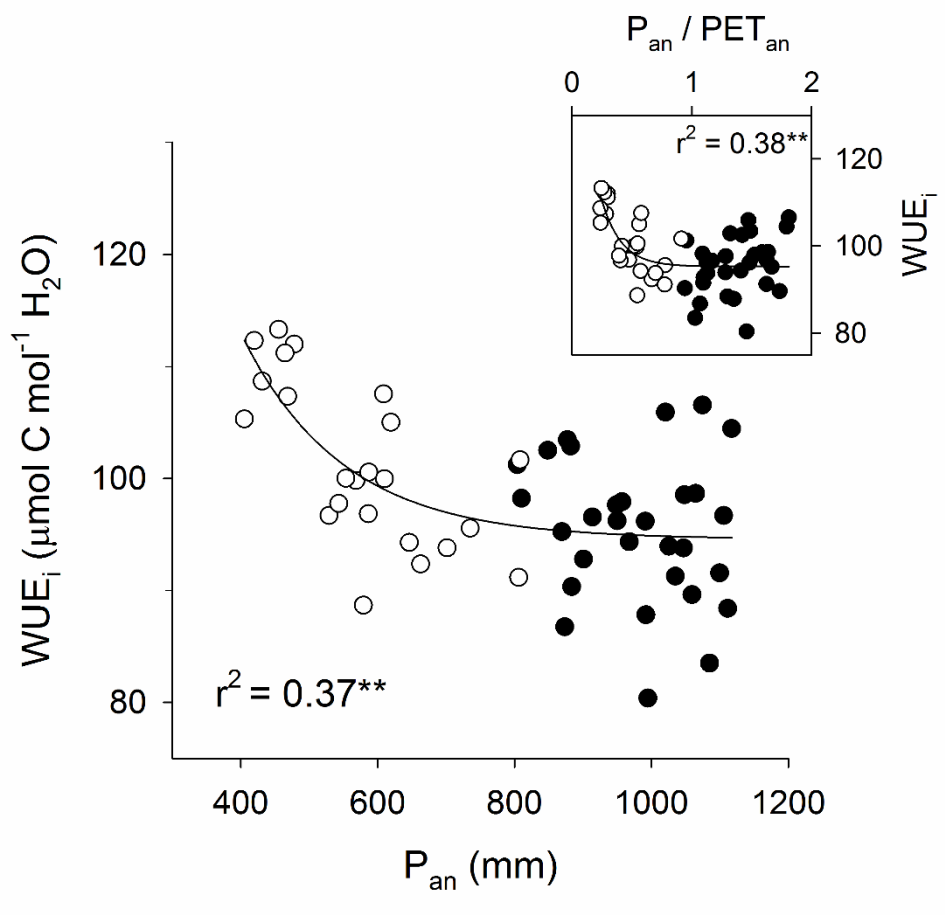

Figure 6. Regression plot (negative exponential function) of WUE_i on mean annual precipitation combining records of *Pinus sylvestris* (present study; closed circles) and *Pinus halepensis* stands (original data published in Ferrio and Voltas (2005); open circles) sampled across north-eastern Iberian Peninsula. WUE_i was estimated from carbon isotope discrimination ($\Delta^{13}C$) of tree rings corresponding to different time periods (2000-2007 for *P. sylvestris*; 1975-1999 for *P. halepensis*). WUE_i values were estimated using the mean atmospheric CO_2 concentration (C_a) for the period of 1975-2007 in order to allow a direct comparison of both datasets. We assumed constant $\Delta^{13}C$ values over time (i.e. C_i/C_a is maintained constant), as previously observed in the Iberian Peninsula for Scots pine (Voltas *et al.*, 2013; Hereş *et al.*, 2014). The insert shows the regression plot of WUE_i on the ratio of annual precipitation to annual potential evapotranspiration. Both regressions are significant at $p < 0.01$ (**).

Chapter V – Appendix

Table S1. Main characteristics of the 22 populations of Pinus sylvestris evaluated in the provenance trial of Aragüés del Puerto (Spanish Pyrenees). Data refer to the site of origin of each population.

Country	Provenance	Latitude	Longitude	Elevation (m a.s.l.)	T_{an} (°C)	P_{an} (mm)	P_s (mm)	PET_{an} (mm)
Germany	Gartow	53° 02' 03" N	11° 25' 03" E	50	8.7	582	186	698
Germany	Laufen	47° 57' 08" N	12° 54' 00" E	430	8.7	1113	423	839
Germany	Otterberg	49° 30' 03" N	07° 45' 02" E	300	8.5	681	205	764
Germany	Selb	50° 12' 03" N	12° 10' 03" E	570	6.5	702	235	683
Germany	Wiesentheid	49° 48' 03" N	10° 21' 03" E	220	8.8	611	203	793
Germany	Wolfgang	50° 09' 03" N	09° 03' 02" E	177	9.5	662	204	795
Spain	Baza	37° 22' 31" N	02° 51' 34" W	2050	8.1	783	96	1000
Spain	Borau	42° 41' 56" N	00° 34' 44" W	1550	5.9	1093	238	737
Spain	Campisábalos	41° 14' 54" N	03° 05' 34" W	1400	8.5	591	113	930
Spain	Castell de Cabres	40° 38' 57" N	00° 03' 19" E	1150	10.4	649	132	876
Spain	Covaleda	41° 56' 41" N	02° 48' 40" W	1550	7.6	748	147	889
Spain	Galve de Sorbe	41° 13' 14" N	03° 10' 45" W	1400	8.9	592	105	938
Spain	Gúdar	40° 24' 41" N	00° 41' 04" W	1700	7.3	710	163	815
Spain	La Sènia	40° 44' 50" N	00° 11' 29" E	1100	9.9	638	142	858
Spain	Morrano	42° 12' 42" N	00° 05' 54" W	700	8.9	593	178	851
Spain	Navafría	41° 00' 20" N	03° 47' 56" W	1600	10.6	679	78	976
Spain	Navarredonda	40° 21' 18" N	05° 06' 50" W	1550	8.6	603	84	950
Spain	Orihuela	40° 30' 47" N	01° 37' 46" W	1750	6.9	691	150	874
Spain	Pobla de Lillet	42° 13' 46" N	01° 57' 30" E	1100	9.7	895	245	788
Spain	Puebla de Lillo	43° 03' 35" N	05° 15' 12" W	1550	8	1005	161	850
Spain	San Zadornil	42° 51' 11" N	03° 11' 43" W	1000	9.8	935	162	837
Spain	Valsaín	40° 48' 43" N	04° 00' 33" W	1550	8.3	589	100	911

T_{an} (mean annual temperature); P_{an} (total annual precipitation); P_s (June to August precipitation); PET_{an} (annual potential evapotranspiration)

Table S2. Main characteristics of the 30 *Pinus sylvestris* natural stands composing the study area (central/eastern Pyrenees, NE Spain)

Site	Latitude	Longitude	Elevation (m a.s.l.)	T_{an} (°C)	P_{an} (mm)	P_s (mm)	PET_{an} (mm)	Basal area (m^2 ha^{-1})	Density (tree ha^{-1})	Crown cover (%)	Height (m)	DBH (cm)	Age (year)	Rocky outcrops (%)	Rock fragments in soil (%)
Alàs i Cercs (I)	42° 19' 26" N	01° 30' 32" E	1130	9.2	914	256	804	46.2	2500	75	12.5	15.3	50	0	15
Alàs i Cercs (II)	42° 18' 54" N	01° 31' 55" E	1391	7.6	1021	270	741	56.4	1850	80	11.8	19.7	58	0	20
Alp (I)	42° 22' 08" N	01° 53' 24" E	1356	8.9	949	256	773	42.7	1500	80	15.2	19	48	0	40
Alp (II)	42° 21' 25" N	01° 57' 32" E	1468	7	1065	267	705	29.7	725	72	16.6	22.8	64	30	20
Arcalís	42° 22' 24" N	01° 11' 00" E	1150	7.1	1058	276	810	10	1070	50	10.9	26.5	80	20	20
Castellar de n'Hug	42° 16' 01" N	02° 02' 06" E	1314	8.7	968	252	755	37.5	1100	70	12.3	20.8	76	0	5
Codó	42° 08' 17" N	01° 32' 56" E	1300	7.9	991	258	747	44.2	1760	80	20.2	37.5	62	0	35
Espot	42° 34' 05" N	01° 06' 36" E	1324	7.6	1059	282	764	51.7	1219	75	17.7	23.4	54	5	20
Estamariu (I)	42° 24' 18" N	01° 30' 43" E	1609	6.3	1106	283	697	45.7	950	32	15.6	24.7	96	0	60
Estamariu (II)	42° 23' 53" N	01° 30' 36" E	1558	6.8	1075	279	716	46.8	2100	80	12.1	16.8	51	0	50
Fontanals (I)	42° 21' 43" N	01° 56' 42" E	1702	6.2	1117	274	678	43.1	950	65	14.7	24	56	10	20
Fontanals (II)	42° 22' 12" N	01° 57' 43" E	1265	6.3	1111	272	681	43.1	650	70	17.7	29.1	56	5	40
Gisclareny (I)	42° 15' 40" N	01° 46' 19" E	1405	8.7	950	256	767	50.3	1500	80	15.8	20.7	50	5	30
Gisclareny (II)	42° 15' 36" N	01° 49' 16" E	1082	9.8	882	247	803	36.3	1600	70	14	17	67	0	40
Gombreny	42° 15' 47" N	02° 02' 53" E	1242	8.9	957	250	761	41.2	1250	80	15.5	20.5	48	0	20
Guils	42° 21' 32" N	01° 17' 28" E	1463	7.2	1048	276	740	58	1050	70	18.7	26.5	76	5	65
Guixers (I)	42° 09' 36" N	01° 42' 11" E	1523	7.1	1047	264	712	22.8	550	70	16	23	67	0	50
Guixers (II)	42° 08' 42" N	01° 41' 17" E	1112	9.6	884	244	801	45	1100	75	16.6	22.8	70	0	5
Pobla de Lillet (I)	42° 14' 24" N	01° 55' 44" E	818	11.2	804	235	843	33.6	800	65	19.8	23.1	84	5	10
Pobla de Lillet (II)	42° 14' 13" N	01° 55' 55" E	803	11.1	810	236	840	52.1	750	65	24.4	29.7	74	5	35
Queralbs	42° 14' 20" N	02° 98' 53" E	1552	10.6	869	240	810	70.4	1550	75	15.2	24.1	51	5	35
Rialb	42° 26' 49" N	01° 11' 17" E	1671	6.5	1100	285	717	51.9	1750	80	12.7	19.4	58	15	15
Sant Llorenç	42° 07' 48" N	01° 34' 12" E	1075	9.7	873	242	810	25.2	700	75	15.2	21.4	69	35	35
Seira	42° 31' 24" N	0° 23' 01" N	1538	6.1	1085	267	810	76.2	1025	75	17.7	37.38	66	20	10
Soriguera	42° 21' 00" N	01° 05' 20" E	954	9.7	901	252	854	35.8	750	70	15.1	24.7	61	0	40
St Joan Abadesses (I)	42° 12' 58" N	02° 14' 24" E	921	11.4	849	235	830	30.3	500	70	17.7	27.8	94	20	0
St Joan Abadesses (II)	42° 14' 10" N	02° 14' 20" E	999	10.8	877	239	813	22.7	1162	65	10.3	15.9	72	0	10
Vallfogona	42° 19' 37" N	02° 17' 46" E	1407	8.6	995	247	744	35.5	700	75	18.2	25.4	49	0	0
Valls de Valira (I)	42° 24' 50" N	01° 25' 34" E	1357	7.5	1035	275	744	33.5	700	70	15	24.7	101	0	35
Valls de Valira (II)	42° 24' 58" N	01° 25' 34" E	1451	7.6	1026	274	751	36	2500	70	14.3	13.5	125	0	45

T_{an} (mean annual temperature); P_{an} (total annual precipitation); P_s (June to August precipitation); PET_{an} (annual potential evapotranspiration)

Table S3. Pearson correlations between either intrinsic water-use efficiency (WUE_i) or tree-ring width (TRW) and climatic, edaphic and physiographic site characteristics for 30 natural stands of *P. sylvestris*. Significant correlations ($p < 0.05$) are highlighted in bold.

Variable	***r* (WUE_i)**	***p*-value**	***r* (TRW)**	***p*-value**
Elevation	-0.08	0.66	-0.29	0.12
T_{an}	0.22	0.23	0.19	0.33
T_{max}	0.19	0.31	0.21	0.26
T_{min}	0.25	0.18	0.16	0.41
P_{an}	-0.19	0.3	-0.25	0.18
P_s	-0.1	0.61	-0.05	0.79
P_s/P_{an}	0.28	0.13	**-0.55**	**<0.01**
PET_{an}	0.06	0.77	**-0.4**	**0.03**
Soil depth	**-0.66**	**<0.01**	0.05	0.79
Basal area	0.2	0.31	-0.02	0.93
Density	0.28	0.15	**-0.43**	**0.02**
Slope	-0.09	0.64	-0.23	0.24
Position	-0.03	0.87	-0.13	0.51
Aspect	-0.1	0.61	-0.09	0.67
Soil carbonates	0.22	0.27	-0.1	0.62
Height	-0.18	0.33	0.15	0.42
Age	-0.15	0.12	**-0.39**	**< 0.01**
TRW	-0.04	0.66		

T_{an} (mean annual temperature); T_{max} (average maximum annual temperature); T_{min} (average minimum annual temperature); P_{an} (total annual precipitation); P_s (June to August precipitation); PET_{an} (annual potential evapotranspiration)

Table S4. Linear mixed-effects models for intrinsic water-use efficiency (WUEi) and tree-ring width (TRW) for the provenance trial of Aragüés del Puerto, a set of 30 natural stands located in the central and eastern Pyrenees mountains and two temporal chronologies from the same area. For chronologies, variance components were estimated based on annually-resolved Ca WUEi values or absolute TRW records (not high-pass filtered) Only the random effects of the models are shown.

	Source of variation	Variance component	% of total variance	Chi-Square value[a]	Likelihood ratio test (*p*-value)[a]
WUE_i					
Provenance trial					
	Population	3.38±3.73[b]	11.2	0.87	p=0.35
	Population×Block	4.14±4.50	13.73	1.14	p=0.28
	Residual	22.68±3.87	75.07		
Natural stands					
	Site	34.47±12.37[c]	50.77	38.63	p<0.01
	Residual	33.42±5.41	49.23		
Chronologies					
	Tree [Site]	20.89±8.58d	25.56	102.56	p<0.01
	Year	40.77±12.57e	49.88	19.96	p<0.01
	Year×Site	3.00±2.47	3.67	3.25	p=0.07
	Residual	17.07±2.51	20.89		
TRW					
Provenance trial					
	Population	0.03±0.02[b]	3.97	3.7	p=0.05
	Population×Block	0.07±0.02	10.31	32.81	p<0.01
	Residual	0.58±0.03	85.72		
Natural stands					
	Site	0.15±0.05[c]	54.27	31.67	p<0.01
	Residual	0.13±0.02	45.73		
Chronologies					
	Tree [Site]	0.55±0.10[d]	40.64	1128.67	p<0.01
	Year	0.00±0.00[e]	0	0	p=1.00
	Year×Site	0.25±0.05	18.45	346.96	p<0.01
	Residual	0.55±0.02	40.91		

[a]Test for the null hypothesis of variance component being equal to 0; [b]estimate of inter-population genetic variation; [c]estimate of spatial phenotypic variation; [d] stimate of temporal phenotypic variation; e estimate of spatiotemporal phenotypic variation

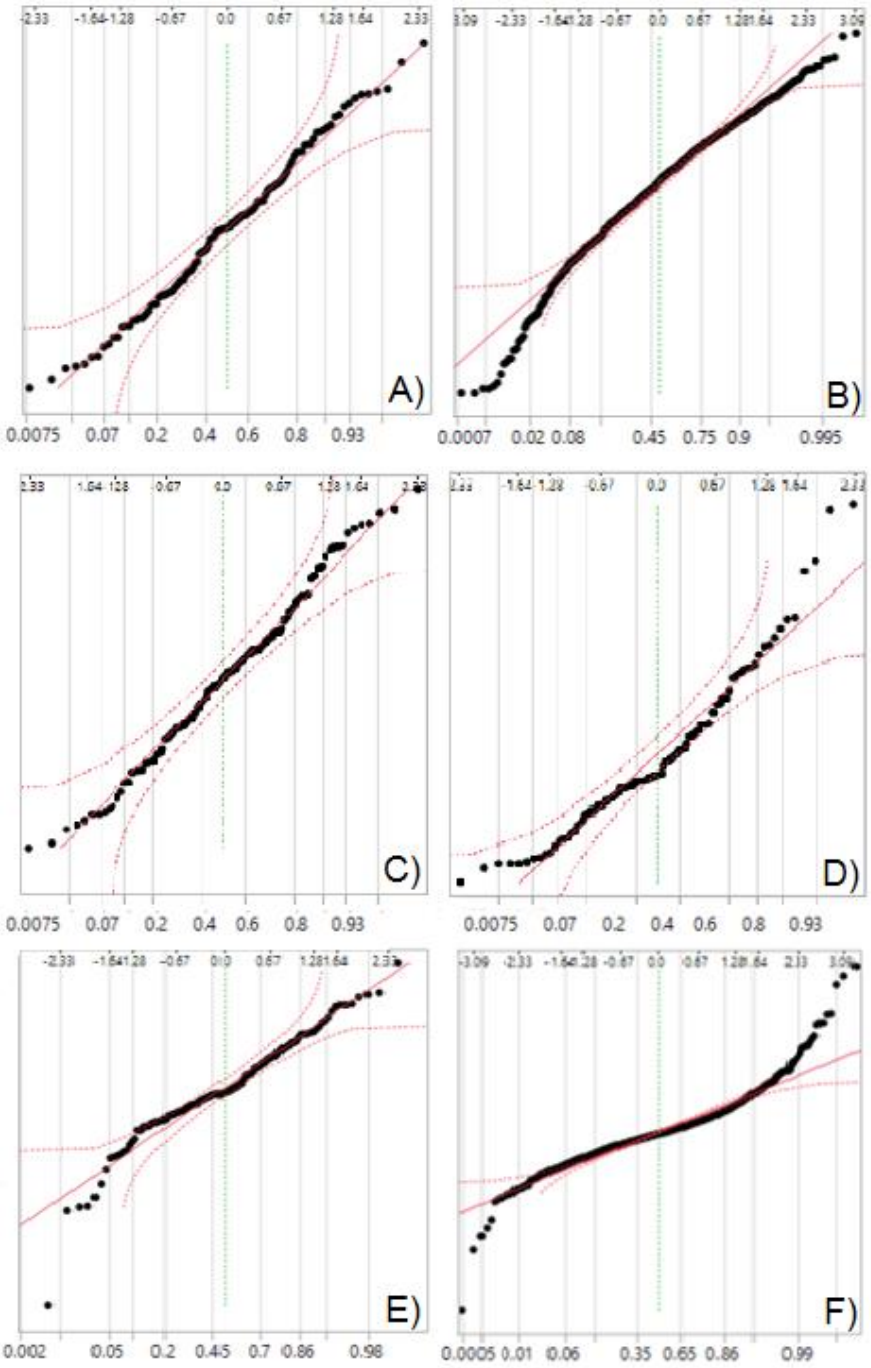

Figure S1. Normal quantile plots of the residuals of the ANOVAs fitted on A) WUE_i and B) TRW in the provenance trial, C) WUE_i and D) TRW in the natural sampled sites and E) WUE_i and F) TRW in the temporal chronologies

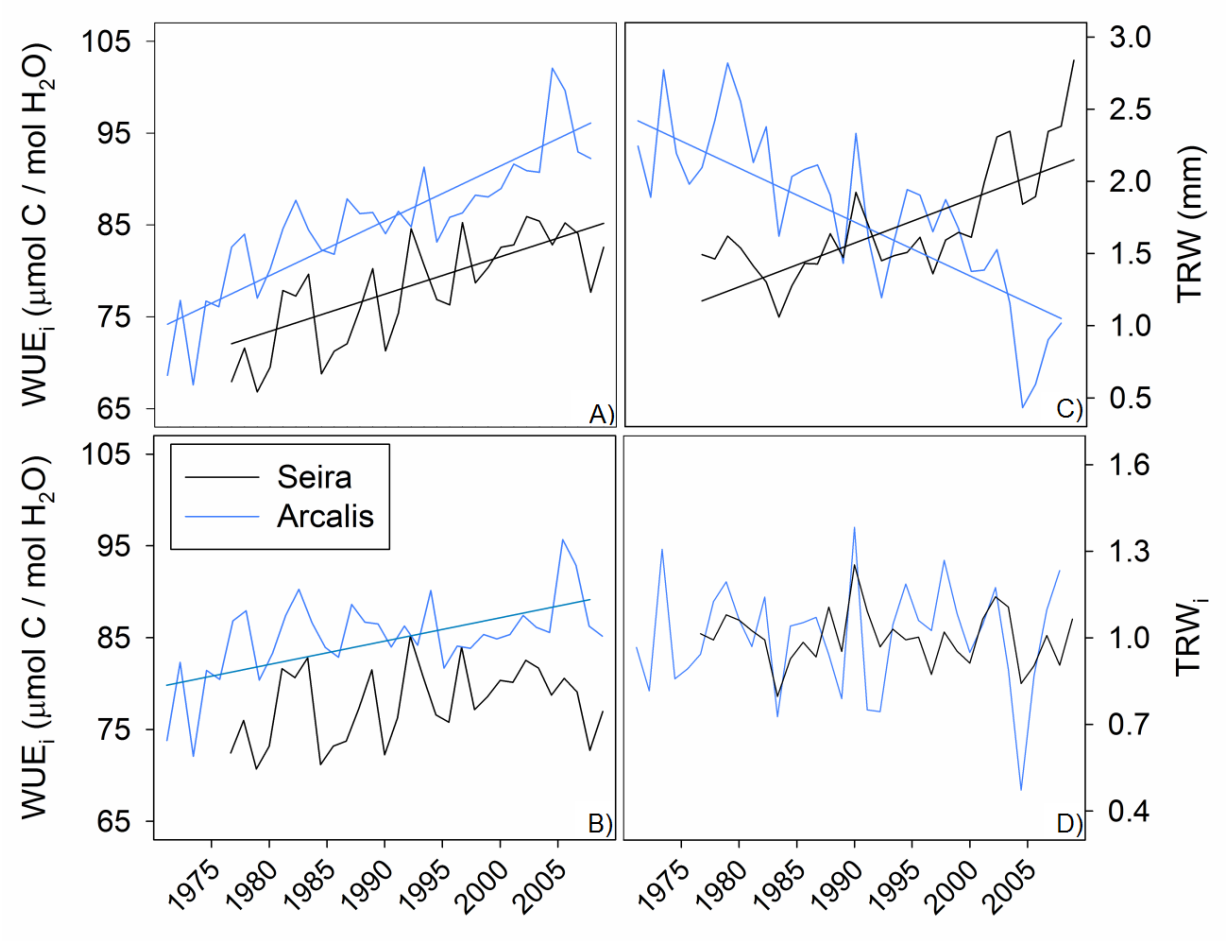

Figure S2. Intrinsic water-use efficiency (WUE_i) and tree-ring width (TRW) chronologies in Seira and Arcalís. Left panels show WUE_i time series estimated using either annually-resolved C_a values (A) or the average C_a over the study period (B). Right panels show absolute TRW records (i.e. not high-pass filtered) (C) and TRW indices (TRW_i) after high-pass filtering (D). Significant linear trends are depicted with lines ($p < 0.05$).

GENERAL DISCUSSION

ADAPTIVE GENETIC VARIATION IN MEDITERRANEAN PINES

Intra-specific differentiation is a fundamental process influencing species capacity to cope with environmental changes (Bussotti *et al.*, 2015). However, it is rarely taken into account when modelling the future performances of forest species in the context of climate change, partially because key information about the extent and distribution of intra-specific variation in functional traits is still lacking even for well-studied trees. In this regard, my thesis provided a deep insight into the intra-specific patterns of variation of three ecologically and socio-economically important Mediterranean pines. These conifers are characterised by contrasting ecological niches and experience different constrains related to the divergent enviroments that they occupy across their Mediterranean distribution (Barbéro *et al.*, 1998). However, common limitations that affect all these species, although with different extent, are water deficit in summer and, at the same time, chilling winter temperatures typical of temperate climates (Flexas *et al.*, 2014). The different impact of these climatic factors largely depends on the altitudinal distribution of the species, with pines of low altitudes more subjected to drought stress and mountain species experiencing harsher winter conditions. The extent of these constrains influences their role as drivers of intra-specific variation, and are reflected in the presence or absence of genetic differentiation in traits among species (Table 1).

Table 1. Presence or absence of inter-population genetic differentiation identified in this thesis in the three trials. The symbol x indicated that the trait was not analysed.

	Species		
Trait	***P. halepensis***	***P. nigra***	***P. sylvestris***
DBH	yes	yes	no
Height	yes	yes	yes
Reserve accumulation	yes	yes	x
WUE_i	yes[1]	no	no
Rooting depth	yes[2]	no	x
Total transpiration (summer)	yes	x	x
Stem water potential	x	no	x
Leaf area	yes	yes	x
Photosynthetic pigments (summer)	no	yes	x

[1]the trait was analysed in the same common garden of this thesis by Voltas *et al.* (2008)
[2]the trait was analysed in the same common garden of this thesis by Voltas *et al.* (2015)

In a low-altitude species such as *P. halepensis*, water limitation turned to be, together with fire occurrence, a key factor driving genetic differentiation across the species range. Indeed, the results of this thesis confirmed the well-known drought-driven differentiation in Aleppo pine (Fady *et al.*, 2003; Tognetti *et al.*, 1997; Voltas *et al.*, 2008, 2015). The populations of *P. halepensis* considered in the thesis originated from regions that greatly differ in terms of annual and summer water availability (Figure 1A), and these factors were the main drivers of genetic differentiation in leaf area and transpiration among populations (Chapters 1 and 2). Indeed, this work revealed that populations thriving in the most arid conditions of the species range have developed a multi-trait adaptive syndrome consisting of reduced transpiration, a deep rooting system and a slow grow rate (Chapter 2). These are strong evidences indicating the presence of slow-growth and drought-adapted populations in contrast with fast-growing but less drought resistant ones across the range of Aleppo pine (Chapters 1 and 2). Combining phenotype data with high-throughput genotyping I also provided an insight into the molecular mechanisms of such phenotypic variation (Chapter 3).

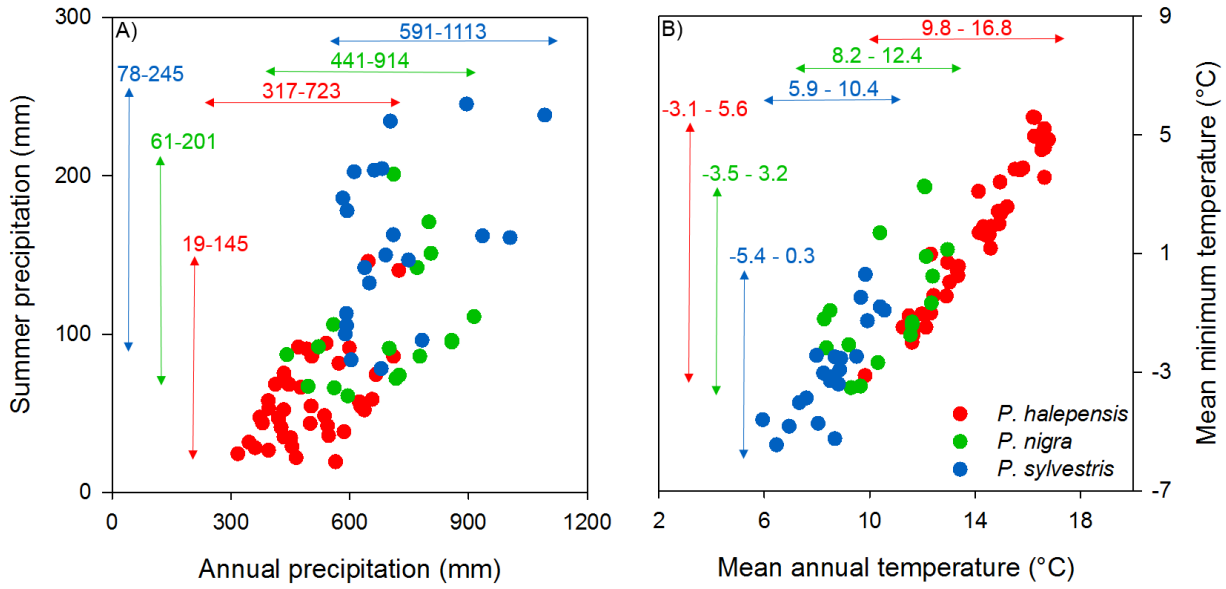

Figure 1 Plots showing the climatic conditions at origin for the populations tested in this thesis, in terms of annual and summer precipitation (A) and annual temperature and winter minimum temperature (B). Populations belonging to the three species are plotted together, to show the different extent of environmental constrains at which each species is subjected. Horizontal arrows indicate the range of annual precipitation and annual temperature among populations of each species. Vertical arrows indicate the range of summer precipitation and mean minimum temperature of the coldest month.

On the other hand, results of this thesis indicated a weak differentiation in traits related to water-use in the medium and high mountain species *P. nigra* and *P. sylvestris* (Table 1). Populations of these species are also subjected to water deficit in summer (Durrant *et al.,* 2016; Enescu *et al.,* 2016), and water availability greatly varies across the distribution range (Figure 1A). However, the wide-range populations tested in this thesis did not show any sign of variation in functional traits related to the tree water economy, such as water use efficiency and, in the case of *P. nigra*, rooting depth and stem water potential (Chapters 4 and 5). Moreover, intra-specific differentiation in growth patterns and reserve accumulation was not related to variation in water availability in *P. nigra* (Chapter 4). Altogether, the evidence emerging from this work indicated that water deficit did not represent a strong selective pressure during the process of population differentiation in *P. nigra* and *P. sylvestris*. Although many populations experienced summer water deficit at their geographical origins, the extent of drought stress was indeed much less important than in the case of *P. halepensis*, indicating that other environmental constraints could act as main drivers of intra-specific differentiation (Figure 1A).

In fact, *P. nigra* and *P. sylvestris* were subjected to lower annual and winter temperature than *P. halepensis* (Figure 1B). In this regard, the results obtained in the common garden of *P. nigra* indicated cold winter conditions and high intra-annual temperature fluctuations as fundamental drivers of intra-specific differentiation in crucial traits such as leaf chlorophyll concentration, growth and reserve accumulation (Chapter 4). European black pine populations differed in their life-history strategies, with individuals originating from areas subject to colder winter conditions experiencing a slower growth and a higher accumulation of carbon reserves. This is in agreement with previous evidence indicating variation in cold resistance among populations of *P. nigra* (Kreyling *et al.,* 2012). On the other hand, winter temperatures and continentality did not influence the variation in functional traits among populations of *P. halepensis*, with the exception of carbon reserves (Chapter 2). Moreover, populations of *P. halepensis* did not show variation in summer photosynthetic capacity, a trait that was found to vary in *P. nigra* and that is typically associated with temperature-limited environments (Oleksyn *et al.,* 1998; Chapters 1 and 4). In the case of *P. sylvestris*, data from this thesis did not allow to speculate on the role of winter temperatures as driver of differentiation. However, this species is subject to harsher winter conditions, in terms of snow precipitation and extended winter frosts, than *P. nigra*, being low winter temperatures known to limit the performance of Scots pine populations in the Iberian Peninsula (Sánchez-Salguero *et al.,* 2015).

In summary, the findings of this thesis suggest that intra-specific genetic variation in the studied pine species is largely related to the ecological niches that they occupy, which correspond

to different environmental constraints. Water availability is a strong limiting factor driving genetic adaptation in the drought-adapted species *P. halepensis*, while *P. nigr*a and *P. sylvestris* thrive under less water-limiting conditions, whose variability among population is a less important determinant of phenotypic variation. On the other hand, populations of black pine exhibit specific strategies to cope with variable level of winter harshness, a differentiation that did not emerged in *P. halepensis*.

PLASTICITY IS A FUNDAMENTAL COMPONENT OF PHENOTYPIC VARIATION

Although the main focus of the thesis was to disentangle patterns of intra-specific genetic differentiation in Mediterranean pines, in Chapter 5 I also provided an insight into phenotypic variation related to plastic adjustments in *P. sylvestris*. As already stressed, plasticity is one of the mechanisms for tree populations to respond *in-situ* to enviromental change (Benito Garzón *et al.,* 2019). Pines are known to be extremely plastic organisms (Tapias *et al.,* 2004; Vizcaíno-Palomar *et al.,* 2016), and the outcome of this thesis indicated that the extent of phenotypic differentiation resulting from phenotypic plasticity may exceed by far the effects of genetic differentiation (Chapter 5). These findings, coupled with already reported evidence of plastic responses in pines (e.g. Mutke *et al.*, 2010; de Luis *et al.*, 2013), suggest that population performances may be largely modulated by phenotypic plasticity of functional characteristics (Feichtinger *et al.,* 2017). This point is particularly important due to the fact that, as showed by the relation between tree-level WUE and ecosystem-level WUE derived by satellite data, plastic variation among populations can have important impacts on ecosystem functioning (Chapter 5).

Although the thesis explored the extent of phenotypic plasticity only in growth and WUE in *P. sylvestris*, it emphasises the necessity of considering plasticity when studying phenotypic variation related to population responses to environmental changes (Valladares *et al.*, 2014). In this regard, data showing appreciable genetic variation in *P. halepensis* and *P. nigra* should be complemented with a characterisation of phenotypic plasticity in meaningful traits in the same species. For this purpose, the UAV-based phenotyping approach could be implemented in multi-environmental trials allowing to study, in parallel with genetic differentiation, the adaptive role of phenotypic plasticity. This extended application of the methodology used in this thesis would be of easy implementation, requiring multiple flights in different trials. As long as flying conditions (i.e. flying date and time, and absence of cloud cover) are consistent across flights in different common gardens, the information that can be collected could provide valuable insights into phenotypic plasticity of functional traits (Bradshaw, 2006). This approach would also allow

exploring the extent of genetic variation in phenotypic plasticity, a third component influencing intra-specific variation (Kusmec *et al.*, 2018).

IMPLICATIONS IN THE CONTEXT OF CLIMATE CHANGE

Forests' response to environmental changes involves several interacting processes including genetic adaptation, migration and phenotypic plasticity (Lindner *et al.*, 2010). Although the objective of this thesis was not to model the future persistence of pine species under the current scenarios of climate change, the evidences emerged from this work could help understanding the vulnerability of populations of Mediterranean pines. In fact, in the actual context of global warming Mediterranean ecosystems will face a double change in environmental constraints. On one side, an increase in intensity and duration of summer drought spells will exacerbate water availability as a limiting factor for forest species (Resco de Dios *et al.*, 2006). On the other hand, milder winters with reduced snow precipitation and frost occurrence will likely be reflected in longer vegetative seasons and in a general reduction of cold limitation for tree performance (Sánchez-Salguero *et al.*, 2015). However, it must be taken into account that the impact of global warming on ecological processes linked to winter conditions could be complex and largely unpredictable, and has received little attention so far (Kreyling, 2010).

Broadly speaking, the result of climate change is likely a rarefaction of the species at their lower altitudinal limit and a simultaneously shift in species distribution towards higher altitudes and/or more humid areas (Benito Garzón *et al.*, 2008). This is particularly true in the case of high mountain species, which will be probably forced to higher altitudes by reduced water availability in summer. However, these processes are strictly related to migration speed which, in the case of forest species, have been demonstrated to be far slower than the speed at which environmental changes are occurring (Pearson, 2006). Therefore, the ability of species to adapt *in-situ* through plastic responses and genetic adaptation will largely determine the fate of forest ecosystems across the Mediterranean.

In the case of *P. halepensis*, the on- going changes will likely favour genotypes which are better adapted to drought conditions. In this regard, the results of this thesis indicated the presence of specific populations which could retain the adaptive potential to future conditions of reduced water availability. These drought-adapted populations are nowadays thriving with the driest conditions of the species range, colonizing areas that, in the future, could experience levels of water deficit too extreme to sustain populations of this conifer (Choury *et al.*, 2017). However, genetic variants that show the highest drought tolerance could represent the basis for species subsistence in the context of climate change. Indeed, *in-situ* selection of drought-adapted

individuals (i.e. within-population genetic variation) could boost local evolution in areas that will experience more arid conditions in the future (Bussotti *et al.,* 2015). In addition, the migration of drought-adapted genotypes through natural or human-assisted gene flow could ensure the survival of less drought-adapted populations that nowadays colonize the most humid part of the species range (Kremer *et al.,* 2012; Aitken and Whitlock, 2013).

Remarkably, similar conclusions cannot be drawn in the case of *P. nigra* and *P. sylvestris*. As already stressed, the results of this thesis confirm previous evidences indicating a weak differentiation in traits that are typically involved in drought resistance (Chapters 4 and 5). In this sense, Mediterranean populations of these species might lack the adaptive potential necessary to cope with future reduction in water availability. Episodes of forests dieback related to water deficit have already been reported for both *P. nigra* and *P. sylvestris* (Voltas *et al.,* 2013; Camarero *et al.,* 2015, Petrucco *et al.,* 2017) and a contraction in the distribution of these species has been modelled for the Iberian Peninsula under current warming trends (Benito Garzón *et al.,* 2008). Previous evidences coupled with the results of this thesis highlight the vulnerability of Mediterranean populations of black and Scots pine in the context of climate change. On the other hand, plastic responses could partially mitigate the effects of global warming on these pines, thus allowing the persistence of mountain species even under reduced water availability (Chapter 5). Altogether, due to the absence of evidence of a potential genetic adaptation of mountain pine species to conditions of water deficit, the persistence and future distribution of *P. nigra* and *P. sylvestris* around the Mediterranean basin will likely rely on the extent of phenotypic plasticity and on the colonization of higher altitude areas, where available (Sánchez-Salguero *et al.,* 2015).

UAV IMAGERY AS PHENOTYPING TOOL OF FOREST GENETIC TRIALS

A fundamental part of the thesis was to test the suitability of remote sensing data derived with UAVs as a phenotyping tool of forest genetic trials. In fact, UAV imagery has become a common approach in evaluating varieties in trials of economically important crop species (Sankaran *et al.,* 2015; Lobos *et al.,* 2017) and several examples of UAV applications in tree phenotyping are also available for fruit orchards. Here, I showed the potential to apply UAV-derived remote sensing data to phenotype forest trees in common gardens. Indeed, UAV imagery used to derive well-established vegetation indices revealed as valid high-throughput phenotypic tool to characterise variation in pine species (Ludovisi *et al.,* 2017; Chapters 1, 3 and 4).

Different approaches involving varying computational efforts were used in this work. Information can be derived at plot level, not requiring individual tree identification and thus resulting in low necessity of computational power. Despite its simplicity, this approach provided

valuable data to characterise the adaptive variation of *P. halepensis* (Chapter 1). In this regard, the results from Chapter 1 also indicated that RGB-derived indices, which require costumer-level cameras to be calculated, can be used as valuable alternative to well-established, but less cost-effective, multispectral indices (Casadesús and Villegas, 2014; Kefauver *et al.*, 2015). Altogether, these results suggest that simple approaches involving semi-professional UAVs equipped with cheap sensors can be effectively used to retrieve valuable information in forest genetic trials (Chapter 1).

However, data retrieving on an individual base provide a higher accuracy in the analysis of phenotypic differentiation. For this purpose, individual tree records can be obtained by implementing a more complex approach which allows the straightforward (automatic) phenotyping of hundreds or thousands of individuals. In this regard, canopy segmentation based on structure-from-motion approaches are widely used in forest sciences to identify single trees (Wallace *et al.*, 2016). In Chapter 3, I showed that this approach can be successfully implemented in the case of common gardens of forest trees, requiring low-cost RGB cameras and widely available software. This approach demands a computationally greater effort than a plot-level one, but can automatically provide individual data that are suitable for a wide range of applications. First, these data can provide a better insight into phenotypic differentiation in genetic trials thus enhancing the capacity to study adaptive variation. Second, high-throughput phenotyping tools based on UAV-imagery can be coupled with modern genotyping techniques to investigate the genetic basis of phenotypic variation. In this regard, in Chapter 3 I showed the feasibility of using UAV-derived images to perform genotype-phenotype association studies. The availability of high-throughput phenotyping tools represents a valid support for this research field, with possible applications in tree breeding through genomic selection (Grattapaglia and Resende, 2011; Jaramillo-Correa *et al.*, 2015).

UAV-mounted sensors

Different sensors were used to retrieve information on vegetation characteristics in this thesis. Well-established vegetation indices were derived from multi-spectral cameras (Roberts *et al.*, 2016). These indices have been used for long time to investigate different phenotypic traits in plants (Aparicio *et al.*, 2000). On the other hand, RGB-derived indices were also tested in Chapter 1 and provided information which partially overlapped with that derived from multispectral images. RGB cameras are far cheaper than multispectral ones, and the results of Chapter 1 suggest that this kind of cameras could be successfully employed for tree phenotyping (Gracia-Romero *et al.*, 2017). However, the interpretation of RGB indices is less clear, since

they have only recently been proposed in addition to multispectral-derived indices as surrogates of plant traits (Großkinsky *et al.,* 2015; Kefauver *et al.,* 2015). In this regard, RGB information was not considered in the case of *P. nigra*, due to the difficulties in interpreting the obtained results. Altogether, I suggest that multispectral cameras should be used, if feasible, to calculate well-established vegetation indices as surrogates of vegetation characteristics, being RGB a suitable alternative if low-cost options should be considered. On the other hand, RGB images can be also used for 3D reconstruction of trees, providing a parallel source of information on tree morphological parameters and being suitable for automatic crown segmentation (Mathews and Jensen, 2013; Díaz-Varela *et al.*, 2015).

Finally, thermal images were used only in the case of *P. halepensis*, due to technical problems in images alignment in the case of *P. nigra* (see below). Thermal images provided fundamental information on variation in water status, which had a considerable influence on tree performance (Chapters 1 and 2). These results indicate the high potential of thermal cameras in evaluating traits related to tree water use (Gonzalez-Dugo *et al.,* 2013). Records of canopy temperature are, therefore, particularly relevant in the case of species in which water-related functional traits play a fundamental role in determining individual performance.

Methodological problems and technical limitations of UAV-based phenotyping

Despite the encouraging results of this thesis, the approach used requires a careful consideration of the issues that could prevent a wide application of UAV-based phenotyping of forest trials. The methodology used in several part of this thesis relies on the possibility of producing high-quality aerial orthomosaics of the common garden tests. This result was achieved in the case of *P. halepensis*, while in the common garden of *P. nigra* an orthomosaic could be produced only for a part of the trial and for multispectral images. The main problem with the trial of *P. nigra* was that the software used for orthorectifying the images were unable to correctly align pictures in the case of the thermal images and part of the multispectral ones. This issue was related to the low altitude (50 m in the case of *P. nigra* vs 100 m in the case of *P. halepensis*) at which the images were collected. The low altitude generated higher resolutions of the pictures and potential higher quality data. However, common gardens of pine species are homogenous areas, and pictures taken too close to the vegetation surface did not contain enough reference points that can be used for images alignment. For this reason, I suggest that, in case of highly dense common gardens with trees reaching altitude of 10 m, images should be taken at different altitudes (50 and 100 meters) during the same flight. Combining pictures obtained at different altitudes can ensure both a high resolution and a correct alignment of the images.

Even in cases in which the orthomosaics can be correctly produced, the recovery of meaningful data requires specific trial conditions. Firstly, a fundamental requirement is the possibility of manual or automatic identification of single individuals or experimental units in aerial images. This is a minor issue in the case of crop trials in which UAV-based phenotyping is widely applied, but growing conditions of common gardens of forests species, coupled with the extreme plasticity in trees' development, often prevent a straightforward identification of the units of interest (Chapter 1). As an example, the non-homogenous growing conditions of the trial of *P. sylvestris* prevented the use of the UAV in that case, due to the impossibility of recognizing experimental units or single trees in aerial images of the trial. A second issue is related to the existence of unwanted shading effects, which may affect vegetation reflectance and impact on the estimation of vegetation indices (Yamazaki *et al.,* 2009). To minimize this problem, flights should be performed at noon and in spring or summer, when the sun elevation over the horizon is at its maximum. Finally, an intrinsic limitation in UAV-based phenotyping is that aerial images retrieve information mainly from the top crown of the tree, not capturing the within-crown differences that may be relevant in forest species (Yamazaki *et al.,* 2009). In this regard, an issue that remained unexplored is the possibility of using RGB data to derive dense point clouds points of the trials, which allows a 3D reconstruction of tree crown. This approach may allow retrieving morphological variation within crowns that cannot be detected from simple orthomosaic images (Díaz-Varela *et al.,* 2015).

REFERENCES

Aitken S.N., Whitlock M.C. (2013) Assisted gene flow to facilitate local adaptation to climate change. *Annual Review of Ecology, Evolution, and Systematics*, 44, 367–388.

Aparicio N., Villegas D., Casadesus J., Araus J.L., Royo C. (2000) Spectral vegetation indices as nondestructive tools for determining durum wheat yield. *Agronomy Journal*, 92, 83.

Barbéro M., Loisel R., Quézel P., Richardson D.M., Romane F. (1998). Pines of the Mediterranean basin. In Richardson D.M. (eds) *Ecology and Biogeography of Pinus*, pp. 153-170..

Benito Garzón M., Sánchez de Dios R., Sainz Ollero H. (2008) Effects of climate change on the distribution of Iberian tree species. *Applied Vegetation Science*, 11, 169–178.

Benito Garzón M., Robson T.M., Hampe A. (2019) ΔTrait SDMs : species distribution models that account for local adaptation and phenotypic plasticity. *New Phytologist*, 222, 1757–1765.

Bradshaw A.D. (2006) Unravelling phenotypic plasticity ? Why should we bother? *New Phytologist*, 170, 644–648.

Bussotti F., Pollastrini M., Holland V., Brüggemann W. (2015) Functional traits and adaptive capacity of European forests to climate change. *Environmental and Experimental Botany*, 111, 91–113.

Camarero J.J., Gazol A., Sangüesa-Barreda G., Oliva J., Vicente-Serrano S.M. (2015) To die or not to die: early warnings of tree dieback in response to a severe drought. *Journal of Ecology*, 103, 44–57.

Casadesús J., Villegas D. (2014) Conventional digital cameras as a tool for assessing leaf area index and biomass for cereal breeding: Conventional digital cameras for cereal breeding. *Journal of Integrative Plant Biology*, 56, 7–14.

Choury Z., Shestakova T.A., Himrane H., Touchan R., Kherchouche D., Camarero J.J., Voltas J. (2017) Quarantining the Sahara desert: growth and water-use efficiency of Aleppo pine in the Algerian Green Barrier. *European Journal of Forest Research*, 136, 139–152.

de Luis M., Čufar K., Di Filippo A., Novak K., Papadopoulos A., Piovesan G., Rathgeber C.B.K., Raventós J., Saz M.A., Smith K.T. (2013) Plasticity in dendroclimatic response across the distribution range of aleppo pine (*Pinus halepensis*). *PLoS ONE*, 8, e83550.

Díaz-Varela R., de la Rosa R., León L., Zarco-Tejada P. (2015) High-resolution airborne UAV imagery to assess olive tree crown parameters using 3D photo reconstruction: application in breeding trials. *Remote Sensing*, 7, 4213–4232.

Durrant T.H., De Rigo D., Caudullo G. (2016) *Pinus sylvestris* in Europe: distribution, habitat, usage and threats. In: San-Miguel-Ayanz J., de Rigo D., Caudullo G., Houston Durrant T., Mauri A. (eds) *European Atlas of Forest Tree Species*, pp. 132-133. Publ Off EU, Luxembourg.

Enescu C.M., de Rigo D., Caudullo G., Mauri A., Houston Durrant T. (2016) *Pinus nigra* in Europe: distribution, habitat, usage and threats. In: San-Miguel-Ayanz J., de Rigo D., Caudullo G., Houston Durrant T., Mauri A. (eds) *European Atlas of Forest Tree Species*, pp. 126–127. Publ Off EU, Luxembourg.

Fady B., Semerci H., Vendramin G.G. (2003) EUFORGEN Technical Guidelines for genetic conservation and use for Aleppo pine (*Pinus halepensis*) and Brutia pine (*Pinus brutia*). International Plant Genetic Resources Institute, Rome, Italy

Feichtinger L.M., Siegwolf R.T.W., Gessler A., Buchmann N., Lévesque M., Rigling A. (2017) Plasticity in gas-exchange physiology of mature Scots pine and European larch drive short- and long-term adjustments to changes in water availability. *Plant, Cell and Environment*, 40, 1972–1983.

Flexas J., Diaz-Espejo A., Gago J., Gallé A., Galmés J., Gulías J., Medrano H. (2014) Photosynthetic limitations in Mediterranean plants: A review. *Environmental and Experimental Botany*, 103, 12–23.

Gonzalez-Dugo V., Zarco-Tejada P., Nicolás E., Nortes P.A., Alarcón J.J., Intrigliolo D.S., Fereres E. (2013) Using high resolution UAV thermal imagery to assess the variability in the water status of five fruit tree species within a commercial orchard. *Precision Agriculture*, 14, 660–678.

Gracia-Romero A., Kefauver S.C., Vergara-Díaz O., Zaman-Allah M.A., Prasanna B.M., Cairns J.E., Araus J.L. (2017) Comparative performance of ground vs. aerially assessed rgb and multispectral indices for early-growth evaluation of maize performance under phosphorus fertilization. *Frontiers in Plant Science*, 8.

Grattapaglia D., Resende M.D.V. (2011) Genomic selection in forest tree breeding. *Tree Genetics and Genomes*, 7, 241–255.

Großkinsky D.K., Svensgaard J., Christensen S., Roitsch T. (2015) Plant phenomics and the need for physiological phenotyping across scales to narrow the genotype-to-phenotype knowledge gap. *Journal of Experimental Botany*, 66, 5429–5440.

Jaramillo-Correa J.P., Prunier J., Vázquez-Lobo A., Keller S.R., Moreno-Letelier A. (2015) Molecular Signatures of adaptation and selection in forest trees. *Advances in Botanical Research*, 74, 265–306.

Kefauver S.C., El-Haddad G., Vergara-Diaz O., Araus J.L. (2015) RGB Picture vegetation indexes for high-throughput phenotyping platforms (HTPPs). In *Remote Sensing for Agriculture, Ecosystems, and Hydrology XVII* (Vol. 9637, p. 96370J). International Society for Optics and Photonics.

Kremer A., Ronce O., Robledo-Arnuncio J.J., *et al*. (2012) Long-distance gene flow and adaptation of forest trees to rapid climate change: Long-distance gene flow and adaptation. *Ecology Letters*, 15, 378–392.

Kreyling J. (2010) Winter climate change: a critical factor for temperate vegetation performance. *Ecology*, 91, 1939–1948.

Kreyling J., Wiesenberg G.L.B., Thiel D., Wohlfart C., Huber G., Walter J., Jentsch A., Konnert M., Beierkuhnlein C. (2012) Cold hardiness of *Pinus nigra* Arnold as influenced by geographic origin, warming, and extreme summer drought. *Environmental and Experimental Botany*, 78, 99–108.

Kusmec A., de Leon N., Schnable P.S. (2018) Harnessing phenotypic plasticity to improve maize yields. *Frontiers in Plant Science*, 9.

Lindner M., Maroschek M., Netherer S., *et al.* (2010) Climate change impacts, adaptive capacity, and vulnerability of European forest ecosystems. *Forest Ecology and Management*, 259, 698–709.

Lobos G.A., Camargo A.V., del Pozo A., Araus J.L., Ortiz R., Doonan J.H. (2017) Editorial: plant phenotyping and phenomics for plant breeding. *Frontiers in Plant Science*, 8.

Ludovisi R., Tauro F., Salvati R., Khoury S., Mugnozza Scarascia G., Harfouche A. (2017) UAV-based thermal imaging for high-throughput field phenotyping of black poplar response to drought. *Frontiers in Plant Science*, 8.

Mathews A., Jensen J. (2013) Visualizing and quantifying vineyard canopy lai using an unmanned aerial vehicle (UAV) collected high density structure from motion point cloud. *Remote Sensing*, 5, 2164–2183.

Mutke S., Gordo J., Chambel M.R., Prada M.A., Álvarez D., Iglesias S., Gil L. (2010) Phenotypic plasticity is stronger than adaptative differentiation among Mediterranean stone pine provenances. *Forest Systems*, 19, 354.

Oleksyn J., Tjoelker M., Reich P. (1998) Adaptation to changing environment in Scots pine populations across a latitudinal gradient. *Silva Fennica*, 32.

Pearson R. (2006) Climate change and the migration capacity of species. *Trends in Ecology and Evolution*, 21, 111–113.

Petrucco L., Nardini A., Von Arx G., Saurer M., Cherubini P. (2017) Isotope signals and anatomical features in tree rings suggest a role for hydraulic strategies in diffuse drought-induced die-back of *Pinus nigra*. *Tree physiology*, 37, 523-535

Resco de Dios V., Fischer C., Colinas C. (2006) Climate change effects on Mediterranean forests and preventive measures. *New Forests*, 33, 29–40.

Roberts D.A., Roth K.L., Perroy R.L. (2016) Hyperspectral vegetation indices. In: Huete A., Lyon J.G., Thenkabail P.S. (eds.) *Hyperspectral Remote Sensing of Vegetation*. pp. 309–328, Boca Raton, FL: CRC Press.

Sánchez-Salguero R., Camarero J.J., Hevia A., *et al.* (2015) What drives growth of Scots pine in continental Mediterranean climates: drought, low temperatures or both? *Agricultural and Forest Meteorology*, 206, 151–162.

Sankaran S., Khot L.R., Espinoza C.Z., *et al.* (2015) Low-altitude, high-resolution aerial imaging systems for row and field crop phenotyping: A review. *European Journal of Agronomy*, 70, 112–123.

Tapias R., Climent J., Pardos J.A., Gil L. (2004) Life histories of Mediterranean pines. *Plant Ecology*, 171, 53–68.

Tognetti R., Michelozzi M., Giovannelli A. (1997) Geographical variation in water relations, hydraulic architecture and terpene composition of Aleppo pine seedlings from Italian provinces. *Tree Physiology*, 17, 241–250.

Valladares F., Matesanz S., Guilhaumon F., *et al.* (2014) The effects of phenotypic plasticity and local adaptation on forecasts of species range shifts under climate change. *Ecology Letters*, 17, 1351–1364.

Vizcaíno-Palomar N., Ibáñez I., González-Martínez S.C., Zavala M.A., Alía R. (2016) Adaptation and plasticity in aboveground allometry variation of four pine species along environmental gradients. *Ecology and Evolution*, 6, 7561–7573.

Voltas J., Camarero J.J., Carulla D., Aguilera M., Ortiz A., Ferrio J.P. (2013) A retrospective, dual-isotope approach reveals individual predispositions to winter-drought induced tree dieback in the southernmost distribution limit of Scots pine: Scots pine disposition to winter-drought dieback. *Plant, Cell and Environment*, 36, 1435–1448.

Voltas J., Chambel M.R., Prada M.A., Ferrio J.P. (2008) Climate-related variability in carbon and oxygen stable isotopes among populations of Aleppo pine grown in common-garden tests. *Trees*, 22, 759–769.

Voltas J., Lucabaugh D., Chambel M.R., Ferrio J.P. (2015) Intraspecific variation in the use of water sources by the circum-Mediterranean conifer *Pinus halepensis*. *New Phytologist*, 208, 1031–1041.

Wallace L., Lucieer A., Malenovský Z., Turner D., Vopěnka P. (2016) Assessment of forest structure using two uav techniques: a comparison of airborne laser scanning and structure from motion (SfM) point clouds. *Forests*, 7, 62.

Yamazaki F., Liu W., Takasaki M. (2009) Characteristics of shadow and removal of its effects for remote sensing imagery, In: *Geoscience and Remote Sensing Symposium, IEEE*, pp. IV–426. Ed. IEEE International, IGARSS.

CONCLUSIONS

Phenotypic variation in functional traits of Mediterranean pines as the combined result of intra-specific genetic variation and phenotypic plasticity

1. Intra-specific genetic variation was extensive in the lowland species *P. halepensis* and in the mid-mountain *P. nigra*, while the role of plastic differentiation was important in determining phenotypic variation in the high-mountain species *P. sylvestris.*

2. Populations of *P. halepensis* were characterised by genetic differentiation in leaf area, transpiration in summer and in photosynthetic pigments and reserves accumulation in spring.

3. Phenotypic integration of functional traits indicated contrasting adaptive syndromes in populations of Aleppo pine. Slow-growing populations showing a deep rooting system, a reduced transpiration and low chlorophyll concentration in spring emerged in contrast to fast-growing populations, which were characterised by a higher transpiration rate and a reduced investment in reproduction and reserves.

4. In Aleppo pine, variation in genes involved in cellulose and carbohydrates metabolism influenced growth traits at individual level. Transpiration and water concentration in the leaves were associated with variation in genes encoding for proteins involved in stomata dynamics. Differentiation in leaves pigments and leaf area was associated with variation in genes mainly involved in plant signalling and peroxisomes metabolisms.

5. Evolutionary differentiation in morpho-physiological traits including growth, reserve accumulation, leaf area and chlorophyll concentration was present in *P. nigra*. At the same time, populations' divergence was weak in traits related to water use.

6. Intra-specific genetic variation in WUE_i was weak in *P. sylvestris*. On the other hand, plastic variation had a primary role in determining tree performance in terms of stomatal conductance and carbon assimilation rate in this species.

7. Spatial differentiation in WUE_i related to plastic adjustment of individual phenotypes influenced variation in ecosystem WUE in stands of *P. sylvestris*.

Environmental drivers of phenotypic variation

1. Phenotypic variation was influenced by different factors in *P. halepensis*, *P. nigra* and *P. sylvestris*, as the consequence of different environmental constraints to which each species is subjected in its particular ecological niche.

2. Differences in the extent of water availability at the geographical origin of each population acted as main driver of genetic differentiation in Aleppo pine.

3. Winter temperatures and continentality were the main drivers of phenotypic variation in *P. nigra*, in contrast with the weak role played by water availability.

4. Spatial and temporal plastic variation of WUE_i in *P. sylvestris* was mainly influenced by soil water holding capacity.

UAV-derived remote sensing data to characterise morpho-physiological features of forest species in common gardens

1. UAV imagery is an effective high-throughput tool for phenotyping forest trees growing in common gardens. Low-cost approaches combining cheap sensors (i.e. RGB cameras) and reduced computational effort can provide valuable information on phenotypic adaptive variation in forest species. However, expensive multispectral and thermal cameras generate more informative data which are also easier to interpret.

2. UAV-imagery is a high-throughput phenotyping tool that can be combined with genomic data to study patterns of molecular adaptation in forest trees, with potential applications in tree breeding.

3. The use of UAV imagery requires a careful evaluation of trial conditions, which should allow the identification of single individuals or experimental units. Flights should be performed in spring/summer and at noon, to minimize unwanted shading effects.

ACKNOWLEDGMENTS

This work is the result of three intense years, and long is the list of people who contributed to the success of my PhD.

Firstly, a big thank to Jordi, who was probably the best supervisor I could have. It's funny the fact that "Plant physiology" was the only exam I had to repeat during my career. The fact that now I'm fascinated by this topic, although still limited to its forestry part, is clearly a success of Jordi, who kept feeding my interest during these years. I am very thankful for all his suggestions and ideas, which never missed, for his patience in constantly revising my work and for giving me the opportunity of travelling and living an all-round PhD.

Together with Jordi, I would like to thank all the people from the Laboratory of Silvicolture of the University of Lleida. Your kindness and your passion for work has been an example for me, and I wish the best to all of you. I'd particularly like to thank Tatiana, for shared lunches, for teaching me dendrochronology and for a nice week in Kaliningrad. Warmest thanks also to Pilar, Maria J. and Sveta, for always being kind and for the help they gave me with my lab work. You have thaught me a lot and you have made my life much easier. Thanks to Luis and Monica, for their explanation about physiological stuffs and for having always something to speak about. Finally, I'm really grateful to Mamun, who gave me a fundamental help regarding not-structural carbohydrates in Chapter 4. Beside my labmates**,** I'm also really thankfull to all the people of the Department of Crop and Forest Sciences of Lleida University. It was a pleasure to work here and I am going to miss this place.

Thanks to Jose Luis Araus and Shawn Kefauver from the Laboratory of Crop Ecophysiology of the University of Barcelona, for providing the drone that was used in in this thesis and for the support in data collection and analysis. Particularly, I would like to acknowledge the work of Shawn, who flew the drone, assembled the images and thaught me how to analyse them, also providing the necessary codes. Without him, this work would not have been possible.

I'm also grateful to Paco Rodríguez and Saray Martín from Föra, who hosted me in Soria for part of my data analysis. Particularly, warm and sincere thanks to Saray, who, during that week, introduced me to point cloud analysis and who fundamentally contributed to develop the code that I used in Chapter 3.

I truly appreciate the effort of all the co-authors of my papers, who contributed to the success of my research with sampling, data analysis or simply by critically reviewing my work. In particular, I'm very grateful to José Climent from INIA, for providing part of the data used in

Chapter 2 and for helping with the interpretation of the results. Thanks also to Delphine Grivet and Ricardo Alía (CIFOR-INIA), for providing the genomic data that I used in Chapter 3.

I'd also like to thank Larry López of Yamagata University Research Forest, for giving me the opportunity of spending two months in his lab in Tsuruoka. It was a very delightful experience, thanks to all the people I met in Japan, who made me to really appreciate the time we spent together. Thanks a lot to Mika, Cho, Alex, Sara, Satoru, Otsu, Saiako, Yurie and Felix, for showing me the crazy country in which you live. A big thank to Carles, for being my travel mate, for sharing this experience with me and for helping me with sampling.

A huge hug to all the friends I've met during my PhD in Lleida. Mirko, Helga, Carles, Carles, Joan, Albert, Habiba, JK, Hector, Iris, Lale, Jimit, Ni, Roberto, Irene, Diego, Marco, Albert, Paula, Audrey, Addy, Jordan, Aurore, Berta, Rut, Deokjoo, Tetsuto and more that I probably forget. Each of you have contributed with a word, a laugh, a smile, a dinner, a shared trip to this experience, that started as a PhD but went much further. In different ways, you all have enriched my life and I wish you all the best.

Thank to Alicia and Priya for having been my family in Lleida. You are the best side effect of having come to Spain for a PhD, and your contribution to my life deserves a much bigger space than few lines in the "Acknowledgments" section of my thesis. However, you have hundoubtfully made the difficulties of this work much easier to overcome, and I don't know how I would have finished my thesis without your support.

Thanks to my family, for being a warm "hogar" (a wonderful Spanish word – "focolare"- that, unfortunately, is rarely used in Italian) where to come back.

Thanks to Giulia, for countless reasons.